

Some parts of this thesis may have been removed for copyright restrictions.

If you have discovered material in AURA which is unlawful e.g. breaches copyright, (either yours or that of a third party) or any other law, including but not limited to those relating to patent, trademark, confidentiality, data protection, obscenity, defamation, libel, then please read our [Takedown Policy](#) and [contact the service](#) immediately

HEAT TRANSFER IN SUBCOOLED POOL FILM BOILING

BY

JACK BOLITHO SIVIOUR

A thesis submitted for the degree of

Doctor of Philosophy

in the

University of Aston in Birmingham

November 1970

*Thesis
b21.101 SIV*

-3 JUN 71 137945

Supervisor: Professor A.J. Ede

Department of Mechanical Engineering

University of Aston in Birmingham

Birmingham 4

Best Copy Available

Variable Print Quality

SUMMARY

Experimental heat transfer data are presented for the steady film boiling of water, aqueous detergent solution, and ethanol on horizontal cylinders of nominal diameters of $1/8$, $1/4$ and $1/2$ inch. The data for water and detergent solution were obtained for values of subcooling from zero, that is for saturated film boiling, to about 150 deg F, and at superheat temperatures of 1612°F, 1312°F and 1012°F. For ethanol, the values of subcooling ranged from zero to about 100 deg F, and the superheat temperatures were 698°F, 590°F and 486°F, (which in dimensionless form are the same as for water).

Rates of heat transfer were found to increase with increasing subcooling and superheat, and to decrease with increasing diameter. For the detergent solution, two stable values of heat flux were obtained for some values of superheat when subcooling was greater than about 50 deg F.

Photographic data are presented of film boiling under the above conditions and also on 8 inch high vertical cylinders, 2 x 2 inch vertical flat surfaces, a 4 inch diameter sphere, and a 2 x 9 inch horizontal surface.

Correlations for subcooled film boiling were derived from the test data in conjunction with existing correlations and some new approximate theoretical solutions for heat transfer in the liquid phase. The correlations take the form of adding a heat flux for saturated film boiling to a heat flux which is calculated from liquid parameters only.

The photographic results show quite clearly that the liquid vapour interface is generally chaotic at small values of subcooling (less than about 20 deg F) but is generally smooth when subcooling is greater than about 50 deg F. New physical models for subcooled film boiling are proposed from these results.

ACKNOWLEDGEMENTS

I wish to thank Professor A.J. Ede, formerly Research Professor, now head of the Department of Mechanical Engineering for his help and guidance given throughout the period during which the work was carried out. I would also like to thank Professor A.C. Walshaw, who was head of the department of Mechanical Engineering when the project was started, and who is now Professor Emeritus of the University of Aston in Birmingham.

I am grateful to the laboratory staff and library staff of the University who helped me carry out the project.

Finally, I would like to thank Mrs. W. Croft who typed the thesis and the friends who read the final draft.

CONTENTS

Chapter	Page
Nomenclature	5
Conversion factors into SI units	10
List of tables	11
List of figures	12
1. Introduction	17
1.1	17
1.2 Description of pool film boiling	18
1.3 A note on units	21
2. Quenching as a heat transfer problem	22
2.1 Introduction	22
2.2 General	22
2.3 Heat transfer considerations	23
2.4 Heat transfer by conduction	24
2.5 Heat transfer from the surface	24
2.5.1 Quenching in a tank of liquid	24
2.5.2 Quenching by jets and sprays	25
2.5.3 Quenching in other media	26
2.6 Conclusions	26
3. Literature Review	28
3.1	28
3.2	28
3.3 Saturated film boiling	29
3.3.1 Horizontal cylinders	29
3.3.2 Vertical surfaces	33
3.3.3 Spheres	34
3.3.4 Horizontal surfaces	35
3.4 Modifications of coefficients of formulae	36
3.5 The superheat term $f(Sp)$	37
3.6 Effects of Radiation	38
3.7 Subcooled film boiling	39
3.7.1 Theoretical solutions	39
3.7.2 Experimental data	44
3.7.3 Comparison of earlier work	44

Chapter		Page
3.8	Interfacial dynamics and vapour flow	46
3.8.1	Saturated film boiling	46
3.8.2	Subcooled film boiling	50
3.8.3	Further considerations	50
3.9	Conclusions	52
4.	The test conditions	53
4.1		53
4.2		53
4.3		53
4.4		54
4.5		55
5.	Apparatus and procedure	56
5.1		56
5.2	Development of the test-piece	56
5.3	Test-pieces for the photographic study	58
5.4	Apparatus	58
5.5	Normal procedure	60
5.6	Experimental difficulties	60
6.	Accuracies and errors	63
6.1		63
6.2	Temperatures	63
6.3	Heat flux	65
6.4	Fluid properties	66
6.5	Calculations	66
7.	Results	67
7.1		67
7.2		67
7.3	Water	67
7.4	Detergent solution	69
7.5	Self-generated noise	73
7.6	Ethanol	74
8.	Analyses and Correlations	76
8.1		76
8.2	Interfacial dynamics and vapour flow	76
8.3	Correlation of the heat transfer results	79

Chapter	Page
8.3.1 Vapour heat transfer	80
8.3.2 Liquid heat transfer	82
8.4 Discussion	85
8.4.1 Vapour heat transfer	85
8.4.2 Liquid heat transfer	86
8.5 Comparison of the correlations and the test data	92
8.5.1 Summary of the correlations for subcooled film boiling	92
8.5.2 General comments on the comparison	94
8.5.3 Best correlation for water	94
8.5.4 Best correlation for ethanol	95
8.5.5 All correlations	95
8.6 Film boiling in detergent solution	96
9. General discussion and conclusions	98
9.1	98
9.2 Reproducibility and accuracy of the test results	98
9.3 Comparison of earlier work and the present results for heat transfer	100
9.4 New physical models for subcooled film boiling	101
9.4.1 Vertical surfaces	101
9.4.2 Horizontal cylinders	102
9.4.3 Spheres	103
9.4.4 Horizontal surfaces	103
9.5 Summary of the analyses and correlations	104
9.6 Summary of film boiling in detergent solution	106
9.7 Film boiling at high subcooling	107
9.8 Application of the data	108
9.9 Advances represented by the present work	110
9.10 Further work	110
Tables 1 and 2	113 - 117
Figures 1 - 63	118 - 182
Appendices	
A Circumferential variations of surface temperature and heat flux	183

	Page
B Solution of the intergrated boundary layer equations for the liquid phase	185
C Experimental results : table C	191
D Fluid properties : tables D1, D2 and D3	216
E Reduction of the test data : tables E1, E2, E3	220
F Comparison of the correlations for heat transfer and the experimental data : tables F1, F2, F3	227
References	231

NOMENCLATURE

English Letters		Units
B	radiation parameter, equation 32	
C	specific heat at constant pressure	Btu/lb degF
D	diameter	ft, in
f	denotes a function of	
g	gravitational acceleration	ft ² /s, ft ² /h
g_c	constant relating force and mass = 32.174	ft lb _m /lb _f s ²
h	heat transfer coefficient	Btu/hft ² degF
h_{fg}	latent heat of vaporization	Btu/lb
h'_{fg}	modified latent heat of vaporization (see section 3.5)	Btu/lb
k	thermal conductivity	Btu/hft degF
L	height	ft, in
L_c	critical height	ft, in
I	length	ft
MIMC	abbreviation for mineral insulated metal covered	
N	numerical coefficient	
n	numerical index	
Q	heating rate	Btu/h
q	heat flux	Btu/hft ²
R	parameters defined where used	
T	temperature	°F
ΔT_L	liquid subcooling $T_s - T_L$	degF
ΔT_v	vapour superheat $T_w - T_s$	degF
t_v	vapour film thickness	ft
t_w	tube wall thickness, equation 51	ft
u	velocity in the vertical direction	ft/s
v	velocity in the horizontal direction	ft/s
x	vertical axis	
y	horizontal axis	

Greek Letters

α	thermal diffusivity	ft^2/h
β	coefficient of thermal expansion	$/\text{degF}$
Δ	designates a difference when used as a prefix	
δ	boundary layer thickness	ft, in
ϵ	radiative emissivity	
λ_c	critical wavelength, equation 8	ft, in
λ'_c	modified critical wavelength, equation 48	ft, in
λ_{md}	"most dangerous" wavelength, section 3.8.1	ft, in
μ	viscosity	$\text{lb}/\text{ft}\cdot\text{h}, \text{lb}/\text{ft}\cdot\text{s}$
ν	kinematic viscosity	ft^2/h
ρ	density	lb/ft^3
σ	surface tension	lb/ft
σ_r	Stefan-Boltzmann constant	$\text{Btu}/\text{hft}^2\cdot\text{degF}^4$

Dimensionless Groups

Bo_1	Bond number	$(\rho_L - \rho_v)gD t_v / \sigma g_c,$ $D t_v (2\pi / \lambda_c)^2$
Bo_2	Bond number	$t_v \sqrt{D t_v} (2\pi / \lambda_c)^2.$
Gr	Grashof number	$g \beta \rho^2 \Delta T D^3 / \mu^2,$ $g \beta \rho^2 \Delta T L^3 / \mu^2.$
Gr^*	modified Grashof number	$g(\rho_L - \rho_v) \rho_v D^3 / \mu_v^2,$ $g(\rho_L - \rho_v) \rho_v L^3 / \mu_v^2.$
$\text{Gr}^*_{\lambda_c}$	modified Grashof number	$g(\rho_L - \rho_v) \rho_v \lambda_c^3 / \mu_v^2.$

Nu	Nusselt number	$qD / \Delta T_k,$ $qL / \Delta T_k.$
Nu_{λ_c}	Nusselt number	$q \lambda_c / \Delta T_k.$
Pr	Prandtl number	$\mu C / k, \eta / \alpha$
Ra	Rayleigh number	(Gr, Pr)
Ra^*	modified Rayleigh number	$(Gr^*, Pr, f(Sp))$
Ra_1^*		$(Gr^* Pr) \left(\frac{1}{2} + \frac{1}{Sp} \right)$
Ra_2^*		$(Gr^* Pr) \left(\frac{1}{Sp} (1 + 0.34 Sp)^2 \right)$
Ra_3^*		$(Gr^* Pr) \frac{1}{Sp}$
$Ra_{\lambda_c}^*$		$(Gr_{\lambda_c}^* Pr) \left(\frac{1}{2} + \frac{1}{Sp} \right) \left\{ 1 + 0.585 \frac{\lambda_c}{D} + \frac{1}{228} \left(\frac{\lambda_c}{D} \right)^3 \right\}$
Re	Reynolds number	$\rho v D / \mu$
Re^*	modified Reynolds number, equation 49	$\rho_v u_v t_v / \mu_v$

Sc	dimensionless subcooling	$C_L \Delta T_L / h_{fg}$
Sp	dimensionless superheat	$C_v \Delta T_v / h_{fg}$

Subscripts

Vapour properties and parameters are generally written without the subscript v where it is unambiguous to do so.

c	refers to a critical value
co	convective only; see section 3.6
fg	see h_{fg}
i	at the liquid-vapour interface
L	refers to the liquid, or bulk liquid
m	mean value
r	radiation
s	at the saturation temperature (boiling point)
T	temperature
t	based on vapour film thickness
tcl	turbulent single phase convection, equation 41
tot	total
u	velocity
v	refers to the vapour
w	at the wall, or hot surface

Units

Btu	British thermal unit
°F	temperature on the Fahrenheit scale
degF	temperature difference on the Fahrenheit scale
ft	foot
h	hour
inch	inch

lb, lb_m	pound mass
lb_f	pound force
s	second.

CONVERSION FACTORS INTO SI UNITS

<u>Multiply</u>	<u>By</u>	<u>To obtain</u>
ft	0.3048	m
inch	25.4	mm
lb, lb _m	0.4536	kg
lb _f	4.448	N
°F-32	5/9	°C
degF	5/9	K
Btu	1.055	kJ
Btu/h	0.2931	W
(q) Btu/hft ²	3.155	W/m ²
(h) Btu/hft ² degF	5.678	W/m ² K
(k) Btu/hft degF	1.731	W/mK
(C) Btu/lb degF	4.187	kJ/kgK
(h _{fg}) Btu/lb	2.326	kJ/kg
(μ) lb/fth	0.4134	kg/kms
(μ) lb/fts	1.488	kg/ms
(ρ) lb/ft ³	16.019	kg/m ³
(σ) lb _f /ft	14.57	N/m
(σ _r) = 1.73×10 ⁻⁹ B/hft ² R ⁴ = 5.66×10 ⁻⁸ W/m ² K ⁴		

LIST OF TABLES

Table 1 Ranges of test results

- 1a Heat transfer on horizontal cylinders
- 1b Photos of steady film boiling
- 1c Photos of transient film boiling

Table 2 Values of Bond number

- 2a Bo_1 for water
- 2b Bo_1 for ethanol
- 2c Bo_2 for water
- 2d Bo_2 for ethanol.

(Other tables are included in the appendices).

LIST OF FIGURES

1. Typical boiling curves.
2. Simplified transformation diagram for a carbon steel.
3. Comparison of values of superheat terms from earlier work.
4. Values of the radiation parameter "B".
5. Comparison of data for the film boiling of water.
6. Interfacial wave pattern and bubble release for saturated film boiling on horizontal surfaces.
7. Comparison of published data for the values of the critical height, L_c , in the saturated film boiling of water.
8. Sketch of a test-piece with which the experimental data for the horizontal cylinders were obtained.
9. Sketches of the additional test pieces used in the photographic study.
10. Present experimental data for the steady film boiling of water on 1/8-inch diameter horizontal cylinders.
11. Present experimental data for the steady film boiling of water on 1/4-inch diameter horizontal cylinders.
12. Present experimental data for the steady film boiling of water on 1/2-inch diameter horizontal cylinders.
13. Present experimental data for the steady film boiling of detergent solution on 1/8-inch diameter horizontal cylinders.
14. Present experimental data for the steady film boiling of 0.025% detergent solution on 1/4-inch diameter horizontal cylinders.
15. Present experimental data for the steady film boiling of ethanol on 1/8-inch diameter horizontal cylinders.
16. Present experimental data for the steady film boiling of ethanol on 1/4-inch diameter horizontal cylinders.
17. Present experimental data for the steady film boiling of ethanol on 1/2-inch diameter horizontal cylinders.
18. Present experimental data for the steady film boiling of ethanol on 1/4-inch diameter horizontal cylinders at the surface temperature of 1012°F.

19. Summary of the photographic results for film boiling at small values of subcooling ($\Delta T_L < \text{about } 20 \text{ degF}$).
20. Summary of the photographic results for film boiling at large values of subcooling ($\Delta T_L > \text{about } 50 \text{ degF}$).
21. Steady film boiling of water on $\frac{1}{4}$ -inch diameter horizontal cylinders.
22. Steady film boiling of 0.025% detergent solution on $\frac{1}{4}$ -inch diameter horizontal cylinders.
23. Steady film boiling of ethanol on $\frac{1}{4}$ -inch diameter horizontal cylinders.
24. Steady film boiling of 0.025% detergent solution of $\frac{1}{4}$ -inch diameter horizontal cylinders at high and low values of heat flux.
25. Steady film boiling of water on $\frac{1}{8}$ -inch and $\frac{1}{2}$ -inch diameter horizontal cylinders .
26. Steady film boiling of water on $\frac{1}{2}$ -inch diameter horizontal cylinders at $T_w = 1312^\circ\text{F}$.
27. Steady film boiling of water on 8 inch high vertical cylinders.
28. Steady film boiling of 0.025% detergent solution on 8 inch high vertical cylinders.
29. Steady film boiling of ethanol on 8 inch high vertical cylinders.
30. Transient film boiling of water on 2 inch high vertical surfaces.
31. Transient film boiling of ethanol on 2 inch high vertical surfaces.
32. Transient film boiling of water on a 4 inch diameter sphere.
33. Transient film boiling of 0.025% detergent solution on a 4 inch diameter sphere.
34. Transient film boiling of water on a 2.x 9 inch horizontal surface.
35. Dimensionless correlations of the results for saturated film boiling with $\epsilon_w = 0.75$ and 1.0, and $f(Sp) = \frac{1}{2} + \frac{1}{Sp}$.

36. Dimensionless correlation of the results for saturated film boiling: the final correlation with $\epsilon_w = 0.9$ and $f(Sp) = (\frac{1}{2} + \frac{1}{Sp})$.
37. Dimensionless correlations of the results for saturated film boiling with $\epsilon_w = 0.9$ and $f(Sp) = \frac{1}{Sp} (1 + 0.34Sp)^2$ and $\frac{1}{Sp}$.
38. Dimensionless correlation of the results for saturated film boiling according to equation 12.
39. Dimensionless correlation of the results for the liquid heat flux, q_L : Nu_L verses $(GrPr)_L$.
40. Dimensionless correlation of the results for the liquid heat flux, q_L : Nu_L verses $(GrPr^2)_L$.
41. Dimensionless correlation of the results for the liquid heat flux q_L : Nu_L verses $(GrPr^{\frac{3}{2}})_L$.
42. Film boiling of water on 1/8-inch diameter horizontal cylinders. Comparison of the experimental data with the proposed correlation of best fit for water.
43. Film boiling of water on 1/4-inch diameter horizontal cylinders. Comparison of the experimental data with the proposed correlation of best fit for water.
44. Film boiling of water on 1/2-inch diameter horizontal cylinders. Comparison of the experimental data with the proposed correlation of best fit for water.
45. Film boiling of ethanol on 1/8-inch diameter horizontal cylinders. Comparison of the experimental data with the proposed correlation of best fit for ethanol.
46. Film boiling of ethanol on 1/4-inch diameter horizontal cylinders. Comparison of the experimental data with the proposed correlation of best fit for ethanol.
47. Film boiling of ethanol on 1/2-inch diameter horizontal cylinders. Comparison of the experimental data with the proposed correlation of best fit for ethanol.
48. Film boiling of water on 1/8-inch diameter horizontal cylinders. Comparison of the experimental data with

- the proposed correlations at $T_w = 1012^\circ\text{F}$.
49. Film boiling of water on 1/8-inch diameter horizontal cylinders. Comparison of the experimental data with the proposed correlations at $T_w = 1312^\circ\text{F}$.
 50. Film boiling of water on 1/8-inch diameter horizontal cylinders. Comparison of the experimental data with the proposed correlations at $T_w = 1612^\circ\text{F}$.
 51. Film boiling of water on 1/4-inch diameter horizontal cylinders. Comparison of the experimental data with the proposed correlations at $T_w = 1012^\circ\text{F}$.
 52. Film boiling of water on 1/4-inch diameter horizontal cylinders. Comparison of the experimental data with the proposed correlations at $T_w = 1312^\circ\text{F}$.
 53. Film boiling of water on 1/4-inch diameter horizontal cylinders. Comparisons of the experimental data with the proposed correlations at $T_w = 1612^\circ\text{F}$.
 54. Film boiling of water on 1/2-inch diameter horizontal cylinders. Comparison of the experimental data with the proposed correlations at $T_w = 1012^\circ\text{F}$ and 1312°F .
 55. Film boiling of ethanol on 1/8-inch diameter horizontal cylinders. Comparison of the experimental data with the proposed correlations at $T_w = 486^\circ\text{F}$.
 56. Film boiling of ethanol on 1/8-inch diameter horizontal cylinders. Comparison of the experimental data with the proposed correlations at $T_w = 590^\circ\text{F}$.
 57. Film boiling of ethanol on 1/8-inch diameter horizontal cylinders. Comparison of the experimental data with the proposed correlations at $T_w = 698^\circ\text{F}$.
 58. Film boiling of ethanol on 1/4-inch diameter horizontal cylinders. Comparison of the experimental data with the proposed correlations at $T_w = 486^\circ\text{F}$.

59. Film boiling of ethanol on $\frac{1}{4}$ -inch diameter horizontal cylinders. Comparison of the experimental data with the proposed correlations at $T_w = 590^\circ\text{F}$.
60. Film boiling of ethanol on $\frac{1}{4}$ -inch diameter horizontal cylinders. Comparison of the experimental data with the proposed correlations at $T_w = 698^\circ\text{F}$.
61. Film boiling of ethanol on $\frac{1}{2}$ -inch diameter horizontal cylinders. Comparison of the experimental data with the proposed correlations at $T_w = 486^\circ\text{F}$.
62. Film boiling of ethanol on $\frac{1}{2}$ -inch diameter horizontal cylinders. Comparison of the experimental data with the proposed correlations at $T_w = 590^\circ\text{F}$.
63. Film boiling of ethanol on $\frac{1}{2}$ -inch diameter horizontal cylinders. Comparison of the experimental data with the proposed correlations at $T_w = 698^\circ\text{F}$.

Chapter 1

INTRODUCTION

1.1 Film boiling is a mode of heat transfer which occurs when a surface that is considerably hotter than the boiling point of a liquid comes into contact with the liquid. It is characterised by the development of a layer of vapour which separates the liquid from the surface, and can occur in a number of situations :- a) when a body is immersed in a tank of liquid, b) when a liquid spray strikes a surface, and c) when a liquid flows inside a tube. These are termed pool, spray and flow film boiling respectively. The process is termed saturated film boiling when all the liquid is at its boiling point, and subcooled film boiling when the bulk of the liquid is below its boiling point. In any liquid, film boiling does not normally develop on surfaces cooler than the Leidenfrost temperature, corresponding to the minimum heat flux in figure 1, but is replaced by transitional and nucleate boiling. A description of all the regimes of boiling can be obtained from standard texts, (e.g. ref. 4). A more detailed introduction to film boiling is given later in this chapter (section 1.2). The Leidenfrost temperature in cryogenic liquids may be well below normal ambient temperature, and the film boiling of such liquids can occur on cold surfaces. In substances that are liquids at normal ambient conditions, the Leidenfrost temperature is usually well above ambient temperature, and high surface temperatures are required for film boiling to develop, such as in the metallurgical process of quenching.

It is well known that subcooled film boiling, both pool and spray, occurs during quenching. The fact that it is a relatively slow mode of heat transfer and that it occurs during the critical initial stages of cooling are both generally appreciated. Yet a literature search under the terms of reference "Quenching as a heat transfer problem" showed that there is little published heat transfer data appertaining to quenching which would enable cooling curves to be calculated.

It was therefore decided to investigate the problem of heat transfer during quenching, restricting the scope of the investigation to subcooled

pool film boiling. The results of this investigation are presented in this thesis.

A literature search was first conducted under the terms of reference "subcooled pool film boiling". The search was extended to include saturated film boiling when it was found that much of the data for subcooled film boiling were extensions of data for saturated film boiling. A few theoretical solutions were discovered for subcooled film boiling, but were found to predict widely differing heat transfer rates. Insufficient experimental data were found to substantiate any of the theoretical solutions.

It was decided therefore to concentrate on obtaining, firstly, accurate experimental data for subcooled pool film boiling, and secondly, a semi-empirical correlation derived from these data, in conjunction with existing theories as far as possible. Both these objectives have been achieved. Experimental data have been obtained for the steady film boiling of water, solutions of a detergent in water, and ethanol, on horizontal cylinders of diameters of $1/8$, $1/4$ and $1/2$ inch. The bulk liquid temperatures cover the range from ambient to near the boiling points. The correlations take the form of adding a heat flux calculated from vapour parameters to one calculated from liquid parameters.

A photographic study has also been carried out with the above cylinders, and with a sphere of 4 inches diameter, a 2 inch high vertical surface, an 8 inch high vertical tube, and 2×9 inch flat horizontal surface. The study illustrates some of the physical aspects of film boiling. In particular it illustrates how the waviness of the liquid-vapour interface and the release of bubbles of vapour vary with subcooling, superheat and the liquid.

1.2 Description of pool film boiling

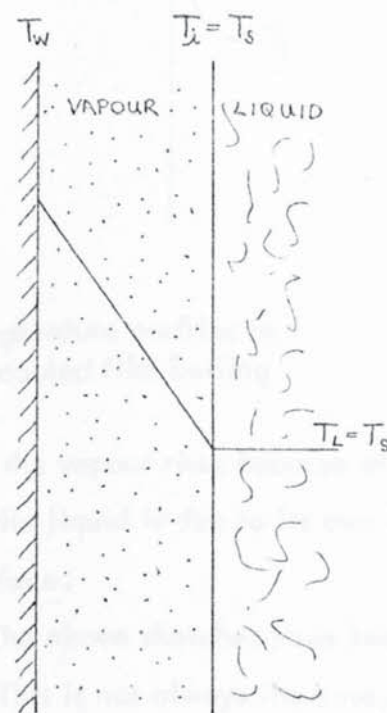
Film boiling generally occurs only on surfaces hotter than the Leidenfrost temperature which is the surface temperature at which the minimum heat flux occurs in the boiling curve, figure 1. The value of the Leidenfrost temperature may be considerably different in different fluids. Under normal

ambient conditions the value in water may be several hundred degrees Fahrenheit, in common organic liquids about $100 - 300^{\circ}\text{F}$, and in cryogenic liquids it may be colder than normal ambient temperature.

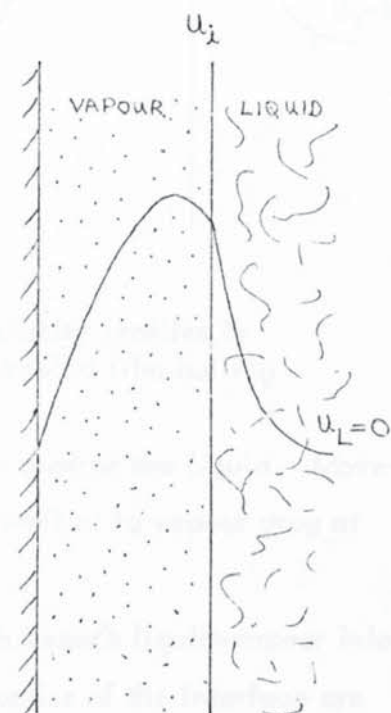
No upper limit of surface temperature has been defined for the film boiling regime. Radiation, therefore, can be of considerable importance as a mode of heat transfer.

It is generally assumed that a complete film of vapour separates the surface from the liquid. The bulk liquid is stationary in pool boiling.

In saturated film boiling, all the liquid is at the boiling point, and therefore temperature gradients exist only in the vapour as shown in the sketch. The temperature difference between the surface and the boiling point of the liquid is



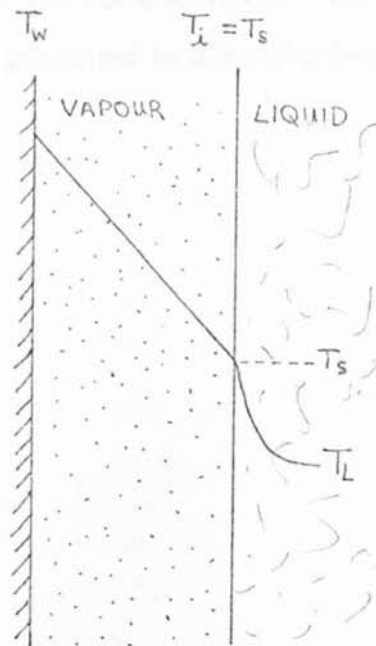
temperature profiles in
saturated film boiling



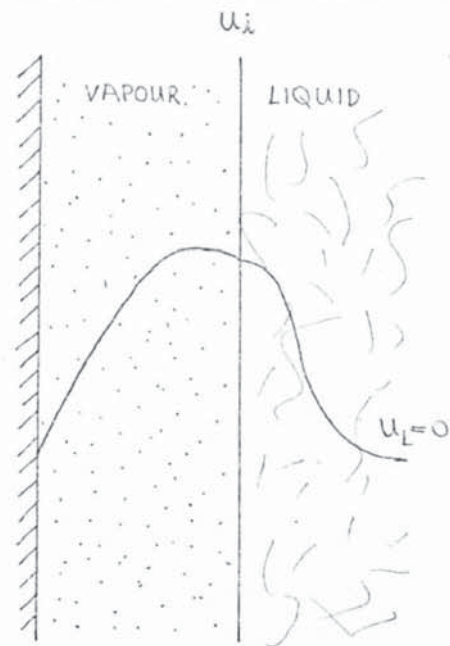
velocity profiles in
saturated film boiling

often termed the superheat, or vapour superheat. The vapour has a tendency to rise because of its buoyancy against the liquid. The movement of the vapour is constrained by the stationary surface, and by shear forces at the liquid-vapour interface. Liquid therefore rises with the vapour, resulting in velocity profiles in both phases as sketched.

In subcooled film boiling the bulk liquid temperature is below the boiling point, although the interface remains at that temperature. The temperature difference between the bulk liquid and the boiling point is known as the subcooling or liquid subcooling. Temperature gradients exist in both the vapour and the liquid as shown. As in the case of saturated film



Temperature profiles in subcooled film boiling



Velocity profiles in subcooled film boiling

boiling, the vapour rises because of its buoyancy against the liquid. Movement of the liquid is due to its own buoyancy as well as to vapour drag at the interface.

The above sketches have been drawn with smooth liquid-vapour interfaces. This is not always the case, but the dynamics of the interface are too complex to be dealt with here. They are discussed in detail in later chapters.

In saturated film boiling, heat is transferred by evaporation of the liquid, subsequent heating of the vapour, and the eventual vapour removal. Thus large quantities of vapour are emitted from the upper regions of surfaces on which the film boiling occurs. In subcooled film boiling, heat can be transported by convection into the liquid, and the quantity of vapour emitted may diminish and become zero. Heat transfer rates are generally increased by subcooling.

1.3 A note on units

The British system of units has been used in this thesis because most previous work, much of which is from the United States of America, have used this system. This applies to papers appertaining to quenching as well as to film boiling. Some conversion factors to S I units have been included after the nomenclature. The system of units is of course irrelevant when data are presented in dimensionless terms.

Chapter 2

QUENCHING AS A HEAT TRANSFER PROBLEM

2.1 The subject of this thesis was decided after a literature search and review under the heading "Quenching as a heat transfer problem" had been carried out. The results of this work, which are discussed briefly in this chapter, indicated, for heat transfer during quenching:

- the present state of knowledge,
- where present heat transfer knowledge might be applied,
- areas requiring research.

2.2 General

Quenching is the rapid cooling of a metal part to give it the desirable properties of strength and hardness. These two properties depend on the structure of the metal after quenching, which in turn depend on a) the composition of the metal, which is a metallurgical problem, and b) the speed of cooling, which is a heat transfer problem. All this can be conveniently illustrated by drawing cooling curves on a transformation diagram.

A simplified transformation diagram for a carbon steel is shown in figure 2, with some cooling curves, $C_1 - C_4$. Typically, a steel would be soaked at about 1600°F until the transformation to austenite is complete. Transformation from austenite begins at about 1300°F . The "nose" of the transformation curve is at about 1000°F and one second. If heat transfer rates are high the metal might cool along curve C_1 , and if they are low along curve C_4 . The hardest steel is obtained by cooling rapidly, as shown by curves C_1 and C_2 , to miss the nose of the transformation curve and thus form 100% martensite. Cooling along curve C_3 would result in some ferrite being formed in the martensite and would produce a softer steel. Slow cooling along curve C_4 would produce a very soft steel.

When a solid body is quenched, the cooling rate is fastest at the surface and becomes progressively slower towards the centre. Thus it is

possible for the surface to cool as curve C_1 , and the centre as C_3 , resulting in complete hardening only near the surface. The proportion of unhardened core increases with the size of the body. It is possible however to harden throughout by using an alloy steel. For such steels the nose of the curve, whilst remaining at about 1000°F , moves along the time axis and could have a value of several hours for a high alloy steel. But since alloy steels are more expensive than carbon steels, the development of a quenching technique which satisfactorily hardens the cheaper steels is economically desirable.

Rapid cooling as shown by curve C_2 is required to pass the nose of the transformation curve, but subsequent cooling may be much slower as shown by curve C'_2 : In fact such slower cooling may be advantageous because it reduces temperature gradients and consequent stresses in the part during quenching, and so reduces the risk of cracking and distortion.

Thus an ideal quenchant would cool very rapidly at first and then more slowly. However, the reverse occurs in most cases because quenching usually involves boiling. At the higher surface temperatures film boiling occurs (usually termed the vapour blanket stage in quenching literature), which has low rates of heat transfer, see figure 1. As the temperature of the surface falls, transitional and nucleate boiling occur, with much higher rates of heat transfer.

2.3 Heat transfer considerations

Calculation of cooling curves can be considered in two parts :

1. heat transfer by conduction within the body,
2. heat transfer from the surface.

Both are quite complex: heat transfer from the surface because it usually involves boiling; and heat transfer by conduction because it is transient, the thermal properties are temperature-dependent, heats of transformation have to be considered, and the rates of heat transfer from the surface must be known.

The problem was set out in this way as early as 1922 by Heindhofer (6), but until recently his definition has not been repeated in the majority of publications. Much experimental data have been published as cooling curves for the quenching of spheres and similar shapes. In this unanalysed

form the application of the data is restricted to situations very similar to those for which the data were obtained. Grossman and co-workers (7) devised the concept of severity of quench, which largely eliminates heat transfer considerations. A discussion of this concept is beyond the scope of the present work, but can be obtained from the review by Dardel (8). His review also covers work on heat transfer during quenching that was published before about 1960.

2.4 Heat transfer by conduction

The problem of calculating the heat transfer by conduction in a part during quenching has been treated with some success by Economopolous and co-workers. Numerical solutions of the conduction equations by computer has enabled temperature-dependent thermal properties and heats of transformation to be taken into account. Calculated and experimental cooling curves were compared (9) for a large shaft of about $3\frac{1}{2}$ ft. in diameter with a 4 inch diameter hole along the axis, and show satisfactory agreement. Thermocouples were positioned at five radii, and the readings of the innermost and outermost thermocouples were used as boundary values to calculate the cooling curves at the other positions.

2.5 Heat transfer from the surface

Quenching is most often carried out either in a tank of liquid, or with jets or sprays. These methods cover a very wide range of heat transfer rates. Both involve the boiling of the liquid, but they are otherwise quite different. Less often, streams of gases, molten salt baths and lead baths are used, and fluidised beds are reported to have some application.

2.5.1 Quenching in a tank of liquid - pool film boiling. Heat transfer takes place from the surface according to the boiling curve figure 1. Experimental data have been published occasionally in the form of boiling curves, but most often as cooling curves or cooling velocity curves. No theoretical solutions or empirical correlations were discovered.

Paschakis and co-workers (10 - 14) have presented experimental boiling curves obtained from the cooling of a two inch diameter sphere from a temperature of 1600°F in water, aqueous solutions of sodium hydroxide and

oils. In water, increasing the degree of subcooling increased the rates of heat transfer over the whole range of superheat. The addition of sodium hydroxide to water caused the replacement of film boiling by transition boiling at higher body temperatures. This happened because sodium hydroxide was deposited on the surface of the metal sphere as water was evaporated at the interface. The surface on which boiling took place was therefore one of sodium hydroxide. The relatively poor thermal conductivity of sodium hydroxide meant that the surface on which boiling occurred was considerably cooler than the body temperature. Heat transfer rates for "slow", "medium" and "fast" oils do not differ significantly in the film boiling regime. Fast oils achieve higher overall rates of heat transfer because film boiling terminates at a higher surface temperature than in slow and medium oils, and rates of heat transfer are higher in the transitional and nucleate boiling regimes. Similar data have been reported by Stenzle and Schultze (15).

Much comparative data were found, in the form of cooling curves and cooling velocity curves, which illustrate that a wide range of rates of heat transfer can be achieved from water based (16) and oil quenchents (17). The quenching speed of water can be increased by adding a salt which acts in a similar manner to sodium hydroxide described above, and can be decreased by adding polyvinyl alcohol (PVA) to give a quench as slow as a fast oil (18). The reduced quenching speed in the PVA solution is attributed to the layer of viscous gel which forms in the liquid at the interface. The quenching speeds in oils differ because of their composition (10 - 14). Heat transfer rates can be improved by agitation, and by forced circulation of the liquid. Raising the temperature of the bulk liquid usually decreases cooling speeds, and vice versa. Special methods of ultrasonic vibrations (19) and electric fields (20) have been found to increase rates of heat transfer.

2.5.2 Quenching by jets and sprays. This type of quenching is usually carried out with air-water mixtures issuing from a number of nozzles adjusted and distributed to give an even coverage of the surface. The liquid boils, and rates of heat transfer vary with surface temperature in a manner similar to that for pool boiling shown by the boiling curve in figure 1. Rates of heat transfer depend on spray parameters such as drop size and velocity, composition and intensity of the spray, and on the fluids. It is stated (21) that the more

powerful sprays disrupt the vapour film at higher temperatures, possibly as high as 1300°F.

No theoretical analysis was found, but a number of publications presenting experimental data were discovered. Unfortunately the experimental data, even when presented in the form of boiling curves (22) have been presented in terms of nozzle parameters, e.g. fluid supply pressures. Such a presentation severely limits comparison and application of the data.

Approximate rates of heat transfer in spray quenching can be obtained from references (23) and (24) in which a boiling curve for a tank of quiescent water has been included with the spray boiling curves. Depending on supply pressures, the rates of heat transfer achieved by the sprays may be greater or less than the rates of heat transfer in the tank of water.

The following correlation is presented (25) for steady film boiling with a 100% water spray on a steel sheet,

$$Nu = N Re^n$$

Application is restricted however, because N and n vary with surface temperature, and the width of the test specimen is used as the characteristic length in the Reynolds number.

2.5.3 Quenching in other media. Occasionally quenching is carried out in air or gas streams, molten salt and lead baths, and fluidised beds. Heat transfer rates are somewhat low, being no better than oil in the film boiling or vapour blanket stage (26). The rates of heat transfer do not become extremely high at the lower surface temperatures in the manner associated with the nucleate boiling of liquids. The empirical correlation

$$h = 0.93 e^{0.0015(T_s - T_L)}$$

has been derived for a quiescent salt bath (27). The possible use of fluidised beds has been assessed by estimating probable heat transfer rates from existing heat transfer knowledge (28,29).

2.6 Conclusions

This brief review has illustrated how the structure of a steel after quenching might be predicted by drawing cooling curves on a transformation

diagram. The calculation of the cooling curve has been considered as a heat transfer problem and divided into heat transfer by conduction within the material, and heat transfer by convection from the surface.

The problem of conduction within the material has been tackled by Economopolous and co-workers, who have used numerical methods to solve the conduction equations.

Almost all the work for surface heat transfer is experimental and unfortunately much of it has been published in unanalysed form such as cooling curves. Therefore, much of the data are suitable only for comparative purposes. Only a small proportion has been published as boiling curves, many of which for spray quenching are suitable for comparative purposes only because they have been presented in terms of nozzle parameters, rather than spray parameters.

The application of the principles of heat transfer should ensure that all experimental data are analysed to have the widest possible application, and to avoid the shortcomings mentioned in the previous paragraph. It should also ensure that the latest heat transfer knowledge is used, and that experiments are designed to obtain data which apply to a wide range of conditions.

It was therefore decided to examine heat transfer from the surface under conditions appertaining to quenching in a tank of liquid. Because the most critical cooling period usually occurs when surface temperatures are high, it was decided to restrict the examination to film boiling, and in particular to subcooled film boiling since the bulk liquid temperature in quenching is usually less than the boiling point.

Chapter 3

LITERATURE REVIEW

3.1 The literature search at first covered only subcooled pool film boiling, but was soon extended to include saturated film boiling when it became apparent that most work on subcooled film boiling was in fact an extension of work on saturated film boiling.

Work on saturated film boiling is reviewed only if it is relevant to subcooled film boiling. The review is restricted as far as possible to natural convection pool film boiling at normal gravity and atmospheric pressure. Emphasis is placed on the film boiling of substances normally liquid under these conditions rather than on cryogenic liquids. Other reviews are available with different emphases (31, 37, 92), but they are mostly restricted to saturated film boiling.

3.2 Saturated film boiling on the four simple geometries is first reviewed. Horizontal cylinders and spheres are well covered by both theoretical and experimental work; vertical and horizontal surfaces are not so well covered though cover is adequate. Some methods are included for modifying the coefficients of equations for horizontal cylinders, or spheres or vertical surfaces so that the equations for one of these geometries can apply to the other two. Various methods of including the enthalpy difference between the liquid at its boiling point and vapour at its mean temperature are compared.

The effects of radiation on film boiling and its inclusion in the heat transfer correlations is next reviewed.

Considerably less literature was discovered for subcooled film boiling than for saturated film boiling. The theoretical solutions are extensions of solutions already obtained for saturated film boiling but are more complex because of the appearance of the liquid as well as the vapour properties. In most cases the results have been presented either graphically or as equations with graphical parameters, and often the information applies only to water. It is not possible to present a single non-dimensional equation

for subcooled film boiling because two phases are involved. None of the theoretical solutions have been supported by experimental work - little of which was discovered anyway - and no empirical correlation has been found. Most of the experimental work is for water and has been obtained from the cooling of spheres and similar bodies, or for steady film boiling on small diameter wires. Consequently comparison of the data has been made for water only and, as far as possible, for horizontal cylinders of $\frac{1}{4}$ inch diameter by modifying equations to apply to this geometry.

The final section of the review deals with interfacial dynamics, flow stability and breakdown of the vapour film.

3.3 Saturated film boiling

3.3.1 Horizontal Cylinder. The first theoretical treatment for film boiling on a horizontal cylinder was carried out by Bromley (30) who, after making a number of simplifying assumptions and by considering the buoyancy of the vapour, derived a relation which in non-dimensional form is:

$$Nu = N [Gr^* Pr]^{\frac{1}{4}} \left[\frac{1}{2} + \frac{1}{Sp} \right]^{\frac{1}{4}}. \quad (2)$$

The complete derivation can be found in reference (31).

The value of the coefficient N is 0.512 if the liquid surrounding the cylinder is assumed to be stagnant, and 0.724 if the liquid moves freely with the vapour. Bromley obtained experimental data for film boiling on tubes of $\frac{3}{16}$, $\frac{1}{4}$, $\frac{3}{8}$, $\frac{1}{2}$ inch diameter in water, n-pentane, liquid nitrogen, ethanol, benzene and carbon tetrachloride which fell between the limits given by these two values of the coefficient. He therefore recommended the mean value of 0.62.

The equation, like most others of similar type, predict a "convection only" heat flux, q_{co} , to which a heat flux for radiation is added in the manner described in section 3.6.

The assumptions made were: 1) a continuous film of vapour separates the liquid from the hot tube. 2) The film is very thin compared with the diameter of the tube. 3) Heat travels through the vapour film by conduction and radiation only. 4) The vapour film is laminar and is controlled by buoyant forces and shear forces at the wall and interface. 5) The interface

is smooth except in the region of vapour removal. 6) The vapour removal region is small compared with the periphery, but there is no constraint on its removal. 7) Kinetic energy of the vapour film is negligible. 8) Vapour properties are evaluated at mean film temperature $\frac{1}{2} (T_w + T_s)$. 9) The latent heat of vaporization is the major item in the heat supplied to the vapour film. 10) The temperature of the wall is uniform. 11) The interface is at the liquid saturation temperature and so is the bulk of the liquid. 12) Pressure in the film is not affected by surface tension.

Errors introduced by these assumptions were assumed to be accounted for by the selection of the coefficient from experimental data.

The superheat term, $\frac{1}{2} + \frac{1}{Sp}$, arises from the way in which the enthalpy change from liquid to vapour is included in the dimensional equation. In this case the simple form of latent heat plus mean superheat is used,

$$h'_{fg} = h_{fg} + \frac{1}{2} (C \Delta T)_v. \quad (3)$$

Later Bromley (32) suggested that this enthalpy difference is better approximated by

$$h'_{fg} = h_{fg} (1 + 0.4Sp)^2, \quad (4)$$

and the heat transfer equation then becomes

$$Nu = 0.62 [Gr^* Pr]^{\frac{1}{4}} \left[\frac{1}{Sp} (1 + 0.4Sp)^2 \right]^{\frac{1}{4}}. \quad (5)$$

This equation correlated the experimental data better than equation 2, though the difference was slight. Because there are a number of expressions for the enthalpy difference, a separate section 3.5, has been included to compare them.

The equations derived by Bromley use the cylinder diameter D as the characteristic length predicting that the heat flux varies inversely as the fourth root of the diameter, $q \propto D^{-\frac{1}{4}}$. The equations therefore fail when the values of diameter are small and large because rates of heat transfer on small and large cylinders do not tend to infinity and zero respectively. (Under such conditions assumptions 2, 6, 12 and 4, 5 are contravened). Empirical modifications were suggested by Banchemo et al (33)

resulting in the following equation,

$$Nu = a \left(\frac{1}{D} + c \right) D^{\frac{1}{4}} [Gr^* Pr]^{\frac{1}{4}} f(Sp) \quad (6)$$

The superheat term was not specified. From this equation the heat flux is independent of diameter for large cylinders, and varies inversely with diameter on small sizes (i.e. the total heat transfer is independent of diameter). The values of a and c were obtained from experimental data. They differ for each liquid tested and are also dimensional.

The unsatisfactory state of affairs represented by the dimensional parameters a and c was eliminated by Breen and Westwater (34). They presented test data for horizontal cylinders of diameters from 0.00012 to 1.85 inches in a variety of liquids which were correlated over the whole range by:

$$Nu_{\lambda_c} = \left(0.59 + 0.069 \frac{\lambda_c}{D} \right) [Gr^*_{\lambda_c} Pr]^{\frac{1}{4}} \left[\frac{1}{Sp} (1 + 0.34Sp)^2 \right]^{\frac{1}{4}} \quad (7)$$

The diameter appears only in the coefficient and all terms are dimensionless. Again for large diameters the heat flux is independent of size and for small diameters heat flux varies inversely with size.

The characteristic length is the critical wavelength, λ_c , where

$$\lambda_c = 2\pi \sqrt{\frac{g_c \sigma}{g(\rho_L - \rho)}} \quad (8)$$

It is the smallest wavelength that can grow in amplitude and allow the release of vapour (section 3.8.1). This dimension had already been used in equations for film boiling above horizontal plates.

For more accurate predictions of heat transfer, Breen and Westwater recommended three equations, to be used according to the value of λ_c/D . For large cylinders, $\lambda_c/D < 0.8$

$$Nu_{\lambda_c} = 0.6 [Gr^*_{\lambda_c} Pr]^{\frac{1}{4}} \left[\frac{1}{Sp} (1 + 0.34Sp)^2 \right]^{\frac{1}{4}} \quad (9)$$

Medium cylinders, $0.8 < \lambda_c/D < 8$

$$Nu = 0.62 [Gr^* Pr]^{\frac{1}{4}} \left[\frac{1}{Sp} (1 + 0.34Sp)^2 \right]^{\frac{1}{4}} \quad (10)$$

Small cylinders, $8 < \lambda_c/D$

$$Nu_{\lambda_c} = 0.16 \left(\frac{\lambda_c}{D} \right)^{0.83} [Gr_{\lambda_c}^* Pr]^{\frac{1}{4}} \left[\frac{1}{Sp} (1 + 0.34Sp)^2 \right]^{\frac{1}{4}}. \quad (11)$$

The first and third of these are asymptotic values of the general solution with slightly modified coefficients to improve fit. The second is Bromley's equation. The first still shows heat flux to be independent of diameter, and the third shows the total heat transfer Q is weakly dependent on diameter ($Q \propto D^{0.17}$). They suggest that this nearindependence at very small diameters is because heat transfer is controlled mainly by the bubble release mechanism, which for small wires is controlled largely by surface tension.

Photographic studies showed that for $D < \lambda_c$ the wave pattern at the top of the tube was one-dimensional, and for $D = 1.7 \lambda_c$ the wave pattern was two-dimensional (section 3.8.1). This change corresponds to the change between the medium and large cylinder equations 10 and 9.

A semi-theoretical solution has been derived by Baumeister and Hamill (35) which correlates the experimental data of Breen and Westwater somewhat better than equation 7. The solution when simplified to apply to standard gravity is:

$$Nu_{\lambda_c} = 0.59 \left[1 + 0.585 \frac{\lambda_c}{D} + \frac{1}{228} \left(\frac{\lambda_c}{D} \right)^3 \right]^{\frac{1}{4}} \times [Gr_{\lambda_c}^* Pr]^{\frac{1}{4}} \left[\frac{1}{Sp} (1 + 0.34Sp)^2 \right]^{\frac{1}{4}}. \quad (12)$$

For small diameters $q \propto D^{-\frac{3}{4}}$ compared with $D^{-0.83}$ and D^{-1} from equations 11 and 7. The equation is really a modification of equation 7 because in the derivation it was assumed that equation 7 was correct for large diameters. This assumption is well supported by experimental data. The additional assumption, which has been made frequently by Baumeister et al, is that the bubble release pattern adjusts to maximise heat transfer.

Two correlations have been proposed which do not use the index of $\frac{1}{4}$. Sarma (36) by dimensional analysis of bubble release derived the equation:

$$Nu = N [Gr^* Pr (B + \frac{1}{Sp})]^{1/3} \quad (13)$$

where B and N are values to be determined experimentally. Science et al (93) have correlated experimental data at atmospheric and reduced pressure by

$$Nu_{\lambda_c} = 0.532 [Gr_{\lambda_c}^* Pr(\frac{1}{2} + \frac{1}{Sp})]^{0.267} \left[\left(\frac{T}{T_c} \right)^2 \right]^{0.267} \quad (14)$$

But as pointed out by Clark (37) the data would almost be as well correlated using the index $\frac{1}{4}$. The significance of the value of the index is discussed in section 3.8.

3.3.2 Vertical Surfaces. For laminar film boiling on vertical flat surfaces, Bromley (30) proposed an equation similar to that for the horizontal cylinder, using as characteristic length the height, L, of the surface.

$$Nu = N [Gr^* Pr]^{1/4} \left[\frac{1}{2} + \frac{1}{Sp} \right]^{1/4} \quad (15)$$

The value of the coefficient N was not given by Bromley, but evaluated by Hsu and Westwater (38) to be 0.667 if the liquid is stagnant, and 0.943 if the liquid moves freely with the vapour.

A solution of the conservation equations for saturated film boiling assuming the vapour flow to be laminar and the interface smooth has been presented graphically by Koh (39). At atmospheric pressure the results lie between those given by the two values of the coefficient and equation 15. Frederking (40) also carried out an analysis of the conservation equations and presented the simplified theoretical solution as

$$Nu = \frac{2}{3} [Gr^* Pr]^{1/4} \left[\frac{1}{Sp} \right]^{1/4} \quad (16)$$

In the light of experimental data (the source of which is not stated) modifications are recommended (41), and the equation then becomes

$$Nu = 0.8 [Gr^* Pr]^{1/4} \left[\frac{1}{2} + \frac{1}{Sp} \right]^{1/4} \quad (17)$$

This is of course the equation 15 with the average value of the two coefficients.

The above equations were compared by Hsu and Westwater (42) with experimental data for vertical tubes from 2.6 to 6.5 inch high. They found that the equations were reasonably accurate only for short tubes, and underpredicted the rates of heat transfer on the others. Because of this they concluded that the equations apply only when flow is laminar, (which is what they were derived for) and therefore derived the following composite equation to include both laminar and turbulent flows :

$$Nu = \frac{2h'_{fg} \mu_v Re^*}{3k_v \Delta T} + f(Tur) . \quad (18)$$

The first term on the right hand side is a modification of equation 15 with the coefficient of $\frac{2}{3}$, and applies to the lower regions where the vapour flow is still laminar. The second term is too complex to reproduce here, but applies to the higher regions on the surface where the vapour flow is turbulent. The position of transition is automatically included in the equation, (see also section 3.8.1).

Much simpler empirical correlations for organic fluids on vertical tubes, including the data of Hsu and Westwater, have been proposed by Borishanskii and Fokin (43) :-

$$\text{For } 2.8 \times 10^4 < Gr_t^* < 1.4 \times 10^6, \quad Nu_t = 0.28 (Gr_t^*)^{\frac{1}{3}}, \quad (19)$$

$$1.4 \times 10^6 < Gr_t^* < 1.5 \times 10^7, \quad Nu_t = 0.0094 (Gr_t^*)^{0.57}. \quad (20)$$

The characteristic length is the thickness of the vapour film t_v . This means that the values of the Nusselt and modified Grashof numbers are much smaller than the corresponding values based on the diameter D . The Prandtl number has been excluded since the values for the vapours correlated differ only slightly.

3.3.3 Spheres Frederking et al (44,45) have carried out an analysis of the conservation equations for the sphere similar to that for the vertical plate and presented the solution in the following simplified form,

$$Nu = 0.586 [Gr^* Pr]^{\frac{1}{4}} \left[\frac{1}{Sp} \right]^{\frac{1}{4}} . \quad (21)$$

This, they contended, is only a guide and in the light of experimental

work recommend (45),

$$Nu = \frac{2}{3} [Gr^* Pr]^{\frac{1}{4}} \left[\frac{1}{2} + \frac{1}{Sp} \right]^{\frac{1}{4}} = \frac{2}{3} [Ra_1^*]^{\frac{1}{4}} \quad (22)$$

This equation correlated test data between values of Ra_1^* of 10^5 and 10^8 .

For values of Ra_1^* between 10^7 and 10^9 the following equation is recommended

$$Nu = 0.14 [Gr^* Pr]^{\frac{1}{3}} \left[\frac{1}{2} + \frac{1}{Sp} \right]^{\frac{1}{3}} \quad (23)$$

Equation 23 is said to be suitable for vertical surfaces and horizontal cylinders when sizes are large enough for the heat flux to be independent of geometry.

A rigorous analysis has been carried out by Hendricks and Baumeister (46) by dividing the film boiling into two parts, one for the heat transfer across the laminar vapour film on the lower regions of the sphere, and two, for heat transfer in the bubble release region. The two parts were added on an area weighted basis. Two solutions were presented, for small spheres on which there is one vapour dome, and for large spheres on which there are many. The two solutions were matched at $\lambda_c/D = 1.35$ to give a general solution which takes the form,

$$Nu = f(Ra_1^{*\frac{1}{4}}, Bo^{\frac{1}{4}}) \quad (24)$$

The full expression is too complex to present here partly because the dependence on Bond number is presented graphically. The experimental data of Frederking et al (45) are well correlated by the expression.

The small sphere solution for single domes is valid for $\lambda_c/D > 0.7$ which, although representing a diameter somewhat larger than the matching position, compares with the values of λ_c/D of 0.6 and 1 reported by Breen and Westwater (p 32), between which the change from a one- to a two-dimensional wavepattern occurred on the horizontal cylinder.

3.3.4 Horizontal Surfaces The first analysis for film boiling above a horizontal surface based on hydrodynamic considerations was by Chang (47) whose resulting equation for saturated film boiling can take the

non-dimensional form,

$$Nu = 0.294 [Gr^* Pr]^{\frac{1}{3}} \left[\frac{1}{Sp} \right]^{\frac{1}{3}} \quad (25)$$

The choice of characteristic length does not matter.

The analysis by Berenson (48) based on the Taylor-Helmholtz instability and model of the four models in section 3.8.1 resulted in the equation

$$Nu = 0.673 [Gr^* Pr]^{\frac{1}{4}} \left[\frac{1}{2} + \frac{1}{Sp} \right]^{\frac{1}{4}} \quad (26)$$

Both these equations were compared with experimental data by Hosler and Westwater for film boiling of water and Freon above an 8 x 8 inch horizontal plate (49). Equation 26 was found to be satisfactory, generally predicting rates of heat transfer a little less than the experimental data, but equation 25 was found to predict rates of heat transfer of about twice the experimental values. Equation 25 does however satisfactorily predict rates of heat transfer for film boiling in cryogenic liquids (37 p.437).

A further analysis, based on instability and including the assumption that the configuration of the vapour domes adjusted to maximise entropy production, was carried out by Hamill and Baumeister (50). The resulting equation is

$$Nu = 0.65 [Gr^* Pr]^{\frac{1}{4}} \left[\frac{19}{20} + \frac{1}{Sp} \right]^{\frac{1}{4}} \quad (27)$$

which is similar to that of Berenson (equation 26).

3.4 Modification of Coefficients of Formulae

The formulae for any of the three geometries, horizontal cylinder, sphere and vertical surface, may be applied to the other two by modifying the coefficient. Eckert (51) states that if the height of a vertical plate is 2.5 times the diameter of a horizontal cylinder then the values of heat flux are the same. Frederking (40) (after Nusselt) quotes the ratio of height to diameter as 2.85.

Substitution of these ratios in equations of the form

$$Nu \propto [Gr^*]^{\frac{1}{4}}, \quad (28)$$

in which the diameter D , or height L , has been used as the characteristic

dimension, results in the following ratios of coefficients :

Vertical Surface	Horizontal Cylinder
1	0.796 (Eckert)
1	0.77 (Frederking)

The value of 0.77 was also obtained from data presented by Nishikawa and Ito (53) for the subcooled film boiling of water. For the sphere, Frederking et al (45) state that the corresponding ratio is 0.88.

3.5 The Superheat Term $f(Sp)$

A number of different forms of the superheat term have been encountered (see figure 3). They arise from the different expressions for the enthalpy difference ($h_v - h_L$) between the saturated liquid and the vapour.

In his original work Bromley (30) suggested that the enthalpy difference, often called the modified latent heat h'_{fg} , may be calculated from

$$h_v - h_L = h'_{fg} = h_{fg} + \int_{T_s}^{\frac{1}{2}(T_w + T_s)} (C \Delta T)_v , \quad (29)$$

which for constant specific heat becomes

$$h'_{fg} = h_{fg} + \frac{1}{2} (C \Delta T)_v . \quad (3)$$

Later (32) he stated that the following is a better approximation

$$h'_{fg} = h_{fg} \left(1 + 0.4 \frac{(C \Delta T)_v}{h_{fg}} \right)^2 , \quad (4)$$

which was further improved by Roshenow (31,54) to

$$h'_{fg} = h_{fg} \left(1 + 0.34 \frac{(C \Delta T)_v}{h_{fg}} \right)^2 . \quad (30)$$

Two other expressions for the enthalpy difference have been found, $h_{fg} + 0.4 (C \Delta T)_v$ and $h_{fg} + \frac{19}{20} (C \Delta T)_v$, and sometimes the unmodified latent heat h_{fg} is used. All these expressions, and the resulting superheat terms are given in figure 3.

The commonest of the superheat terms is the original, $\frac{1}{2} + \frac{1}{Sp}$, very likely because of its simplicity.

All the terms have been compared in figure 3 by calculating their values to the power of $\frac{1}{4}$. The values of superheat, Sp , at which the present tests were carried out are also marked on the graph. Differences are small especially at the lower superheats. Over the range from 0.3 to 1.0 the value of the term $\left[\frac{1}{2} + \frac{1}{Sp}\right]^{\frac{1}{4}}$ compared with the "correct" term of

$\left[\frac{1}{Sp} (1 + 0.34Sp)^2\right]^{\frac{1}{4}}$ varies from 2 to 5% lower. Thus the additional error introduced by using the term $\left[\frac{1}{2} + \frac{1}{Sp}\right]^{\frac{1}{4}}$ is only 1 to 2% provided that the coefficient of the equation is suitably altered.

3.6 Effects of Radiation

The equations for film boiling usually give a value for convective heat transfer q_{co} only, to which a value for heat transfer by radiation must be added. The simple original analysis by Bromley (30) has been shown to be accurate and to apply to other geometries.

The simple addition of the radiative and convective heat fluxes is not valid because they are not mutually exclusive. Accepting Bromley's assumption that heat transfer through the vapour film is by conduction and radiation only, then additional radiation causes additional evaporation thus thickening the vapour film and reducing conduction. By the order of magnitude argument Bromley derived the equation

$$q_s = q_{co} \left(\frac{q_{co}}{\epsilon_w q_r} \right)^{\frac{1}{3}} \epsilon_w q_r. \quad (31)$$

For $(\epsilon_w q_r / q_{co}) < 10$ this equation is approximated to an error of less than 0.3% by

$$\begin{aligned} q_s &= q_{co} + \epsilon_w q_r \left[\frac{3}{4} + \frac{1}{4} \frac{\epsilon_w q_r}{q_{co}} \left(2.62 + \frac{\epsilon_w q_r}{q_{co}} \right)^{-1} \right] \\ &= q_{co} + \epsilon_w B q_r. \end{aligned} \quad (32)$$

The value of B can be obtained from figure 4. The term q_r is the black body radiation between two parallel plates,

$$q_r = \sigma_r (T_w^4 - T_s^4). \quad (33)$$

Equation 32 implies that the vapour is transparent and that the absorptivity of the liquid-vapour interface is unity, both of which have been shown to be valid (55). Furthermore the results of the rigorous analysis in this reference, which included radiative effects in the solution of the boundary layer equations, agree with the simple analysis of Bromley to within a few per cent.

The analysis of Lubin (56) for a vertical surface also resulted in the equation 31, thus substantiating the derivation by Bromley and extending his results to apply to the vertical surface. In the case of film boiling above a horizontal surface (57 and section 3.7.1), B is assigned a value of 0.88 in the simplified version of a theoretical solution.

3.7 Subcooled film boiling

3.7.1 Theoretical Solutions. Among the early theoretical solutions for subcooled film boiling was that by Chang (47) who extended his solution for saturated film boiling which had been based on the instability of the interface. The solution takes the form:

$$Nu = N [Gr^* Pr^*]^n \quad (34)$$

where for horizontal surfaces $N = 0.234$ and $n = \frac{1}{3}$

and for vertical surfaces $N = 0.72$ and $n = \frac{1}{4}$.

The Nusselt number is based on the thermal conductivity of the vapour and the superheat ΔT_v . The effects of subcooling are included in the modified Prandtl number Pr^* which is calculated from an equivalent thermal diffusivity α^* . Chang presented α^* graphically for water for ΔT_v from 600 to 1600°F and at subcoolings of 5, 10, 50 and 100 deg.F. It can also be evaluated from a complex implicit equation.

A number of solutions were discovered which apply to laminar film boiling on a vertical isothermal surface. Sparrow and Cess (58) were the first to publish a solution obtained by considering the problem as one of two-phase natural convection. The six conservation equations (three for each phase) were first transformed in the manner carried out by Polhausen (59), and then solved numerically for the following boundary conditions:

at the surface	$u = 0$	No-slip
	$v = 0$	Non-porous
	$T = T_w$	temperature continuity, isothermal surface
in the bulk liquid	$u_L = 0$	stationary liquid
	$T = T_L$	
at the liquid-vapour interface	$u_i = 0$	stationary interface vertically
	$m_L = m = m_v$	mass continuity
	$T_v = T_L = T_s$	temperature continuity
	$\left[k \frac{\partial T}{\partial y} \right] dx = m_i h_{fg} - \left[k \frac{\partial T}{\partial y} \right]_L dx$	energy continuity
	$\tau_i = 0$	zero interfacial shear

It was assumed that the vapour formed a continuous film over the surface, and that the interface was smooth.

The assumption of a stationary interface was made because, they state, an earlier analysis showed that for the saturated film boiling of water, the velocity of the interface was unimportant. The assumption made the solution of the equations easier. Setting the interfacial shear at zero was based on the assumption that buoyancy would dominate motion, and mean that movement in each phase would depend on its own buoyancy only. Slip would therefore occur at the interface.

The results were presented graphically in terms of a computational parameter P , and five fluid parameters. The range of fluid parameters were selected with water in mind and are :

$$Pr = 1$$

$$Pr_L = 1, 2.$$

$$Sp = 0 \text{ to } 2$$

$$Sc = 0.05, 0.15, 0.3, 0.5 .$$

$$R = \left[\frac{\rho \mu}{(\rho \mu)_L} \right]^{\frac{1}{4}} \left[\frac{\rho_L - \rho}{\rho} \right]^{\frac{1}{4}} \left[\frac{C_L}{\beta_L h_{fg}} \right]^{\frac{1}{4}}$$

$$= 0.05, 0.1, 0.15, 0.25 .$$

Under normal ambient conditions $R \approx 0.05$; the higher values of R would apply at higher pressures. The value of $Pr = 1$ is a close approximation for water vapour.

Heat transfer results are obtained by substituting P in the equation,

$$Nu = \frac{2}{3} [Gr^*]^{\frac{1}{4}} \left[0.84 + \frac{1}{P} \right]^{\frac{1}{4}} . \quad (35)$$

For saturated film boiling $P = Sp$, and therefore,

$$Nu = \frac{2}{3} [Gr^*]^{\frac{1}{4}} \left[0.84 + \frac{1}{Sp} \right]^{\frac{1}{4}} . \quad (36)$$

At very high subcooling, when interfacial evaporation becomes zero, the solution became exactly that for single phase natural convection. This is a consequence of the assumption of a stationary interface.

The conservation equations have been solved by Nishikawa and Ito (53) without making the assumption of a stationary interface. Heat transfer results were presented graphically for the laminar film boiling of water at atmospheric pressure on vertical surfaces and horizontal cylinders, and the results are significantly different from the values obtained from the solution of Sparrow and Cess (see section 3.7.3 and figure 5). Their solution for the velocity profiles shows that the liquid reaches its maximum velocity at the interface.

Frederking and Hopenfield (41) have obtained theoretical solutions for film boiling on vertical isothermal surfaces using the integrated boundary layer equations. The assumption of a stationary interface was not made, but otherwise the boundary conditions were much the same as those set out by Sparrow and Cess. Two solutions were presented, one for small subcooling ($Sc < 1$) and the other for large subcooling ($Sc \gg 1$). The results were presented as general equations which include parameters that have to be obtained from graphs.

At small subcooling, the liquid buoyancy was assumed to be zero so that liquid motion was induced only by shear forces at the interface. At

atmospheric pressure the general solution can be reduced to,

$$Nu = \frac{2}{3} [Gr^* Pr (1 + A \cdot Sc)]^{\frac{1}{4}} \left[\frac{1}{Sc} \right]^{\frac{1}{4}} \quad (37)$$

where A has an approximate value of 700 for water and 420 for ethanol.

The recommendations for solutions by Frederking et al of increasing the coefficient and altering the superheat term were made and the equation then becomes :

$$Nu = 0.8 [Gr^* Pr (1 + A \cdot Sc)]^{\frac{1}{4}} \left[\frac{1}{2} + \frac{1}{Sc} \right]^{\frac{1}{4}} \quad (38)$$

At large subcooling, when $Sc \gg 1$, it was assumed that liquid buoyancy was large and that the maximum velocity in the liquid occurred at the interface. Vapour convection was zero. The general solution at atmospheric pressure can be reduced to :

$$Nu_L = 0.75 [Gr_L \cdot Pr_L^2]^{\frac{1}{4}} \quad (39)$$

which involves only liquid properties. The appearance of the square of the Prandtl number, which is characteristic of inviscid flow, in this case arises from the assumption of a freely moving interface. The application of equation 39 is restricted by the condition that $Sc \gg 1$. The maximum value for water at atmospheric pressure is about 0.185, and occurs when the bulk liquid is at the freezing point, so then equation 39 is inapplicable.

The interpolation for moderate subcooling between the solutions for small and large subcooling was given as :

$$q_{\text{moderate}} = \left[q_{\text{small}}^4 + q_{\text{large}}^4 \right]^{\frac{1}{4}} \quad (40)$$

The results of Frederking and Hopfield (41), and Sparrow and Cess (58) have been compared by Burmeister (61) with the results of his own work for water at atmospheric pressure and the surface temperature of 612°F. Burmeister obtained his solution for film boiling subjected to pressure fluctuations, but since below a certain rate of fluctuation heat transfer was independent of frequency the results can be adapted to constant pressure film boiling. He found that his own solution agreed closely with the sum of the effects of subcooling of the other two solutions. This he argues is reasonable since whereas Sparrow and Cess assumed zero

interfacial velocity but included liquid buoyancy, and Frederking and Hopenfield neglected liquid buoyancy but assumed a freely moving interface, he included both.

For film boiling on a horizontal flat surface, Hamill and Baumeister have extended their solution for saturated film boiling (section 3.3.4) to obtain a solution for subcooled film boiling (57). A regular pattern of vapour domes was assumed with the major portion of the heat transfer occurring across the thin portions of the vapour film. Radiation was included in the solution assuming a view factor of unity and no vapour absorption. Inertia terms were assumed to be negligible and convective effects in the vapour were taken to be zero. Thus the temperature gradient in the vapour was linear. The assumption of maximum entropy production was also applied.

The complete solution was presented in parametric form involving the three modes of heat transfer - film boiling, radiation and single phase convection. A simple equation was presented which is valid for many practical applications when $|q_T - q_{tcl}| < 2q_{co}$, namely,

$$q_{tot} = q_{co} + 0.88 \epsilon_w q_T + 0.12 q_{tcl} . \quad (41)$$

The effect of radiation is added in a similar way to that recommended by Bromley (3.6). The film boiling component, q_{co} , is obtained from the solution for saturated film boiling (equation 27). The heat flux due to subcooling is calculated from the single phase turbulent free convection equation for heat transfer on a horizontal surface namely,

$$Nu_L = 0.14 [Gr_L Pr_L]^{\frac{1}{3}} . \quad (42)$$

The effect of subcooling on heat transfer is quite small, (see figure 5), because of the small value of 0.12 in equation 41.

The solution also predicts that film boiling is not possible at very strong subcooling, when

$$q_T - q_{tcl} < - 1.27 q_{co} .$$

Heat transfer then occurs by turbulent single phase convection. Thus for example, in cold water at 75°F film boiling would not be possible on

a surface colder than about 1000°F .

3.7.2 Experimental Data. A limited amount of experimental data have been found for the cooling of spheres and cylinders, and for steady film boiling on wires of small diameter. Data for the latter cover only small degrees of subcooling. Most of the data are for water, some details for which are given in the next section. Data are also available for other liquids as listed below. The data obtained in the steady state seems to show better reproducibility than that obtained by the transient technique.

Liquid	Subcooling deg F	Geometry and Size	Authors
Methanol	0-27	Horizontal Wires 0.0315 in dia.	Tachibana & Fukui (62)
Carbon Tetrachloride	0-27	ditto	ditto
Oil	20-200	Cylinder 1 in. x 0.32 in. dia.	Stenzle & Schultze (15)
Oil	$T_L = 20, 60^{\circ}\text{F}$	0.8 in. dia. sphere	Loskiewicz & Gorczyca (63)
Oil	$T_L = 110^{\circ}\text{F}$	2 in. dia. sphere	Paschkis et al (10 - 14)
NaOH soln.	ditto	ditto	"

3.7.3 Comparison of earlier work. A comparison of the theoretical and experimental data for the subcooled film boiling of water has been made and is shown in figure 5. The fact that there are two phases and two temperature differences, ΔT_v and ΔT_L , means that it is not possible to compare the data in dimensionless terms. The comparison was made only for water because much of the data, even from the theoretical solutions, applies to water only. Wherever possible data have been taken for, or adjusted to apply to the $\frac{1}{4}$ inch diameter horizontal cylinder. The

equations for vertical surfaces were modified to apply to horizontal cylinders by changing the coefficient in the way recommended by Frederking et al (section 3.4). The data for the $\frac{1}{4}$ inch diameter horizontal cylinder therefore apply to vertical surfaces of height 0.685 inch, $(\frac{1}{4} \div (0.77)^4)$, and spheres of diameter 0.417 inch, $(\frac{1}{4} \div (0.88)^4)$. Sparrow and Cess did not present an equation for film boiling at very high subcooling, but stated that the solution was exactly as for single phase free convection. Therefore the following equation was used, taken from Jakob (60),

$$Nu_L = 0.55 [Gr_L Pr_L]^{\frac{1}{4}} \quad (43)$$

The experimental data for spheres and wires have not been adjusted because their sizes fall outside the range of application, given by Breen and Westwater (section 3.3.1), of equations for film boiling involving the fourth root of the Rayleigh number. Radiation has been included where necessary in the way described in section 3.6, taking $\epsilon_w = 0.9$. The value of $\epsilon_w = 0.9$ was used because this value was found to apply to the present results, section (8.3.1).

The comparison shows that, in general, agreement is relatively poor. The data which apply to horizontal cylinders were obtained from theoretical analyses. They show close agreement at the boiling point, but differ increasingly with subcooling. It was expected that the data of Nishikawa and Ito (53) would be greater than that of Sparrow and Cess (58) because of the assumption of a stationary interface by the latter. The steep increase in heat flux with small subcooling as predicted by the solution of Frederking and Hopenfield (41) is rather surprising because the solution neglected the buoyancy of the liquid. The very steep increase in heat flux predicted by Chang (47) is due to the strong dependence on subcooling of the value of the modified Prandtl number, Pr^* .

The heat transfer rates given by the equations for large subcooling are somewhat low. This is not surprising since they are not strictly applicable at the relatively small values of subcooling ($Sc < 0.185$) represented in the figure. The data of Sparrow and Cess are lower than that of Frederking and Hopenfield because the former assumed the interface to be stationary.

Rates of heat transfer are independent of superheat because only liquid properties appear in equations 39 and 43, and because the diameter of the cylinder was used as the characteristic dimension.

The theoretical solutions for the horizontal surfaces differ widely, one showing almost no change of heat flux with subcooling and the other showing a very large increase.

The experimental data for both wires and spheres do not show particularly close agreement, and do not substantiate any of the theoretical solutions.

3.8 Interfacial Dynamics and Vapour Flow

In film boiling the vapour flow may be laminar or turbulent, and the interface may be smooth, wavy, or involve bubble release. When the liquid is subcooled, the flow of the liquid may also be relevant. From the literature the situation for saturated film boiling can be adequately described. Very little has been published that describes the situation in subcooled film boiling.

3.8.1 Saturated film boiling. When saturated film boiling occurs no heat can be convected into the bulk liquid because all the liquid is at the boiling point. Heat transfer is effected by evaporation of the liquid, and the removal of the vapour thereby produced. The situation is unstable because a more dense liquid is being supported by a less dense vapour (the Taylor instability) and the interface becomes wavy. Vapour can be released only when the wavelength of the interfacial waves exceeds the critical value, λ_c , because only then can the waves grow in amplitude and ultimately form bubbles. The value of the critical wavelength on a horizontal surface is given by ;

$$\lambda_c = 2\pi \sqrt{\frac{g_c \sigma}{g(\rho_L - \rho)}} \quad (8)$$

The wavelength at which the amplitude grows the fastest is generally termed "the most dangerous, λ_{md} " where $\lambda_{md} = \sqrt{3} \lambda_c$.

The instability approach was first applied by Chang (47) and later by Berenson (48) for the saturated film boiling on the upper surface of a horizontal plate (section 3.3.4). Berenson postulated that the dominant

wavelength was the one which allowed the amplitude to grow the fastest, λ_{md} . The vapour generated flowed into a two-dimensional pattern of domes or cells formed by the waves above the surface and was subsequently released as bubbles (figure 6). The whole interface was chaotic, but the configuration could be time averaged to which the principles of conservation could be applied. A similar model was later used by Hamill and Baumeister (50, 57).

From the above model Frederking et al (67) proposed four thermo-hydrodynamic cases which resulted in four forms of the heat transfer equation.

$$\begin{array}{ll} 1. \text{ laminar vapour flow} & Nu = N_1 [Gr^* Pr]^{\frac{1}{4}} [f(Sp)]^{\frac{1}{4}} \\ \text{regular cell pattern} & \end{array} \quad (44)$$

$$\begin{array}{ll} 2. \text{ laminar vapour flow} & Nu = N_2 [Gr^* Pr]^{\frac{1}{3}} [f(Sp)]^{\frac{1}{3}} \\ \text{random cell pattern} & \end{array} \quad (45)$$

$$\begin{array}{ll} 3. \text{ turbulent vapour flow} & Nu = N_3 [Gr^* Pr^2]^{\frac{1}{4}} [f(Sp)]^{\frac{1}{4}} \\ \text{regular cell pattern} & \end{array} \quad (46)$$

$$\begin{array}{ll} 4. \text{ turbulent vapour flow} & Nu = N_4 [Gr^* Pr^2]^{\frac{1}{3}} [f(Sp)]^{\frac{1}{3}} \\ \text{random cell pattern} & \end{array} \quad (47)$$

The indices of $\frac{1}{4}$ and $\frac{1}{3}$, which occur in single phase convection for laminar and turbulent flows are now governed by cell pattern. When the index is $\frac{1}{3}$ the choice of characteristic length is immaterial. The assumption of turbulent vapour flow with inertia forces dominating viscous forces gives rise to the square of the Prandtl number which is characteristic of inviscid flow.

When film boiling occurs on the other three simple geometries - the horizontal cylinder, sphere and vertical surface - the interfacial dynamics are somewhat different (46) see figure 19. Consider firstly a high vertical surface. At and near the leading edge the interface is relatively smooth because the thin vapour film which exists there tends to damp out interfacial disturbances. The film is thin because the heat transfer rates are locally high. With increasing distance from the leading edge the vapour film increases in thickness, because the local heat transfer rates decrease, and small interfacial capillary waves appear which may have been generated at the lower stagnation points (68). However, if the wavelength is less than the critical value λ_c

the waves cannot grow in amplitude. These two regions have been termed the laminar and pseudo-laminar regions (46). With further increase in distance from the leading edge the capillary waves move further apart, because of the increasing velocity of the interface, and eventually the wavelength becomes λ_c . This marks the onset of transition at which the amplitude of the wave starts to grow. Eventually the amplitude will be such that bubbles of vapour will depart from the interface, which marks the onset of turbulence.

In the cases of horizontal cylinders and spheres the interfacial dynamics are greatly influenced by diameter, and in particular by the ratio λ_c/D (46). On small diameter cylinders ($D \ll \lambda_c$) a single line of vapour domes form above the wire and vapour flow is predominantly axial into the domes because the dome spacing is considerably greater than the diameter of the wire. Diameter has little effect on total heat transfer (p. 32). On intermediate diameters ($D \simeq \lambda_c$) vapour flow becomes increasingly circumferential but the one-dimensional wave pattern at the trailing edge is retained. This is the region of Bromley's model. In both the above cases the interface that is not in the bubble release region is relatively smooth resembling the laminar and pseudo-laminar regions on the vertical surface. On large diameter cylinders ($D > \lambda_c$) vapour flow remains circumferential but the wave pattern becomes two-dimensional thus permitting a multiple dome configuration similar to that above a horizontal surface. The change in wave pattern has been reported by Breen and Westwater (34) (p. 32) from photographic studies to occur between diameters of about λ_c and $\lambda_{md}, (\sqrt{3} \lambda_c)$. All the regions described for the vertical surface may exist on a large cylinder.

The behaviour on spheres is very similar to that on horizontal cylinders, the difference being that on spheres of small and intermediate diameters a single vapour dome occurs on the upper surface. The largest diameter for the existence of the single dome was obtained theoretically (46) as $D = 1.47 \lambda_c$.

The value of the critical wavelength λ_c has so far been calculated for a flat surface. On a horizontal cylinder the critical wavelength λ'_c decreases with decreasing diameter thus (69),

$$\lambda'_c = 2\pi \left[\frac{g(\ell L - \ell)}{g_c \sigma} + \frac{2}{D^2} \right]^{-\frac{1}{2}} \quad (48)$$

and $\lambda'_{md} = \sqrt{3} \lambda'_c$. The value of λ'_c becomes significantly less than the value of λ_c for ratios of $\lambda_c/D > 3$. The dominant wavelength of the comb on the trailing edge on a horizontal cylinder has been observed to be slightly greater than the most dangerous wavelength λ'_{md} (69,64), being about $2 \lambda'_c$ (69). (This compares with the postulation by Berenson above that λ'_{md} is the dominant wavelength in film boiling above a horizontal plate.) Therefore the spacing between the positions of bubble release diminishes with the diameter of the cylinder.

The transition from laminar to turbulent film boiling on vertical surfaces has been based on the transition of the vapour flow from laminar to turbulent as well as on the dynamics of the interface as discussed above. The analysis by Hsu and Westwater (42) was based on the vapour film thickness increasing with distance from zero at the leading edge to a critical value according to the one-fourth-root power relationship. At the critical value transition in the vapour began and their sketch indicates that the interface starts to become wavy. The critical distance from the leading edge can be calculated from the following expression :

$$(Gr^*_{Lc})^{\frac{1}{3}} = \left(\frac{Re^{*4}}{4} \right)^{\frac{1}{3}} \left(\frac{1}{2} + \frac{1}{Sp} \right) Pr. \quad (49)$$

Values calculated from this expression for water are shown in figure 7. The critical Reynolds number Re^* is based on the critical film thickness and was given the value of 100.

A simpler approach by Burmeister (61) was to apply the single phase natural convection criterion that transition occurs between Grashof-Prandtl product ($Gr^* Pr$) of 10^9 and 10^{10} . Another simple approach suggested by Frederking et al (44,45) was that when heat transfer data can be correlated without reference to geometry the flow could be assumed turbulent. From their results transition begins and ends at values of $Gr^* Pr \left(\frac{1}{2} + \frac{1}{Sp} \right)$ of about 3×10^7 and 2×10^8 respectively. Critical heights calculated from these criteria are also shown in figure 7.

There is evidence to support the trend predicted by Hsu and Westwater that the critical height increases as the surface temperature decreases. Firstly it has been observed that the interface is smoother at the lower surface temperatures. Secondly, from conduction and radiation considerations of heat transfer through the vapour film, the film is thinner at the lower surface temperatures. The increasing critical height predicted by the other two criteria is due to the decreasing value of Gr^* as the surface temperature increases. The effects of the vapour film thickness are not included in either of them.

The theoretical values of critical height by Hsu and Westwater, and Burmeister have not been supported by experimental work. The criterion of Frederking et al was deduced from experimental data, and the values of critical height correspond roughly to the value of the diameter of horizontal cylinders at which the change from dependence to independence on diameter occurs, equations 10 and 11.

It has been suggested (46) that on the horizontal cylinder and sphere transition would occur at the position where the distance on the circumference from the leading edge equals the critical height for the vertical surface as given by Hsu and Westwater. Alternatively for the horizontal cylinder, Burmeister suggested using the single phase criterion of $GrPr = 4 \times 10^8$ given by Hermann (70).

3.8.2 Subcooled film boiling. It has been reported that bubble release from wires (64) and spheres (13) diminish^{es} with increasing subcooling, and that the interface becomes increasingly smooth (68).

3.8.3 Further considerations on interfacial dynamics and the breakdown of film boiling. In film condensation it is common to increase heat transfer rates, calculated by assuming a smooth interface, to account for the effects of waviness (71). One might say that this is done in film boiling too because the theoretical equations, at least for saturated film boiling have been modified according to experimental data. An analysis has been carried out by O'Brien (73) who compared heat transfer rates through a wavy layer and a slab containing the same volume of material. The results can be stated simply to be the influence of geometry on conduction. Increases in the rates of heat transfer occur because the surface area is increased whilst thickness

is reduced. Applying this to film boiling then the greatest effect should occur when the interface is most wavy.

The existence of waves in the liquid-vapour interface means that some parts of it are closer to the hot surface than others, and receive excess heat by conduction. The excess heat causes local excess evaporation which locally pushes the interface away (15). Thus film boiling is stable.

It is generally assumed that in stable film boiling no liquid-solid contact occurs. Bradfield (74), however, has shown experimentally that liquid-solid contact does occur, increasingly so, as the superheat decreases towards the Leidenfrost point. Film boiling continues, however, because immediately on contact, the liquid is rapidly vaporized and thrown back.

Bearing this in mind, the onset of transition boiling, in which liquid-solid contact is generally accepted, does not involve a sudden change of process, and the so-called film breakdown at the Leidenfrost temperature does not occur. The Leidenfrost temperature can be defined as the temperature at which the minimum heat flux occurs in a continuously changing process from no liquid-solid contact through a little, to liquid-solid contact occurring over a considerable proportion of the surface. The sudden changes attributed to take place at the Leidenfrost temperature have probably arisen because most experiments have been carried out with the heat flux as the independent parameter. As soon as the temperature is reached where the slope of the boiling curve is negative (figure 1) the extra heat demanded by the boiling process is obtained by cooling the test piece, and generally the rate of cooling is very rapid.

A tentative explanation as to why the Leidenfrost temperature for water is considerably higher than other liquids has been put forward by Stenzel and Schultze (15). Liquid water has high values of surface tension, latent heat of vaporization and thermal conductivity. On contact with the solid the water tends to spread rapidly. A large quantity of heat is required to cause evaporation and if the liquid is subcooled then even more heat is required to supply that which is conducted into the liquid. Consequently a large temperature difference is required to supply enough heat so that sufficient evaporation occurs to maintain film boiling.

3.9 Conclusions

In general saturated film boiling is well covered both by theoretical and experimental work. Many of the equations for predicting heat transfer take the form,

$$Nu = N [Gr^* Pr]^n [f(Sp)]^n \quad (50)$$

where $n = \frac{1}{4}$ or $\frac{1}{3}$. On small bodies vapour flow is laminar. On larger bodies vapour flow can be turbulent. Dependence of heat transfer on size has been eliminated from the above equation by using either $n = \frac{1}{3}$ or the critical wavelength, λ_c , as the characteristic dimension.

The values of the coefficient N may be modified so that equations for the horizontal cylinder, or vertical surface, or sphere, can apply to the other two geometries. In fact, equations for all four simple geometries vary little in both form and coefficient. For example if $n = \frac{1}{4}$ and the characteristic length is λ_c , then N has the values of 0.6, 0.8, 0.67, 0.67 for horizontal cylinders, vertical surfaces, spheres, and horizontal surfaces.

Stability of the vapour and interface have been well discussed. There are two possible transitions; one, the vapour flow can become turbulent and two, the interface can become wavy. It is not essential for the vapour to be in turbulent flow when the interface is wavy and bubbles are released.

Subcooled film boiling is relatively poorly covered compared with saturated film boiling. The theoretical solutions show wide disagreements, and there are insufficient experimental data to support any of them. The photographic studies are so few that an adequate visual picture of subcooled film boiling cannot be described.

Chapter 4

THE TEST CONDITIONS

4.1 Following the review it was decided that the main objectives of this work would be firstly to obtain experimental data over a wide range of subcooling, and secondly to derive a simple correlation for subcooled film boiling. The additional objective of a photographic study was included after early tests showed that the visual picture varied considerably with test conditions. The range of test conditions is summarised in table 1.

4.2 The choice of liquids was made bearing in mind that the heat transfer correlation would require the knowledge of both liquid and vapour properties, and that the vapour must be able to withstand without decomposing the relatively high surface temperatures necessary for film boiling to take place. These requirements limited the choice considerably. Water, based on these requirements, is an obvious choice. In addition it is used in quenching, is cheap, easily available, non-toxic and non-flammable. Ethanol was chosen as the second liquid because its liquid and vapour properties are known, under normal ambient conditions its boiling point is well above normal ambient temperature, and it is available in pure form. Although flammable, it burns quietly, and is easily extinguished by a blanket of carbon dioxide gas. Solutions of detergent in water were tested as a third liquid. Detergent had been added to water in initial tests to try to reduce the random breakdown of the vapour film. Heat transfer tests were carried out when it was found that two stable values of heat flux could exist during film boiling at moderate and high values of subcooling.

4.3 The ranges of temperatures over which the tests were to be carried out were decided firstly for water. Since the main concern of the work was to obtain data for subcooled film boiling, the tests were to cover as far as possible the full range of subcooling from boiling point to freezing point. Three surface temperatures were selected, 1612°F , 1312°F , and

1012°F which in the quenching of steel correspond approximately to the temperatures of respectively, immersion, transformation begins, and the nose of the transformation curve (figure 2). The detergent solutions were tested over the same ranges. Ethanol was tested over the same ranges of dimensionless subcooling and superheat, and also at the surface temperature of 1012°F so that a comparison of the rates of heat transfer could be made for the film boiling of water and ethanol on surfaces at the same temperature.

4.4 The selection of the size and geometry of the test piece, whether a steady state or transient technique should be used, and the method of heating are largely interrelated. If it is accepted that correlations for horizontal cylinders, vertical surfaces and spheres can be modified to apply to any of these geometries in the way given in section 3.4, and that on larger geometries rates of heat transfer are independent of geometry (p 35, 49), then the choice of geometry can be made mainly for reasons of convenience.

No reliable evidence was discovered showing that rates of heat transfer obtained from steady state tests were any different from those obtained from transient tests. Chromium plated spheres (65,66) and silver spheres (10 - 14) have been used to obtain experimental data for the transient film boiling of water at high subcooling, but reproducibility was not good (14). Cylinders of up to about 1½ inch diameter, heated both electrically and by condensing vapours, have been used to obtain data for steady saturated film boiling. In subcooled liquids data have been discovered for steady film boiling only on electrically heated wires of diameters up to about 0.04 inch (62,64).

The high values of heat flux and surface temperatures required for the film boiling of water eliminate all methods of heating for steady film boiling except heat pipes and direct electrical heating. Of these two electrical heating is the simpler. For cylinders of sizes larger than wires it was thought preferable to use a tube to keep the current as small as possible. Even so a tube of one inch diameter and 0.02 inch wall thickness would require about 1000 ampere to generate a heat flux of

10^5 Btu/hft^2 . If a metal strip is used instead of a tube, it can be easily rolled to thinner than 0.02 inch and require less than the 1000 ampere, but the problem of locating the thermocouple arises (it can go inside a tube).

The problem of the power requirement is also relevant. The one inch diameter tube already mentioned would require, at the heat flux of 10^5 B/hft^2 , about 8 kW per foot length continuously. In contrast, a transient test piece of the same size could be heated slowly in a furnace of much lower rating.

4.5 It was therefore decided to try to develop an electrically heated tube on which the subcooled film boiling of water in the steady state could take place. It was thought that any test section developed to withstand the high surface temperatures and generate the high values of heat flux necessary for film boiling in water would be satisfactory for the other liquids. Initially sizes were restricted to $1/8$ and $1/4$ inch diameter horizontal tubes. Chromium plated copper spheres of larger diameters were considered for obtaining experimental data for larger sizes, and also if the steady state test cylinders of $1/8$ and $1/4$ inch diameter could not be developed to obtain experimental data for high subcooling in water. In fact the steady state tests were extended to include tubes of $1/2$ inch diameter, and the spheres were excluded from the heat transfer tests. The range of conditions covered by the heat transfer tests are summarised in table 1a.

The photographic study was carried out over the same range of conditions as the heat transfer tests. In addition, some larger geometries shown in figure 9 were included. The conditions of the photographic study are summarised in tables 1b and 1c.

Chapter 5

APPARATUS AND PROCEDURE

5.1 The development of a satisfactory design of test-piece on which the heat transfer data were obtained is described first. The additional test-pieces used to obtain the photographic results and the rest of the apparatus are described briefly. The normal experimental procedure is next described and finally some experimental difficulties are discussed.

5.2 Development of the test-piece .

A test-piece was developed on which the steady film boiling of water could take place over the range of test conditions given in the preceding chapter. As was expected, the design required no modification for the film boiling of the other two liquids, namely detergent solution and ethanol.

Initially a test-piece comprising a straight length of stainless steel tubing about 0.1 inch diameter and six inches long was used. It was electrically heated, and supported and held horizontally by two current terminals. A quartz-fibre insulated chromel-alumel thermocouple placed inside the tube was used to measure the surface temperature. Film boiling was established by first heating the test piece in air to above the Leidenfrost temperature, and then immersing it in the water and at the same time increasing the heating rate.

With such a test-piece results could be taken only at the intermediate surface temperature of 1312°F and at bulk water temperatures greater than about 200°F . At the surface temperature of 1612°F the stainless steel corroded and scaled badly and the thermocouple burnt out. At the surface temperature of 1012°F and bulk liquid temperatures less than about 200°F , local excess cooling of the tube occurred at the terminals resulting in local nucleate boiling which would spread and displace film boiling from the whole tube.

To prevent the spread of nucleate boiling, two ceramic collars were attached around the tube near each terminal as recommended by

Nishikawa (64). Film boiling was then possible between the collars at the surface temperature of 1312°F in water down to a bulk temperature of about 170°F . The addition of a small quantity of detergent (0.025%) teepol) allowed film boiling to persist down to bulk temperatures of about 150°F .

A satisfactory design of test-piece (figure 8) was developed from this preliminary work by making three major changes :

1. The tube was bent into a wide U-shape so that the terminals and a short length of hot tube were held out of water during testing. This prevented the occurrence of local nucleate boiling at the terminals.
2. The test-pieces were made from tubing of nickel-chromium alloy, Nimonic 75, which has good corrosion resistance properties under the conditions of testing. The alloy C262 by Fine Tubes Limited was also used.
3. MMC thermocouples were used which were capable of operating at temperatures of up to 2200°F . The metal cover of the thermocouples were insulated from the test piece by a silica-fibre sheath (trade name Refrasil).

To make the experimental data applicable to horizontal cylinders, the sensing junctions of the thermocouples were positioned approximately in the middle of the horizontal section. End effects were eliminated by making the length of the horizontal section of the $\frac{1}{8}$ and $\frac{1}{4}$ inch diameter test-pieces greater than 15 diameters. The length of the horizontal section in the $\frac{1}{2}$ inch diameter test piece had to be limited to 10 diameters because of power supply limitations (section 5.5), but this was considered sufficient.

The sensing junctions of the thermocouples were located approximately on the axis of the tube in the $\frac{1}{4}$ and $\frac{1}{2}$ inch diameter tubes using ceramic and asbestos bushes. Allowing them to be free to move resulted in poor reproducibility of the value for the surface temperature (appendix A). The thermocouples and insulating sheath were put into position before bending the tube. The radius of the bends were made relatively large, at least $1\frac{1}{2}$ inch, otherwise there was a tendency for the film to breakdown at the

bends.

The test-pieces were held in position by clamping each end into a closely fitting groove in the end of each current terminal. The terminals were made from copper and brass, and were nickel plated to prevent corrosion. The voltage tappings were welded to each tube after it had been clamped in place, in such a way that during testing the tappings were above the surface of the liquid.

All the test-pieces were made from four sizes of tubing :- $1/8$ inch diameter of 0.01 inch wall thickness; $1/4$ inch diameter of 0.012 and 0.02 inch wall thicknesses; and $1/2$ inch diameter of 0.02 inch wall thickness.

5.3 Test-pieces for the photographic study

Photographs were taken of steady film boiling on the $1/8$, $1/4$ and $1/2$ inch diameter test-pieces which have been described in the preceding section, and also of film boiling on 8 inch high vertical cylinders, a 2 inch high vertical surface, a 4 inch diameter sphere, and a 2×9 inch horizontal surface. These additional test pieces are sketched in figure 9.

The 8 inch high vertical cylinders were made from tubing of $1/4$ inch diameter, of the same type used to make the other test-pieces of this diameter. Electrical heating was used and photos were taken of steady film boiling. The thermocouple was positioned approximately three inches from the top of the cylinder.

Photos were taken of transient film boiling on the other test-pieces. They were made from copper and were chromium plated to prevent corrosion. All were heated by gas flame. The thermocouples were positioned as shown, in closely fitting holes. The sphere was hollow, having been made in halves which were screwed together.

5.4 Apparatus

The immersion apparatus comprised a gantry and a moveable cross-member to which the current terminals were fixed and which could be raised and lowered by a hand lever to effect immersion.

Glass and metal tanks were used to hold the liquids. Initially glass tanks of about two and six gallons capacity were used so that the film

boiling could be seen, and were used again later when photographs were taken. Metal tanks of larger capacity (10 and 18 gallons) were used when rates of heat dissipation were high, so that the change of the bulk temperature of the liquid during a single test was insignificant. A portable immersion heater-stirrer was used to heat the liquids in the glass tanks with the aid of the test-piece itself. The metal tanks had fixed immersion heaters. Covers for the tanks were used when the liquids were hot to reduce heat loss by evaporation.

The ethanol was tested in the 10 gallon metal tank except when taking photographs. To prevent the ignition of the ethanol by the hot test-piece, the tank was partially filled with ethanol to about three inches from the top and gaseous carbon dioxide fed into this space at a rate of between about three and six litres per minute. A carbon dioxide fire extinguisher was kept handy to put the flame out on the few occasions when ignition did occur.

The heating circuit comprised a fixed transformer driven by a variable transformer which enabled the power generated to be varied between zero and maximum. The fixed transformer was rated at 16V, 250A continuous output, 240V input. Much higher currents could be taken for short periods, for example 500A for 10 minutes. In cases when the small step change of the variable transformer was too large for accurate measurements of power dissipation to be made, a rheostat was included in the primary circuit.

The heating rate was measured between the voltageappings using a current transformer and wattmeter. The temperature of the bulk liquid as well as the surface temperatures was measured using MIMC thermocouples and a digital voltmeter. The sensing junction of the thermocouple measuring the bulk temperature was positioned at about the same level as the horizontal section of the test-piece, and about $\frac{1}{2}$ inch from it. Details of the calibration of the thermocouples are given in section 6.2.

The photographs were taken of film boiling in the glass tanks. Some were taken as silhouette pictures against a background of diffuse lighting, and the others under direct lighting. Generally a high shutter speed

($\frac{1}{125}$ s) was used in order to stop the movement of the bubbles and the

interface.

5.5 Normal Procedure .

The liquid was heated or allowed to cool to the bulk temperature required, and then stirred thoroughly. Ice was added to water and detergent solution to speed up cooling. The test-piece was heated in air to approximately the surface temperature required for the test. The test-piece was then immersed and at the same time the heating rate was increased. Short lengths of the hot tube were left above the liquid surface, and the power input adjusted precisely to give the required surface temperature. Readings for the surface and bulk liquid temperatures, and for heat dissipation were taken.

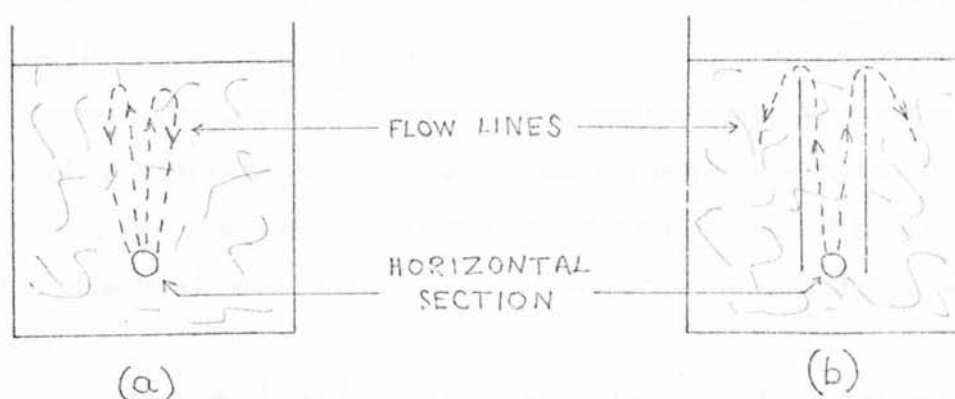
When the temperature of the bulk liquid was within about 20 deg F of the boiling point it was possible to take readings for all three surface temperatures from one immersion. At other bulk temperatures it was usual to take, from each immersion, one set of readings for only one surface temperature because temperature stratification occurred in the liquid. Normally a set of readings could be taken within one minute of immersion.

5.6 Experimental difficulties.

The simple open tank apparatus enabled results for film boiling to be taken to within only one or two °F of the boiling points of the liquids. High heat losses prevented the temperature of the liquid being maintained at the boiling point. Special efforts were made to enable results to be taken at the boiling point for the $\frac{1}{4}$ inch diameter test-piece in water. These involved using two tanks, the one in which the film boiling took place was immersed in water in the second which was kept boiling and stirred. The tanks were covered to reduce evaporation.

Temperature stratification of the liquid occurred during testing when the subcooling was greater than about 20 deg F. This happened because there was little evaporation to reduce the temperature of the liquid at the surface, and because there were few bubbles to cause mixing. Therefore to avoid uncertainty in the value of the readings for the bulk temperature, only one set of readings for one surface temperature were taken from

each immersion. The reading for the bulk temperature was taken just before immersion, and if there was any change from this value when the surface temperatures were taken then the whole set was discarded. The problem was particularly acute when the liquids were cold because the circulation of the liquids would "short-circuit" in a matter of seconds as shown in sketch (a). To prevent this, two vertical plates were positioned parallel to the tube and



about 6 - 12 diameters apart (sketch (b)). The plates extended along the whole length of the test piece, to about $\frac{1}{2}$ inch below it, and to within $\frac{1}{4}$ inch of the surface. Even so, to get a reliable set of readings for cold liquid it was essential that on immersion the surface temperature was within 10 deg F of the required value, and that the rate of power generation was set to the correct value immediately. To do this, a few preliminary runs had to be made.

The remainder of the experimental difficulties arose because the heat flux was the independent parameter rather than the surface temperature.

The method used to establish film boiling was not satisfactory at high subcooling in water ($T_L < 100^\circ\text{F}$). It was necessary to balance rather precisely the rate of immersion of the test-piece against the simultaneous increase in the heating rate, and not allow the temperature of the surface either to fall below the Leidenfrost temperature or exceed its melting point. The balancing of the rates of immersion and increase in heating rate was less critical for the test-pieces made from the thicker walled tubing, probably because of the higher thermal capacity of the test-pieces.

On occasions, film boiling would be replaced locally by nucleate boiling which would then spread over the whole test-piece. The position of the breakdown of the film occurred almost anywhere on the test-pieces. The causes were not established, but it did seem beneficial to clean the tube periodically with very mild abrasive, and to make the radius of the bends greater than about $1\frac{1}{2}$ inches. The speed at which the nucleate boiling spread was found to increase as the temperatures of the surface and the bulk liquid were reduced. The chance of the breakdown occurring also increased. The resulting thermal shock could cause considerable distortion especially in cold water. The tube could become oval, and the straight horizontal and vertical sections become bent so badly that the test-piece eventually had to be discarded. The test-pieces made from the thicker walled tubing were better able to withstand the shock than those made from the thinner walled tubing.

In the case of the $\frac{1}{2}$ inch diameter test-piece, it was not possible to take readings for $T_w = 1012^\circ\text{F}$ in water below about 150°F because breakdown of the film occurred on the vertical sections. These sections were found to be considerably colder than the horizontal section.

Chapter 6

ACCURACIES AND ERRORS

6.1 In this section factors affecting the accuracies of the results are discussed, and estimates of the errors in the heat transfer results are made. The accuracies of the temperatures and heat fluxes are influenced by errors in instrumentation, the system, measurements and calculations. The accuracies of the correlations depend on the accuracies of the fluid properties as well.

In the photographic study, less attention was paid to obtaining accurate values of both bulk liquid and surface temperatures. Errors are therefore about twice those of the heat transfer results.

The errors have been combined, where appropriate, according to the square-square root method given in B.S.1042 (75).

6.2 Temperature

The bulk liquid temperatures were measured using a MIMC thermocouple, ice point reference and digital voltmeter. This circuit was calibrated over the temperature range from 60 to 220°F to an accuracy of $\pm \frac{1}{2}$ deg F. This was the maximum accuracy of the digital voltmeter. A check calibration carried out about halfway through the test programme revealed no change from the original one. The error in the bulk liquid temperature was estimated to be ± 1 deg F, which includes uncertainties arising from the fact that liquid temperature was not uniform throughout the test tank.

The surface temperatures were subject to errors in the thermocouple circuit, and to the temperature differences between the sensing junctions on the axis of the tube and the outer surface of the tube.

The thermocouple circuits comprised MIMC thermocouples, ice reference points and digital voltmeter (DVM). The errors in the readings had to be estimated from the manufacturers data because the maximum temperature of the calibration bath was about 500°F. However, the thermocouples were checked at this temperature and rejected if the reading was outside the limit given by the thermocouple manufacturer.

The accuracies stated by the manufacturers of the equipment are :-

Thermocouples: below 750°F	$\pm 5.4 \text{ deg F } (\pm 3\text{K})$
above 750°F	$\pm 0.75\%$
DVM: range up to 23 mV (about 1030°F)	$\pm 10 \mu\text{V } (\pm \frac{1}{2} \text{ deg F})$
range up to 100 mV	$\pm 100 \mu\text{V } (\pm 4 \text{ deg F})$

The discrimination of the DVM was also $\pm 10 \mu\text{V}$ on the 23 mV range and $\pm 100 \mu\text{V}$ on the 100 mV range.

Usually during steady film boiling the reading of the DVM remained constant. Under difficult conditions, however, reading errors of $\pm 100 \mu\text{V}$ ($\pm 4 \text{ deg F}$) in water, and $\pm 30 \mu\text{V}$ ($\pm 1\frac{1}{2} \text{ deg F}$) in ethanol were accepted.

From the above data, the accuracies of the readings of the thermocouples used to measure surface temperatures were estimated to be :

ethanol	$\pm 7 \text{ deg F}$
water and detergent solution	$(T_w = 1012^\circ\text{F}) \pm 10 \text{ deg F}$ $(1312^\circ\text{F}) \pm 12 \text{ deg F}$ $(1612^\circ\text{F}) \pm 14 \text{ deg F}$

These values represent random errors for ΔT_v of approximately $\pm 1.7\%$ in ethanol and $\pm 1.1\%$ in water.

The position of the sensing junctions on the axis of the tube meant that average temperatures of the inside surface of the tube were measured. Assuming that the surface temperature is uniform (see appendix A), the temperature difference between the inside and outside surfaces can be calculated from the following equation (72),

$$\Delta T \div q \frac{t_w}{k} \left[\frac{1}{2} + \frac{t_w}{6D} \right] \approx \frac{1}{2} q \frac{t_w}{k} \quad (51)$$

Taking a value of 14 Btu/hftF for the thermal conductivity of the tube material, the values of the temperature difference work out to be : in ethanol, 0.4 to 2 deg F; in water, 1 to 6 deg F generally, but up to 9 deg F when a test-piece made from the tubing of $\frac{1}{4}$ inch diameter and 0.02 inch wall thickness was being tested at 1612°F in cold water. Because

the differences were usually small, and generally well inside the accuracies of the thermocouple readings, no allowances were made for them.

Two thermocouples were used to indicate the hot surface temperature, so that one could be checked against the other. Normally readings from the two agreed to within $\pm 100 \mu V$ ($\pm 4 \text{ deg F}$) in water and $\pm 50 \mu V$ ($\pm 2 \text{ deg F}$) in ethanol, so readings were taken from one only, and the reading of the other was checked occasionally. If the differences between the two readings were consistently greater than the above values, the test-piece was discarded. It was considered that either one of the sensing junctions had been displaced from the axis of the tube and was no longer registering the mean temperature or one of the thermocouples had lost its accuracy.

6.3 Heat Flux

The value of the heat flux in the horizontal section was taken to be the same as the mean value between the voltageappings. Errors in the values of heat flux therefore arose from errors in the values of surface area and heating rate, and also because the heat flux in the horizontal section usually differed slightly from the mean value.

The accuracy of the values of the mean heat flux was estimated to be better than $\pm 1.75\%$. The surface area was calculated at the test temperature from measurements of diameter and length of the test-piece when cold. An allowance for expansion was made of 0.16% for each 100 deg F rise above ambient. The accuracies of the values of the areas have been estimated to be better than $\pm 1\%$. The heating rate was measured using a wattmeter and current transformer. The manufacturers accuracies for these instruments are 0.5% of full scale deflection (FSD) for the wattmeter and $\pm 0.15\%$ for the current transformer. At 40% FSD, which was the smallest deflection used, the accuracy of the wattmeter was therefore $\pm 1.25\%$. At 40% FSD the wattmeter could be read to $\pm 0.5\%$ of the reading.

The values of the heat flux in the horizontal sections were generally a little different from the mean values because the electrical resistance of the tubing varied slightly with temperature. Usually the vertical sections were colder than the horizontal section. In ethanol the errors in the values of the heat flux arising from this source were estimated to be less than $\pm \frac{1}{2}\%$.

In water, the errors in the values of the heat flux were generally less than $\pm 1\frac{1}{2}\%$. Worse cases occurred in warm and cold water when the values of the heat flux in the horizontal sections were estimated to be 2 - 3% higher than the mean.

6.4 Fluid Properties

The values of the fluid properties were taken from a number of sources, not all of which stated the accuracies of the values. However, indications are that the property values for water, water vapour and ethanol liquid are accurate to within $\pm 4\%$. For ethanol vapour the figure is probably slightly worse, about $\pm 6\%$.

6.5 Calculations

The calculations were carried out using an electronic desk calculator, and the results were usually recorded to four significant figures.

For simple calculations, for example that for heat flux, the error due to calculation (including rounding off) was estimated to be no more than $\pm \frac{1}{8}\%$.

Fluid properties were evaluated at the mean temperatures, $\frac{1}{2}(T_w + T_s)$ and $\frac{1}{2}(T_L + T_s)$. In the calculation of the vapour Grashof number, $Gr^* =$

$$g D^3 \rho_v (\rho_L - \rho_v) / \mu_v^2, \text{ a mean value for the density difference}$$

$(\rho_L - \rho_v)$ was taken. It was evaluated (see appendix D), from the mean value of the liquid density at the boiling point and at the largest subcooling, and the value of the vapour density at the mean temperature between the boiling point and the middle surface temperature.

The values of Gr^* calculated thus are too large when the liquid is at and near the boiling point, and too small when the liquid is cold.

Maximum errors _{in Gr^*} have been estimated to be $\pm 2.2\%$ in water, and $\pm 3.5\%$ in ethanol. However in correlations for heat transfer where the $\frac{1}{3}$ or $\frac{1}{4}$ root of Gr^* is taken, effective error would be only about 1% or less.

Chapter 7

RESULTS

7.1 The heat transfer and photographic results are presented in this chapter, first in general terms and then for each liquid. Some observations on self-generated noise that occurred when film boiling took place in water and detergent solution are included. The range of conditions covered by the results are summarised in table 1 (a, b and c).

7.2 The heat transfer results are presented graphically in figures 10 - 12 for water, 13 and 14 for the detergent solution, and 15 - 18 for ethanol; and are tabulated in appendix C. The heat flux q_{tot} , is plotted against the liquid subcooling, ΔT_L , with the surface temperature, T_w , as the third parameter. The graphs show that in all cases heat flux increases with subcooling and with superheat. Reproducibility is good in all cases. Lines have been drawn through the points to represent average values. In some cases the lines are smooth curves, increasing monotonically, and in others the lines show distinct changes of slope.

The photographic results are presented in figures 21 to 34 and summarised in the sketches of figures 19 and 20. They show that near the boiling point much vapour is released as bubbles, and most of the interface is chaotic. With increasing subcooling bubble release decreases, and the interface becomes increasingly smooth. With increasing superheat both bubble release and interfacial waviness increase.

7.3 Water

The heat transfer results were taken at surface temperatures of 1012°F, 1312°F and 1612°F for the cylinders of 1/8 and 1/4 inch diameters (figures 10 and 11), and at 1012°F and 1312°F for the cylinder of 1/2 inch diameter (figure 12).

Results for the 1/2 inch diameter cylinder at 1312°F could not be taken at values of subcooling greater than about 120 deg F because of limitations of the power supply; and for the same reason, results were not

taken at $T_w = 1612^\circ\text{F}$. At the surface temperature of 1012°F , results could not be obtained at values of subcooling greater than about 90 deg F for the $1/8$ inch diameter cylinder, and 50 deg F for the $1/2$ inch diameter cylinder, because film boiling could not be established under these conditions. If film boiling was established at higher values of surface temperature, and then the heating rate slowly reduced, the surface temperature would fall but, before the temperature of 1012°F was reached, film boiling was replaced locally by nucleate boiling which then spread over the whole test-piece (see section 5.6). Otherwise the highest subcooling for which results could be obtained were limited by the difficulty of matching the speed of immersion with the increase in the heating rate (section 5.6).

Special efforts were made (section 5.6) to enable results for saturated film boiling on the $1/4$ inch diameter cylinder to be obtained so that the trend of the results between 0 and 2 deg F of subcooling could be checked.

The heat transfer results for the $1/8$ inch diameter cylinder, which were obtained first, include results for distilled, de-ionised and tapwater, and for tapwater that had been a) aerated (by bubbling air through the water for several hours), and b) partially de-aerated (by boiling for a few minutes and allowing the water to cool). Because there were no noticeable differences, only tapwater was used in subsequent tests.

The trends of the results for the $1/8$ inch diameter cylinder are shown by the faired lines which are smooth curves approximately parallel. The results for the $1/4$ inch diameter cylinder behave likewise, except at the surface temperatures of 1312°F and 1612°F between values of subcooling of about 10 - 50 deg F. The results are then a little higher than smooth curves would indicate. The results for the $1/2$ inch diameter cylinder at 1312°F show a distinct change of slope, and between 60 and 72 deg F the heat flux remains constant. It seems that there are different modes of heat transfer which depend on superheat, subcooling and diameter.

The silhouette photographs of film boiling on the horizontal cylinders, figures 21 and 25, show clearly that the release of bubbles and the trailing edge comb diminish rapidly with increasing subcooling, especially at the lowest superheat (figure 21) resulting eventually in a smooth interface

at the trailing edge. (The slight blips in some frames at high values of subcooling are caused by air which has come out of solution). The comb persists to a greater subcooling on the larger cylinders, figure 25.

The photos taken under direct lighting, figures 25 - 27, 30, 32, are summarised in figures 19 and 20. The pronounced effects of subcooling on bubble release and interfacial disturbances are well illustrated. Most of the photographs are for the surface temperature of 1312°F only, because the effects of superheat on interfacial disturbances were only slight.

At moderate and high values of subcooling, of greater than about 50°F , the interface is relatively smooth and the release of bubbles virtually eliminated. Figure 25 shows that on the $1/8$ inch diameter cylinder the whole of the interface is smooth. Figures 25 and 26 show that on the $1/2$ inch diameter cylinder the interface is smooth except for the slight waviness above the upper surface. Figure 34 shows that even on the horizontal surface the interface is relatively smooth especially at $\Delta T_L = 89^{\circ}\text{F}$, except for disturbances caused by air that has come out of solution. On the vertical cylinders (figure 27) and sphere (figure 32), the interface is only slightly wavy in the upper regions, and quite smooth in the lower regions. (It was not possible to establish film boiling on the vertical cylinders at about 90°F because of power supply limitations).

At the very small value of subcooling of 5°F , the interface is fairly smooth close to the leading edge only. Elsewhere it is highly chaotic, and bubbles of vapour are released from above the upward facing surface of the sphere (figure 32) and from over most of the vertical surfaces (figures 27 and 30).

The relatively small degree of subcooling of about 22°F almost eliminates bubble release from the vertical surfaces (figures 27 and 30), and the interface is much smoother than for $\Delta T_L = 5^{\circ}\text{F}$. On the horizontal cylinders bubbles are released from the trailing edge. On the cylinder of $1/8$ inch diameter the interface is otherwise smooth (figure 25). On the cylinder of $1/2$ inch diameter the interface is relatively wavy (figure 25).

7.4 Solution of detergent in water

The addition of 0.025% and 0.01% of detergent to water had some pronounced effects on both the rates of heat transfer and the trailing edge

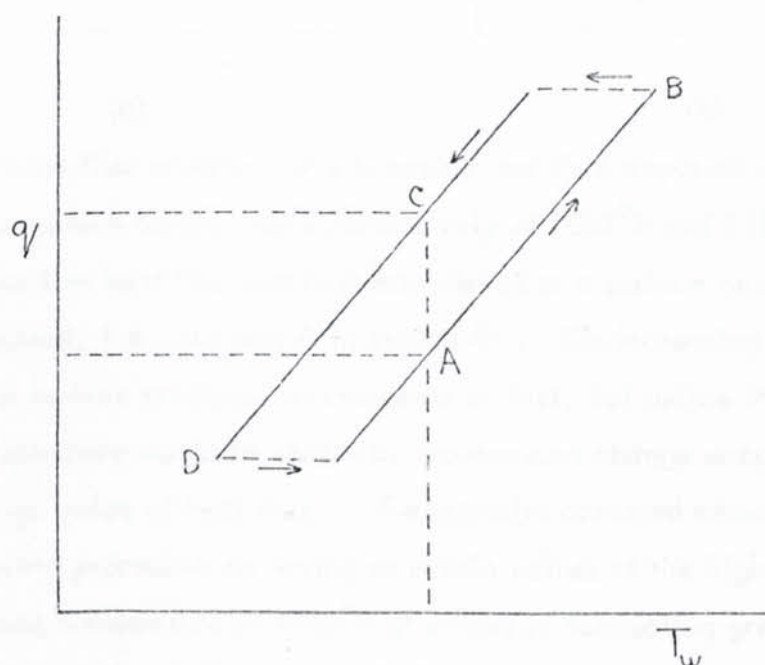
comb. The results for heat transfer on the $1/8$ inch and $1/4$ inch diameter cylinders are presented in figures 13 and 14, and show that at moderate and high subcooling there could be more than one stable value of heat flux for each value of superheat and subcooling. The silhouette photos, figure 22, show that the trailing edge comb persisted to much greater values of subcooling than in water.

The discovery of these effects of detergent happened by chance. Originally the detergent had been added to water to reduce the chance of the random breakdown of the vapour film (sections 5.1 and 5.6. It was never conclusively established whether it did this or not). Tests were carried out first for the $1/8$ inch diameter cylinder over a wide range of subcooling. In general, no differences were detected in the rates of heat transfer from those for water, compare figures 13 and 10, except for a few results for values of subcooling between 60 and 90 deg F, which were somewhat lower than the rest. At the time they were thought to be spurious, but would be investigated further after testing the $1/4$ inch diameter cylinder in water. Because it was so much easier to establish film boiling on the $1/4$ inch diameter tube, this size was used to carry out further tests in the detergent solution.

The results of the tests for the $1/4$ inch diameter cylinder are presented in figure 14. Included, are the average values for water for the same diameter. Results were not taken at values of subcooling less than 50 deg F, which are outside the range of "multi-stability", because the tests for the $1/8$ inch diameter cylinder indicated that the results would be the same as those for water.

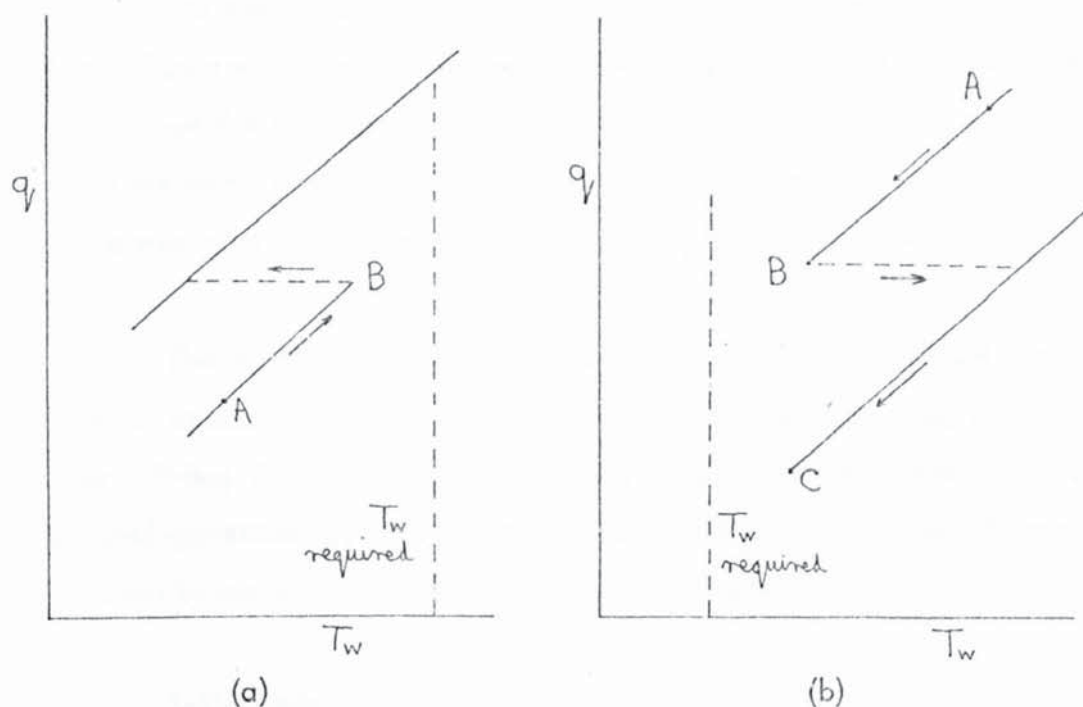
The results in figure 14 show that at the surface temperatures of 1012°F and 1312°F two values of heat flux may occur at moderate and high values of subcooling. The higher of the two values of heat flux are slightly smaller than the corresponding values for water, and the other, lower values are considerably smaller. The lower values are only slightly dependent on subcooling. The "duo-stability" at the surface temperature of 1012°F was found to occur between values of subcooling of about 60 deg F and 90 deg F. At the surface temperature of 1312°F the duo-stability was found to occur from 75 deg F of subcooling to at least 150 deg F which was the maximum value of subcooling at which tests were taken.

It was comparatively easy, within these ranges of subcooling, to obtain either value of heat flux both on immersion and after film boiling had been established. The normal procedure of heating the test-piece in air was carried out. Then, on immersion the heating rate was set to give a value of heat flux slightly less than the lower value of heat flux if the lower was required, or slightly greater than the higher value if that was required. The heating rate could be set correctly after about 20 seconds. The change from one value of heat flux to the other after film boiling had been established is illustrated in the sketch. If film boiling was taking place at the lower value



of heat flux, point A, the heating rate was increased slowly. At first the surface temperature also increased, but when the change occurred, at point B, the surface temperature suddenly decreased. To change the other way, from point C, the heating rate was slowly reduced until, at point D, the surface temperature suddenly increased. In both cases adjustment of the heating rate was necessary after the change to obtain the required surface temperature.

Difficulties arose which prevented results from being obtained outside the ranges of subcooling given above. The difficulties can be explained with the aid of the following sketches. When trying to obtain the value of



the low heat flux at values of subcooling less than about 60 deg F and 75 deg F at surface temperatures respectively of 1012°F and 1312°F, film boiling at the low heat flux was first established at a surface temperature below that required, i.e. at point A in sketch (a). On increasing the heating rate, the surface temperature increased at first, but before the required surface temperature could be reached, spontaneous change occurred at point B to the high value of heat flux. The opposite occurred when carrying out the opposite procedure for trying to obtain values of the high heat flux at the surface temperature of 1012°F at values of subcooling greater than about 90 deg F, see sketch (b). Film boiling at the high value of heat flux, point A, changed to film boiling at the low value at point B before the surface temperature could be reached.

Results for the low value of heat flux could not be obtained for the surface temperature of 1012°F at values of subcooling greater than 90 deg F because breakdown of film boiling occurred at surface temperatures higher than 1012°F - point C, sketch (b).

The surface temperatures at which the changes occurred (points B and C) varied considerably from test to test, by up to 100 deg F. The changes seemed to happen quite spontaneously. The limits of duo-stability are therefore only approximate, and with perseverance and improvements in technique it may be possible to extend the ranges.

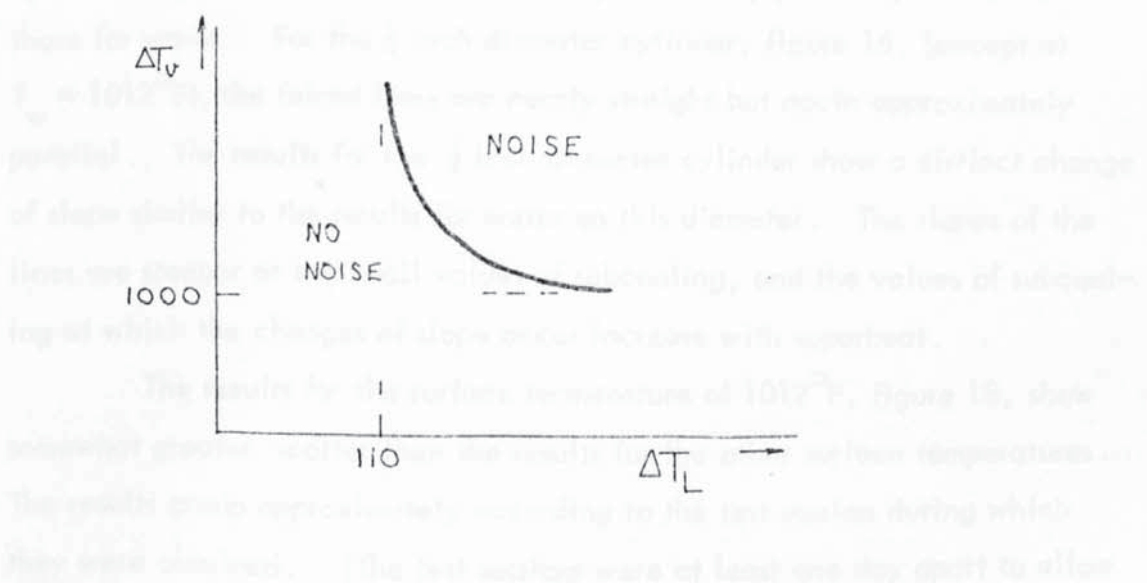
The slight visual difference between film boiling at the high values of heat flux and at the low values is shown in figure 24. At the high values the comb on the trailing edge is regular and well formed, whilst at the low values the comb tends to be ragged without all the peaks existing. The difference was more noticable during testing than the photos show.

The results for the surface temperature of 1612°F_A (fig. 14) indicate that numerous values of heat flux are possible at values of subcooling greater than about 110 deg F. Some of the additional values of heat flux were associated with self-generated noise, discussed in section 7.5. A thorough investigation could not be carried out because of the lack of time.

7.5 Self-generated noise

Self-generated noise accompanied film boiling in water and detergent solution at high values of superheat ($\Delta T_v > 1000$ deg F) and subcooling ($\Delta T_L > 110$ deg F). Because of a shortage of time, only a superficial study of the occurrence and the effects could be made.

Whether the noise was generated or not was governed by the values of both temperature differences in the manner shown in the sketch. The noise



would fade quickly at the temperature limits indicated, through changes in subcooling of about 5 deg F, and in superheat of about 20 deg F. The noise was easily audible, and the frequency varied over a limited range, which was estimated to be between 60 Hz and 100 Hz.

The onset and loss of noise generally showed a hysteresis, and the indications were that rates of heat transfer were slightly less when noise was being generated than otherwise. At a subcooling of 112 deg F, and with a heat flux of $115,000 \text{ Btu/hft}^2$, the surface temperature stabilised at about 1550°F without noise, and at about 1590°F when noise was being generated. This is equivalent to a change in the value of heat flux of about $2\frac{1}{2}\%$.

When noise was being generated, alternate light and dark lines were seen in the interface on the trailing edge of the cylinders. The lines were about 1 mm apart, at right angles to the axis of the tube, and were assumed to be the waves associated with the generation of the noise.

7.6 Ethanol

The results for ethanol were obtained for the same values of dimensionless superheat and over the same range of dimensionless subcooling as the results for water. The corresponding surface temperatures are 486°F , 590°F and 698°F , and the results are presented graphically in figures 15, 16 and 17. Results were also obtained at the surface temperature of 1012°F for horizontal cylinders of $\frac{1}{4}$ inch diameter (figure 18) to compare with the results for water at this surface temperature.

The faired lines obtained for the results for the $\frac{1}{8}$ inch diameter cylinder (figure 15) are smooth curves approximately parallel, similar to those for water. For the $\frac{1}{4}$ inch diameter cylinder, figure 16, (except at $T_w = 1012^\circ\text{F}$), the faired lines are nearly straight but again approximately parallel. The results for the $\frac{1}{2}$ inch diameter cylinder show a distinct change of slope similar to the results for water on this diameter. The slopes of the lines are steeper at the small values of subcooling, and the values of subcooling at which the changes of slope occur increase with superheat.

The results for the surface temperature of 1012°F , figure 18, show somewhat greater scatter than the results for the other surface temperatures. The results group approximately according to the test session during which they were obtained. (The test sessions were at least one day apart to allow the ethanol, which became hot during testing, to cool down). Carbon was often deposited on the surface of the tube during testing. It had to be cleaned off before the next test otherwise the vapour film was liable to

break down and nucleate boiling occur. The amount of carbon deposited was very sensitive to the value of heat flux; if this was less than $50,000 \text{ Btu/hft}^2$ the amount deposited was negligible, yet at the value of $53,000 \text{ Btu/hft}^2$ a thick coat was deposited.

The silhouette photographs of film boiling on $\frac{1}{4}$ inch diameter horizontal cylinders, figure 23, show that the comb and bubble release diminish with increasing subcooling, but are not eliminated - as is the case in water - even at the highest values of subcooling (93 deg F). The comb and bubble release are more pronounced at the highest surface temperature.

The photos of film boiling of ethanol on the 2 inch high vertical surface, figure 31, illustrate very well the effects of subcooling and superheat on interfacial waviness and bubble release. At the surface temperature of 698°F , and with $\Delta T_L = 28 \text{ deg F}$, the interface is chaotic and much vapour is released as bubbles. With decreasing superheat and with increasing subcooling, bubble release diminishes, and the interface becomes smooth near the leading edge and takes on a distinctive wave pattern on much of the rest of the interface.

The photos of film boiling on the vertical cylinders, figure 29, show that bubbles of vapour are not released even at the relatively small subcooling of 28 deg F. This resembles film boiling on this geometry of the other two liquids at similar degrees of subcooling (figures 27 and 28). At $\Delta T_L = 90 \text{ deg F}$ the interface is a little more wavy than the interface in the film boiling of detergent solution at about the same degree of subcooling and dimensionless superheat.

Chapter 8

ANALYSES AND CORRELATIONS

8.1 In this chapter the photographic results are analysed first, and the phenomena of the interfacial disturbances and the stability of the flows of the vapour and liquid are discussed. From the heat transfer results some correlations for subcooled film boiling are developed in two parts : 1) equations for the "vapour heat flux, q_v " are developed from existing correlations for saturated film boiling, and 2) equations for the "liquid heat flux, q_L " are developed from approximate theoretical solutions. The validity of the correlations are discussed bearing in mind the analysis of the photographic data. The values of heat flux calculated from the correlations are compared with the original experimental data. Finally, the results for the detergent solution are discussed.

8.2 Interfacial dynamics and flow stabilities

In subcooled film boiling the flow of the liquid is governed not only by its own buoyancy, but also by upward movement and waviness of the interface. The dynamics of the interface, and the stability of the vapour flow are extensions of those for saturated film boiling which were introduced in chapter 1 and discussed in section 3.8.1. A brief summary of the vapour flow and interfacial dynamics is as follows : on horizontal cylinders, spheres and vertical surfaces the vapour moves upwards because of its buoyancy against the liquid, and, because of interfacial shear forces, the interface and adjacent liquid also rise. The vapour flow is laminar near the leading edge and the interface is relatively smooth. With increasing distance from the leading edge the interface becomes increasingly wavy, bubbles of vapour are released and the vapour flow becomes turbulent. Above a horizontal surface the interface is chaotic with bubble release over the whole surface.

The photographic results were presented in the preceding chapter, and have been summarised in figures 19 and 20. The pictures of film boiling at small degrees of subcooling largely substantiate the earlier descriptions for saturated film boiling, although in some cases the interface does not appear to be very smooth at and near the leading edge, for example on the sphere

(figures 32 and 33) and vertical surface (figure 30) at $\Delta T_L = 5$ deg F. This may be because film boiling is also occurring underneath downward facing surfaces.

The most noticable effects of increased subcooling are the progressive extension of the smooth interface downstream, and the progressive reduction of the release of bubbles of vapour (figure 20). In water, the release of vapour is completely eliminated even from above the upward facing surfaces of the horizontal cylinders, (figures 21, 25) sphere (figure 32) and horizontal plate (figure 34). On the 8 inch high vertical cylinders, the release of vapour bubbles is completely eliminated in ethanol and detergent solution as well as in water (figures 27 - 29).

The extension of the smooth interface downstream as subcooling increases is an indirect result of the increase in the rates of heat transfer. The smooth interface in the vicinity of the leading edge is due to the high degree of damping imposed on the interface by the thin film of vapour that exists there. The film is thin because heat transfer rates are locally high and because most heat is transferred through the film by conduction. Higher rates of heat transfer due to increased subcooling make the film thinner and thus extend the smooth interface further downstream. Assuming that flow is laminar, local rates of heat transfer, and consequently film thickness, are approximately proportional to the fourth root of the distance downstream. The extent of the smooth interface is therefore highly dependent on the film thickness and heat flux. By doubling the value of heat flux, for example by increasing subcooling in water from about 20 deg F to 120 deg F, the film thickness would be approximately halved, and the extent of the smooth interface increased sixteenfold. This is the sort of increase indicated by the photos. It follows therefore that on smaller geometries, when other conditions are the same, a greater proportion of the interface will be smooth.

The release of bubbles is dependent on subcooling because the increased rates of heat transfer affect the growth in amplitude of the interfacial waves. The growth is influenced in two ways. The first is due to the increased damping of the thinner vapour film as explained above. The onset of bubble release as well as the onset of the wavy interface is moved downstream. The second may be explained as follows; consider a wavy interface.

A bubble is formed by the amplitude growing and the "dome" breaking off. The interface at the top of the dome is most distant from the hot surface and therefore receives less heat than the average over the whole interface. The amount of heat reaching the interface in the dome can be less than that removed locally by the liquid, in which case condensation would occur. The growth of the dome and eventual bubble release depend on the balance of the local condensation and the extent to which vapour moves into the dome from other areas. In subcooled water the local condensation becomes so large that the amplitude of the waves cannot grow sufficiently to form bubbles of vapour, even in the interface above upward facing surfaces.

Figures 21 - 23, 30 and 31 show that the effects of increasing the superheat are opposite to those of increasing the subcooling. This can be explained in terms of the vapour film thickness, because in all cases the film thickness increased with superheat. The increase in film thickness can be deduced from considerations of heat conduction and radiation through the film.

Comparison of figures 21, 22 and 23 for the film boiling of water, detergent solution and ethanol on $\frac{1}{4}$ inch diameter horizontal cylinders, indicates that surface tension may be important in the formation of the comb on the trailing edge. The surface tension of water is about 4.0×10^{-3} lb_f/ft at its boiling point, and the values for detergent solution and ethanol at their boiling points are about 1.5 and 1.2×10^{-3} lb_f/ft respectively (appendix D).

Instabilities in the vapour and the liquid cannot be seen in the photos. In the vapour, the transition from laminar to turbulent flow for saturated film boiling has been discussed in the review (section 3.8.1). In subcooled film boiling, because of the thinner vapour film, the position of the transition would be further downstream. It may be possible to estimate the position, from similar considerations to those used by Hsu and Westwater, and to include the effects of subcooling but this is outside the scope of this thesis. It would involve a discussion on whether it is valid to consider a laminar vapour film when the interface is disturbed.

Instabilities in the liquid in subcooled film boiling may be due to its own buoyancy or to interfacial waviness. At high values of subcooling, when much of the interface is relatively smooth, the effects of interfacial

waviness may be insignificant, and the flow of the liquid would depend on its own buoyancy. The flow could become turbulent at some critical distance from the leading edge. Using the single-phase criterion that transition occurs between values $GrPr$ of 10^8 and 10^{10} , then in water at high subcooling ($\Delta T_L > 100$ deg F), transition would occur at heights from the leading edge of between one and five inches. Therefore on sizes such as the 4-inch sphere and 8 inch vertical cylinders, subcooled film boiling with turbulent liquid flow could occur.

More relevant, however, to the present heat transfer results is an induced or pseudo-turbulence imposed on the liquid by the wavy interface. It has an enormous effect on heat transfer into the liquid as will be shown in the analysis of the heat transfer results, especially at small values of subcooling where the interface is highly chaotic. The pseudo-turbulence may explain the changes in slope in the graphs of the heat transfer results for the $\frac{1}{4}$ inch diameter cylinders (figures 12 and 17). At small subcooling the interface is generally chaotic, and a smooth interface covers only a small proportion of the tube. The effect of pseudo-turbulence could therefore be large. With increasing subcooling the smooth interface moves progressively downstream covering a larger proportion of the tube. The pseudo-turbulence would, therefore, have a decreasing effect and presumably, at the changes of slope, is no longer effective.

The theoretical solutions which have been carried out after making the assumption that the interface is smooth are not, therefore, strictly applicable at small values of subcooling when the interface is wavy. The solution for subcooled film boiling above a horizontal surface (57) in which the interface was assumed to be wavy, is not strictly valid at moderate and high values of subcooling. Some new physical models are proposed in section 9.4.

8.3 Correlation of the heat transfer results

The present heat transfer results for the subcooled film boiling of water on $\frac{1}{4}$ inch diameter horizontal cylinders are compared with earlier work in figure 5. The results do not support any of the solutions which apply to the $\frac{1}{4}$ inch diameter horizontal cylinder except near the boiling point, and there are no earlier experimental data for this size and geometry. Some new correlations have been developed which are based on the properties of both

the liquid and the vapour. This approach had already been suggested by Frederking and Hopfield (41) and Hamill and Baumeister (57) who add a heat flux for the liquid to a heat flux for the vapour according to equations 40 and 41.

The present correlations are based on the assumption that in subcooled film boiling heat is transferred in two ways : 1) by evaporating liquid, and 2) by convection into the liquid. The first gives rise to a vapour heat flux, q_v , dependent on vapour properties, and the second to a liquid heat flux, q_L , dependent on liquid properties. The two values are added to give the total heat flux thus,

$$q_{tot} = q_v + q_L \quad (52)$$

Since the curves in figures 10 - 12 and 15 - 17 are essentially parallel and because the liquid-vapour interface is at the saturation temperature, it was assumed that the vapour heat flux q_v was independent of subcooling. Therefore q_v had the value of the heat flux at the boiling point, q_s , and

$$q_{tot} = q_s + q_L \quad (53)$$

The proposed correlations for subcooled film boiling are therefore in two parts, one for saturated film boiling and the other for liquid heat transfer. The data for water at the three surface temperatures of 1012°F, 1312°F, and 1612°F and for ethanol at 486°F, 590°F and 698°F for the three diameters of 1/8, 1/4 and 1/2 inch (figures 10 - 12 and 15 - 17) have been used to develop the correlations for subcooled film boiling in conjunction with existing equations for saturated film boiling, and some new approximate theoretical solutions for liquid heat transfer. (Some of the present data for the subcooled film boiling of water on 1/8 and 1/4 inch diameter horizontal cylinders were earlier correlated in this manner - see section 8.5.2).

8.3.1 Correlation of the vapour heat flux q_v . A number of correlations for the prediction of heat transfer in saturated film boiling have been reviewed (section 3.3). It was decided to test the present data against first of all equation 2 by Bromley with $N = 0.62$, then equations of this type but with different terms for $f(Sp)$, and finally against equation 12 by Hamill and

Baumeister.

The results for the saturated film boiling of water and ethanol were obtained by extrapolating to the boiling point the faired lines that represent the mean of the results for subcooled film boiling (figures 10 - 12 and 15 - 17; and appendix E). To reduce the results for saturated film boiling to dimensionless form the "convection only" component had to be obtained by subtracting a value for the heat transferred by radiation. This was carried out in the manner given in section 3.6, i.e.

$$q_{co} = q_s - B \epsilon_w q_r \quad (32a)$$

The value of the emissivity of the wall, ϵ_w , was not known so q_{co} was evaluated for the two values of 0.75 and 1.0. (Later a more accurate value of 0.9 was deduced).

The values of the Nusselt numbers, Nu , were calculated from the values of q_{co} and plotted against the modified Rayleigh number $Ra_1^* = Gr^* Pr (\frac{1}{2} + \frac{1}{Sp})$, for each value of emissivity, see figure 35. The vapour properties were evaluated at the mean temperature of the film, $\frac{1}{2}(T_w + T_s)$, (appendix D), and the diameter of the cylinder, after being corrected for thermal expansion was used as the characteristic dimension. Equations of best fit, (nos. 54 and 55), and equation 2 have been drawn.

From the graphs in figure 35 it was possible to deduce a more accurate value of 0.9 for the emissivity, based on the assumption that the one-fourth index of the equations is correct. If the value of the emissivity is correct, the points lie on a line which has a slope of $\frac{1}{4}$. If the value of the emissivity is low, the values of q_{co} are over-estimated and the values of the Nusselt number are too high. Results in which the proportion of heat transfer by radiation is large are affected to a greater extent than those in which the radiative component is small. Therefore, the results at high superheat are affected more than those at low superheat, and a line joining the results for a given liquid and tube diameter, line A figure 35, has a slope of less than $\frac{1}{4}$. Conversely if the value of the emissivity is too large, such a line, line B figure 35, has a slope of greater than $\frac{1}{4}$. Furthermore, the results for water are affected to a greater extent than those for ethanol, and therefore the results for water lie above those for ethanol when the value

of the emissivity is too small, and conversely if the value is too large.

The results were recalculated taking the value of the emissivity to be 0.9, and are plotted in figure 36. The line of best fit, selected visually, has the equation,

$$Nu = 0.55 [Gr^* Pr]^{\frac{1}{4}} \left[\frac{1}{2} + \frac{1}{Sp} \right]^{\frac{1}{4}}. \quad (56)$$

The data is correlated with less scatter than in figure 35, which is a further indication that the value of 0.9 for the emissivity is more accurate than either 0.75 or 1.0.

The value of the coefficient in equation 56 is somewhat smaller than the value of 0.62 recommended by Bromley, but is within the limits of 0.512 and 0.724 given by his simple theory. The values of the coefficient are slightly different when different superheat parameters are used (figure 37). The values become 0.59 and 0.54 respectively, if $\frac{1}{Sp}$ and $\frac{1}{Sp} (1 + 0.34 Sp)^2$ are used (equations 57 and 58). The data is not noticeably better correlated by using the superheat term $\frac{1}{Sp} (1 + 0.34 Sp)^2$. (57)
(58)

The results for saturated film boiling were finally compared with equation 12, taking a value of 0.9 for the emissivity, see figure 38. The ratio of the critical wavelength to diameter (λ_c/D) varies from 4.76 for the 1/8 inch diameter cylinder in water to 0.75 for the 1/2 inch diameter cylinder in ethanol. The agreement between the results and equation 12 depends on the value of this ratio: for the smallest value the agreement is good, for the largest the results are about 15% too small. Consequently, equation 12 has not been considered any further.

8.3.2 Correlation of the liquid heat flux q_L . From equation (53) the values of the liquid heat flux can be calculated by subtracting the heat flux for saturated film boiling from the total heat flux:

$$q_L = q_{tot} - q_s \quad (53a)$$

Values of q_L have been calculated from the results for water and ethanol, taking the mean values of the experimental data (see figures 10 - 12 and 15 - 17). The mean values were taken for each diameter and superheat at intervals of subcooling of 10 deg F in water starting at the bulk temperature

of 200°F, and at intervals of 18 deg F in ethanol starting at a bulk temperature of 158°F. (see appendix E).

At large values of subcooling in water the values of the liquid heat flux, q_L , for the 1/8 inch and for the 1/4 inch diameter cylinders vary little with superheat, and in subsequent calculations the average value of q_L could be used. At large values of subcooling in ethanol on the 1/8 and 1/4 inch diameter cylinders, q_L is slightly dependent on superheat. At small values of subcooling all the values of q_L were noticeably dependent on superheat and no meaningful average could be used.

The first attempt at correlating the results for liquid heat transfer was based on the simplest theory for single phase natural convection: values of the Nusselt number were plotted against the Grashof-Prandtl product, $GrPr$, figure 39. The properties of the liquid were evaluated at the liquid film temperature, $\frac{1}{2}(T_L + T_s)$, and the diameter of the cylinder, corrected for expansion, was used as the characteristic length in both Nu_L and Gr_L (appendix E). The results for small values of subcooling, for which the values of heat flux were noticeably influenced by superheat show considerable scatter. The results for large values of subcooling in water, for which average values for heat flux, q_L were used, seem to be lumped together. (The division of the results according to liquid and diameter, and the equations in these figures will be discussed later).

The use of the diameter of the cylinder as the characteristic dimension is not strictly correct because heat transfer into the liquid occurs at the interface. Estimation of the size of the interface is difficult, especially at small values of subcooling when it is wavy and irregular. Examination of the variation of the liquid heat flux with cylinder diameter showed that only at moderate and high values of subcooling does the heat flux decrease with increasing diameter, indicating laminar flow. At low values of subcooling heat flux increased with diameter.

In view of the fact that at low values of subcooling the liquid heat flux is a relatively small proportion of the total, it was decided to ignore the poor correlation of the results at small subcooling for the time being, and to go ahead with correlating the results for high subcooling, using the

cylinder diameter as the characteristic dimension.

An approximate theoretical solution for liquid heat transfer was carried out (appendix B). The integral boundary layer equations were solved by assuming simple profiles for the velocity and temperature. The resulting equation for heat transfer is

$$Nu_L = N [GrPr^2]^{1/4} \quad (B8)$$

where the value of N varies slightly with the actual profiles chosen. Since the value of N would be selected from experimental data, its theoretical value is unimportant. Equation B8 with $N = 0.75$ is the same as equation 39.

The values for the Nusselt number have been plotted against $GrPr^2$ in figure 40. The water data at high subcooling are well correlated by equation 59, but the ethanol data are moved very much to the right. This is due to the relatively high value of the Prandtl number for ethanol (about 10) compared with the value for water (about $2\frac{1}{2}$), and suggests that the Prandtl number is over-represented.

The appearance of the square of the Prandtl number in the above solution is partly due to the assumption that the velocity and temperature boundary layers are of equal thickness. This is true only for Prandtl numbers of one. At other values of Prandtl number the two thicknesses in natural convection are related thus :

$$\delta_U = \delta_T \sqrt{Pr} \quad (B6)$$

The approximate solution of the boundary layer equations (appendix B) then becomes :

$$Nu = N [GrPr^{3/2}]^{1/4} \left\{ \frac{1}{3} - \frac{1}{10Pr} + \frac{1}{30Pr\sqrt{Pr}} \right\}^{1/2}, \quad (B10)$$

which reduces to

$$Nu = N' [GrPr^{3/2}]^{1/4} \quad (B10a)$$

for large values of Prandtl number.

The value of the term $\left\{ \frac{1}{3} - \frac{1}{10Pr} + \frac{1}{30Pr\sqrt{Pr}} \right\}^{1/2}$ varies only

slightly with the value of the Prandtl number: the term has the values of 0.516, 0.54, 0.569 and 0.576 for values of Pr of 1, 2, 10 and ∞ respectively. Therefore the values of the Nusselt number have been plotted against

the values of the product $(GrPr^{\frac{3}{2}})_L$, see figure 41. The results for water and ethanol are brought somewhat closer together without upsetting too much the results for water at high subcooling.

The equations for liquid heat transfer were selected from figures 39 - 41 to correlate well the results at high subcooling when the liquid heat flux is a large proportion of the total heat flux. Since the data for water and ethanol did not show particularly close agreement, an equation for each liquid was selected :

$$\text{for water} \quad Nu_L = 0.386 (GrPr^{\frac{3}{2}})_L^{0.28}, \quad (59)$$

$$\text{for ethanol} \quad Nu_L = 0.151 (GrPr^{\frac{3}{2}})_L^{\frac{1}{3}}. \quad (60)$$

The index of $\frac{1}{3}$ in single phase convection is normally associated with turbulent flow, and the index of 0.28 could indicate mixed laminar and turbulent flow. These points are discussed in section 8.4.2.

The following equations have been selected for both liquids :

$$\text{based on } GrPr \quad Nu_L = 0.42 (GrPr)_L^{0.29}, \quad (61)$$

$$\text{based on } GrPr^{\frac{3}{2}} \quad Nu_L = 0.34 (GrPr^{\frac{3}{2}})_L^{0.29}, \quad (62)$$

$$\begin{array}{l} \text{based on } GrPr^{\frac{3}{2}} \\ \text{and the index of } \frac{1}{4} \end{array} \quad Nu_L = 0.6 (GrPr^{\frac{3}{2}})_L^{\frac{1}{4}}. \quad (63)$$

All the equations 59 - 63 for liquid heat flux were obtained by visual alignment for best fit.

8.4 Discussion

8.4.1 Vapour heat transfer. The correlation of the results for saturated film boiling presented no great difficulty. The value of 0.55 for the coefficient of the equation 56 is somewhat lower than the value of 0.62 recommended by Bromley, but within the extreme values of 0.512 and 0.724 which were obtained by assuming first a stagnant and then a freely moving interface. The value of 0.55 for the coefficient and the value of 0.9 for

the emissivity of the hot surface were selected because they resulted in the most accurate correlation of the test data. A small change in the value of emissivity from 0.9 to 0.75 would necessitate a change in the value of the coefficient from 0.55 to 0.59, and the correlation of the results is slightly less accurate (figures 35 and 36).

The use of the different superheat terms, $\frac{1}{Sp}$ and $\frac{1}{Sp} (1 + 0.34 Sp)^2$ correlates the results almost equally well provided that coefficients of 0.59 and 0.54 respectively are used (figure 37). From the comparison of the superheat terms presented in figure 3, no difference in accuracy would be expected over the small range of Sp , from 0.39 to 0.73, covered by the results.

The smallest ratio of the critical wavelength to diameter (λ_c/D) is about 0.75 for the $\frac{1}{2}$ inch diameter cylinder in ethanol. According to Breen and Westwater (section 3.3.1) this is about the smallest ratio for which data can be correlated by equations such as equation 56 which use the diameter of the cylinder as the characteristic dimension. The results were tested against equation 12 which used λ_c as the characteristic dimension and so covers a wide range of sizes. The results, however, fall into groups depending on the value of λ_c/D , with only those for large λ_c/D being well correlated.

The fact that the present results for saturated film boiling are not correlated well by existing equations might cast doubts on the accuracy of the results. They were obtained by extrapolating the curves representing the mean of the data for subcooled film boiling. The extrapolation is considered accurate because the slopes of the curves are quite small near the boiling point, and the extrapolation was over one or two deg.F only. The present results fall within the spread of the test data used to substantiate equations 2 and 12.

8.4.2 Liquid heat transfer. The values for the liquid heat flux were obtained by subtracting the values of the heat flux at the boiling points from the mean values of the data for total heat flux. At low subcooling therefore, the small values of q_L were sensitive to errors in the two values of heat flux from which it was calculated. The values of liquid heat flux were in no way affected by the correlation of the results for saturated film boiling. Heat

transfer by radiation was taken to be independent of subcooling because the latter has no effect on the two "surface" temperatures T_w and T_s , or on the emissivity of the hot surface.

The suggested correlations for liquid heat transfer are not entirely satisfactory because the results for water and ethanol are not well correlated together, and also because many of the results at low subcooling are not well correlated (figures 39 - 41).

The division of the experimental data between high and low subcooling may be based on the dependence of the liquid heat flux on diameter. At low subcooling the values of the heat flux increased with diameter, and at high subcooling it decreased. The changes occurred at the following degrees of subcooling :

water	$T_w (^{\circ}\text{F})$ 1012	T_L (deg F) 42 - 52
	1312	about 52
	1612	52 - 62
ethanol	486	about 87
	590	about 87
	698	> 87 .

It was expected that the changes would correspond to the changes of slope in the heat flux-subcooling curves, figures 12 and 17, but this was not found to be the case.

The visual difference between high and low values of subcooling is that the interface is relatively quiescent at high subcooling, but is highly disturbed, due to waviness and bubble release at small subcooling. Interfacial disturbances have therefore some effect on heat transfer into the liquid.

The above division classifies most of the ethanol results as "low subcooling". This is supported by the continuing bubble release from the trailing edge of the cylinders (figure 23) and the relatively poor correlation of many of the results especially for the $\frac{1}{2}$ inch diameter cylinder. For water the results at high subcooling are independent of superheat, and bubbles are no longer released.

The equations for heat transfer into the liquid nos. 59 - 63, were

selected to be accurate at high subcooling because the liquid heat transfer then constitutes a large proportion of the total. The results for water are best correlated by a formula based on $(GrPr^2)_L$. The use of this product is strictly correct only for $Pr = 1$; in the present results the values for water are between about 2 and 3. The ethanol results are best correlated using the product $(GrPr^{\frac{3}{2}})_L$. The use of $(GrPr^{\frac{3}{2}})_L$ is strictly correct only for very large values of Pr , but the values for ethanol, between about 10 and 12 in the present tests, are large enough to be only slightly in error. Equations for both water and ethanol are based on either $(GrPr)_L$, or $(GrPr^{\frac{3}{2}})_L$. The use of $(GrPr^2)_L$ causes separation of the results of the two liquids (figure 4D).

The approximate theoretical solutions for heat transfer into the liquid (appendix B) could serve only as a guide to the form the equations might take, not only because the method of solution was not exact, but also because rather sweeping assumptions were made to simplify the boundary conditions. The values of the coefficients of all the equations have been selected from the experimental data. The equations of best fit, nos. 59 - 62, do not have the index value of $\frac{1}{4}$ which the approximate solutions predicted.

The fact that the indices in equations 59 - 62 are not $\frac{1}{4}$ could indicate that the liquid flow is not entirely laminar. Thus even at high subcooling the interfacial disturbances might still impose a pseudo-turbulence in the flow of the liquid. The index of 0.28 for water differs only slightly from $\frac{1}{4}$, and might indicate that the effect of the pseudo-turbulence was small. This is supported by the photos, figures 21 and 25, which show that the interface is smooth on the $\frac{1}{8}$ inch diameter cylinder, and only slightly wavy on the upward facing surfaces of the $\frac{1}{2}$ inch diameter cylinder. The index of $\frac{1}{3}$ in the equation for ethanol suggests that the flow was pseudo-turbulent over the entire surface. However, the photos of film boiling in ethanol at high subcooling figures 23, 29 and 31 show that this was not the case.

An alternative explanation may be based on the fact that the total effect of the pseudo-turbulent flow on heat transfer depends on the proportion of the cylinder surrounded by the disturbed interface, and how vigorously the turbulence is induced. Since large cylinders are surrounded by a greater proportion of disturbed interface (section 8.2), the enhanced rates of heat

transfer will be greater than on the small diameters, and this will have the effect of steepening the line of best fit.

The poor correlation of most of the results for low subcooling may be explained as over-estimation of the values of the Nusselt number, or under-estimation of the values of the Grashof number, both of which could be caused by the wavy interface. The over-estimation of the values of the Nusselt number could arise from the higher rates of heat transfer associated with the pseudo-turbulent flow of the liquid. The effect of the pseudo-turbulence is greater on larger cylinders, at higher superheats and at small subcooling, because the waviness of the interface and bubble release which induce the pseudo-turbulence are more extensive and vigorous. The results for the 1/8 inch diameter cylinder, and for water on the 1/4 inch diameter cylinder at 1012°F, suggest that the induced turbulence was not effective under these conditions. The most likely explanation is that the smooth interface extended over most of the interface, as figure 25 shows is the case for the film boiling of water on the 1/8 inch diameter cylinder at $\Delta T_L = 22$ deg F.

For reasons of simplicity the characteristic dimension in the Nusselt and Grashof numbers was taken to be the cylinder diameter. It would have been more correct to have used the equivalent diameter of the interface, because it is from the interface that heat transfer into the liquid actually occurs.

The use of the diameter of the cylinder in calculating the Nusselt number does not cause any error because the diameter of the cylinder was used to calculate the value of the heat flux. The Nusselt number is independent of characteristic length as the following equations show :

$$Nu = \frac{qD}{\Delta T k} \quad , \quad q = \frac{Q}{\pi D L} ;$$

$$\text{Hence} \quad Nu = \frac{Q}{\Delta T k \pi L} .$$

In the calculation of the Grashof number the selection of the correct characteristic dimension can be very important because the value of the dimension is cubed. The equivalent diameter of a smooth interface can be estimated after calculating the thickness of the vapour film from conduction and radiation considerations. Simple approximate calculations show that

under such conditions, which correspond to water at high subcooling, the vapour film is thin, and the diameters of the interface are between 4 and 8% greater than the diameter of the cylinder. The values of Grashof would thereby be increased by a relatively small amount of between 10 and 30%. However, the results for water at high subcooling are adequately correlated using the diameter of the cylinder, so there is little point in introducing the equivalent diameter of the interface.

When the interface is wavy and bubbles are released the effective diameter of the interface cannot reasonably be calculated. The photographs show that at small subcooling the average diameter of the interface is considerably larger than the diameter of the cylinder. The waviness increases the effective diameter still further (section 3.8.3). Thus an effective diameter of twice the cylinder diameter seems possible at small subcooling, which would increase the values of the Grashof number eightfold. This is the sort of increase that would be needed to correlate the results at low subcooling with those at high subcooling.

Attempts have been made to define a criterion to indicate when interfacial disturbances have a significant effect on heat transfer into the liquid. From the discussion so far it is apparent that the diameter of the cylinder, and the values of the superheat and subcooling all have some effect on the interfacial disturbances, and it is likely that the buoyancy of the vapour against the liquid does also. The analysis of the photographic results suggests that surface tension should be included because of its effect on the trailing edge comb. From considerations of heat conduction and radiation through the vapour film, the effects of superheat and subcooling could be accommodated by including the thickness of the vapour film. All the foregoing conditions can therefore be included in a Bond number defined as :

$$Bo_1 = \frac{\rho_L - \rho}{\sigma} \frac{g}{g_c} Dt_v = \left(\frac{2\pi}{\lambda_c} \right)^2 Dt_v .$$

The Bond number thus defined is a ratio of buoyancy forces to damping forces, since both surface tension and film thickness influence the damping of the interface.

The values of the Bond number for water and ethanol are presented

in tables 2a and 2b. The tick (✓) and cross (x) indicate whether the results are influenced or not by the interfacial disturbances, and the question mark (?) indicates borderline cases. It is concluded that if $Bo_1 < 0.2$, then for both liquids the results are not affected; if $Bo_1 > 0.32$ in ethanol and > 0.40 in water the results are affected. For values of Bond number between these limits the results may or may not be affected.

The values of Bond number in tables 2a and 2b do in fact show a diameter dependence, yet the critical values agree reasonably well between the two liquids. Therefore the Bond number was re-defined to reduce the significance of the diameter,

$$Bo_2 = \left\{ \frac{2\pi}{\lambda_c} \right\}^2 t_v \sqrt{Dt_v}.$$

The values of the new Bond number are presented in tables 2c and 2b. The new limits for the Bond number are : water, 0.037 to 0.052; and ethanol, 0.027 to 0.05. These limits, however, are no more precise than those for the first definition of Bond number.

In cases when bubbles of vapour are not released, all heat is ultimately transferred into the liquid. It should then be possible to calculate rates of heat transfer from considerations of liquid convection only. The effective diameter of the interface would have to be known because it is from the interface that heat is transferred into the liquid. Therefore vapour properties would be involved as well.

Equations 39 and 43 have been derived from theoretical considerations to apply under the condition of very high subcooling defined as $Sc \gg 1$. Only liquid properties are involved, and therefore the equations predict that rates of heat transfer are independent of superheat, except for any effect superheat may have on the effective diameter of the interface.

The photos in figure 21 for the film boiling of water on the $\frac{1}{4}$ inch diameter cylinder indicate that at the subcooling of 112 deg F ($Sc = 0.115$) the interface is smooth and the liquid flow is laminar. It might therefore be expected that the total heat flux could be calculated from equations involving only liquid properties, even at this relatively small value of dimensionless subcooling, provided that the equivalent diameter of the interface is used. It can easily be shown, however, that this is not the case.

Take, for example, the results for the $\frac{1}{4}$ inch diameter cylinder in water at the subcooling of 132 deg F ($Sc = 0.135$) and at the surface temperatures of 1312°F and 1612°F. The respective heat fluxes are 114 000 and 135 500 Btu/hft². The corresponding thicknesses of the vapour film are 0.0035 inch and 0.0045 inch resulting in equivalent diameters of the interface of 0.263 and 0.266 inch. The heat flux is clearly not inversely proportion to the fourth root of the equivalent diameter.

If either of the equations 39 or 43 is valid at $Sc \gg 1$, then the value of the vapour heat flux q_v must at some stage diminish with increasing subcooling and eventually vanish. The present analysis has been based on the assumption that the vapour heat flux q_v is independent of subcooling, and this has been shown to be essentially correct. The fact that the present results do not detect a reduction in the vapour heat flux with increasing subcooling is probably because only a relatively small degree of subcooling is covered, up to a maximum of about $Sc = 0.18$.

8.5 Comparison of the correlations and the test data.

The correlations are summarised first, and then the comparison between the predicted results, and experimental data discussed in general terms. Comparison of the experimental data with the best correlations is made first for water and then for ethanol. Finally, the comparisons between the experimental data and all the correlations are made.

8.5.1 Summary of the correlations for subcooled film boiling. The proposed correlations take the form of adding a liquid heat flux q_L , to a vapour heat flux q_v , to give the total heat flux q_{tot} :

$$q_{tot} = q_v + q_L . \quad (52)$$

The vapour heat flux is the same as the heat flux at the boiling point. Therefore,

$$q_{tot} = q_{co} + \epsilon_w B q_r + q_L . \quad (64)$$

The individual components making up q_{tot} , namely vapour convection, radiation, and liquid convection are obtained from the following equations:

vapour convection, $q_{co} = Nu \frac{\Delta T_k}{D}$, where;

$$Nu = 0.55 [Gr*Pr]^{\frac{1}{4}} \left[\frac{1}{2} + \frac{1}{Sp} \right]^{\frac{1}{4}}, \quad (56)$$

radiation, $\epsilon_w B q_r$:

$$q_r = \sigma_r (T_w^4 - T_s^4) \quad (33)$$

B is a coefficient from figure 4

ϵ_w is the emissivity of the hot surface,

liquid convection, $q_L = Nu_L \frac{\Delta T_L k_L}{D}$, where;

$$\text{for water} \quad Nu_L = 0.386 [GrPr^2]_L^{0.28} \quad (59)$$

$$\text{for ethanol} \quad Nu_L = 0.151 [GrPr^{\frac{3}{2}}]_L^{\frac{1}{3}} \quad (60)$$

$$\text{for both liquids} \quad Nu_L = 0.42 [GrPr]_L^{0.29} \quad (61)$$

$$Nu_L = 0.34 [GrPr^{\frac{3}{2}}]_L^{0.29} \quad (62)$$

$$Nu_L = 0.6 [GrPr^{\frac{3}{2}}]_L^{\frac{1}{4}} \quad (63)$$

The results for saturated film boiling are well correlated by equation 56, see figure 36. The results for liquid convection are not so well correlated by equations 59 to 63, see figures 39 to 41. The equations for liquid heat transfer were selected visually for best fit at large values of subcooling when the accuracy of the value of q_L is most important since it then forms a relatively large proportion of q_{tot} .

Some of the present experimental data for the film boiling of water on the $\frac{1}{8}$ inch and $\frac{1}{4}$ inch diameter horizontal cylinders were correlated earlier (76) in an exactly similar manner, but with slightly different equations for q_{co} and q_L , namely :

$$Nu = 0.613 [Gr*Pr]^{\frac{1}{4}} \left[\frac{1}{Sp} \right]^{\frac{1}{4}} \quad (65)$$

$$\text{and } Nu_L = 0.59 [GrPr^2]^{1/4} \quad (66)$$

The value of the emissivity ϵ_w was assumed to be 0.75.

8.5.2 General comments on the comparison. It was not possible to compare, in dimensionless terms, the correlations and the test data for total heat flux because neither of the two temperature differences, ΔT_L and ΔT_V , could be used to define the Nusselt number based on q_{tot} . Therefore comparison of the correlations and the test data have been carried out by calculating q_{tot} at intervals of subcooling for both water and ethanol, for all three diameters and superheats, and for all the proposed correlations.

The results of these calculations are tabulated in appendix F together with the corresponding test results, and graphical comparisons are made in figures 42 to 63. Figures 42 - 44 show the test results for water and the correlation of best fit (i.e. using equation 59); figures 45 - 47 show the same for ethanol, and figures 48 to 63 show the test data and all the correlations. The figures are discussed in detail below.

The calculated values of heat flux for saturated film boiling, which are the same whichever equation for q_L is used, show close agreement with the test data. This was expected because the non-dimensional results for saturated film boiling were well correlated by equation 56, figure 36.

In all cases, therefore, significant differences between the correlations and the test data are due to inaccuracies in the prediction of the liquid heat flux q_L . The largest differences between the predicted and experimental values of q_{tot} do not necessarily correspond to the largest deviation of the non-dimensional results for q_L from equations 59 - 63, but represent the combined effect of a fairly large deviation in the non-dimensional results for q_L with a fairly large value of q_L .

8.5.3 Best correlation for water. In figures 42 to 44 the results for water, calculated using the best equation (no. 59) for liquid heat transfer, are compared with the test data. Curves representing $\pm 5\%$ on the mean of the test data are also shown.

On the $1/8$ and $1/4$ inch diameter cylinders the predicted results fall within $\pm 5\%$ of the mean of the experimental data. On the $1/2$ inch diameter

cylinder agreement is with $\pm 5\%$ only for values of subcooling greater than about 70 deg. F, and less than about 10 deg F. Poorest agreement occurs at values of subcooling at which the values of q_L were not well correlated by equation 59 (figure 40), yet constituted a significant proportion of q_{tot} .

8.5.4 Best correlation for ethanol. The calculated results for ethanol using the best equation (no. 60) for q_L are compared with the experimental data in figures 45 - 47. Curves representing $\pm 5\%$ on the mean of the experimental data are also shown. Agreement is excellent in the case of the 1/8 inch diameter cylinder, figure 45. On the 1/4 inch diameter cylinder agreement is generally within $\pm 5\%$ of the mean experimental data, with the largest differences occurring at $\Delta T_L \approx 40$ deg F. On the 1/2 inch diameter cylinders agreement is generally poor. The predicted values for q_{tot} are considerably less than -5% of the mean of the experimental data over much of the range of subcooling. The regions of poor agreement correspond to the conditions under which interfacial disturbances have considerable effect on liquid heat transfer.

8.5.5 All correlations. The experimental data and the values for q_{tot} calculated from all the correlations are compared for water in figures 48 to 54, and for ethanol in figures 55 to 63. Except in the case of the 1/2 inch diameter cylinder in water (figure 54), comparison at only one surface temperature is made in each figure to aid clarity. Lines representing $+10\%$, -10% or $\pm 10\%$ of the mean of the experimental data are shown. The experimental data at the other values of surface temperature are shown. The grid lines have been omitted also to aid clarity. In some cases it has not been possible to represent all the correlations because they predicted results that were too similar to be distinguishable from one another. This is especially so at small values of subcooling.

In water on all three sizes, and in ethanol on the 1/8 and 1/4 inch diameter cylinders, the values of q_{tot} obtained from the correlations generally lie within $\pm 10\%$ of the mean of the experimental data, except when the equation of best fit for the other liquid was used. On the 1/2 inch diameter cylinders in ethanol the results from the correlations lie within $\pm 10\%$ of the

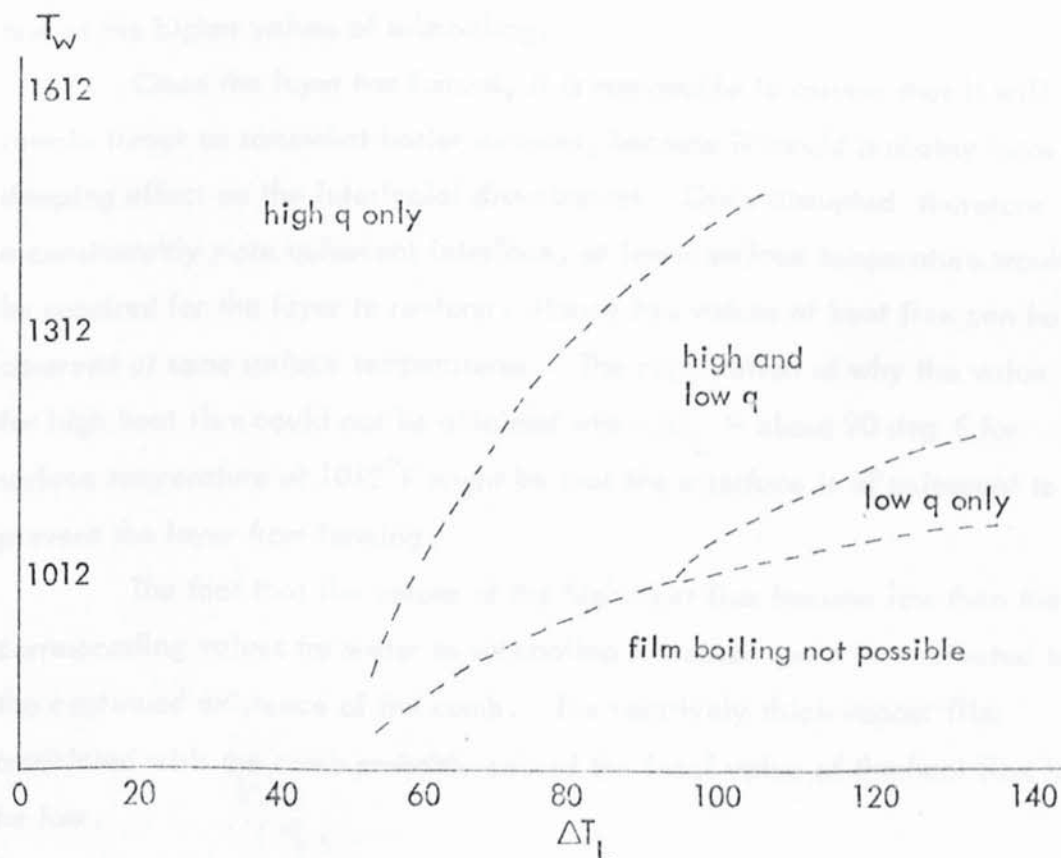
mean of the experimental data at low and high subcooling, but generally fall below -10% at moderate subcooling. The correlation using the equation for water, no. 59, fits the experimental data best except at the highest values of subcooling.

In all cases the values of q_{tot} calculated from the correlation involving equation 59, which had been selected for water, are highest; and the values of q_{tot} , calculated using equation 60, which was selected for ethanol, are the lowest. The values of q_{tot} calculated using the other equations for q_L lie between these two extremes, but not in the same order - compare the correlations using equations 62 and 63 in figures 48 - 50, and figures 51 - 54.

8.6 Film boiling in detergent solution

The heat transfer results for film boiling in the detergent solutions (figures 13 and 14) were not used in the derivation of the correlations. The values for "high" heat flux would be reasonably well predicted by the best correlation for water. No attempt has been made to obtain a formula for the rates of heat transfer at the low heat flux.

A field diagram has been constructed, see below, to show the limits of existence of the duo-stability. The diagram can only be approximate



Detergent Solution Field Diagram

because of the variations in the observed temperatures at which the changes occurred from one heat flux to another (section 7.4).

The one noticeable difference that might have some bearing on the phenomenon of duo-stability was the appearance of the trailing edge comb (figure 24), which was well defined and regular at the high heat flux, but ragged at the low value. No other peculiarities were observed.

The following, tentative, explanation assumes the formation of a layer or "skin" at the liquid-vapour interface somewhat similar perhaps to the layer of gel that forms when film boiling occurs in an aqueous solution of PVA (section 2.5). In the detergent solution the skin might form at the interface where water is evaporated because of the higher concentration of the solution. Such a layer would increase the overall value of the thermal resistance. The value of the low heat flux would be observed if the layer existed, and the value of the high heat flux if there was no layer.

It may be assumed that the layer forms only when the interface is fairly quiescent. The chaotic interface at low subcooling would prevent the layer from forming, and the higher the superheat the greater must be the subcooling before the interface is sufficiently quiescent for the layer to form. The layer is therefore most likely to form at the lower surface temperatures and at the higher values of subcooling.

Once the layer has formed, it is reasonable to assume that it will remain intact on somewhat hotter surfaces, because it would probably have a damping effect on the interfacial disturbances. Once disrupted therefore a considerably more quiescent interface, or lower surface temperature would be required for the layer to re-form. Hence two values of heat flux can be observed at some surface temperatures. The explanation of why the value for high heat flux could not be obtained when $\Delta T_L > \text{about } 90 \text{ deg F}$ for surface temperature of 1012°F might be that the interface is too quiescent to prevent the layer from forming.

The fact that the values of the high heat flux become less than the corresponding values for water as subcooling increases could be attributed to the continued existence of the comb. The relatively thick vapour film associated with the comb probably caused the local value of the heat flux to be low.

Chapter 9

GENERAL DISCUSSION AND CONCLUSIONS

9.1 In this chapter the accuracy of the experimental data, and factors affecting the accuracy are discussed. The comparisons between the present and earlier work are summarised. New physical models for subcooled film boiling are presented. Brief discussions and summaries of the analyses, and the correlation of the heat transfer data are given.

The conditions under which film boiling at very high subcooling ($Sc \gg 1$) may occur are discussed. A section is included on the application of the data presented in this thesis. The advances represented by the present work, are summarised, and some suggestions for further work are outlined.

9.2 Reproducibility and accuracy of the test results

The test results for heat transfer show a high degree of reproducibility as can be seen from figures 42 to 47 in which lines representing $\pm 5\%$ of the mean of the test data are shown. Most of the data fall well within the $\pm 5\%$ limits. The reproducibility is well illustrated in figure 12 by the close agreement of the results for water between values of subcooling of about 60 and 70 deg F on the $\frac{1}{2}$ inch diameter cylinder at the surface temperature of 1312°F .

The sensitivity of the apparatus and instrumentation as a whole is illustrated by the experimental results for the film boiling of ethanol on the $\frac{1}{4}$ inch diameter cylinder at $T_w = 1012^\circ\text{F}$ (figure 18). The grouping of the test results, as described in section 7.6, within the limits of $\pm 5\%$ was detected quite easily.

The accuracy of the measurements has been estimated in chapter 6. Random errors which have contributed to the scatter of the results were calculated to be : $\pm 1^\circ\text{F}$ for T_L , approximately $\pm 1.5\%$ for ΔT_v or $\pm 1\%$ for T_w , and $\pm 1.75\%$ for q . The $\pm 1\%$ error in T_w would result in approximately $\pm 1\%$ error in the total heat flux, q_{tot} , since q_{tot} is approximately proportional to T_w . The combination of these random errors would account for most of the scatter in the test data.

The test data are subject to some systematic errors in T_w and q_{tot}

which were also discussed in chapter 6. The measured value for the surface temperature, T_w , was a mean of the inside surface of the tube. The temperature difference across the wall of the tube was not allowed for; it was generally small (less than 4 deg F), but at high values of heat flux in water the difference could have been as much as 9 deg F. The value of the heat flux in the horizontal section was assumed to be the same as the mean value of heat flux for the whole of the test-piece. For film boiling in cold water it has been calculated that the values of the heat flux in the horizontal sections were thereby underestimated by 2 to 3%. In the worst cases, for film boiling in cold water, the net result of these two systematic errors is that the values of the heat flux may be too small by up to 4%.

The test data might also be subject to error arising from slow changes of the bulk liquid temperature T_L , during the time taken to obtain a set of readings. Inaccuracy could have arisen not only in the recorded value for T_L , but also in the value for the surface temperature if this was also changing slowly, because the thermocouples were located on the axis of the tube, and they could not closely follow changes of surface temperature. To make these errors insignificant, changes in T_L during any single test were kept very small by using a sufficiently large tank of liquid. If any change in T_L was detected over the period, extending from immediately before immersion to when the set of readings was taken, then that set of readings was discarded.

The temperature of the inside surface of the horizontal section of the tube was assumed to be that given by the thermocouples located on the axis of the tube. However, during film boiling in water at the surface temperature of 1312°F and 1612°F, the tube glowed red; and in the horizontal section the shade of red was usually brighter towards the top of the tube than around the rest of the circumference. It was therefore concluded (appendix A) that the surface temperature varied circumferentially, but the matter was not investigated further. It was assumed that the thermocouples on the axis of the tube measured a suitable mean temperature.

A consequence of the variation of the surface temperature around the circumference of the horizontal section was that the heat flux also varied around the circumference, since the electrical resistance of the material of the tube was temperature-dependent. Thus during film boiling in water, the values of the heat flux on the horizontal sections were slightly

larger near the leading edge where the temperature was lowest than around the rest of the circumference.

9.3 Comparison of earlier work and the present results

It was not possible to compare data for subcooled film boiling in non-dimensional terms because there are two temperature differences ΔT_v and ΔT_L , neither of which could be used to define the Nusselt number based on the total heat flux, q_{tot} . For this reason a dimensional comparison of earlier work was made in the review (section 3.7.3 and figure 5). The values for the total heat flux for the film boiling of water have been plotted against a) liquid subcooling at the surface temperature of 1312°F, and b) surface temperature at a subcooling of 100 deg F. As far as possible the data were calculated for, or adjusted to apply to, the $\frac{1}{4}$ inch diameter horizontal cylinder. The comparison was made for water because most of the data applied to this fluid only.

The present test data for the $\frac{1}{4}$ inch diameter cylinder have been included in the diagram. The test data are directly comparable only with the theoretical solutions of Sparrow and Cess (58), Nishikawa and Ito (53), Frederking and Hopenfield (41), and Chang (47) because only these apply to the $\frac{1}{4}$ inch diameter horizontal cylinder. Agreement is good at and near the boiling point only. At larger values of subcooling the test data do not support any of the theoretical solutions. The predictions of Sparrow and Cess (58) underestimate the effects. The predictions of Nishikawa and Ito are marginally the closest to the test data, but their solution was presented graphically for water only and for values of subcooling up to only about 75 deg F.

The present test data for ethanol could be compared only with the theoretical solution of Frederking and Hopenfield (41). The solution of Sparrow and Cess (58) covered values of Pr_L of 1 and 2 only. The solution of Nishikawa and Ito (53) applied to water only and no data were given by Chang (47) for the values of the modified Prandtl number, Pr^* , for ethanol. No comparable experimental data were found.

The comparison of the test data for the film boiling of ethanol on the $\frac{1}{2}$ inch diameter cylinder at the surface temperature of 590°F is given in the following table.

Subcooling ΔT_L deg F	Present test data Btu/hft ²	Theoretical results (41), equation 38 Btu/hft ²
0	14 100	15 300
15	16 800	30 400
33	19 800	33 700
51	21 700	37 200
69	23 300	39 800
87	25 400	41 700

Agreement is poor except at the boiling point. The theoretical solution predicts a very rapid increase in the rates of heat transfer at small subcooling, in a manner similar to the predictions for water given by the same theoretical solution. The comparison was made for the $\frac{1}{2}$ inch diameter cylinder because the test data also exhibits a more rapid increase in the rates of heat transfer at low values of subcooling than at high values.

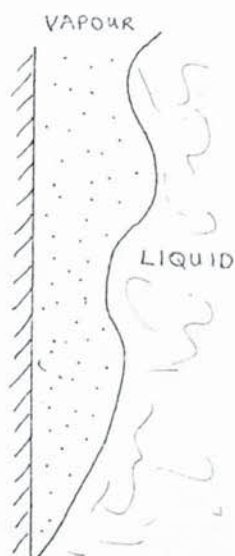
9.4 New physical models for subcooled film boiling

New physical models are presented for subcooled film boiling on vertical surfaces, horizontal cylinders, spheres and horizontal surfaces. Two models are proposed for each geometry: one applies when the interface is relatively smooth and no bubbles are released – for example, to film boiling of water at high subcooling; and the other applies when the interface is disturbed – for example to the film boiling of water at small subcooling and, on some geometries, to the film boiling of ethanol at all values of subcooling.

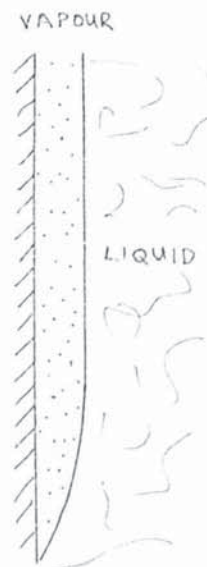
9.4.1 Vertical surfaces. The theoretical solutions for subcooled film boiling on vertical surfaces have included the assumptions that the liquid-vapour interface is smooth, and that the flow of the liquid is laminar.

These assumptions have been found to be incorrect at low and moderate subcooling, especially at high superheat and on large geometries. Under such conditions the interface has been found to be wavy, which induced a pseudo-turbulence in the flow of the liquid. At high subcooling, the assumption of a smooth interface seems to be essentially correct, but there is the possibility of the flow of the liquid becoming turbulent due to its own buoyancy, especially on large geometries.

The following sketches therefore provide more accurate physical pictures of subcooled film boiling on vertical surfaces.



Small and moderate subcooling
(e.g. $\Delta T_L < 50$ deg F in water
and ethanol).



High subcooling
(e.g. $\Delta T_L > 100$ deg F
in water).

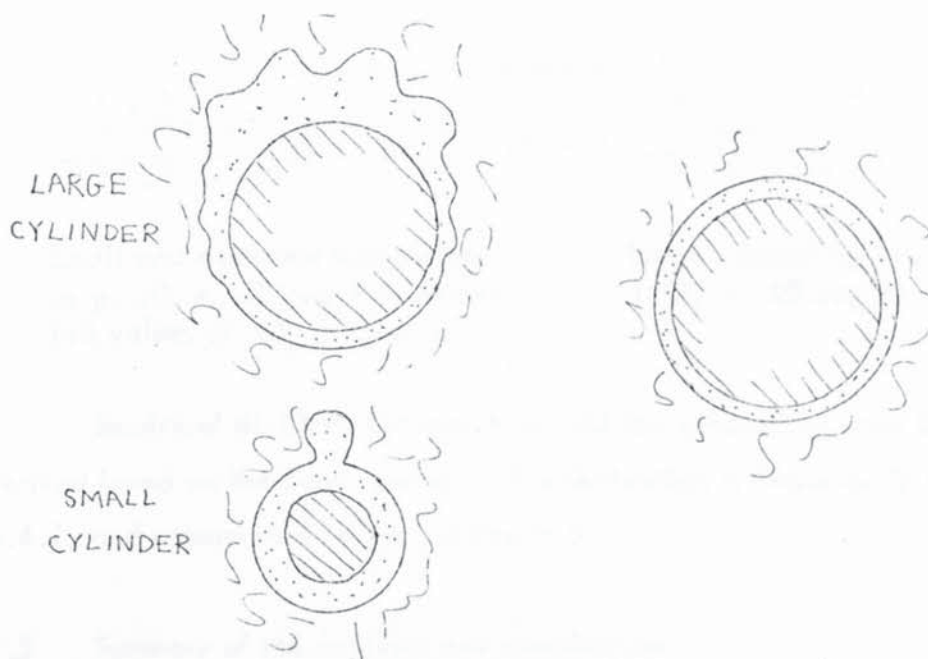
At small and moderate subcooling the interface near the leading edge will be smooth. The distance from the leading edge at which the pseudo-turbulence would have a significant effect on heat transfer is likely to be less than $\frac{1}{4}$ inch, since interfacial disturbances had some effect on heat transfer from the $\frac{1}{4}$ inch diameter horizontal cylinders.

9.4.2 Horizontal cylinders. In the theoretical solutions for subcooled film boiling on horizontal cylinders it has been assumed that the interface was smooth, that there was no bubble release, and that the flow of the liquid was laminar. The present study on horizontal cylinders of $\frac{1}{8}$, $\frac{1}{4}$ and $\frac{1}{2}$ inch diameter has shown that these assumptions are essentially correct only for the film boiling of water at high subcooling.

In the film boiling of both water and ethanol at small subcooling, the interface on the $\frac{1}{4}$ and $\frac{1}{2}$ inch diameter horizontal cylinders was found to be wavy around much of the circumference. On the $\frac{1}{8}$ inch diameter cylinders, the effects of the wavy interface were negligible even at small subcooling, because most of the cylinder was surrounded by a smooth interface. Bubbles of vapour were released from the trailing edge in both liquids at small

values of subcooling, and in ethanol at high values of subcooling.

The following sketches therefore provide more accurate pictures of film boiling on horizontal cylinders.



Small and moderate subcooling
(e.g. $\Delta T_L < 50$ deg F in water)
(all values of ΔT_L in ethanol).

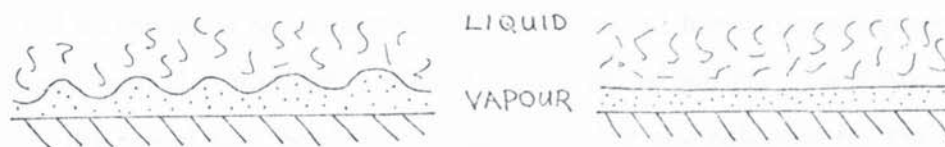
Large subcooling in water
($\Delta T_L > 100$ deg F).

On large cylinders at high subcooling the flow of the liquid may become turbulent due to its own buoyancy.

9.4.3 Spheres. The physical models proposed for subcooled film boiling on spheres are closely similar to those for the horizontal cylinders sketched above.

9.4.4 Horizontal surfaces. In the theoretical solutions for subcooled film boiling above horizontal surfaces, a chaotic interface has been assumed. Such a model is not valid in water at high subcooling, when the interface has been found to be relatively quiescent. No data were obtained for the subcooled film boiling of ethanol above a horizontal surface but it may be assumed that bubbles of vapour would be released at all values of subcooling. The basis of this assumption is that bubbles were released from the trailing edge of horizontal cylinders at all values of subcooling.

The following sketches show the proposed new models for subcooled film boiling above horizontal surfaces.



Small and moderate subcooling
(e.g. $\Delta T_L < 50$ deg F in water)
(all values of ΔT_L in ethanol).

Large subcooling in water
($\Delta T_L > 100$ deg F).

Empirical divisions between high and low subcooling have been derived based on the Bond number. The derivation is discussed in section 8.4.2, and summarized below (section 9.5).

9.5 Summary of the analyses and correlations

The test data were analysed with the main purpose being to obtain correlations for subcooled film boiling. The correlations were developed using the experimental data for water and ethanol in conjunction with existing equations for saturated film boiling and new approximate theoretical solutions for heat transfer into the liquid.

The correlations take the form of adding a liquid heat flux dependent on liquid parameters to a vapour heat flux dependent on vapour parameters. The value of the vapour heat flux was assumed to be independent of subcooling and therefore to have the same value as the heat flux for saturated film boiling. Therefore,

$$q_{\text{tot}} = q_L + q_v = q_L + q_s \quad (52)$$

$$= q_L + q_{\text{co}} + \epsilon_w B q_r. \quad (64)$$

The values of q_L , q_{co} and $\epsilon_w B q_r$ are obtained respectively from equations 59 to 63, equation 56 and equation 33, all of which are given in section 8.5.

The experimental data for q_{co} are well correlated by equation 56, which differs from the Bromley equation 2 only in that the coefficient of

equation 56 is 0.55 instead of 0.62.

The data for the liquid heat flux, q_L , could not be well correlated by a single equation, and therefore an equation for each liquid has been selected, and also some equations for both liquids. All the equations were selected on the basis of correlating the data well at high subcooling when the liquid heat flux represents a large proportion of the total heat flux.

The use of the "best" correlation, i.e. the one selected for the particular liquid, gives predicted values of total heat, for film boiling on the $1/8$ and $1/4$ inch diameter cylinders, which agree to within $\pm 5\%$ of the mean of the test data (figures 42, 43, 45, 46). Agreement with the mean of the test data is within $\pm 10\%$ on these diameters when using the equations which were selected to apply to both liquids (figures 48 to 53 and 55 to 60).

On the $1/2$ inch diameter cylinder at small and moderate subcooling, the values for total heat flux calculated by using the "best" correlation are more than 5% below the experimental values (figures 44, 47). These conditions correspond to the situation when the enhanced rates of heat transfer due to the interfacial disturbances were greatest.

The values for q_L were calculated from the test data at intervals of subcooling by subtracting the values of q_s from the mean values of q_{tot} . At high subcooling, the values of q_L were approximately independent of superheat. At small and moderate subcooling on the $1/4$ and $1/2$ inch diameter cylinders, the values of q_L were strongly dependent on superheat. The dependence has been explained in terms of the interfacial disturbances inducing a pseudo-turbulent flow in the liquid, thereby enhancing rates of liquid heat transfer. The disturbances and therefore the enhanced rates of heat transfer were greater the larger the superheat. A large proportion of the interface surrounding the cylinders of $1/8$ inch diameter was smooth, and therefore rates of heat transfer were not enhanced significantly.

The calculated values for liquid heat transfer were compared graphically in terms of the Nusselt number and Rayleigh Numbers (figure 39 to 41). The Rayleigh number has been defined in three slightly different ways, namely $(GrPr)_L$, $(GrPr^2)_L$ and $(GrPr^{3/2})_L$. The first of these three is the parameter commonly used in single phase convection, and the other two

arose from approximate theory (appendix B). None of the graphs shows particularly close agreement between the data for the two liquids or between data at high subcooling and data at low subcooling. The dependence of the Nusselt number on superheat at low and moderate subcooling has been attributed to the effects of induced turbulence enhancing the values of q_L as mentioned above. It would have been more correct to have used the equivalent diameter of the interface as the characteristic length instead of the diameter of the cylinder. This would have increased considerably, by up to about eight times the values of the Rayleigh numbers at low subcooling. However, at low subcooling the value of the equivalent diameter cannot reasonably be calculated because of the chaotic nature of the interface.

Critical values of Bond numbers have been defined, such that for greater values the disturbances of the interface have a significant effect on heat transfer into the liquid :

$$Bo_1 = \left(\frac{2\pi}{\lambda_c} \right)^2 \quad Dt_v = \frac{\rho_L - \rho}{\sigma} \quad \frac{g}{g_c} \quad Dt_v \quad \text{critical value} = 0.4$$

$$Bo_2 = \left(\frac{2\pi}{\lambda_c} \right)^2 \quad t_v \sqrt{Dt_v} \quad \text{critical value} = 0.05$$

At values of Bond number greater than the critical, the proposed correlations may not be particularly accurate, especially when the value of the liquid heat flux is a significant proportion of the total heat flux.

The Bond numbers defined above obviously include the effects of vapour buoyancy, surface tension, and diameter. The effects of superheat and subcooling are included in the thickness of the vapour film, t_v , because both temperature differences affect the heat flux which in turn affects t_v . The significance of the vapour film thickness is slightly greater in Bo_2 than in Bo_1 , and the significance of the diameter is less in Bo_2 than in Bo_1 .

9.6 Film boiling in detergent solution

Experimental heat transfer data were obtained for film boiling on

the $\frac{1}{8}$ and $\frac{1}{4}$ inch diameter cylinders in 0.01% and 0.025% detergent solutions (figures 13,14). The data show that at moderate and high subcooling more than one stable value of heat flux can occur. Two stable values of heat flux were obtained for the surface temperatures of 1012°F and 1312°F at values of subcooling greater than about 60 and 75 deg F respectively. The larger of the two values are about the same as for water under the same conditions. The smaller values are considerably less than for water, and vary little with subcooling. At the surface temperature of 1612°F , more than two values of heat flux were observed for values of subcooling greater than about 100 deg F, but only a superficial study was carried out at this surface temperature.

The two values of heat flux at 1012°F and 1312°F have been ascribed to the formation of a layer of gel in the liquid at the interface. Such a layer would cause an increase in the overall thermal resistance, and a lower value of heat flux would be observed. Without the layer, the value of heat flux would be about the same as for water. The layer would form near the interface because of the relatively high concentration of detergent due to evaporation of water, but only if the interface was relatively quiescent. The chaotic interface at low subcooling and high superheat prevented the layer from forming.

9.7 Film boiling at high subcooling

At values of dimensionless subcooling, $Sc > 0.1$, in water, no bubbles of vapour were released, and the interface appeared smooth. Under such conditions it might appear that heat transfer would have been independent of the vapour heat flux, i.e. $q_v = 0$, but this was found not to be the case. The theoretical solutions which involve only liquid parameters and therefore imply that $q_v = 0$ are valid for $Sc \gg 1$. These solutions are therefore well outside the range of the present data which extend only to $Sc \approx 0.18$.

The occurrence of film boiling at very large subcooling, when $Sc \gg 1$, is questionable on two counts. Firstly, high values of Sc are possible only if the product $C_L \Delta T_L$ is large, or if h_{fg} is small. Under normal ambient conditions, and with the temperature of the liquid at its freezing point, the maximum values of Sc in water and ethanol are approximately 0.18 and 0.5 respectively, and they may be regarded as typical

liquids in this respect. At high pressure near the critical point, values of h_{fg} become small for all liquids and the condition that $Sc \gg 1$ may be possible.

Secondly, it has been predicted from theory (section 3.7.1) that above a horizontal surface, film boiling is replaced by single phase convection if the value of the liquid heat flux, q_L , becomes much larger than the value of the saturated heat flux q_s . Therefore, if very large subcooling is due to a large value of ΔT_L , and if the value of q_L is thereby also large, then the superheat must also be high to make q_s sufficiently large for film boiling to exist.

9.8 Application of the data

The data presented in this thesis can be applied to circumstances when both saturated and subcooled film boiling occurs. The data for saturated film boiling, both from the review and from the present work can be used to calculate rates of heat transfer for saturated film boiling on a wide range of geometries and sizes. The data could also be used when subcooled film boiling occurs to calculate what would be expected to be minimum rates of heat transfer.

The present data for subcooled film boiling enables accurate values of heat flux to be calculated over the limited range of the test conditions. It could also be used over a wider range of conditions, but with reduced assurance. Some possible methods of extending the application of the present data are as follows :

1. the non-dimensional correlations could be used for other liquids. (Single phase heat transfer data suggests that the correlation incorporating the "best" equation for ethanol would correlate quite well similar organic liquids.)
2. the experimental data and correlations, which have been obtained for the horizontal cylinder, could be modified to apply to other geometries by adjusting the coefficient of the equations in the manner described in section 3.4.
3. it could be assumed that in a given liquid and for the

same degree of subcooling the ratio q_{tot}/q_s is independent of geometry. The present results show this nearly to be the case. At the surface temperature of 1312°F in water (figures 10 - 12), $q_{\text{tot}}/q_s = 2$ at values of subcooling of 107, 103 and 107 deg F for the diameters of $1/8$, $1/4$ and $1/2$ inch respectively. At the surface temperature of 486°F in ethanol (figures 15 - 17), the corresponding values of subcooling are 104, 93 and 85 deg.F. The values of q_{tot}/q_s for water and ethanol could be obtained from the present experimental data, and applied to the data for saturated film boiling which, as mentioned above, covers a relatively wide range of geometries.

4. the value of the liquid heat flux could be estimated from equations for single phase natural convection, and added to the value for saturated film boiling. The equation for single phase laminar convection,

$$\text{Nu} = 0.55 [\text{GrPr}]^{1/4}, \quad (43)$$

has been included in figure 39. The value of q_L would be generally underestimated by this equation.

The above data and procedures would apply only to the film boiling regime. From theoretical considerations some predictions of the Leidenfrost temperature have been made, and in water at 75°F ($\Delta T_L = 137$ deg F) the value works out to be about 1000°F . Random breakdown of film boiling was encountered in the present tests on surfaces at temperatures at which film boiling might at other times exist indefinitely. An analogous, what might be called premature, breakdown of film boiling has been reported in quenching tests (77). Since rates of heat transfer are usually greater in the other boiling regimes than in the film boiling regime, the consequence of premature breakdown is that rates of heat transfer would be higher than the values predicted. Premature breakdown of film boiling due to dirt and scale (section 3.8.3) would likewise result in rates of heat transfer higher

than expected.

9.9 Advances represented by the present work

The new data presented in this thesis represent a number of advances in the field of subcooled film boiling. An experimental technique and suitable test sections have been developed which enabled steady state film boiling to be established and maintained in subcooled liquids. Experimental heat transfer data of high accuracy have been presented for the subcooled film boiling of water, aqueous detergent solution and ethanol on horizontal cylinders of diameters of $1/8$, $1/4$ and $1/2$ inch. The data for water and ethanol have been used to derive correlations for subcooled film boiling. The data for detergent solution led to the discovery that at moderate and high subcooling there may be two, or possibly more, values of heat flux for each value of subcooling and superheat.

Photographic data have been presented for steady film boiling on horizontal and vertical cylinders, and for transient film boiling on vertical and horizontal surfaces, and spheres. These data have enabled new physical models for subcooled film boiling to be defined.

9.10 Further work

There is considerable scope for further work in the field of subcooled film boiling. Using the present apparatus the range of test conditions could be extended to other liquids, higher superheats, and to cylinders of the present sizes in any orientation. Accuracies could be improved by calibrating the thermocouples used to measure the surface temperatures at all operating temperatures, by making corrections for the temperature differences through the wall of the tube, and by making corrections for the differences between the mean heat flux and the heat flux in the horizontal sections. An investigation could be carried out into the variation of the surface temperature around the circumference of the horizontal cylinder.

Better photographs could be obtained by paying more attention to photographic techniques.

Cylinders of larger diameter, in all orientations, could be tested by incorporating a power supply of larger output in the present apparatus.

Tests on such larger sizes at high subcooling could include the study of the

transition of the liquid flow from laminar to turbulent. Tests could be carried out using the present apparatus on other geometries, e.g. vertical and horizontal flat surfaces. It may be advantageous to automate the simultaneous immersion of the test section and the increase in heating rate.

Theoretical solutions are required for the new physical models for subcooled film boiling. The theory at small subcooling would have to take into account the turbulence in the flow of the liquid induced by interfacial disturbances. At large subcooling the possibility of the flow of the liquid becoming turbulent due to its own buoyancy would have to be considered. The development from theoretical consideration of a criterion to differentiate between small and large subcooling may be desirable.

The further new data, both theoretical and experimental would allow the development of correlations for subcooled film boiling of higher accuracy than those presented here, and having a wider range of application.

Further experimental work is required on subcooled film boiling in detergent solution so that an adequate explanation of the occurrence of more than one stable value of heat flux can be developed. It may then be possible to derive some empirical relationships for heat transfer, and ultimately obtain theoretical solutions.

Work in the more distant future may include a theoretical solution for heat transfer in subcooled film boiling in terms of the liquid heat flux only, which would apply under conditions when no vapour is released and $Sc < 1$, for example to some of the present results for water. A special investigation may be useful to find out if, and under what conditions, film boiling with $Sc \gg 1$ is possible. Experimental data on surfaces of uniform temperature, and information in the region of the Leidenfrost temperature, could be obtained for cylinders by using a method involving the condensation of vapours. The condensation of steam may be satisfactory when surface temperatures are low, e.g. in the film boiling of ethanol. It may be possible to use heat pipes to obtain data for the boiling of water in the region of the Leidenfrost temperature.

On the problem of heat transfer during quenching, there is scope

for further work in other areas besides pool film boiling. A better understanding of the mechanisms of the breakdown of film boiling is desirable, and data on the values of the Leidenfrost temperature are required. Data on subcooled pool transitional and nucleate boiling would be necessary to construct complete cooling curves. For spray boiling, an investigation covering all three boiling regimes is necessary.

Table 1. Ranges of test results.

Table 1a. Heat Transfer on horizontal cylinders.

Liquid	Surface Temp. T_w °F (T_w in °C in brackets)	Dimensionless Superheat $C \frac{\Delta T_v}{h_{fg}}$	Subcooling ΔT_L deg F (ΔT_L in K in brackets)		
			1/8" dia.	1/4" dia.	1/2" dia.
Water	1012 (544)	0.397	2- 90 (1- 50)	0-155 (0- 86)	1- 50 (1- 28)
ditto	1312 (711)	0.56	2-135 (1- 75)	0-155 (0- 86)	2-120 (1- 67)
ditto	1612 (890)	0.735	2-135 (1- 75)	0-155 (0- 86)	- -
Detergent solution	1012 (544)		10- 80 (5- 44)	50- 95 (28- 53)	- -
ditto	1312 (711)		20- 95 (11- 53)	50-155 (28- 86)	- -
ditto	1612 (888)		10-135 (5- 75)	50-155 (28- 86)	- -
Ethanol	486 (252)	0.39	2-100 (1- 55)	2-100 (1- 55)	2-100 (1- 55)
ditto	590 (310)	0.55	2-100 (1- 55)	2-100 (1- 55)	2-100 (1- 55)
ditto	698 (370)	0.727	2-100 (1- 55)	2-100 (1- 55)	2-100 (1- 55)
ditto	1012 (544)	1.305	-	10-110 (5- 61)	-

Table 1b. Photos of steady film boiling.

Liquid	size and geometry	Lighting	Surface Temp. T_w °F	Subcooling ΔT_L in deg F	Fig. No.
Water	1/8" diameter horizontal cylinder	Silhouette Direct	1312 "	22,63,89 22,89	} 25
ditto	1/4" diameter horizontal cylinder	Silhouette ditto ditto	1612 1312 1012	22,63,89,112 22,63,89,112 ditto)) 21)
ditto	1/2" diameter horizontal cylinder	Silhouette Direct ditto	1312 "	55,60,65,70,75 ditto 22,63,89) 26) 25
Detergent solution	1/4" diameter horizontal cylinder	Silhouette ditto ditto ditto ditto	1612 1312 1012 1312 1012	22,63,89 ditto ditto 90 high q, 90 low q 60 high q, 60 low q)) 22)) 24)
Ethanol	1/4" diameter horizontal cylinder	Silhouette ditto ditto	698 590 486	10,46,72,97 ditto ditto)) 23)
Water	8" high vertical cylinders	Direct ditto	1312 1290	5,22 50) 27)
Detergent solution	ditto	Direct	1312	22,50,63,89	28
Ethanol	ditto	Direct	590	28,90	29

Table 1c. Photos of transient film boiling.

Liquid	Size and geometry	Lighting	Surface Temp. T_w $^{\circ}\text{F}$	Subcooling ΔT_L in deg F	Fig. No.
Water	2" high vertical surface	Direct "	1312 1012	5,50,89 5,50)) 30
Ethanol	ditto	Direct " " "	698 590 486 300	28,50 28,50,112 28,50 28,50,112))) 31)
Water	4" diameter sphere	Direct	1312	5,50,90	32
Detergent solution	ditto	Direct	1312	5,50,89	33
Water	2" x 9" upward facing horizontal surface	Direct	1312	50,89	34

Table 2. Values of Bond Numbers (see section 8.4.2)

Table 2a. Values of $Bo_1 = \left(\frac{2\pi}{\lambda_c}\right)^2 Dt_v$ for WATER.

ΔT_L deg F	1/8" diameter tube			1/4" diameter tube			1/2" diameter tube	
	T_w °F			T_w °F			T_w °F	
	1012	1312	1612	1012	1312	1612	1012	1312
102		0.06 x	0.08 x	0.09 x	0.14 x	0.20 x		0.32 x
92	0.04 x	0.06 x	0.09 x	0.10 x	0.15 x	0.22 x		0.34 x
82	0.05 x	0.07 x	0.09 x	0.11 x	0.16 x	0.23 x		0.38 x
72	0.05 x	0.07 x	0.10 x	0.12 x	0.18 x	0.25 x		0.40 ?
62	0.06 x	0.08 x	0.11 x	0.13 x	0.19 x	0.26 x		0.41 ✓
52	0.07 x	0.09 x	0.12 x	0.15 x	0.21 ?	0.28 ✓	0.33 ✓	0.44 ✓
42	0.07 x	0.10 x	0.13 x	0.17 x	0.23 ✓	0.29 ✓	0.36 ✓	0.47 ✓
32	0.08 x	0.11 x	0.14 x	0.19 x	0.25 ✓	0.31 ✓	0.39 ✓	0.52 ✓
22	0.09 x	0.12 x	0.15 x	0.21 x	0.27 ✓	0.33 ✓	0.43 ✓	0.59 ✓
12	0.10 x	0.13 x	0.16 x	0.24 x	0.34 ✓	0.38 ✓	0.51 ✓	0.69 ✓

Limits 0.2, 0.4

Table 2b. Values of $Bo_1 = \left(\frac{2\pi}{\lambda_c}\right)^2 Dt_v$ for ETHANOL.

ΔT_L deg F	Diameter D = 1/8"			Diameter D = 1/4"			Diameter D = 1/2"		
	T_w °F			T_w °F			T_w °F		
	486	590	698	486	590	698	486	590	698
105	0.08 x	0.11 x	0.13 x	0.19 x	0.25 x	0.30 x			
87	0.09 x	0.12 x	0.15 x	0.21 x	0.27 x	0.32 x	0.45 ✓	0.58 ✓	0.69 ✓
69	0.11 x	0.13 x	0.16 x	0.23 ✓	0.30 x	0.35 ✓	0.49 ✓	0.63 ✓	0.73 ✓
51	0.12 x	0.15 x	0.18 x	0.26 ✓	0.32 x	0.38 ✓	0.56 ✓	0.69 ✓	0.77 ✓
33	0.14 x	0.17 x	0.19 x	0.30 ✓	0.37 x	0.43 ✓	0.63 ✓	0.75 ✓	0.89 ✓
15	0.16 x	0.19 x	0.22 ?	0.35 ✓	0.42 x	0.48 ✓	0.77 ✓	0.90 ✓	1.04 ✓

Limits 0.2, 0.32

Table 2c. Values of $Bo_2 = \left(\frac{2\pi}{\lambda_c} \right)^2 t_v \sqrt{Dt_v}$ for WATER

ΔT_L deg F	Diameter D = 1/8"			Diameter D = 1/4"			D = 1/2"	
	T_w °F			T_w °F			T_w °F	
	1012	1312	1612	1012	1312	1612	1012	1312
102								0.036x
92								0.039x
82						0.042 x		0.045x
72					0.028 x	0.048 x		0.050?
62	0.011 x	0.018 x	0.029 x	0.019 x	0.033 x	0.052 x		0.051/
52	0.013 x	0.021 x	0.033 x	0.022 x	0.037 ?	0.057 /	0.038 /	0.057/
42	0.018 x	0.024 x	0.037 x	0.027 x	0.043 /	0.062 /	0.042 /	0.063/
32	0.019 x	0.028 x	0.041 x	0.032 x	0.048 /	0.067 /	0.047 /	0.073/
22	0.021 x	0.032 x	0.046 x	0.038 x	0.055 /	0.075 /	0.055 /	0.089/
12	0.024 x	0.035 x	0.051 x	0.045 x	0.065 /	0.089 /	0.072 /	0.112/

Limits 0.037, 0.052

Table 2d. Values of $Bo_2 = \left(\frac{2\pi}{\lambda_c} \right)^2 t_v \sqrt{Dt_v}$ for ETHANOL

ΔT_L deg F	Diameter D = 1/8"			Diameter D = 1/4"			Diameter D = 1/2"		
	T_w °F			T_w °F			T_w °F		
	486	590	698	486	590	698	486	590	698
105	0.012 x	0.017x	0.026 x	0.019x	0.030x	0.039 x			
87	0.014 x	0.020x	0.027 x	0.023x	0.033 x	0.044 x	0.037/	0.053/	0.069/
69	0.017 x	0.024x	0.031 x	0.027/	0.039/	0.050/	0.042/	0.060/	0.075/
51	0.020 x	0.027x	0.036 x	0.032/	0.044/	0.058/	0.051/	0.069/	0.081/
33	0.025 x	0.032x	0.041 x	0.039/	0.053/	0.067/	0.060/	0.079/	0.101/
15	0.030 x	0.038x	0.047 ?	0.050/	0.066/	0.080/	0.081/	0.104/	0.128/

Limits 0.027, 0.05



Illustration removed for copyright restrictions

Figure 1. Typical boiling curves (1,2). The values of q and ΔT_v are approximate only, and apply to water. For other liquids, e.g. ethanol, the values of both q and ΔT_v are smaller (3).



Illustration removed for copyright restrictions

Figure 2. Simplified transformation diagram for a carbon steel (5), (section 2.2).

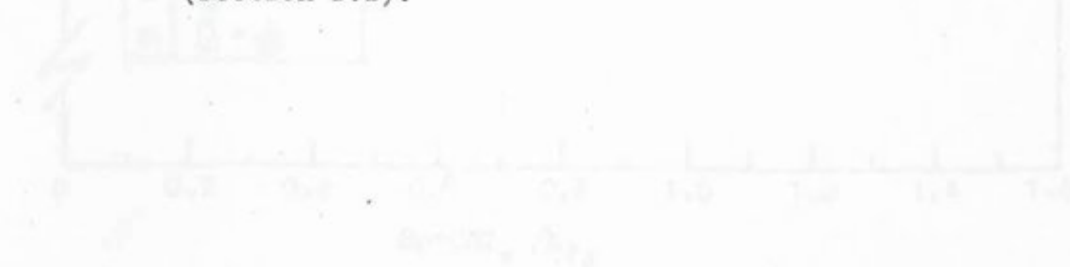


Figure 3. Comparison of the values of the maximum value of the smaller work (see section 1.5). The values of B_0 for the present results are also shown.

Table of the values of $f(Sp)^{\frac{1}{4}}$

$h_{fg} = h_v - h_L$	$f(Sp)$	Sp					ref.
		0	0.3	0.6	1.0	1.5	
$h_{fg} + \frac{1}{2}CAT_v$	$\frac{1}{2} + \frac{1}{Sp}$	∞	1.40	1.21	1.11	1.04	30
$h_{fg}(1+0.4Sp)^2$	$\frac{1}{Sp}(1+0.4Sp)^2$	"	1.43	1.27	1.18	1.14	32
$h_{fg}(1+0.34Sp)^2$	$\frac{1}{Sp}(1+0.34Sp)^2$	"	1.42	1.25	1.16	1.11	31
$h_{fg} + 0.4CAT_v$	$0.4 + \frac{1}{Sp}$	"	1.39	1.20	1.10	1.02	46
h_{fg}	$\frac{1}{Sp}$	"	1.35	1.14	1.00	0.90	41
$h_{fg} + \frac{19}{20}CAT_v$	$\frac{19}{20} + \frac{1}{Sp}$	"	1.44	1.27	1.18	1.13	50

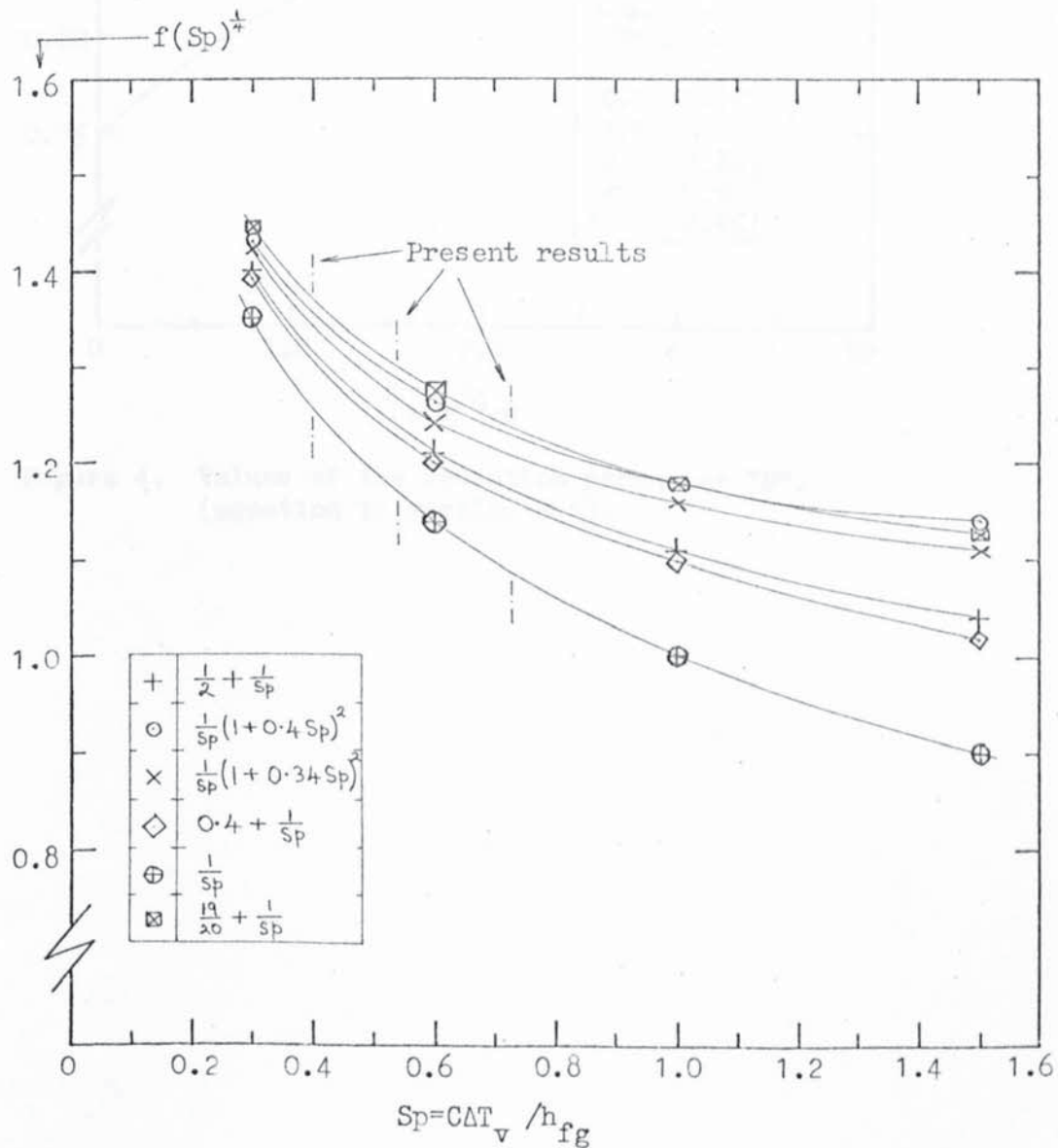


Figure 3. Comparison of the values of the superheat terms from earlier work (see section 3.5). The values of Sp for the present results are also shown.

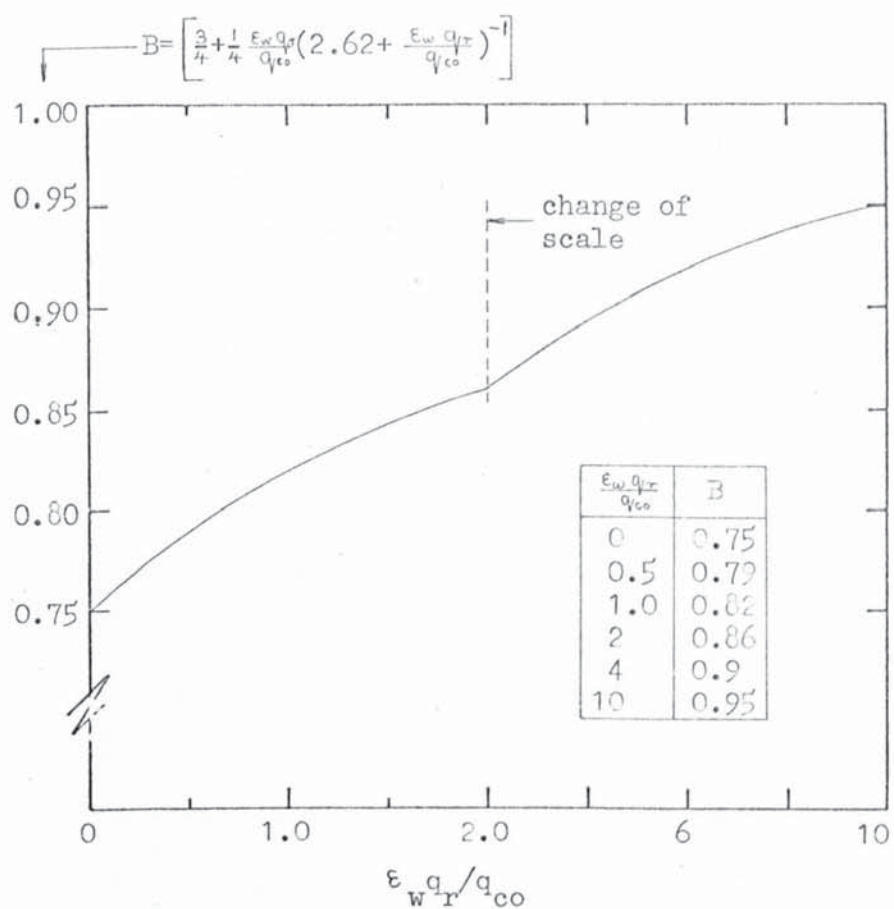


Figure 4. Values of the radiation parameter "B",
(equation 32, section 3.6).

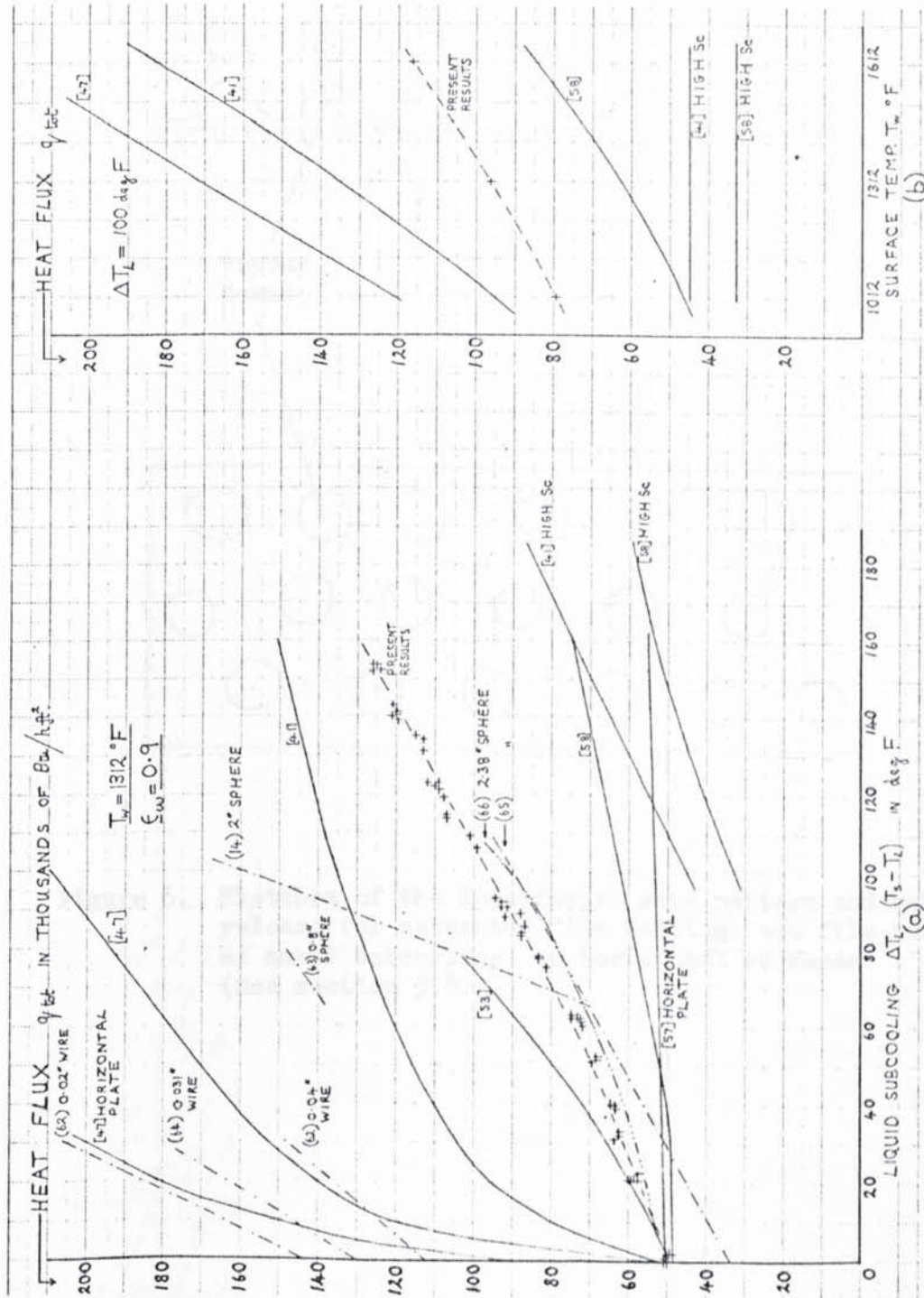


Figure 5 a) and b). Comparison of data for the film boiling of water, a) at the surface temperature of 1312°F, and b) at the subcooling of 100 degF (see section 3.7.3). The key to the diagram is given on the opposite page.

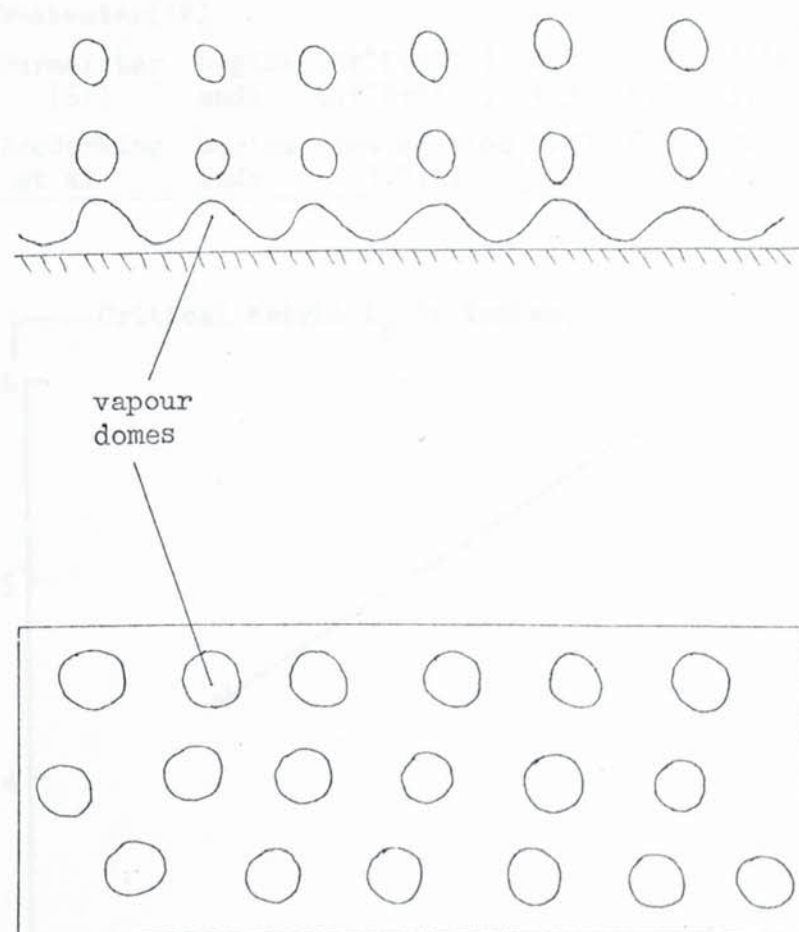


Figure 6. Sketches of the interfacial wave pattern and bubble release for saturated film boiling, and film boiling at small subcooling, on horizontal surfaces. (See section 3.8.1.)

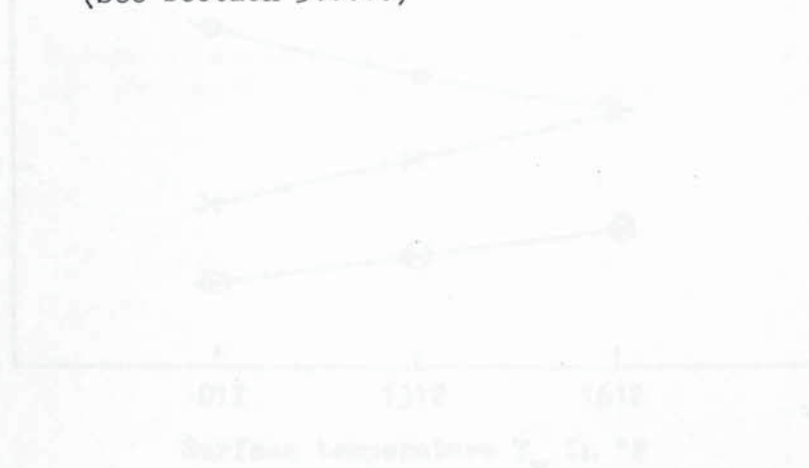


Figure 7. Comparison of the predicted time for the values of the critical height L_c for the transition from laminar to turbulent flow for the saturated film boiling of water on a vertical surface. (See section 3.8.1.)

Table of the values of the critical height L_c in inches.

Authors		T_w °F	1012	1312	1612	
Hsu and Westwater(42)			1.67	1.43	1.29	⊙
Burmeister (61)	begins ($Gr^*Pr=10^9$)		2.03	2.34	2.64	⊕
	ends ($Gr^*Pr=10^{10}$)		4.38	5.04	5.63	+
Frederking et al	begins (see section 3.8.1)		0.43	0.56	0.60	⊗
	ends		0.82	1.05	1.37	×

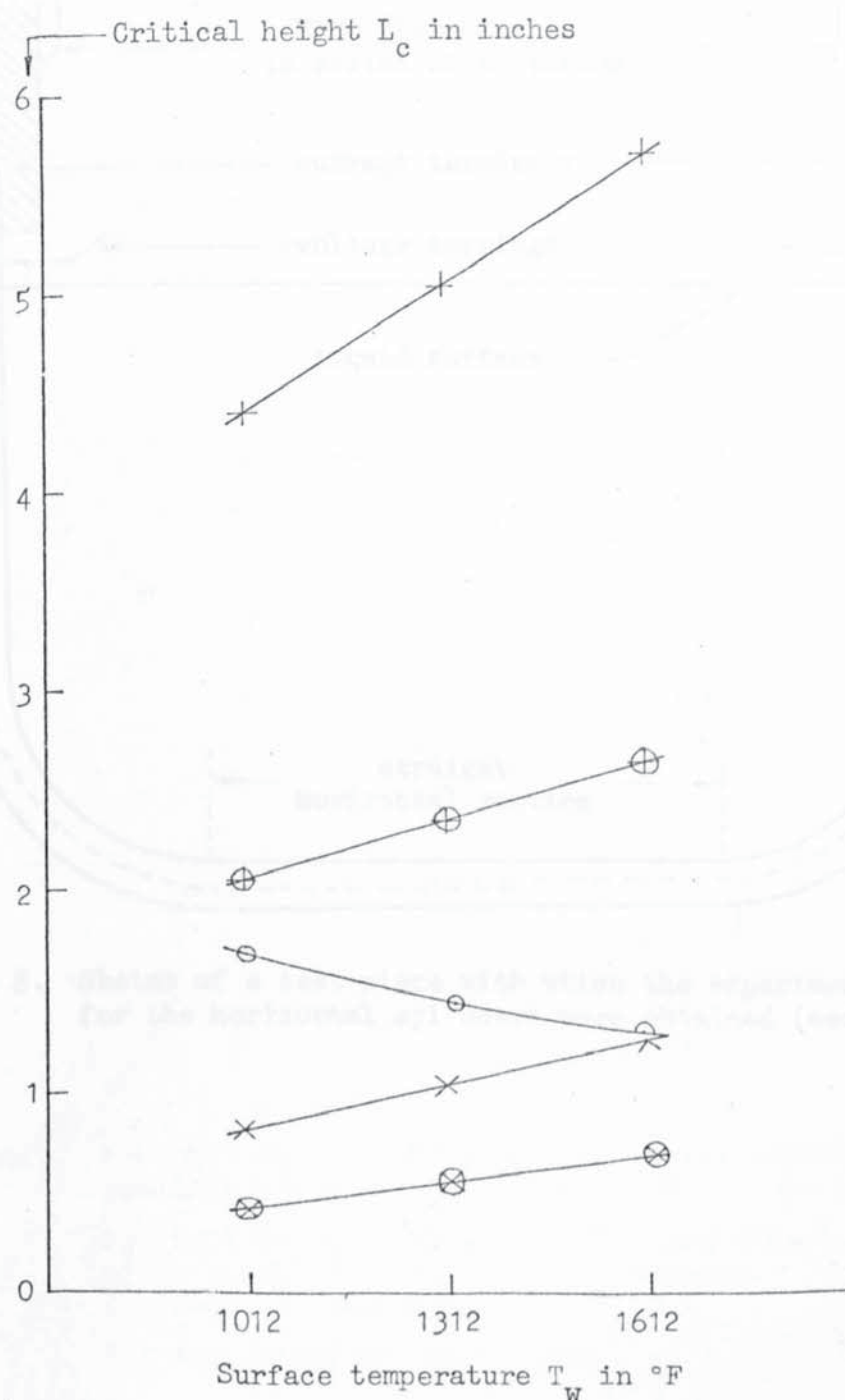


Figure 7. Comparison of the published data for the values of the critical height L_c , for the transition from laminar to turbulent flow for the saturated film boiling of water on a vertical surface. (see section 3.8.1).

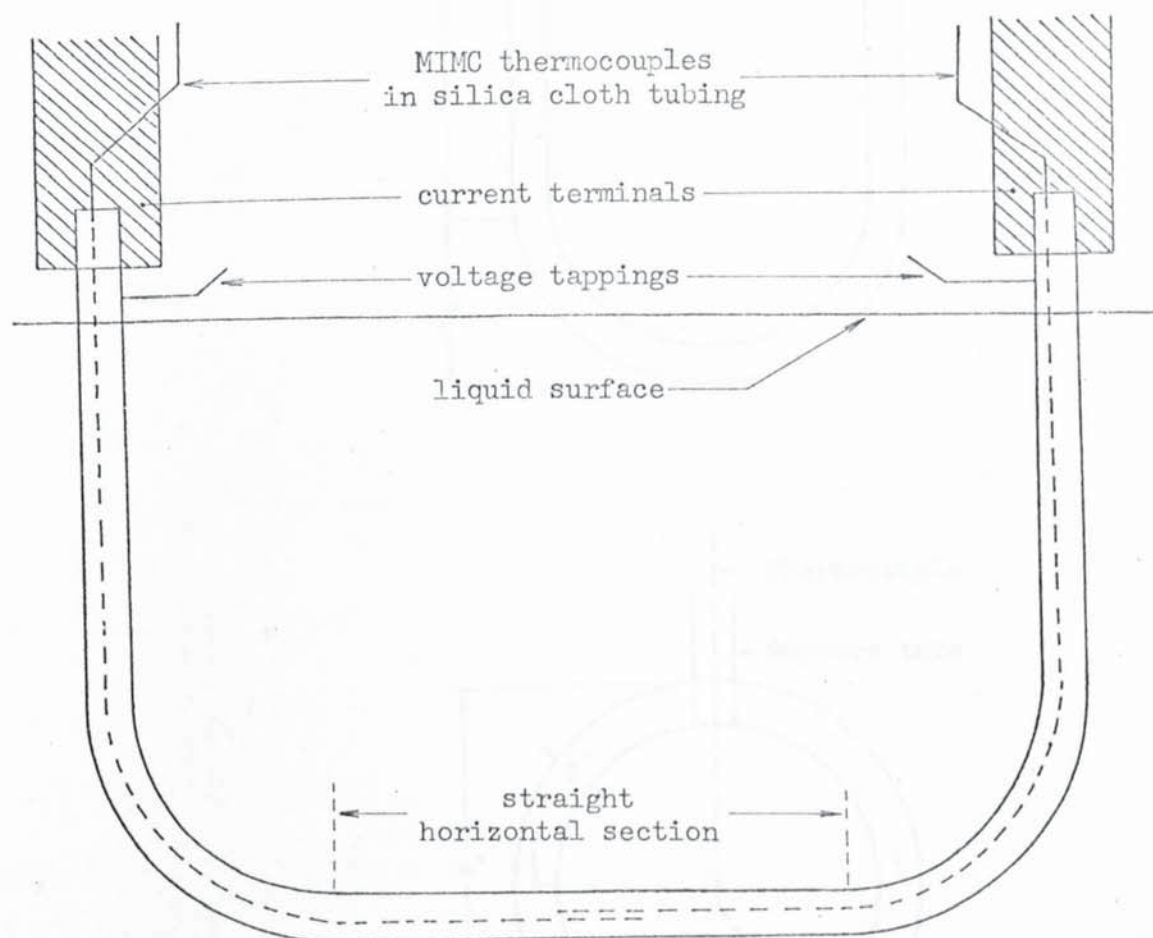


Figure 8. Sketch of a test-piece with which the experimental data for the horizontal cylinders were obtained (section 5.2).

Figure 9. Sketches of the additional test-pieces used in the photographs of Fig. 5.3).

- a) (top) vertical cylinder of 1-inch diameter;
- b) (bottom) sphere of 1-inch diameter;
- c) (center) on next page.

All dimensions are approximate.

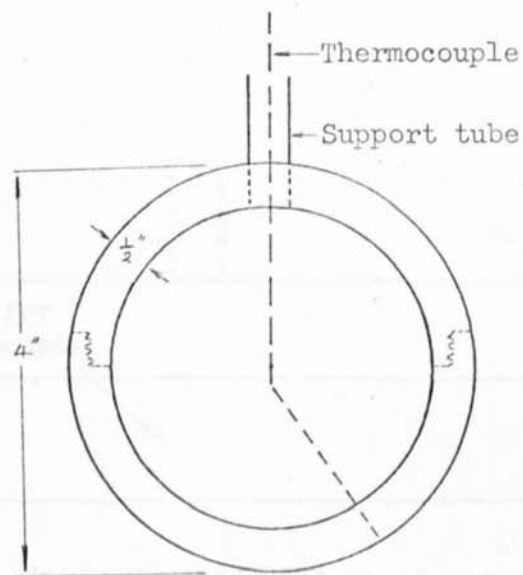
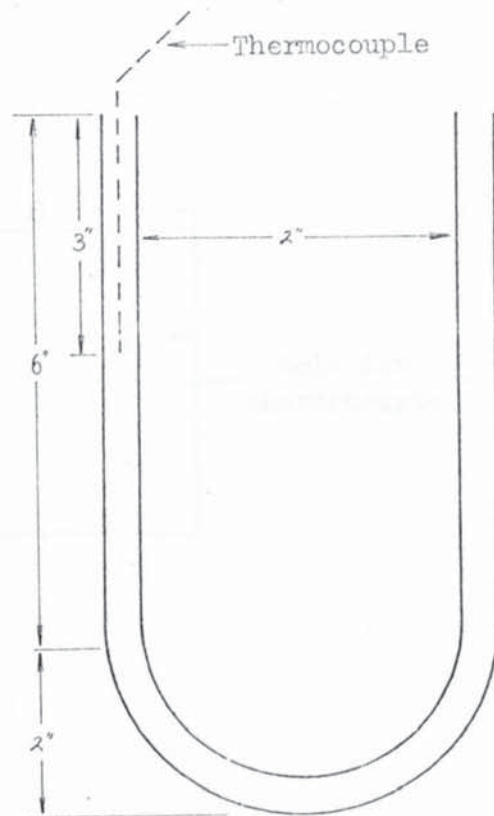


Figure 9. Sketches of the additional test-pieces used in the photographic study (see section 5.3).

- a) (top) vertical cylinders of $\frac{1}{4}$ -inch diameter,
- b) (bottom) sphere of 4 inches diameter,
- c) (cont. on next page).

All dimensions are approximate.

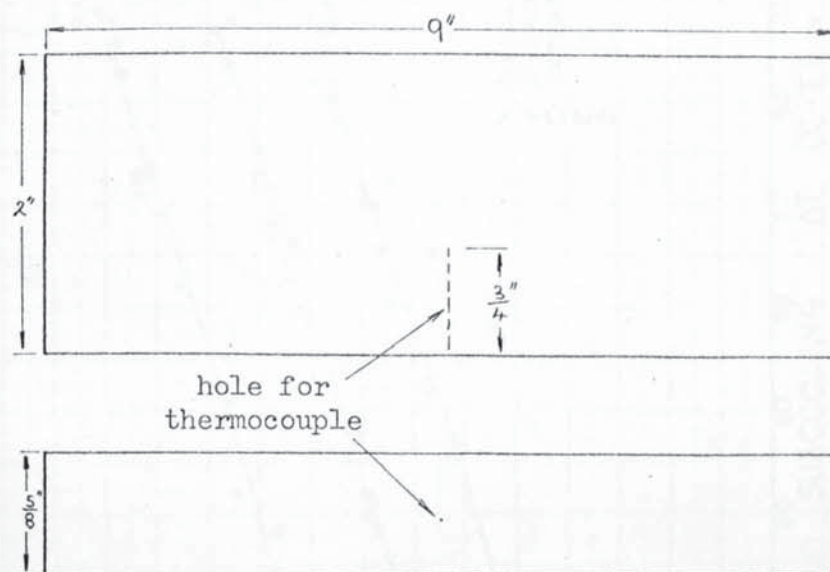
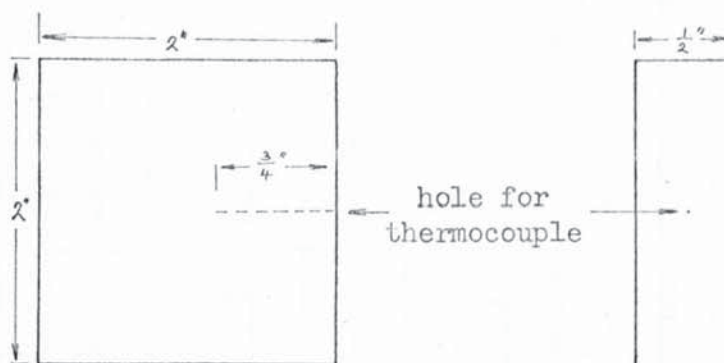


Figure 9 (cont.). Sketches of the additional test-pieces used in the photographic study (see section 5.3).

- c) (top) vertical surface 2 inches high,
- d) (bottom) horizontal surface 2x9 inches.

All dimensions are approximate.

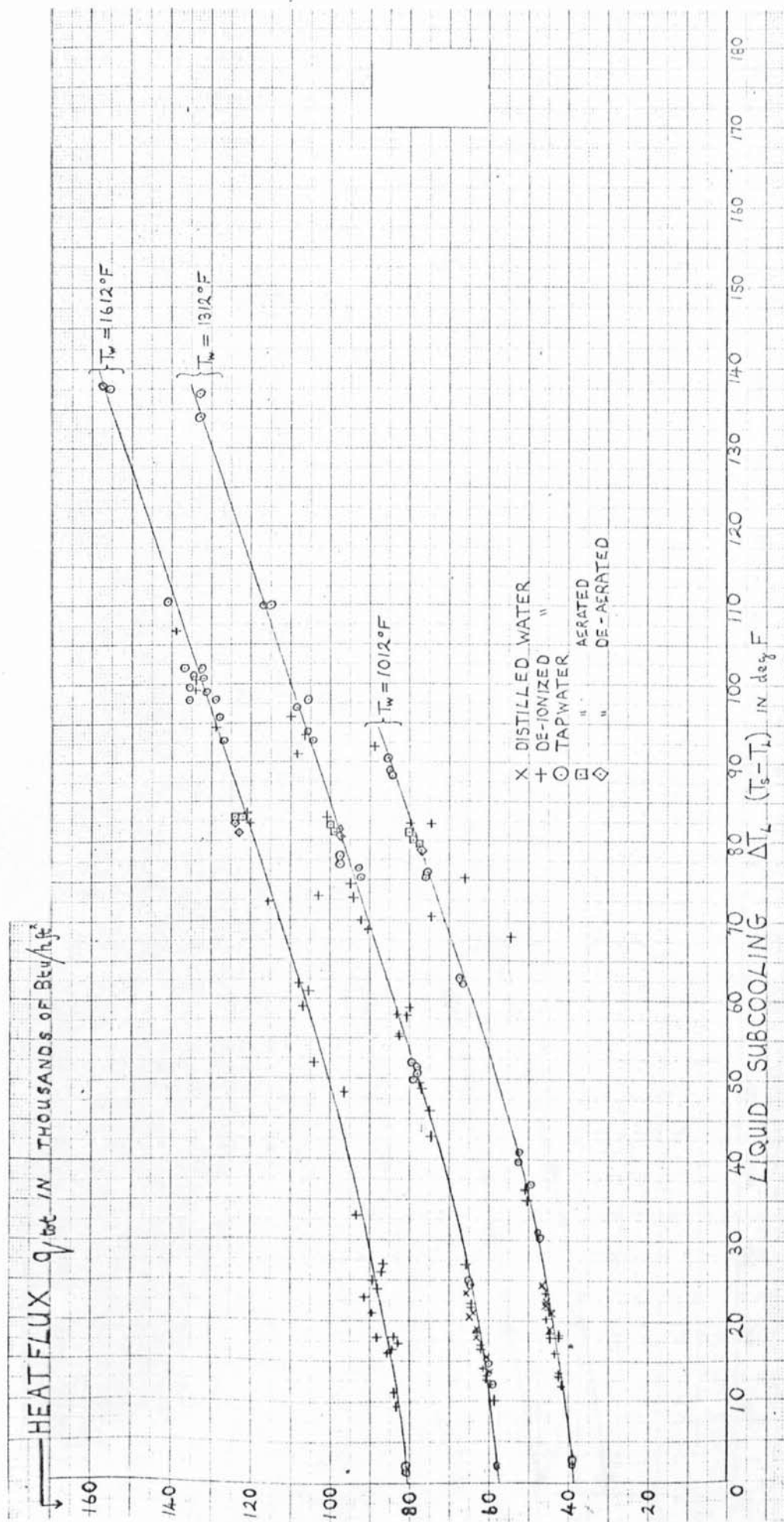


Figure 10. Present experimental data for the steady film boiling of water on $\frac{1}{8}$ -inch diameter horizontal cylinders. The lines represent the mean of the data for each surface temperature.

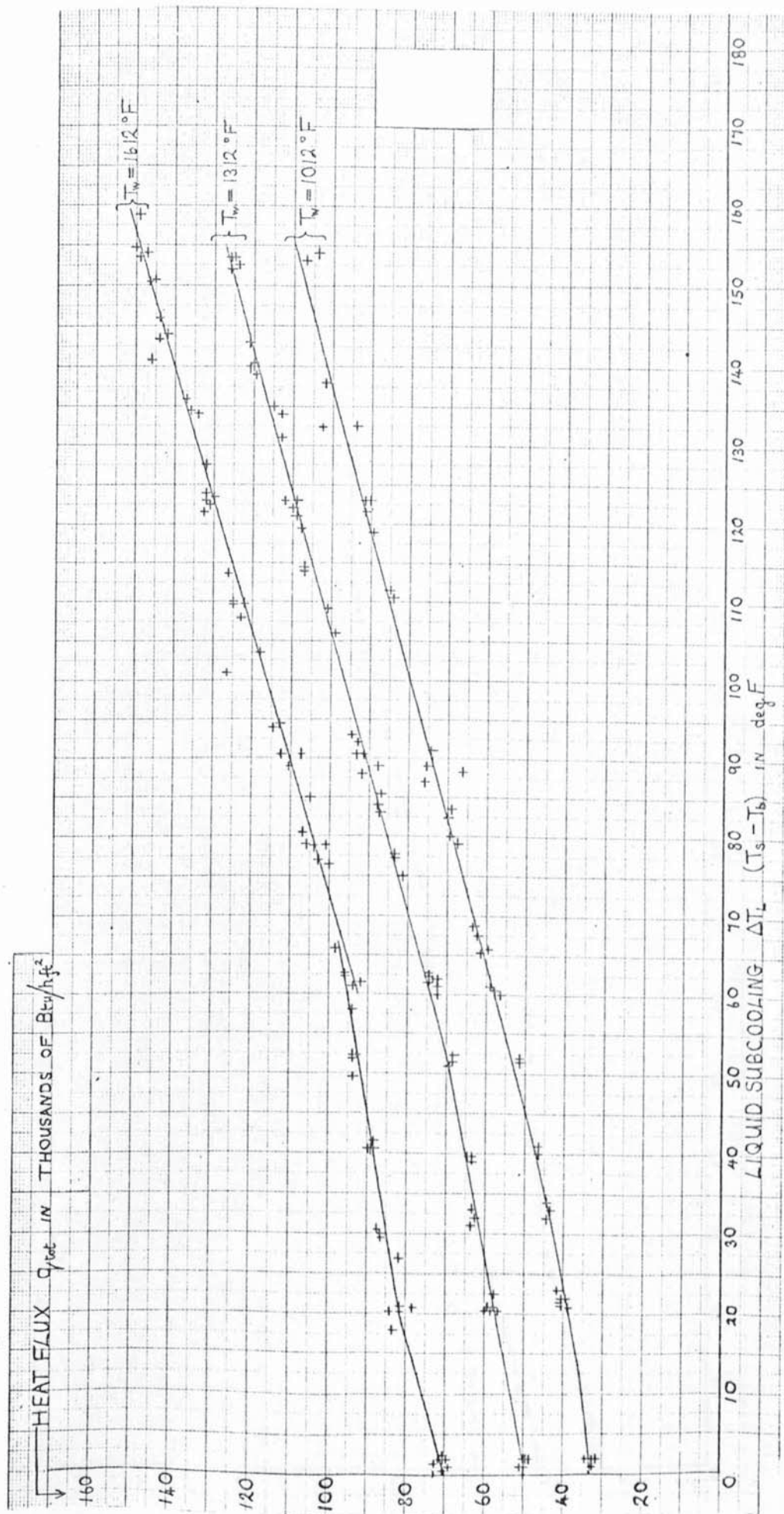


Figure 11. Present experimental data for the steady film boiling of water on 1/4-inch diameter horizontal cylinders. The lines represent the mean of the data for each surface temperature.

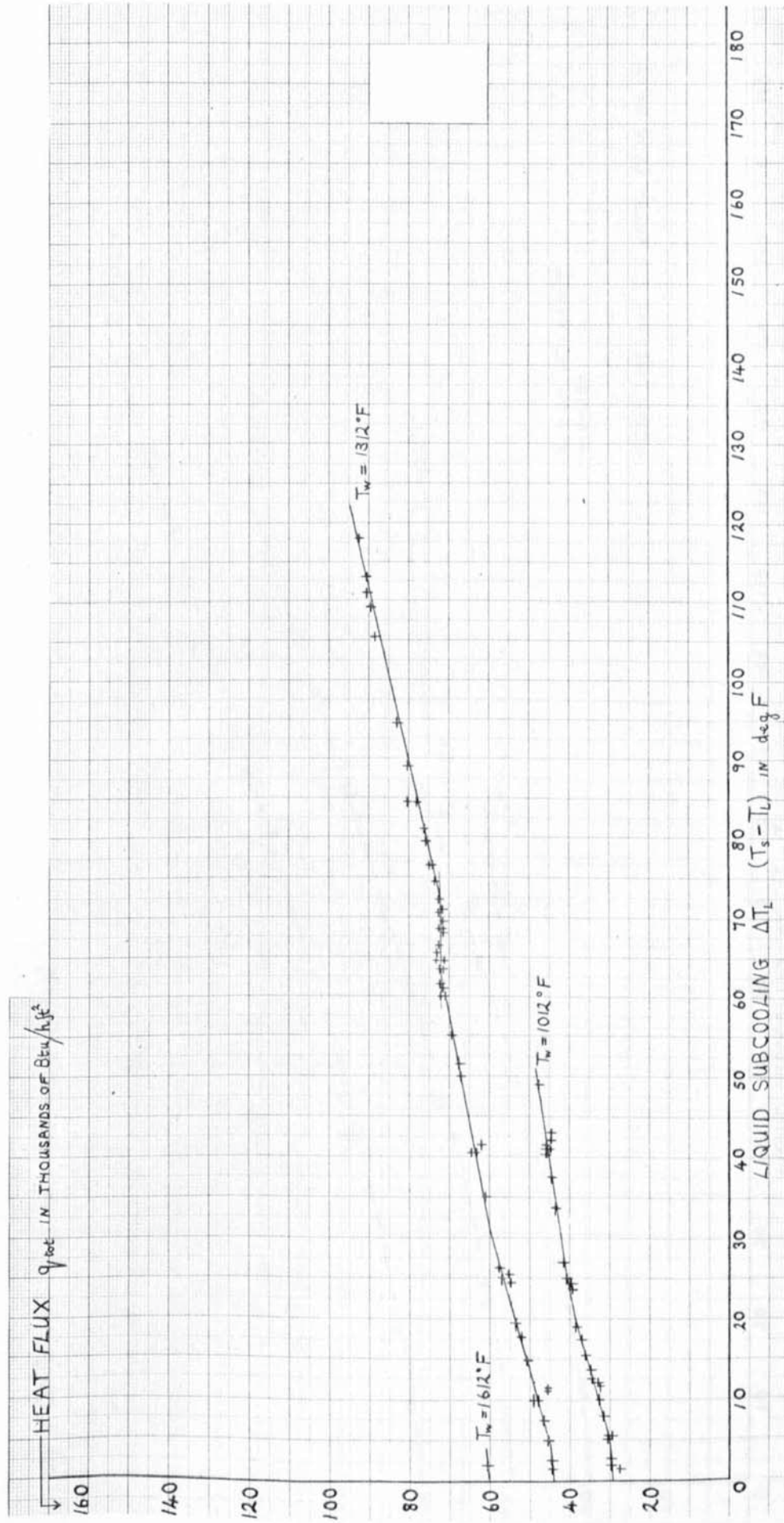


Figure 12. Present experimental data for the steady film boiling of water on $\frac{1}{2}$ -inch diameter horizontal cylinders. The lines represent the mean of the data for each surface temperature.

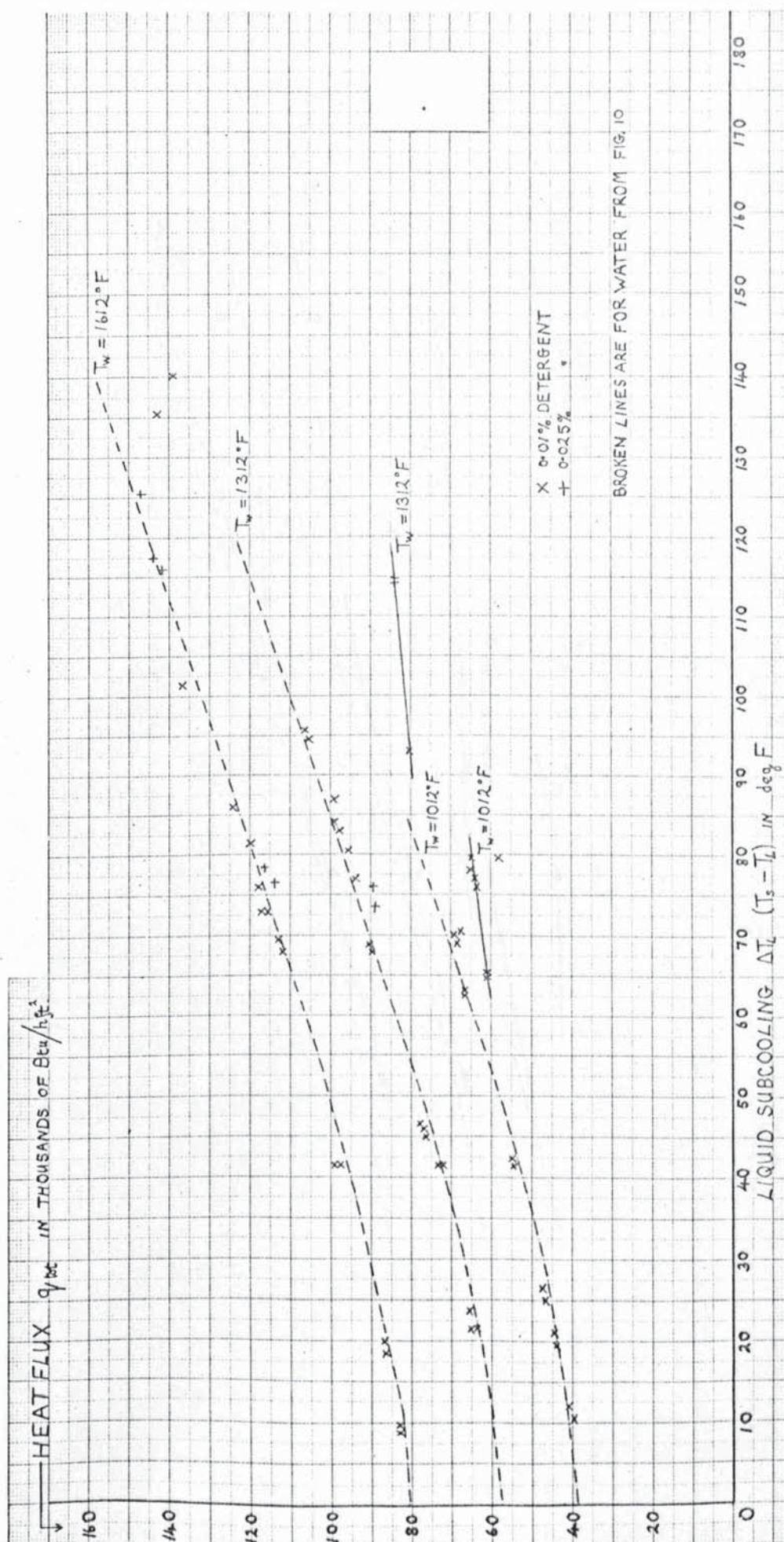


Figure 13. Present experimental data for the steady film boiling of detergent solution on $\frac{1}{8}$ -inch diameter horizontal cylinders.

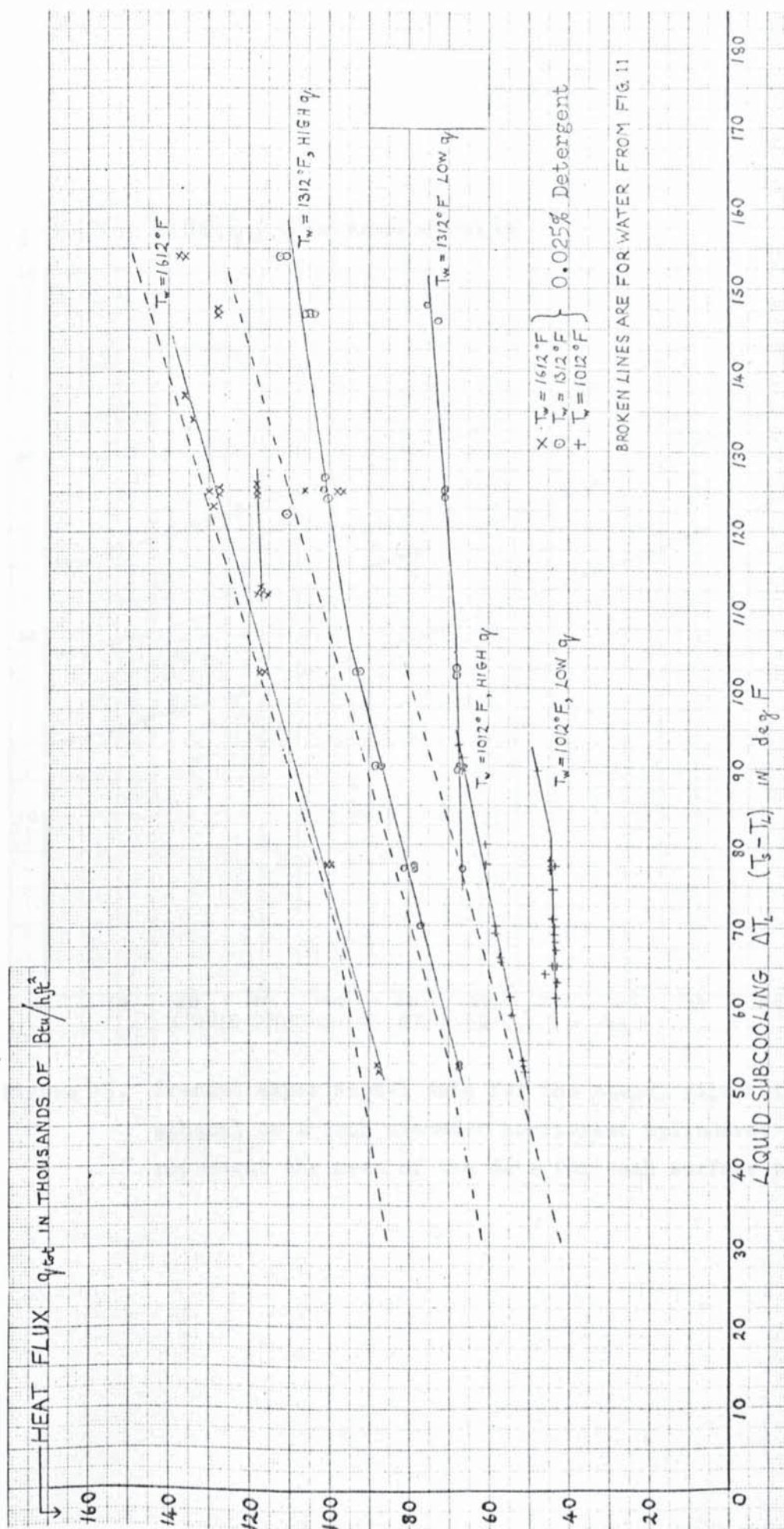


Figure 14. Present experimental data for the steady film boiling of detergent solution on $\frac{1}{8}$ -inch diameter horizontal cylinders. The full lines represent the mean of this data for each surface temperature.

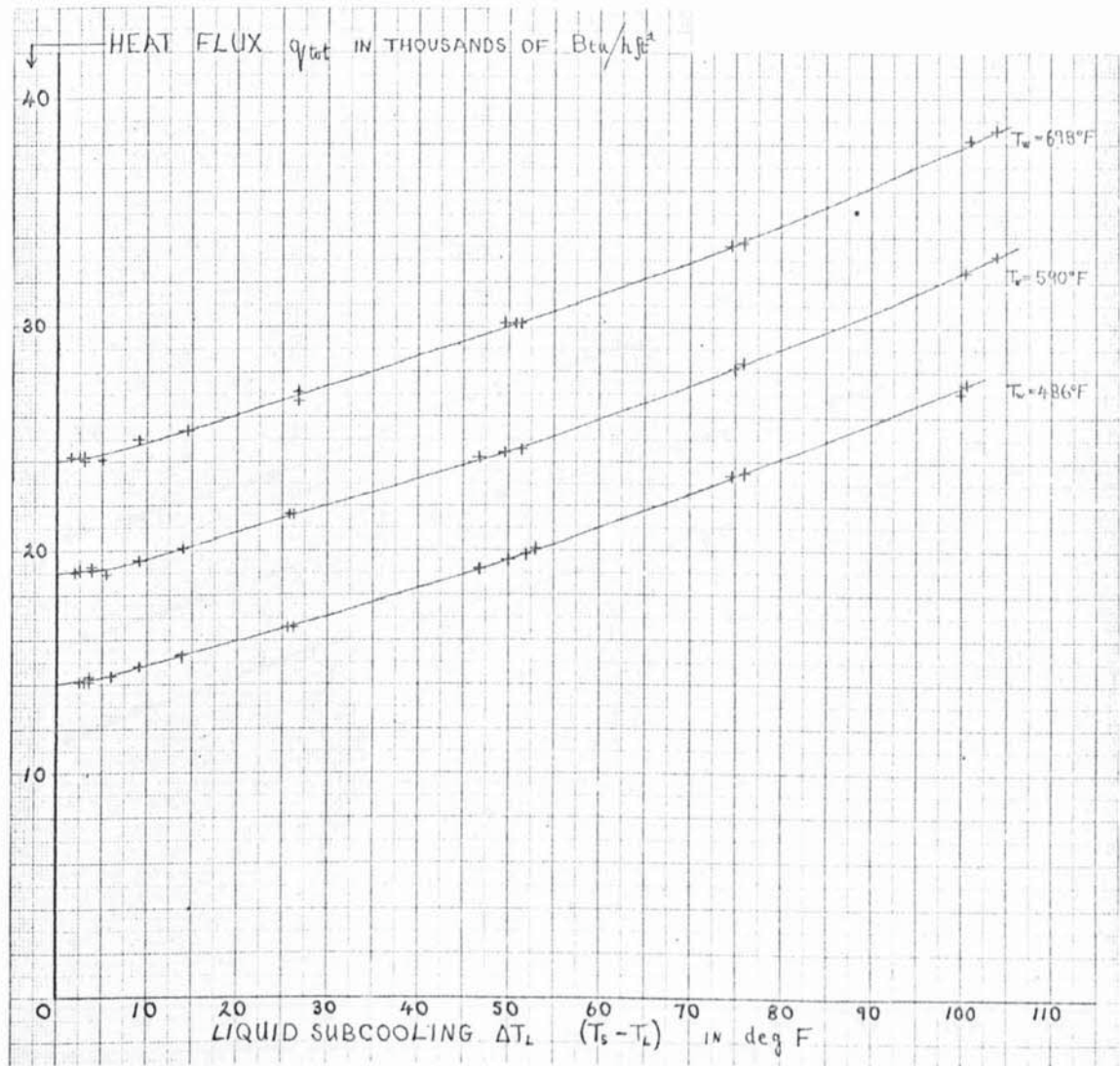


Figure 15. Present experimental data for the steady film boiling of ethanol on $\frac{1}{8}$ -inch diameter horizontal cylinders. The lines represent the mean of the data for each surface temperature.

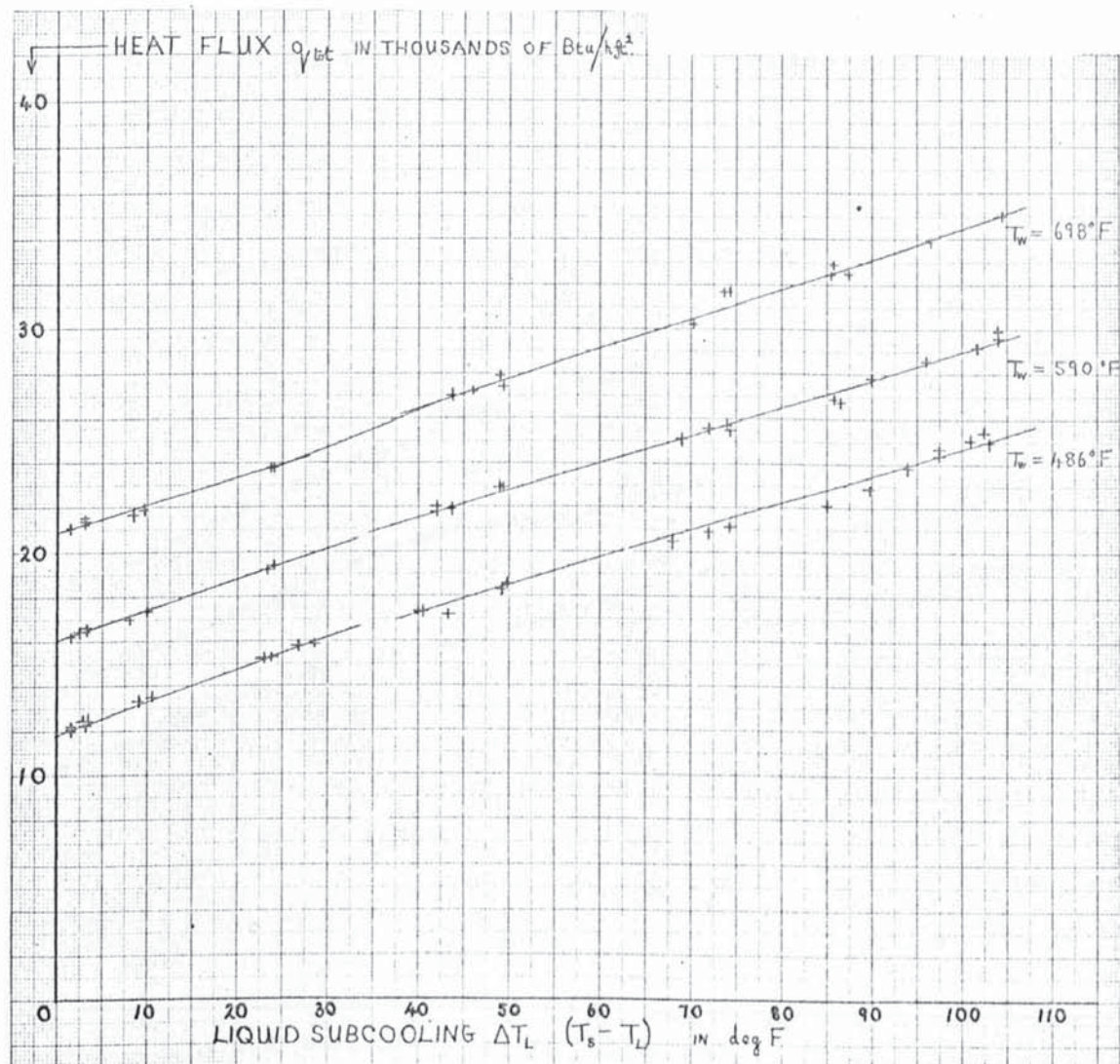


Figure 16. Present experimental data for the steady film boiling of ethanol on $\frac{1}{4}$ -inch diameter horizontal cylinders. The lines represent the mean of the data for each surface temperature.

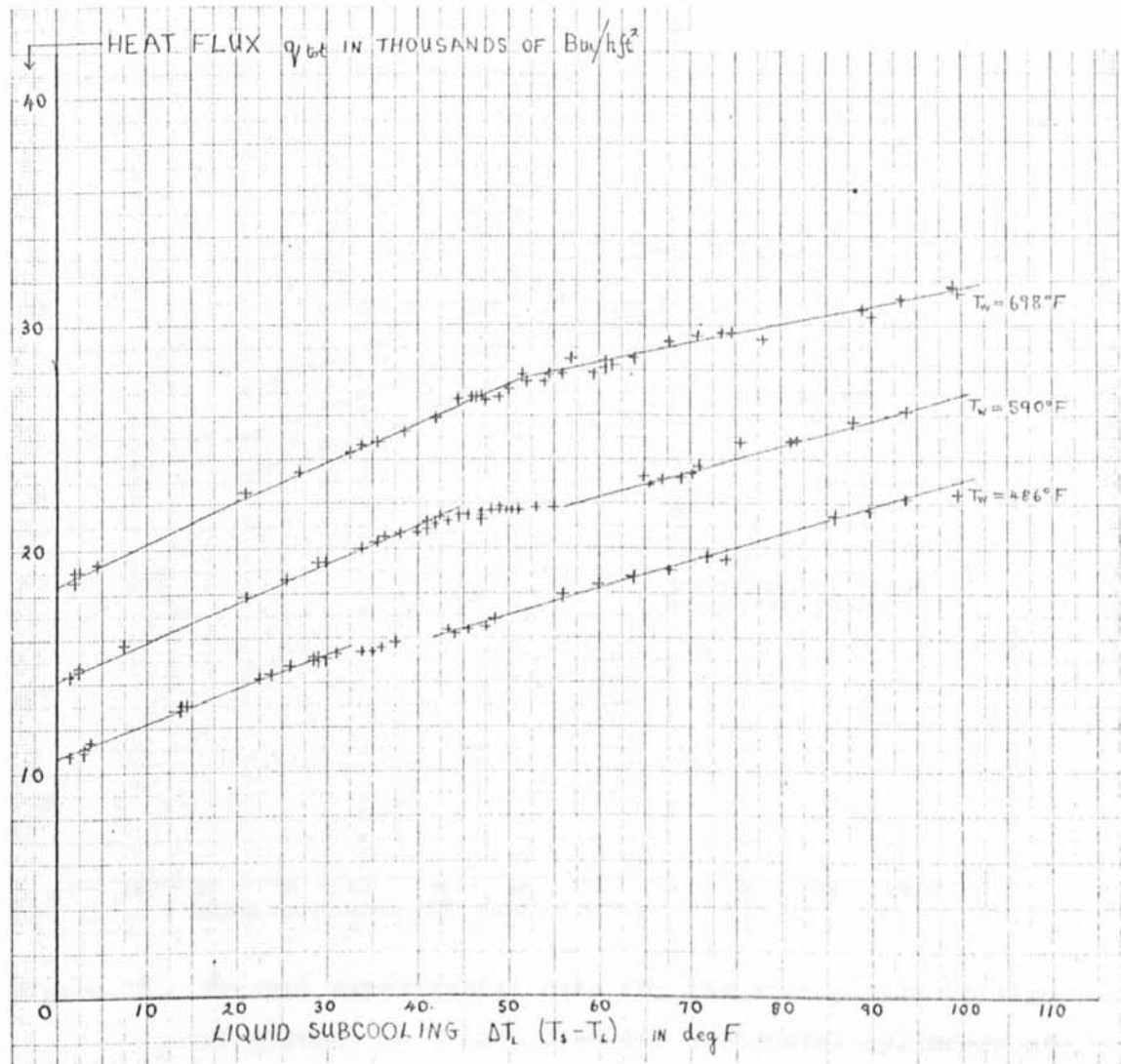


Figure 17. Present experimental data for the steady film boiling of ethanol on $\frac{1}{2}$ -inch diameter horizontal cylinders. The lines represent the mean of the data for each surface temperature.

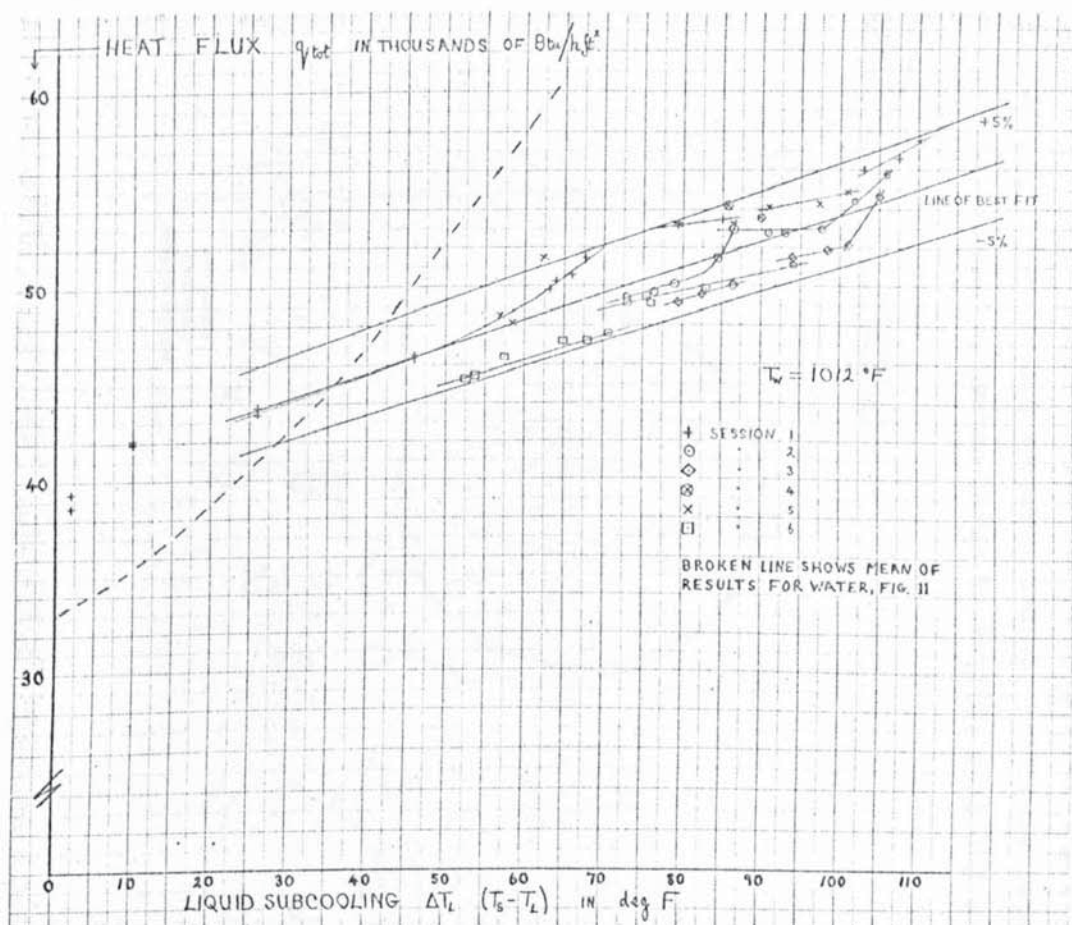


Figure 18. Present experimental data for the steady film boiling of ethanol on $\frac{1}{4}$ -inch diameter horizontal cylinders at the surface temperature of $1012^\circ F$. The lines represent the mean of the data and $\pm 5\%$ of the mean. (See section 7.6).

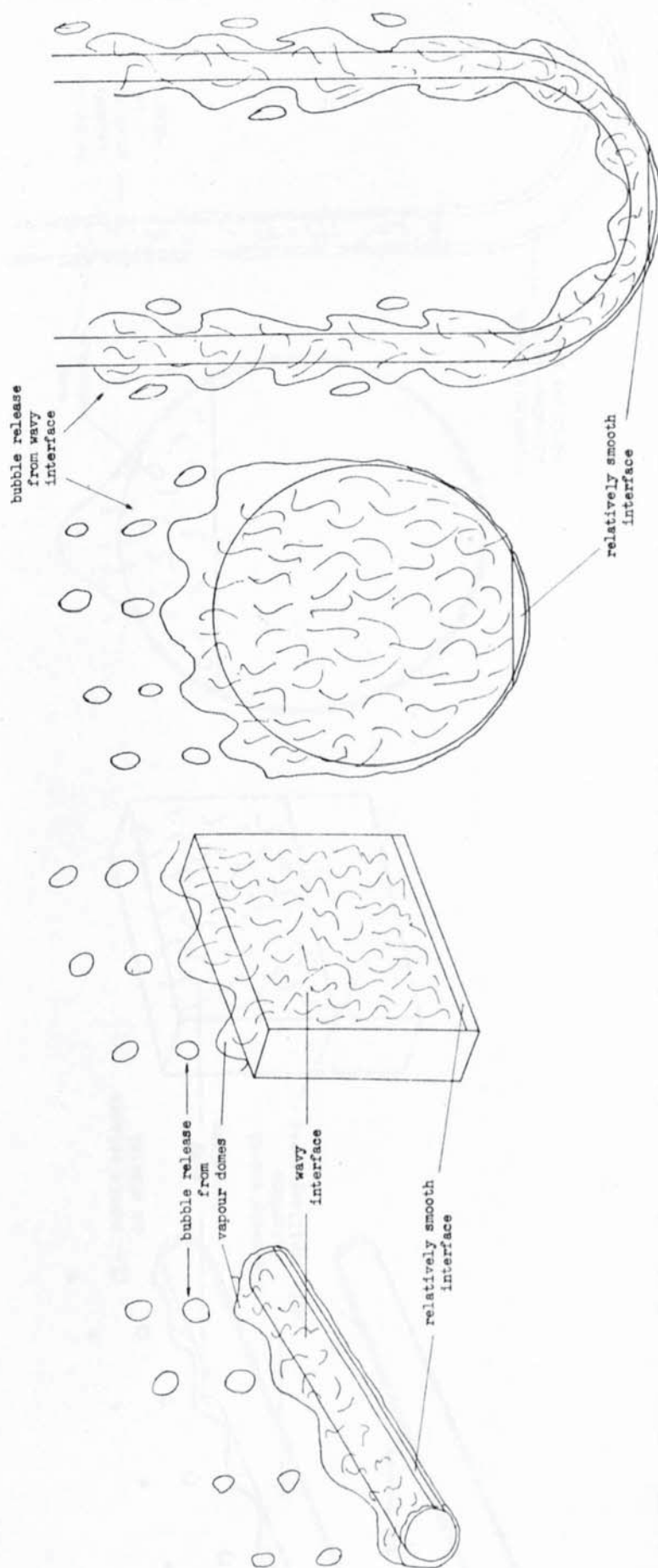


Figure 19. Summary of the photographic results for film boiling at small values of subcooling ($\Delta T_L < \text{about } 20 \text{ degF}$).

Approximate dimensions and geometries are: $\frac{1}{8}$, $\frac{1}{4}$, $\frac{1}{2}$ -inch diameter horizontal cylinders, 2-inch high vertical surface, 4-inch diameter sphere, and 8-inch high vertical cylinders of $\frac{1}{4}$ -inch diameter.

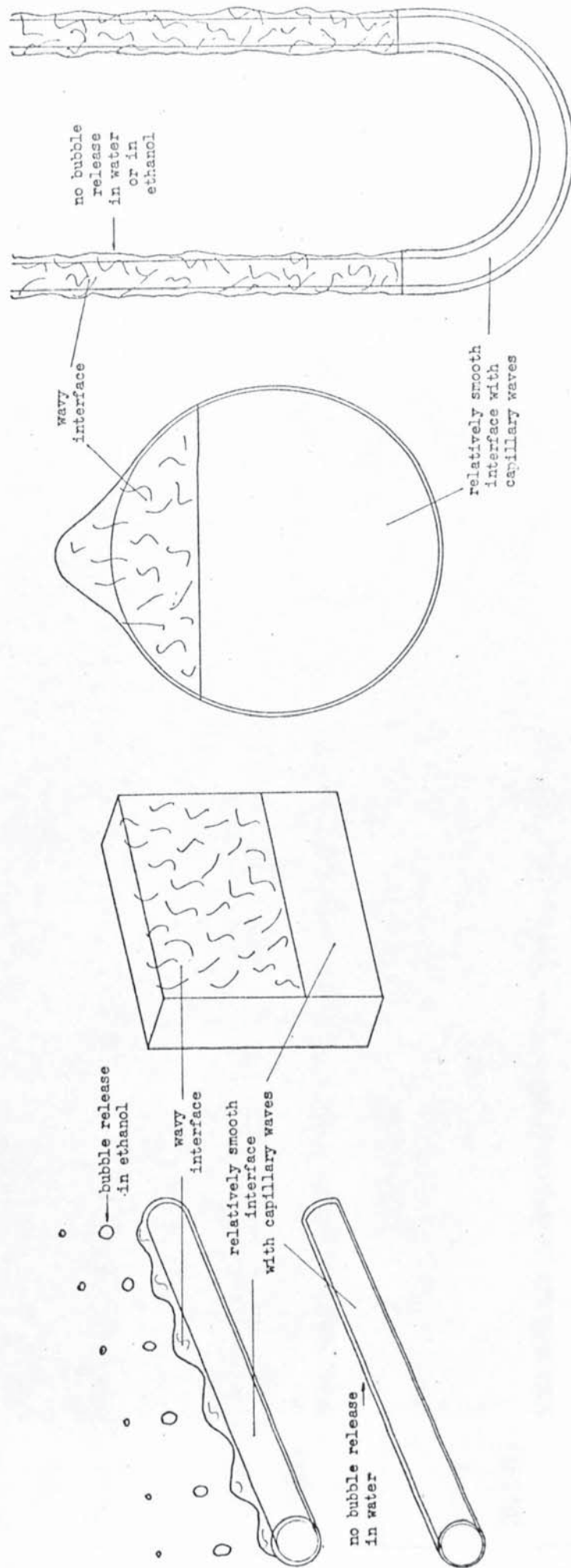


Figure 20. Summary of the photographic results for film boiling at large values of subcooling ($\Delta T_L > \text{about } 50 \text{ degF}$).

Approximate dimensions and geometries are: $\frac{1}{8}$, $\frac{1}{4}$, $\frac{1}{2}$ -inch diameter horizontal cylinders, 2-inch high vertical surface, 4-inch diameter sphere, and 8-inch high vertical cylinders of $\frac{1}{4}$ -inch diameter.

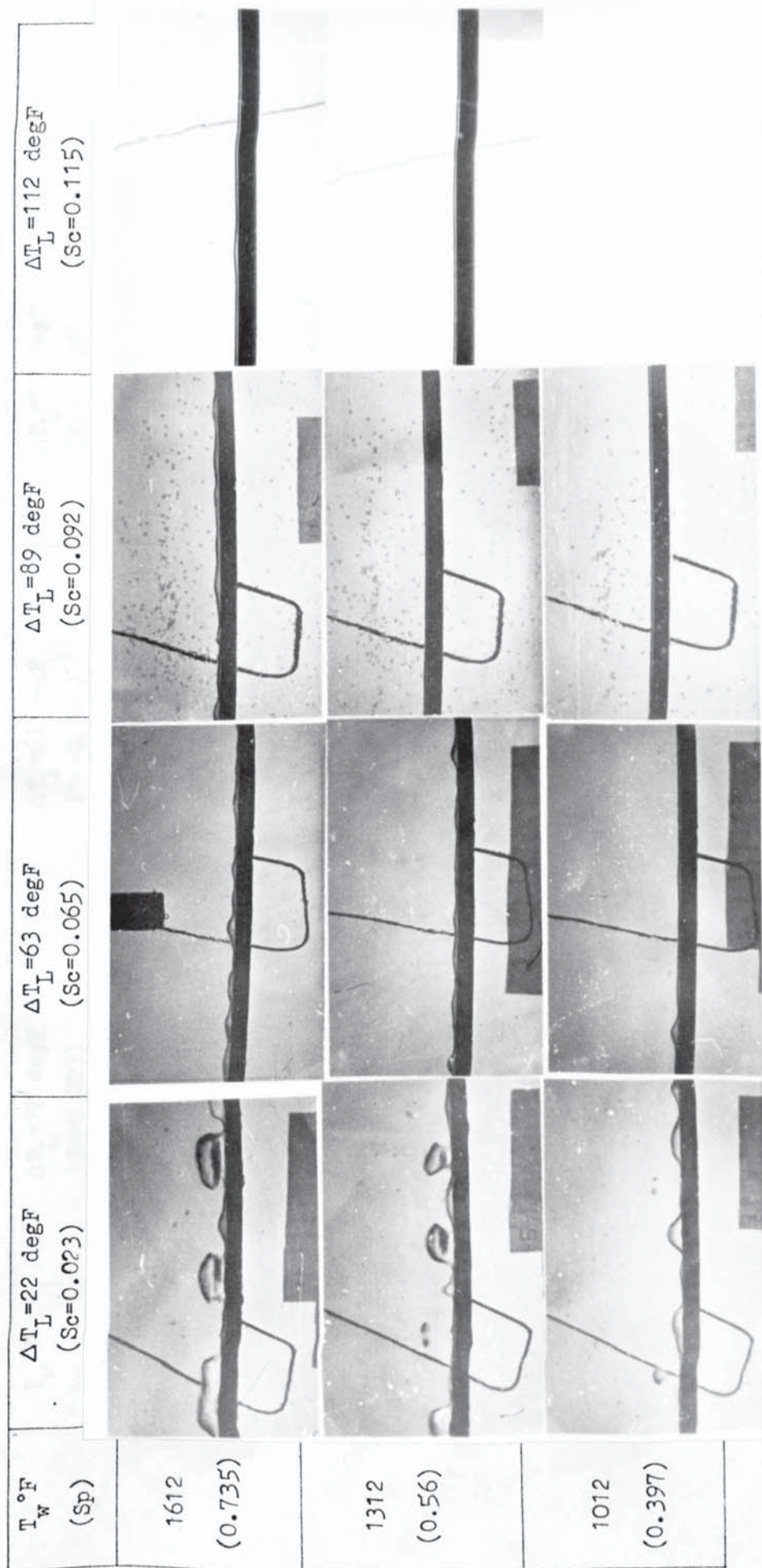


Figure 21. Steady film boiling of water on $\frac{1}{4}$ -inch diameter horizontal cylinders. At the larger values of subcooling bubble release is eliminated and the interface on the trailing edge appears to be smooth.


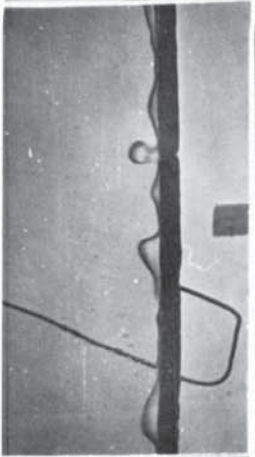

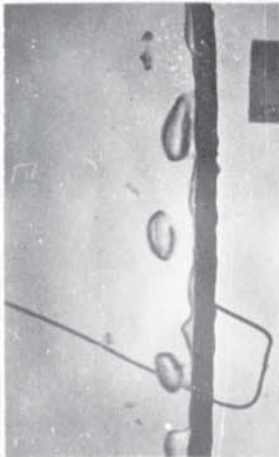
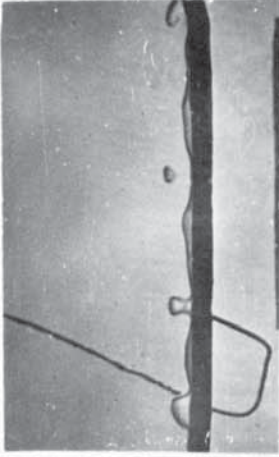

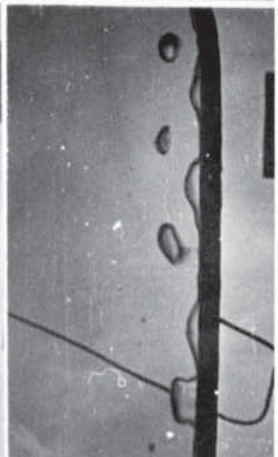


T_w °F (Sp)	$\Delta T_L = 22$ degF (Sc=0.023)	$\Delta T_L = 63$ degF (Sc=0.065)	$\Delta T_L = 89$ degF (Sc=0.092)
1612 (0.735)			
1312 (0.56)			
1012 (0.397)			

Figure 22. Steady film boiling of 0.025% detergent solution on $\frac{1}{4}$ -inch diameter horizontal cylinders. At $\Delta T_L = 22$ degF the interfacial disturbances are not noticeably different from those for water (figure 21), but at the higher values of subcooling bubble release is not entirely eliminated, and a regular comb exists on the trailing edge.

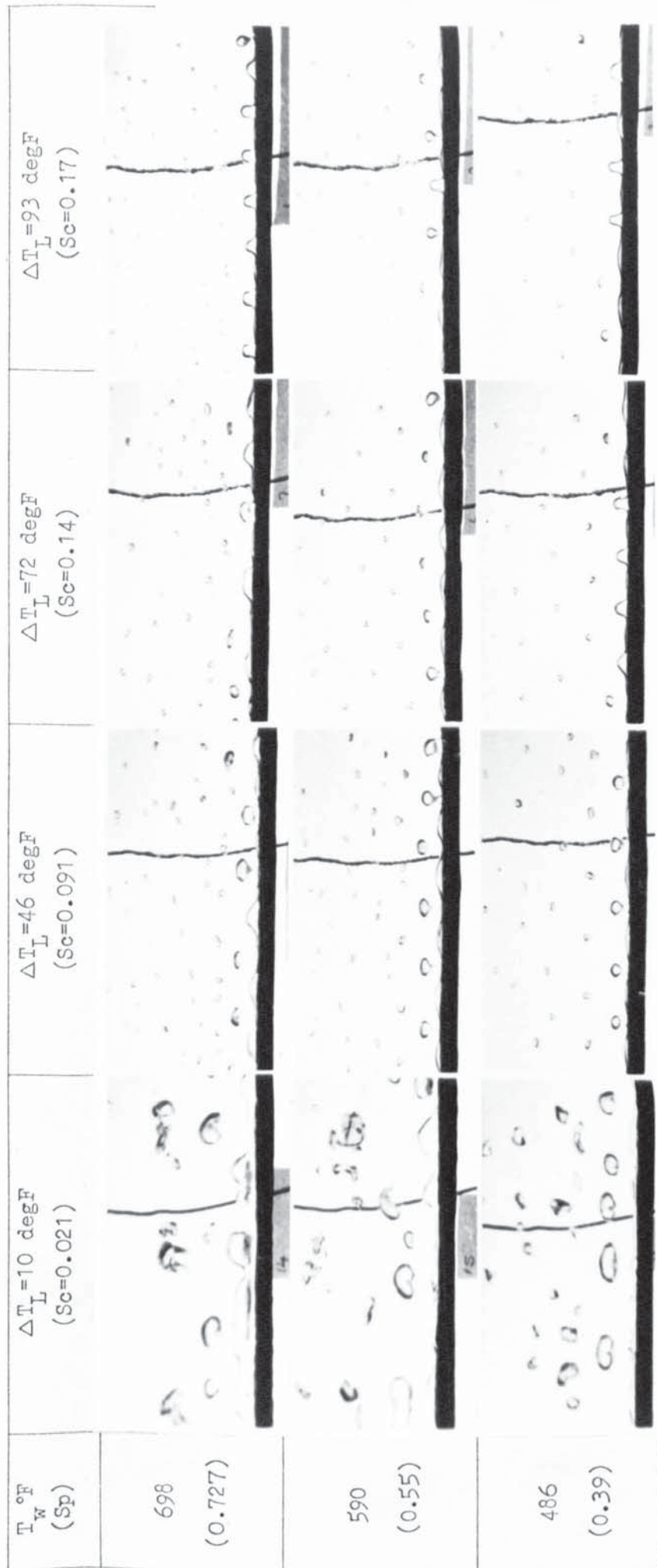


Figure 23. Steady film boiling of ethanol on $\frac{1}{4}$ -inch diameter horizontal cylinders. As the subcooling is increased, bubble release is reduced and becomes evenly spaced, and the comb on the trailing edge becomes regular. The pictures were taken under silhouette lighting.

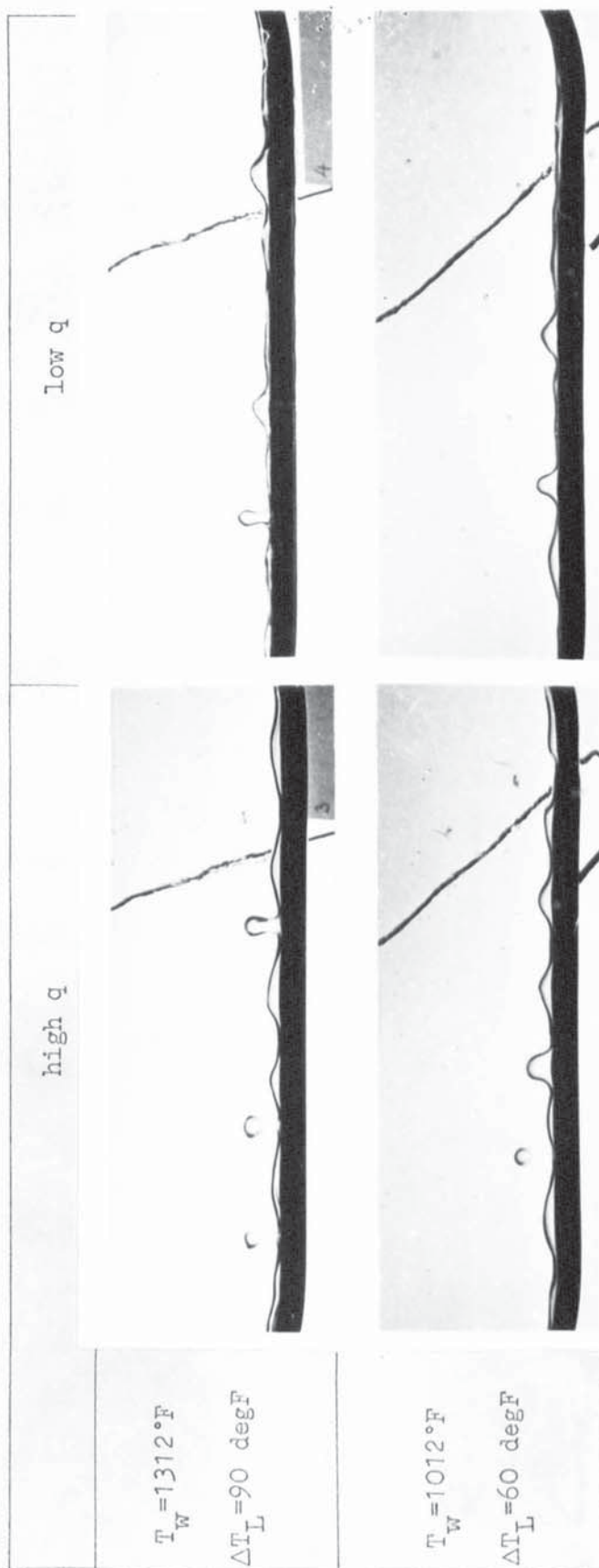


Figure 24. Steady film boiling of 0.025% detergent solution on $\frac{1}{4}$ -inch diameter horizontal cylinders at high and low values of heat flux. The comb appears to be less regular and more ragged at the low values of heat flux. The observed differences were more marked than these photos show. The pictures were taken under silhouette lighting.



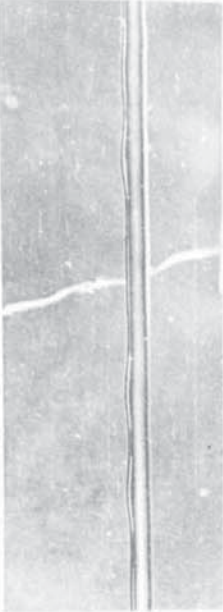




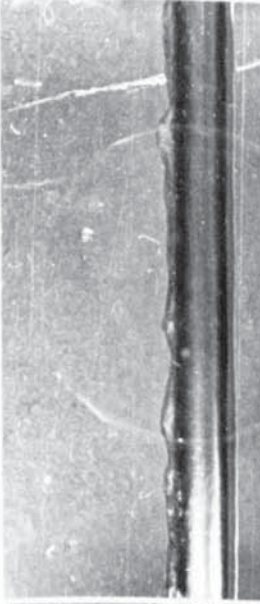

	$\Delta T_L = 22 \text{ degF (Sc=0.023)}$	$\Delta T_L = 63 \text{ degF (Sc=0.065)}$	$\Delta T_L = 89 \text{ degF (Sc=0.092)}$
$\frac{1}{8}$ " dia. (direct lighting)			
$\frac{1}{8}$ " dia. silhouette lighting			
$\frac{1}{2}$ " dia. (direct lighting)			

Figure 25. Steady film boiling of water on $\frac{1}{8}$ and $\frac{1}{2}$ -inch diameter horizontal cylinders at the surface temperature of 1312°F . Direct and silhouette lighting have been used. On the $\frac{1}{8}$ -inch diameter cylinders the interface appears to be smooth except in the region of bubble release, and the pattern of bubble release is much more regular than on the $\frac{1}{2}$ -inch diameter cylinders. On the latter size the interface appears to be slightly wavy even at $\Delta T_L = 89 \text{ degF}$.

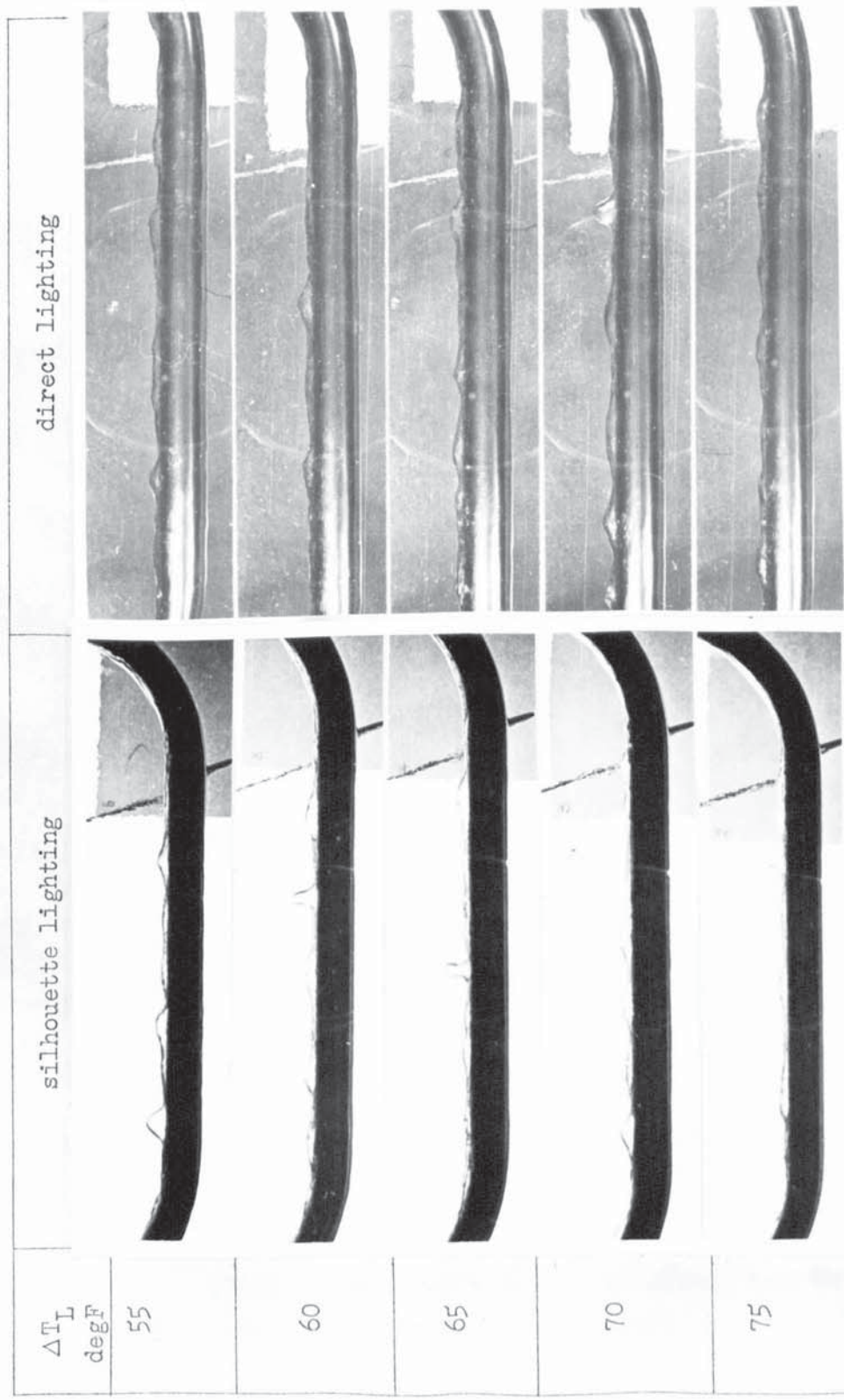


Figure 26. Steady film boiling of water on $\frac{1}{2}$ -inch diameter horizontal cylinders at $T_w = 1312^\circ\text{F}$. The photos cover the range of subcooling in which the change of slope occurs in the q versus ΔT_L curve (figure 12). There appear to be significant changes in the interfacial disturbances.

$T_W = 1312^\circ\text{F}$ $\Delta T_L = 5 \text{ degF}$ $(Sp=0.56)$ $(Sc=0.0051)$	$T_W = 1312^\circ\text{F}$ $\Delta T_L = 22 \text{ degF}$ $(Sp=0.56)$ $(Sc=0.023)$	$T_W = 1250^\circ\text{F}$ $\Delta T_L = 50 \text{ degF}$ $(Sp=0.51)$ $(Sc=0.052)$
---	---	---

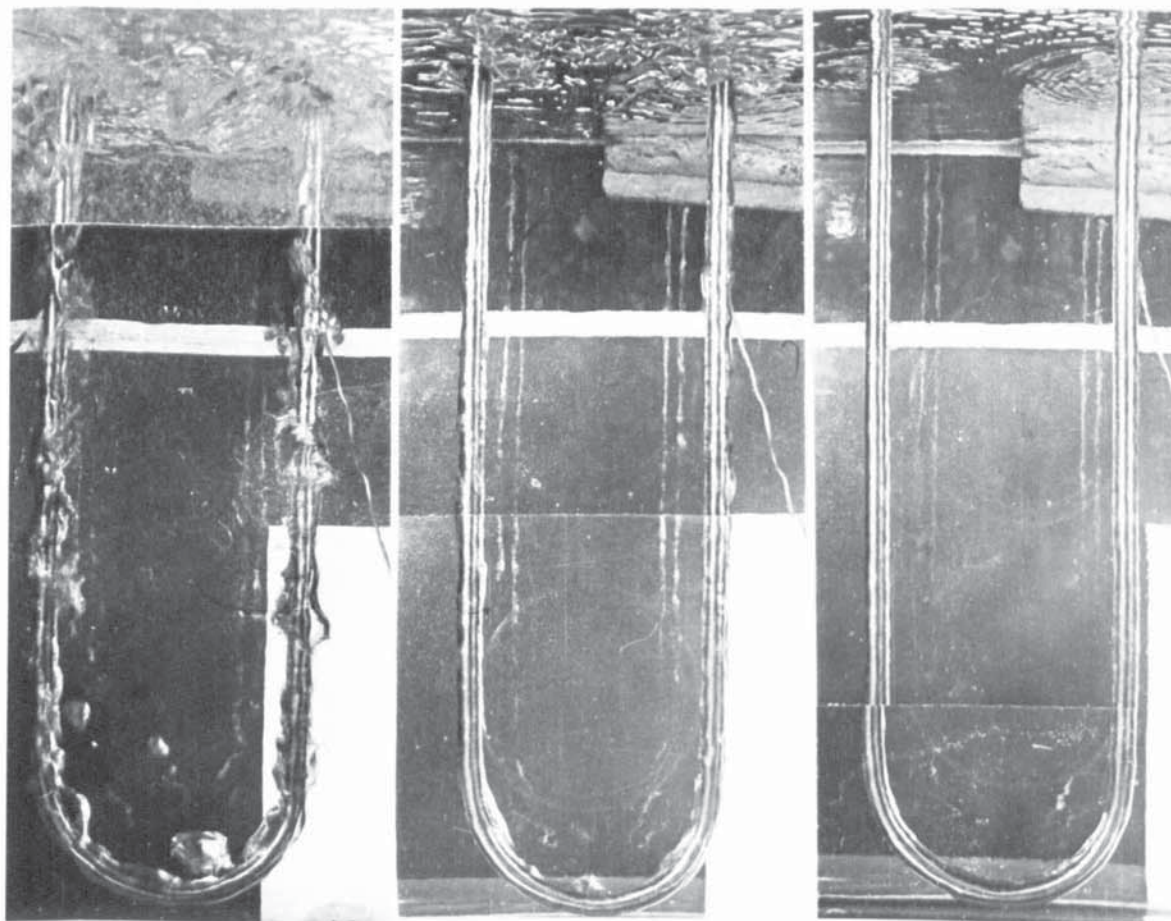


Figure 27. Steady film boiling of water on 8 inch high vertical cylinders of $\frac{1}{4}$ -inch diameter. The interface is highly disturbed at $\Delta T_L = 5 \text{ degF}$, but is relatively smooth at the higher values of subcooling. Bubble release from the vertical sections is eliminated at $\Delta T_L = 22 \text{ degF}$. (Each picture was taken in two parts, and the prints were subsequently joined together.)

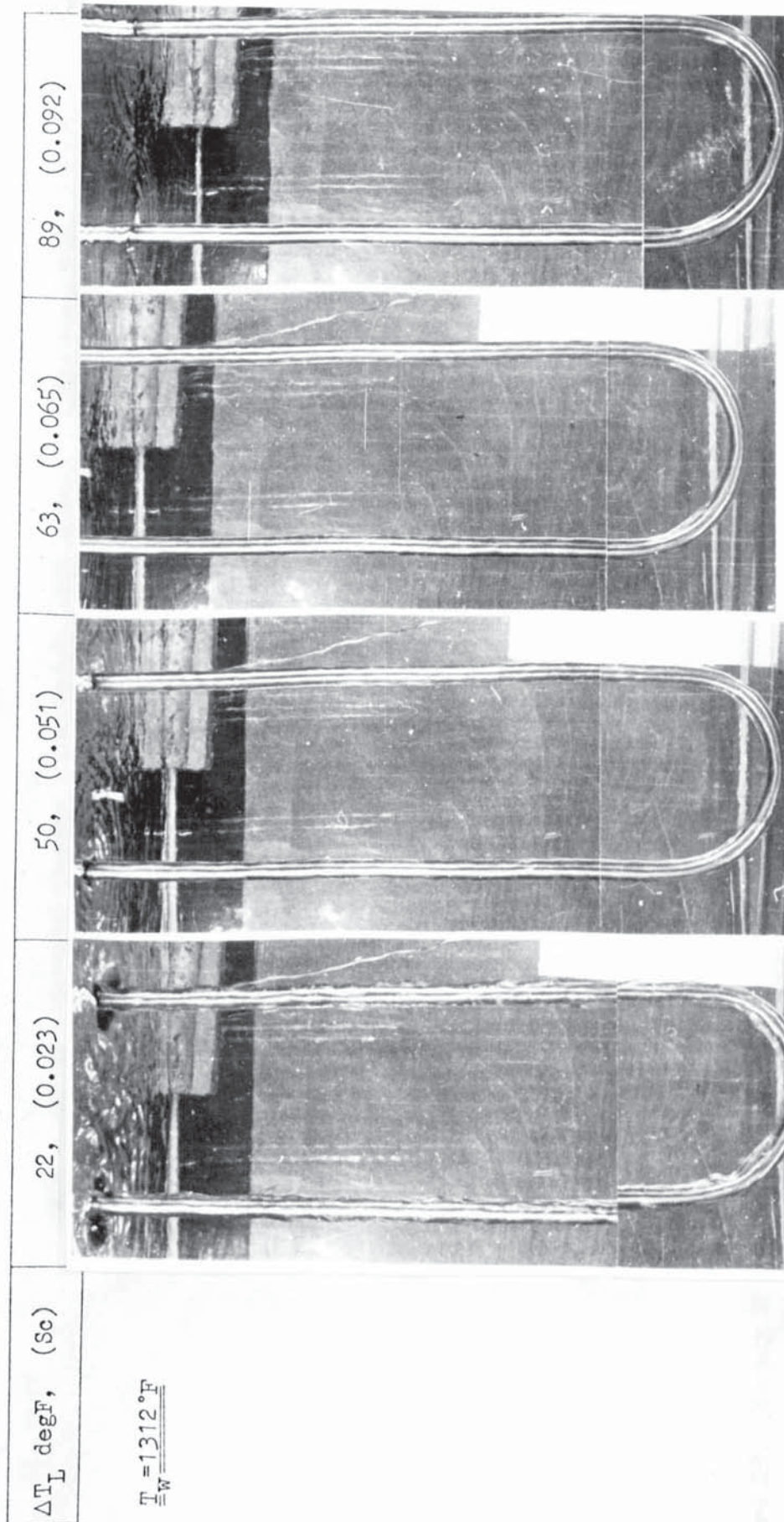


Figure 28. Steady film boiling of 0.025% detergent solution on 8 inch high vertical cylinders of $\frac{1}{4}$ -inch diameter. The interface becomes increasingly smooth with subcooling and the release of bubbles is eliminated at $\Delta T_L = 22$ degF.

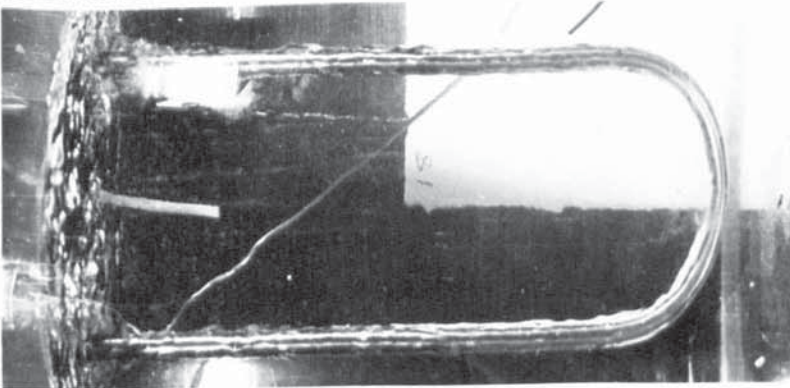
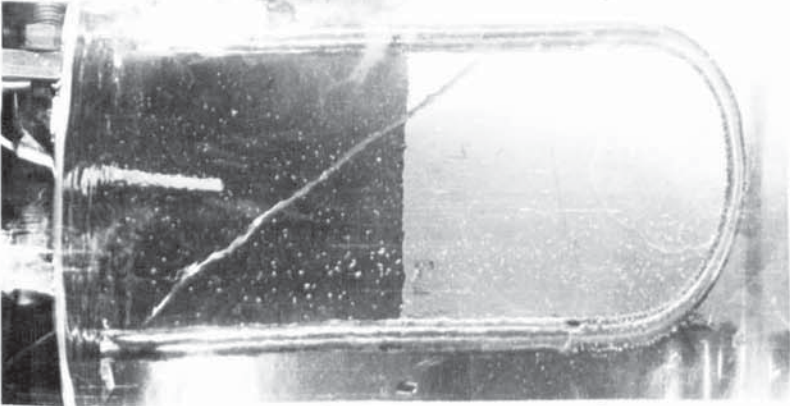
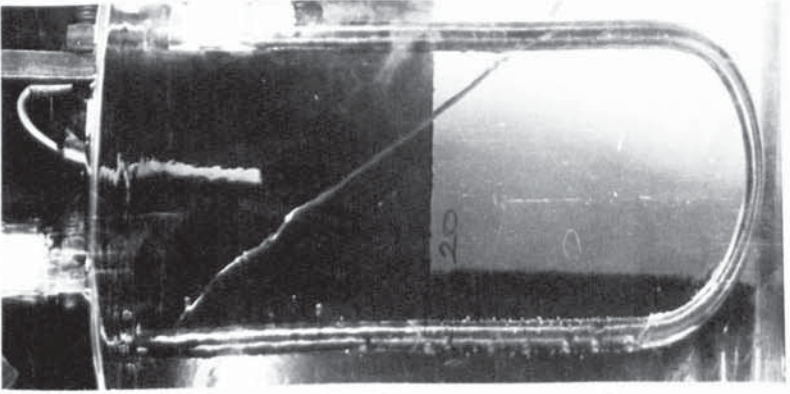
T_w , (Sp) ΔT_L degF, (Sc)	590, (0.55)	590, (0.55)	650, (0.65)
	28, (0.056)	≈ 90 , (0.17)	≈ 90 , (0.17)
			

Figure 29. Steady film boiling of ethanol on 8 inch high vertical cylinders of $\frac{1}{4}$ -inch diameter. Bubble release from the vertical sections is eliminated at $\Delta T_L = 28$ degF. At about $\Delta T_L = 90$ degF the interface is somewhat wavier than for detergent solution at the same degree of subcooling, see figure 28. In places, film boiling has been replaced by nucleate boiling.

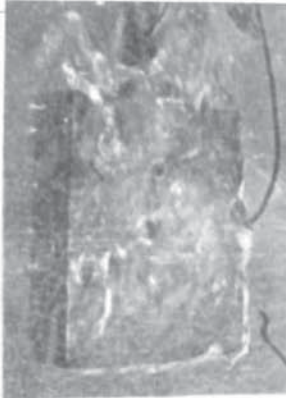
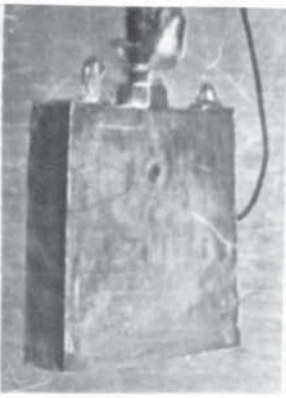


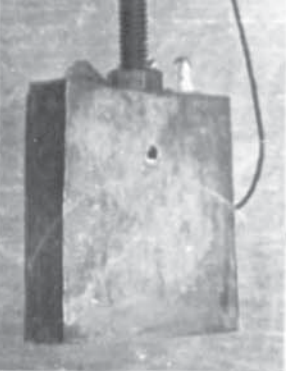
T_w °F (Sp)	$\Delta T_L = 5$ degF (Sc=0.0051)	$\Delta T_L = 50$ degF (Sc=0.023)	$\Delta T_L = 89$ degF (Sc=0.092)
1312 (0.56)			
1012 (0.397)			

Figure 30. Transient film boiling of water on a 2 inch high vertical surface. The interface is chaotic at $\Delta T_L = 5$ degF, but is relatively smooth at $\Delta T_L = 50$ degF and greater.

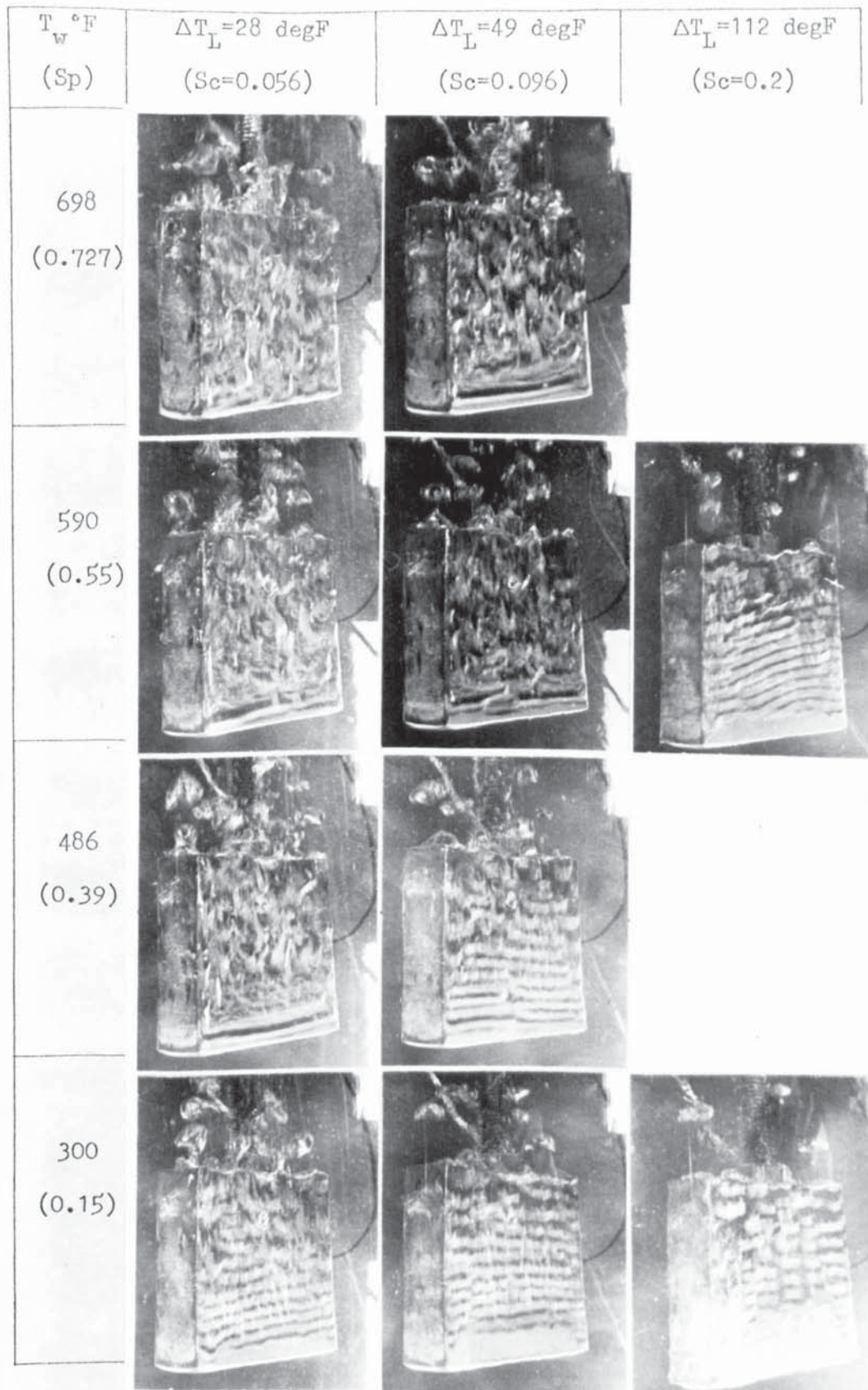


Figure 31. Transient film boiling of ethanol on a 2 inch high vertical surface. At high surface temperatures and small subcooling the interface is chaotic. At low surface temperatures, or when subcooling is large, the interface near the leading edge is smooth, and over much of the rest of the surface the interfacial disturbances take on a distinctive wave pattern.

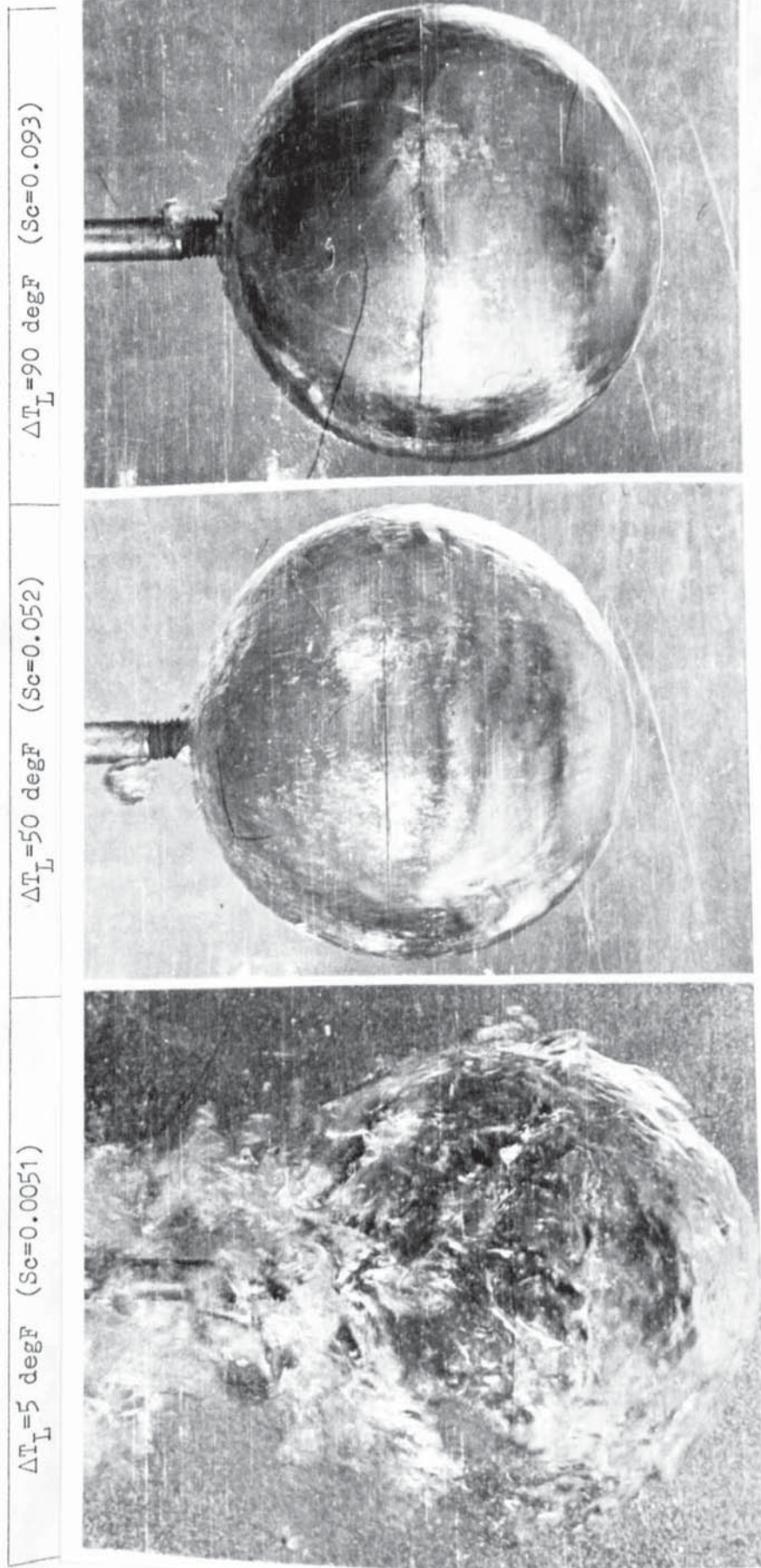


Figure 32. Transient film boiling of water on a 4 inch diameter sphere at $T_w = 1312^\circ\text{F}$. The effects of subcooling on interfacial disturbances and bubble release are clearly seen. At $\Delta T_L = 90 \text{ degF}$ the interface is only slightly wavy on the upward facing surface, and the bubble is one of air.

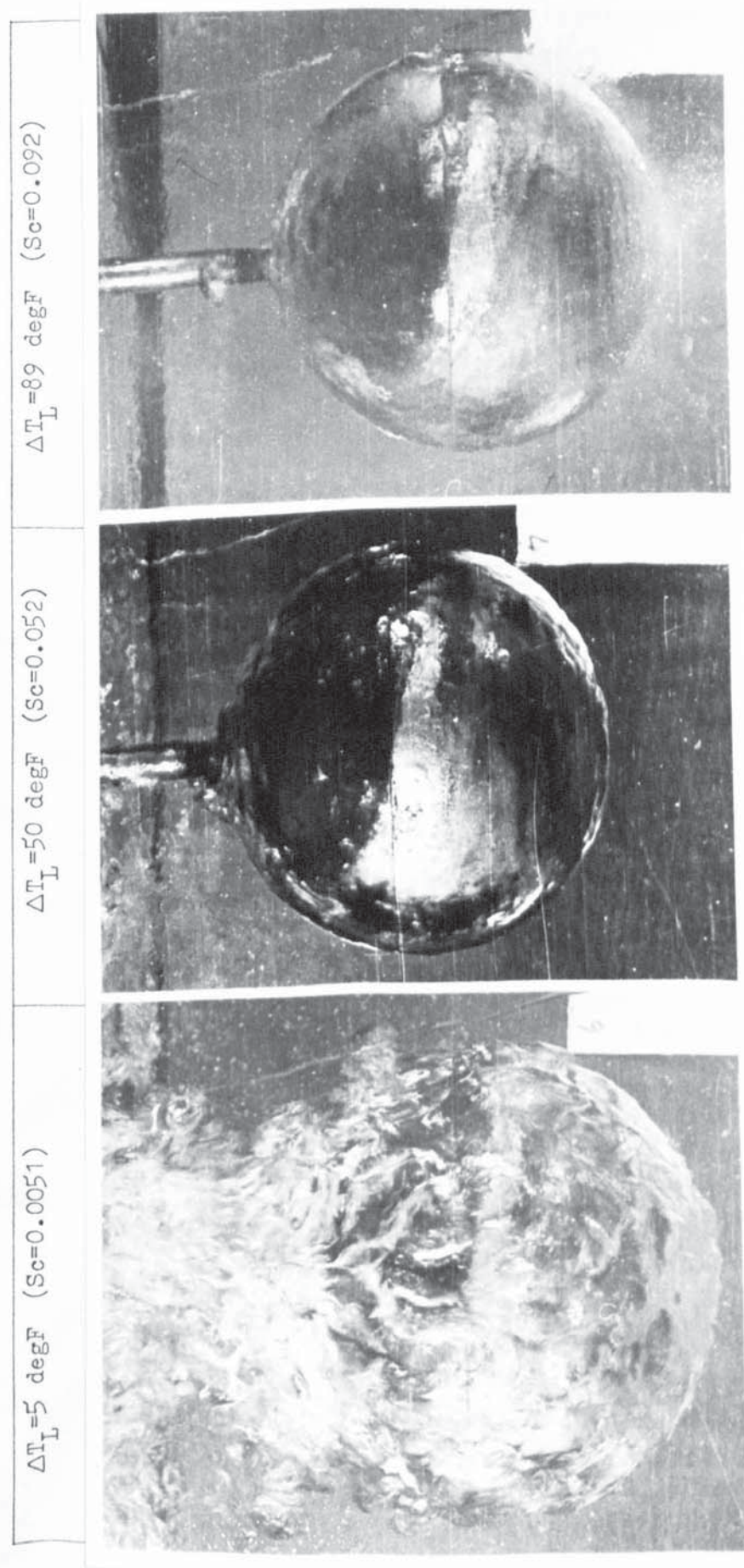


Figure 33. Transient film boiling of 0.025% detergent solution on a 4 inch diameter sphere at $T_w = 1312^\circ\text{F}$. The effects of subcooling are very similar to those in water. At $\Delta T_L = 50$ and 89 degF the interface on the upward facing surface is smooth, in contrast with the interface on the trailing edge of the horizontal cylinders (fig. 22).

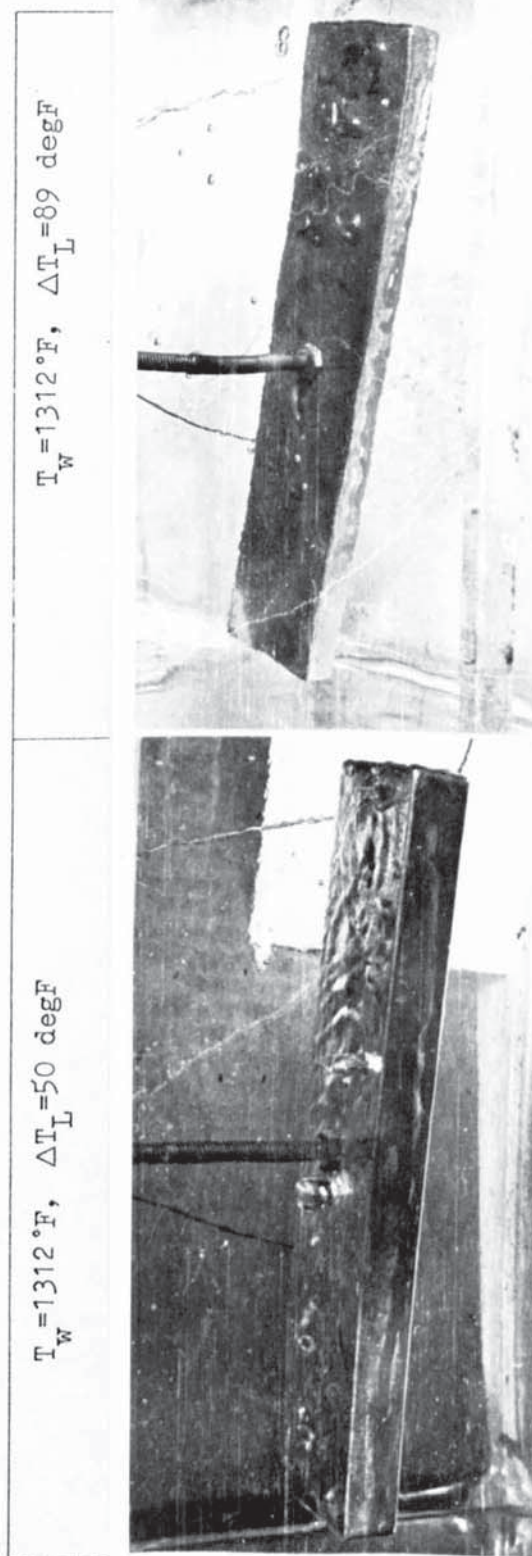


Figure 34. Transient film boiling of water on a 2x9 inch horizontal surface. The interface is relatively smooth especially at $\Delta T_L = 89 \text{ degF}$. The domes and bubbles are ^{partly} caused by air which has come out of solution.

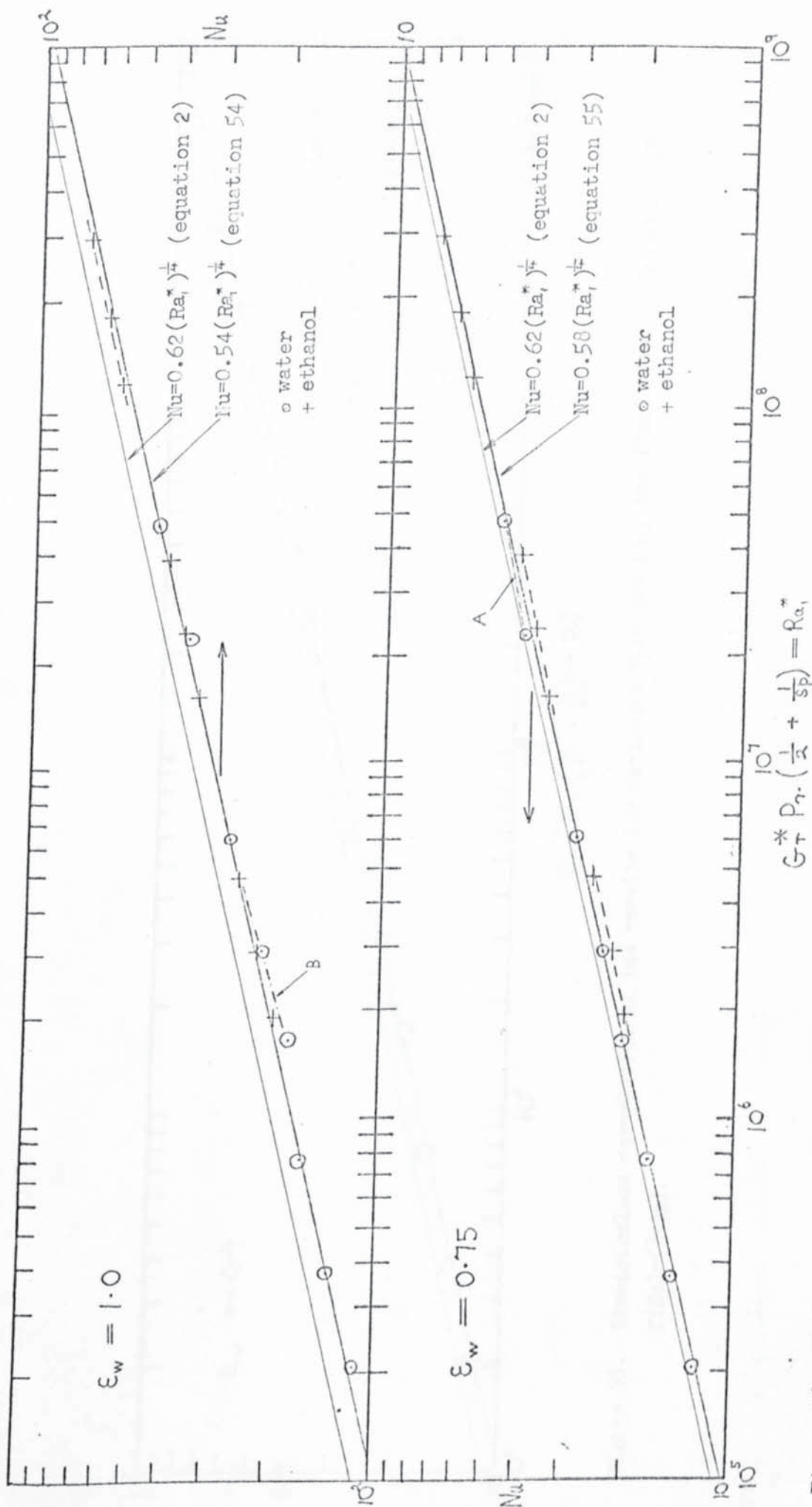


Figure 35. Dimensionless correlations of the results for saturated film boiling with $\epsilon_w = 0.75$ and 1.0 and $f(Sp) = \left(\frac{1}{2} + \frac{1}{Sp} \right)$.

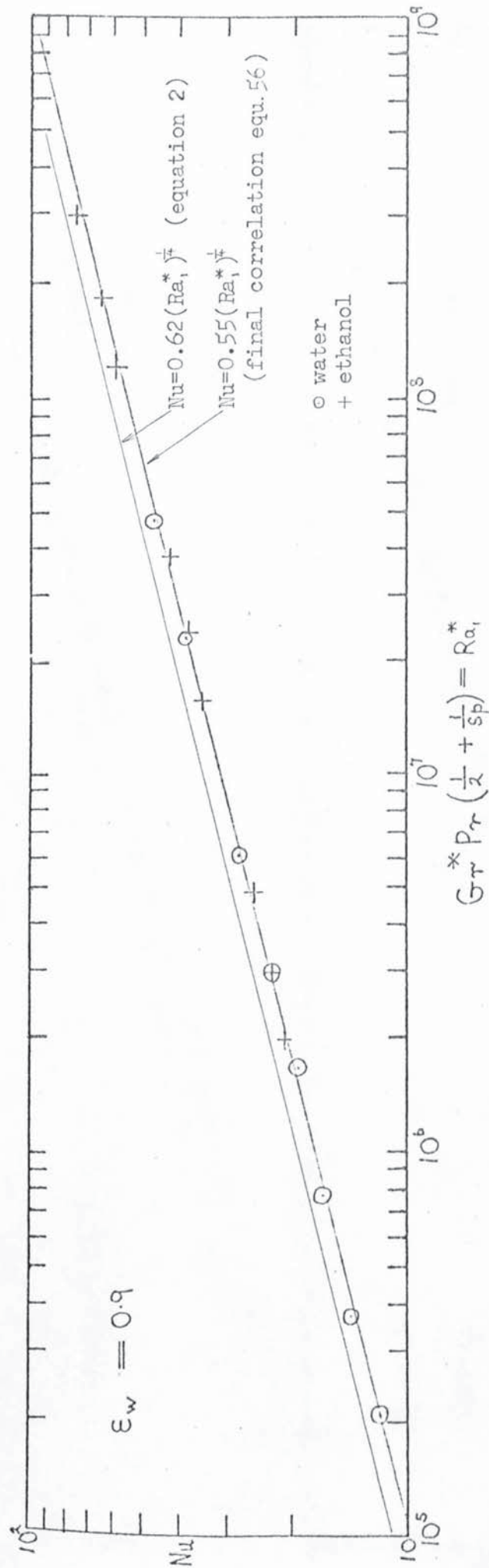


Figure 36. Dimensionless correlation of the results for saturated film boiling: the final correlation with $\epsilon_w = 0.9$ and $f(Sp) = \left(\frac{1}{2} + \frac{1}{s_p} \right)$.

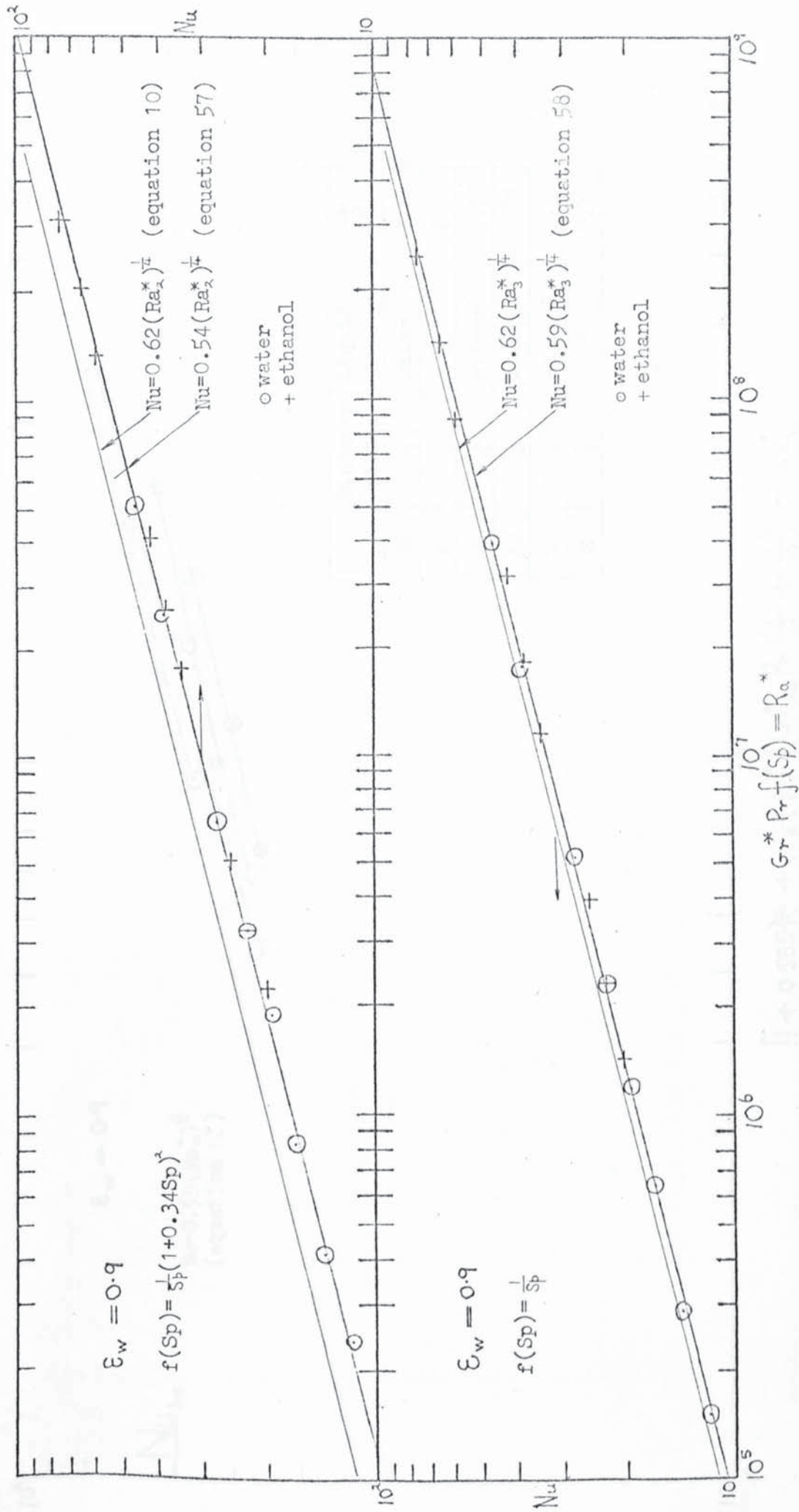


Figure 37. Dimensionless correlations of the results for saturated film boiling with $\epsilon_w = 0.9$ and $f(Sp) = \frac{1}{Sp^2}(1 + 0.34Sp)^2$ and $\frac{1}{Sp}$.

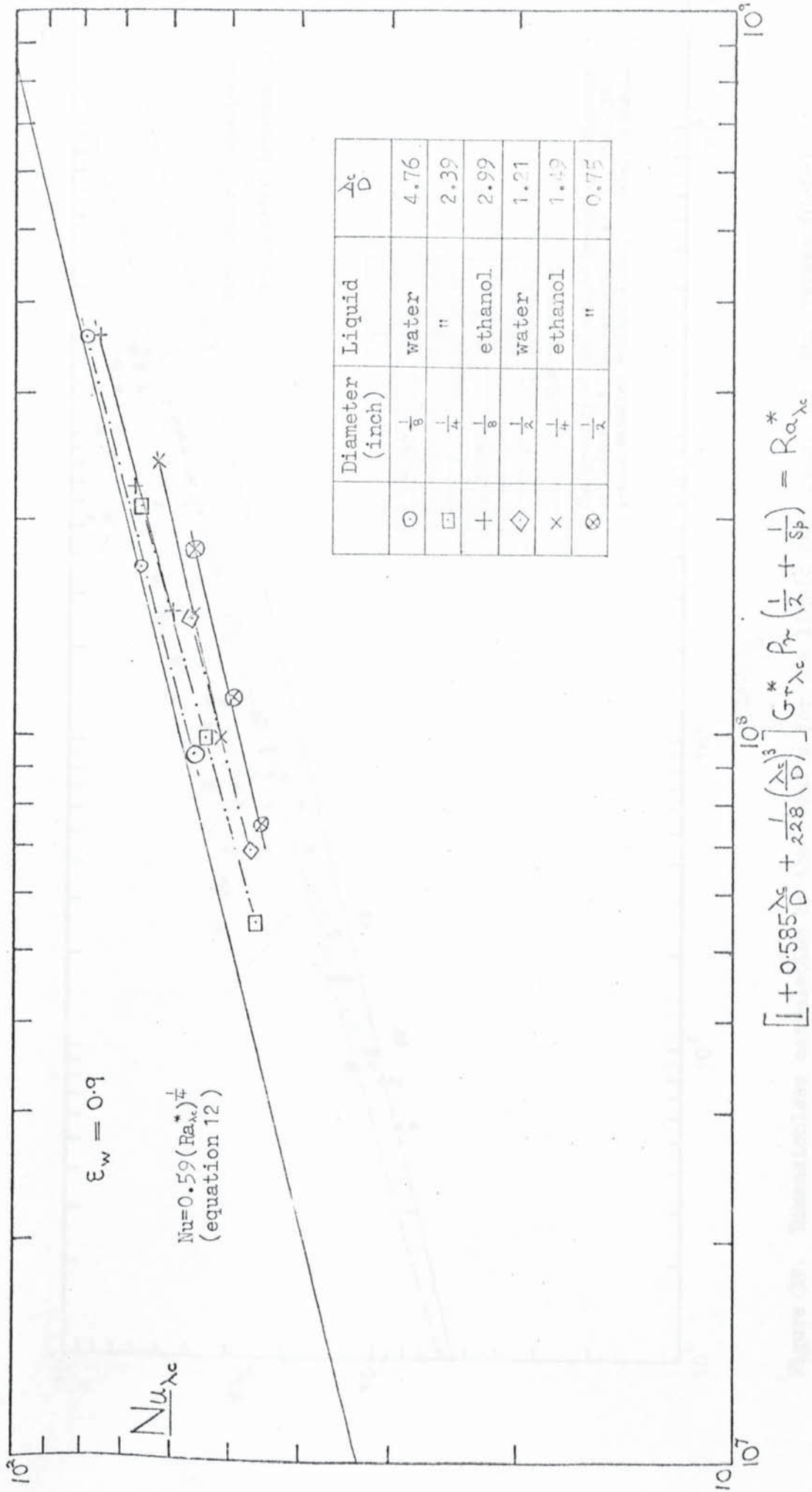


Figure 38. Dimensionless correlation of the results for saturated film boiling according to equation 12.

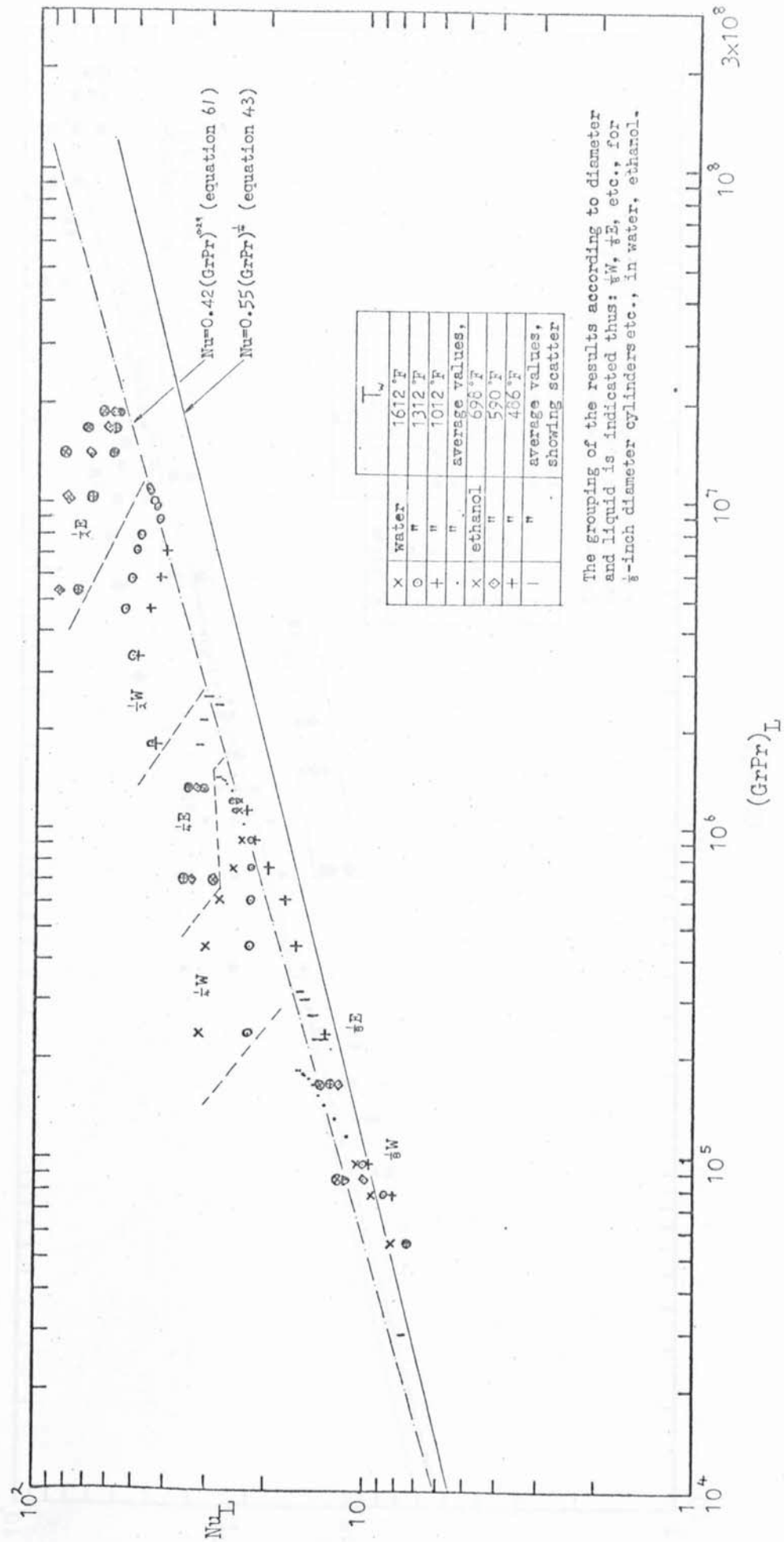


Figure 39. Dimensionless correlation of the results for the liquid heat flux, q_L : Nu_L verses $(GrPr)_L$.

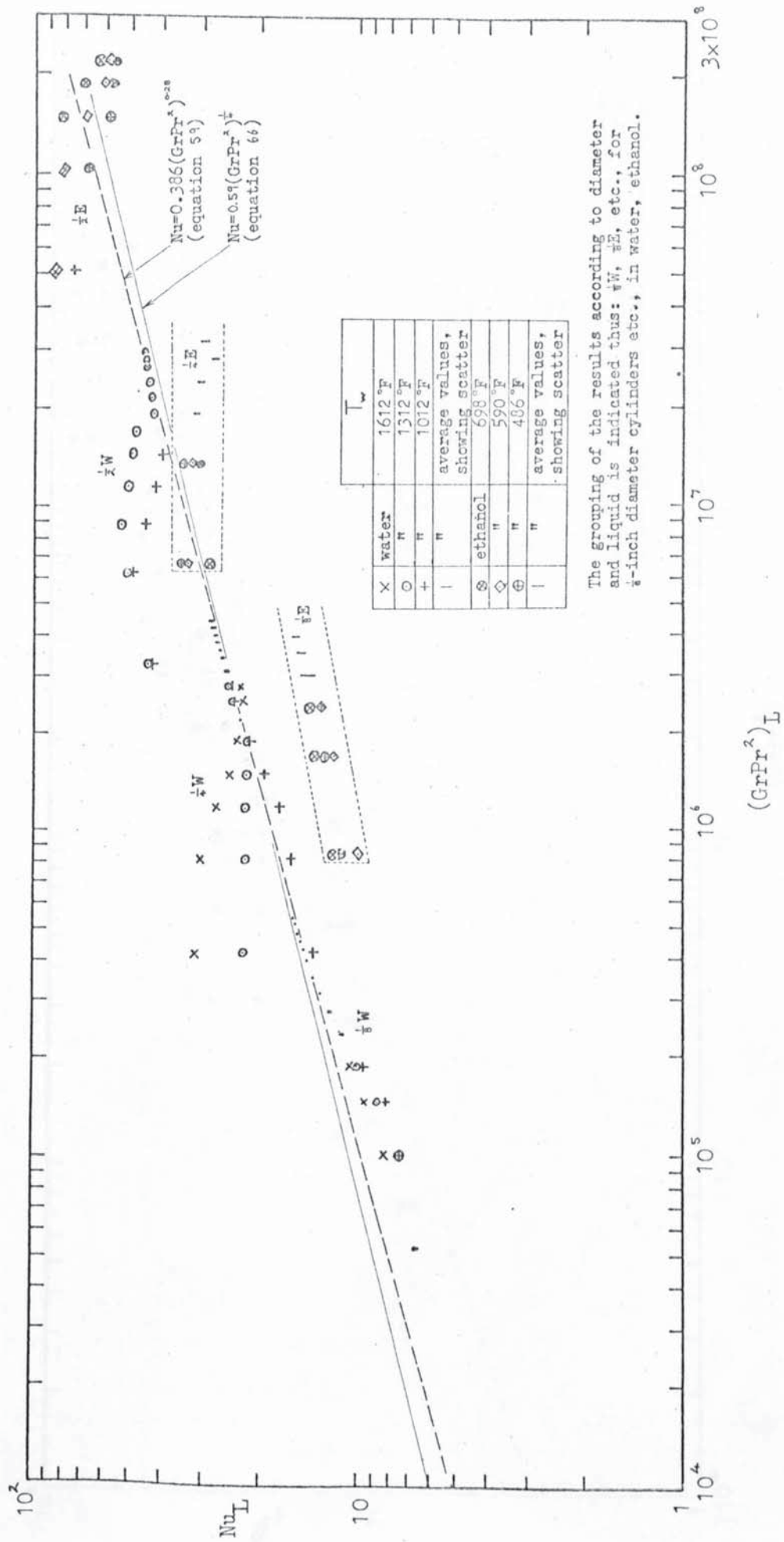


Figure 40. Dimensionless correlation of the results for the liquid heat flux, q_L : Nu_L verses $(GrPr^2)_L$.

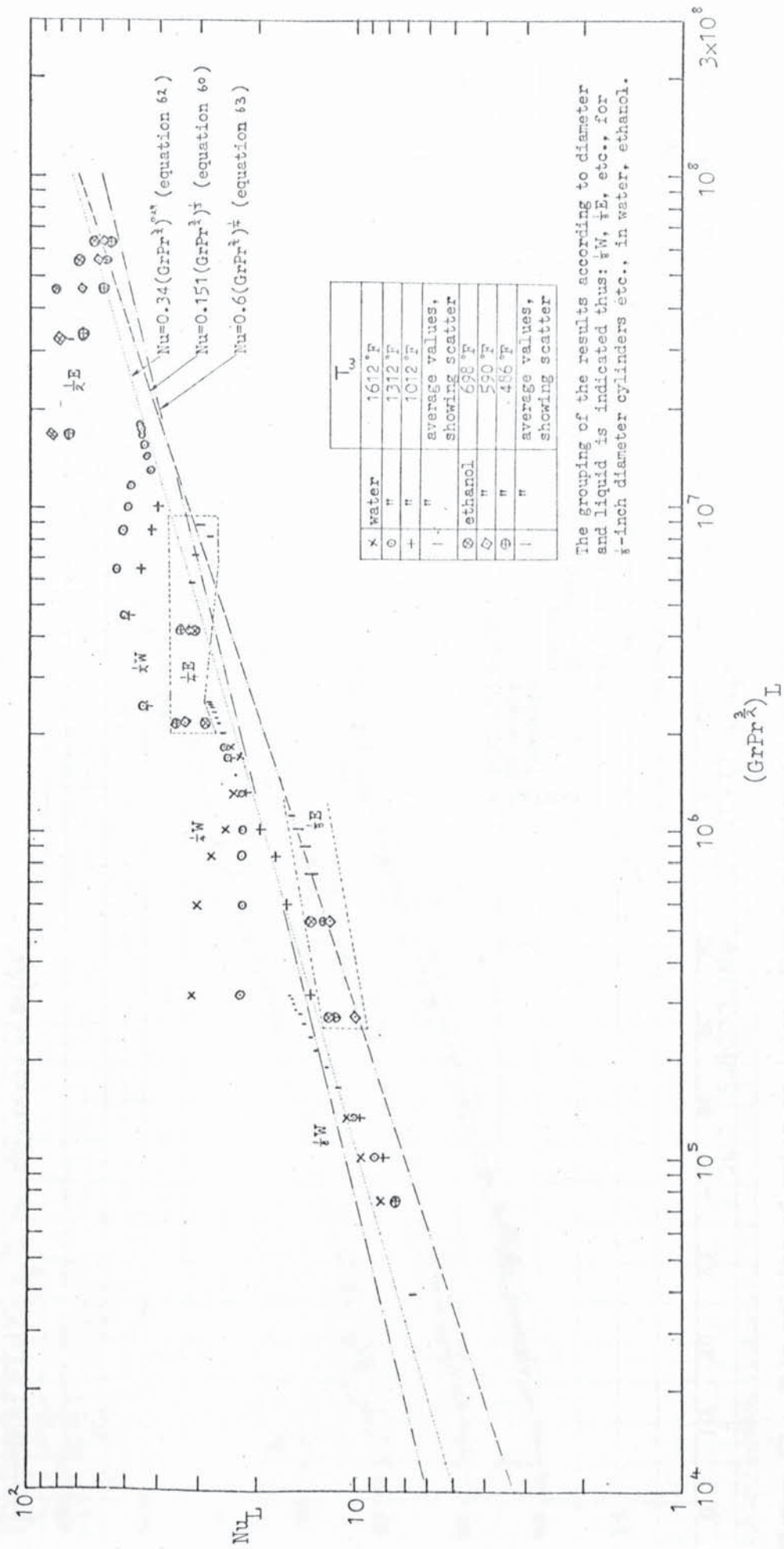


Figure 41. Dimensionless correlation of the results for the liquid heat flux, q_L : Nu versus $(GrPr^2)_L$.

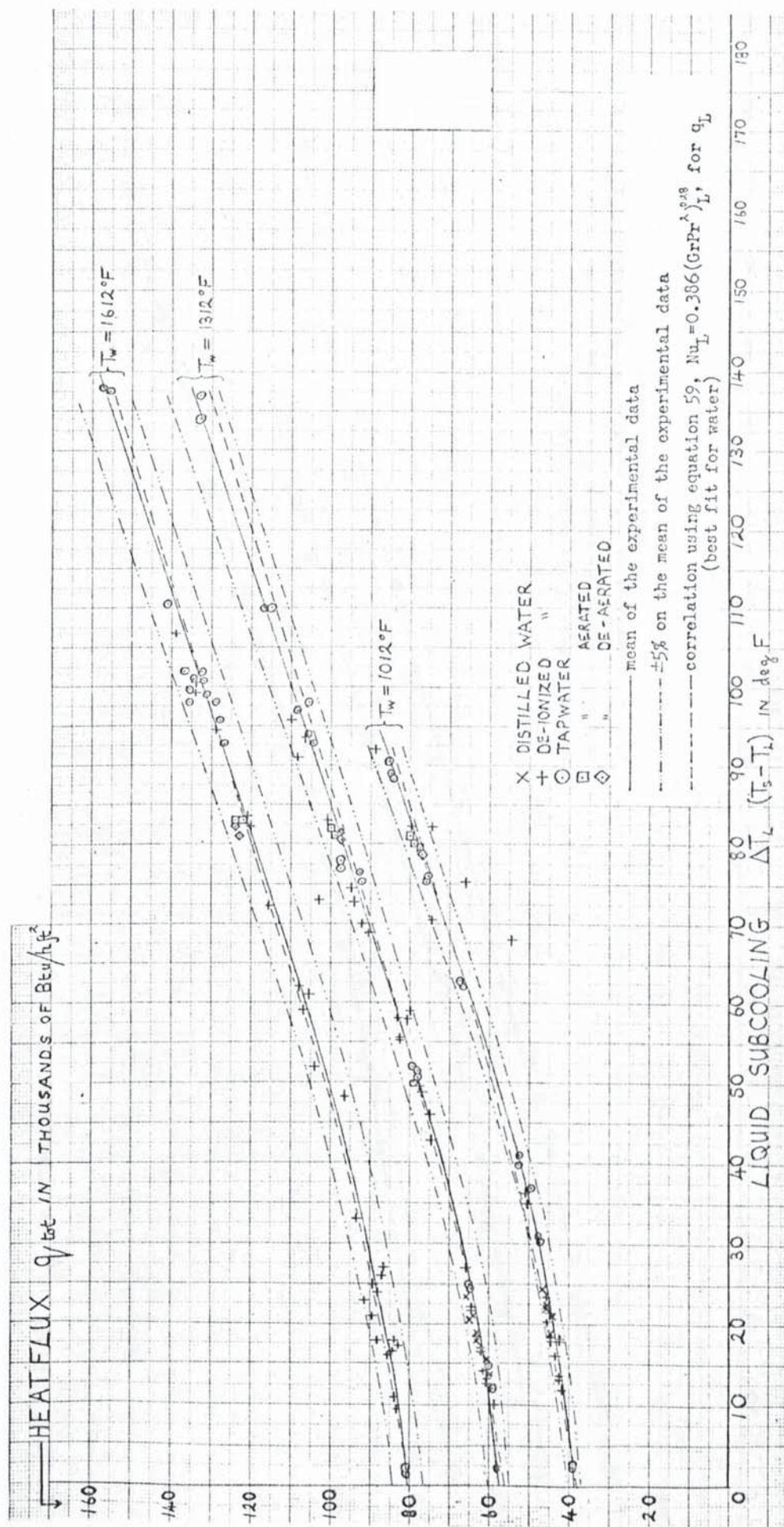


Figure 42. Film boiling of water on $\frac{1}{8}$ -inch diameter horizontal cylinders. Comparison of the experimental data with the proposed correlation of best fit for water (q_L calculated from equation 59). (See section 8.5.)

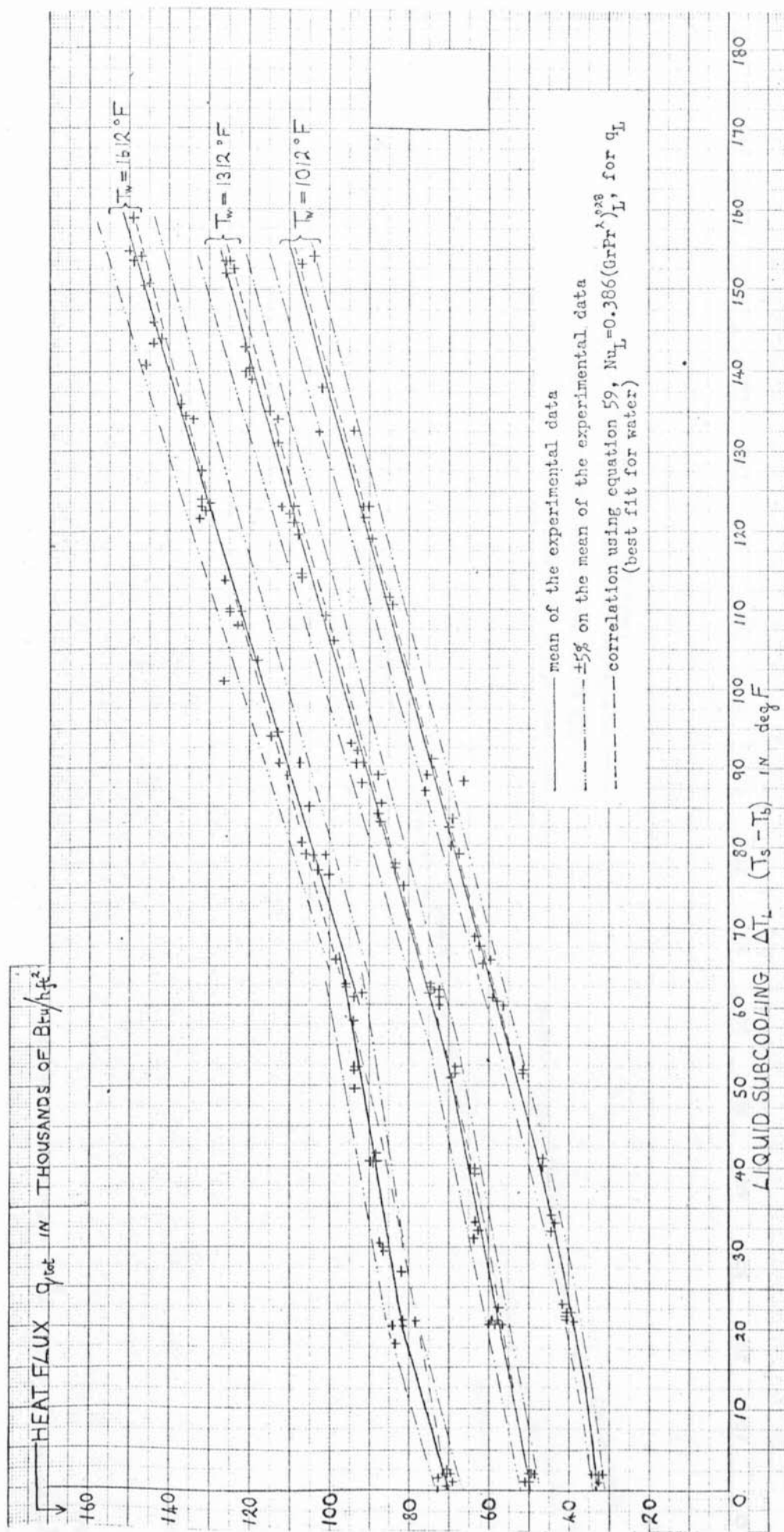


Figure 43. Film boiling of water on $\frac{1}{4}$ -inch diameter horizontal cylinders. Comparison of the experimental data with the proposed correlation of best fit for water (q_L calculated from equation 59). (See section 8.5.)

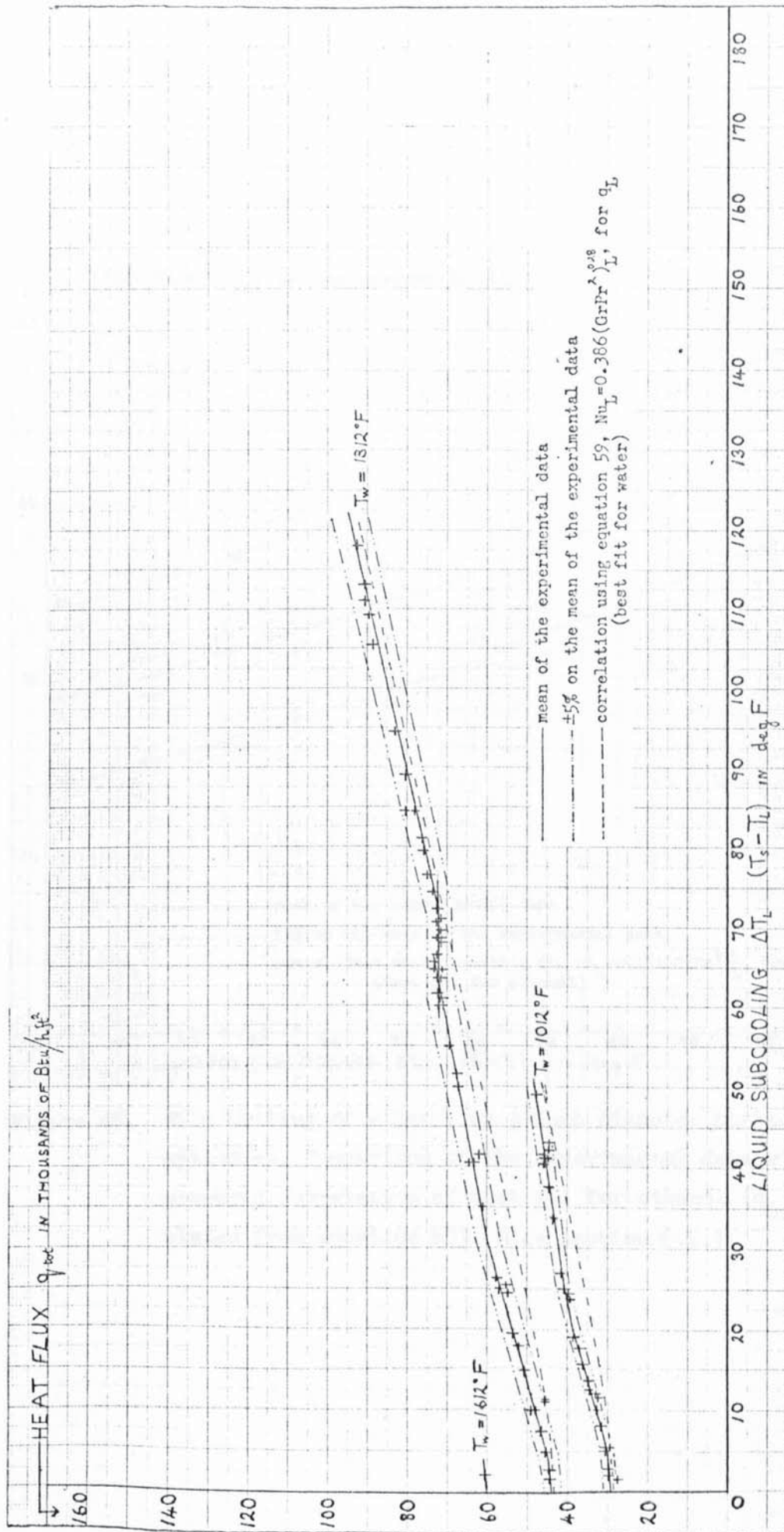


Figure 44. Film boiling of water on $\frac{1}{2}$ -inch diameter horizontal cylinders. Comparison of the experimental data with the proposed correlation of best fit for water (q_L calculated from equation 59). (See section 8.5.)

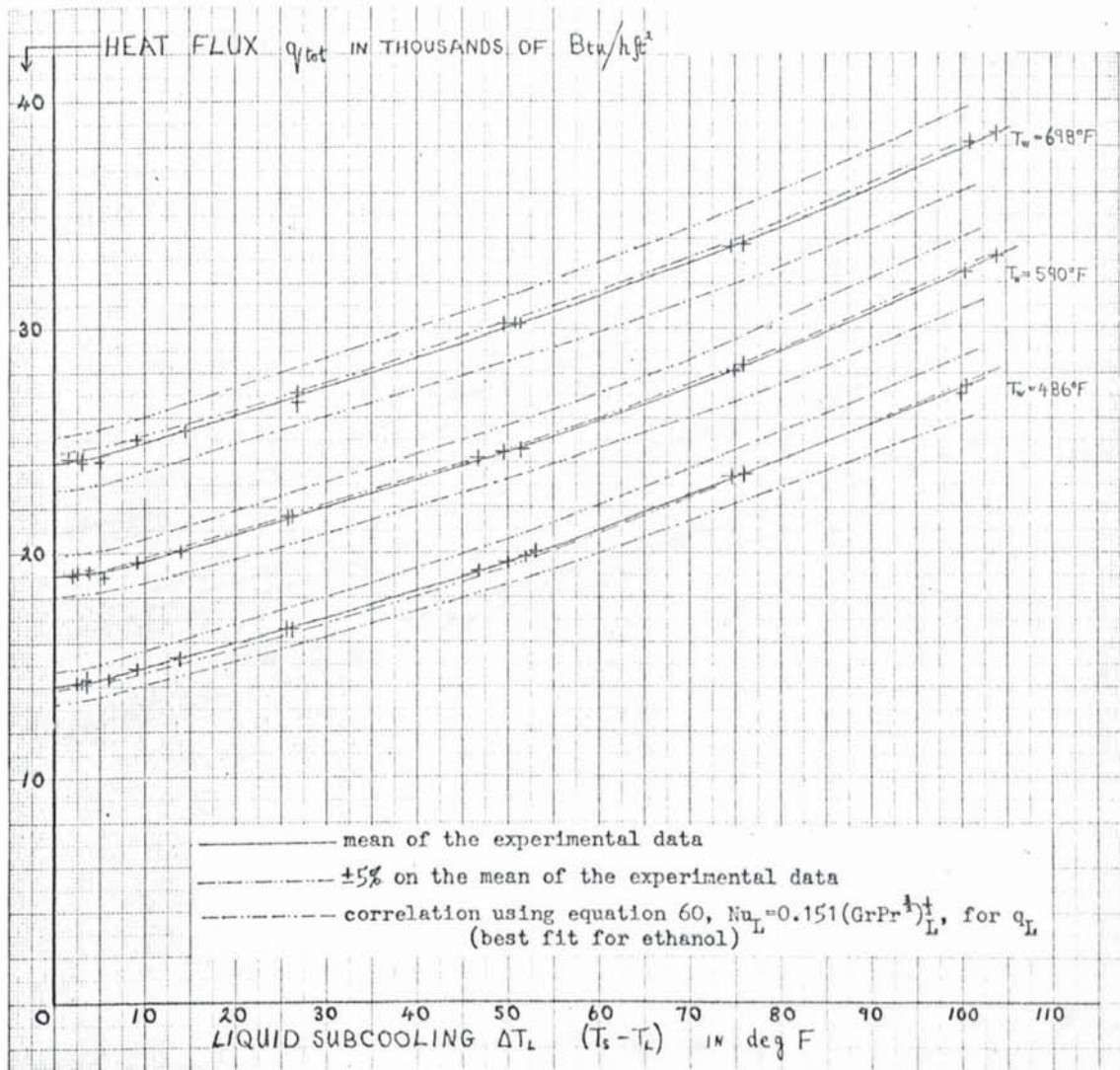


Figure 45. Film boiling of ethanol on $\frac{1}{8}$ -inch diameter horizontal cylinders. Comparison of the experimental data with the proposed correlation of best fit for ethanol (q_L calculated from equation 60). (See section 8.5.)

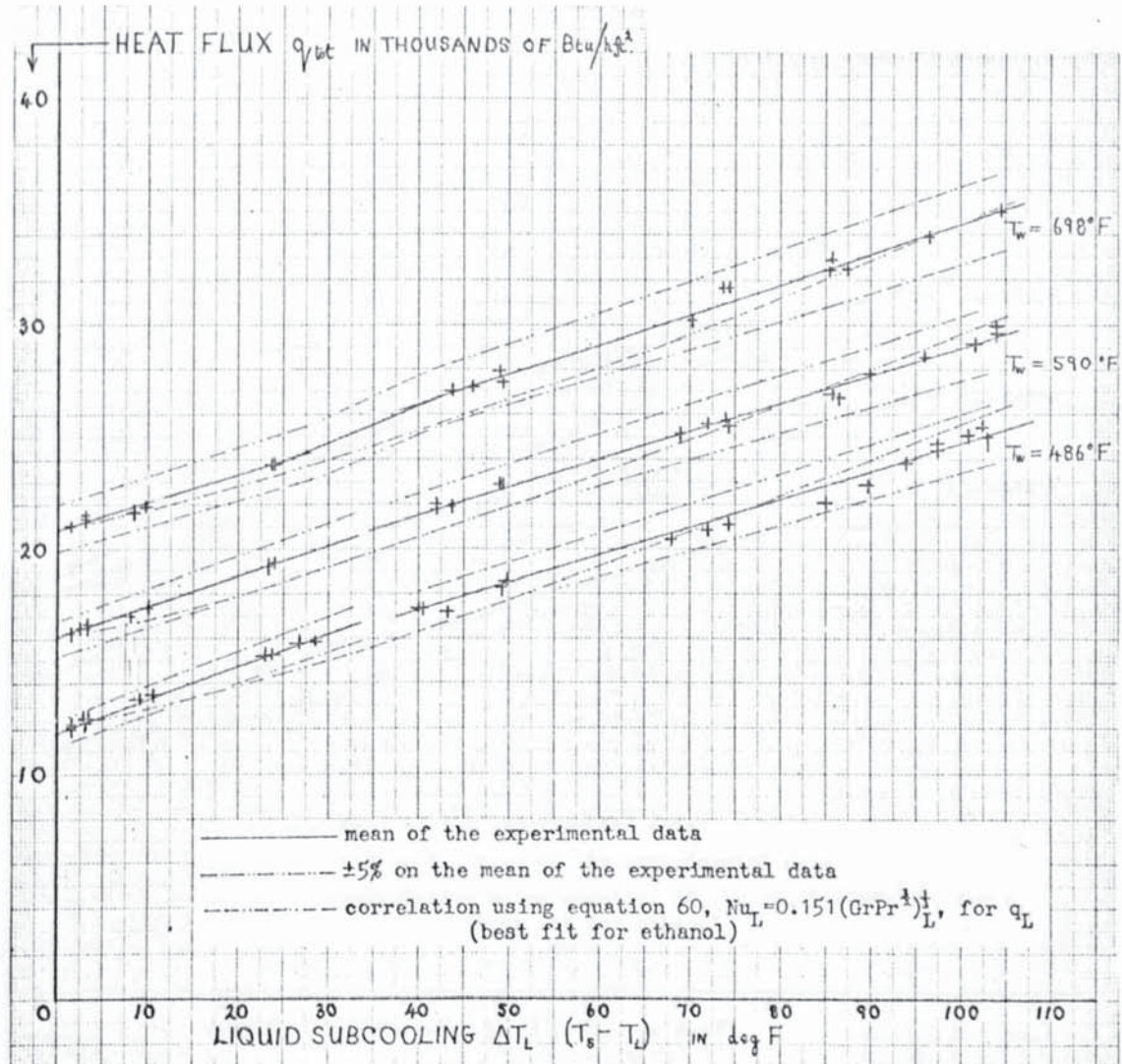


Figure 46. Film boiling of ethanol on $\frac{1}{4}$ -inch diameter horizontal cylinders. Comparison of the experimental data with the proposed correlation of best fit for ethanol (q_L calculated from equation 60). (See section 8.5.)

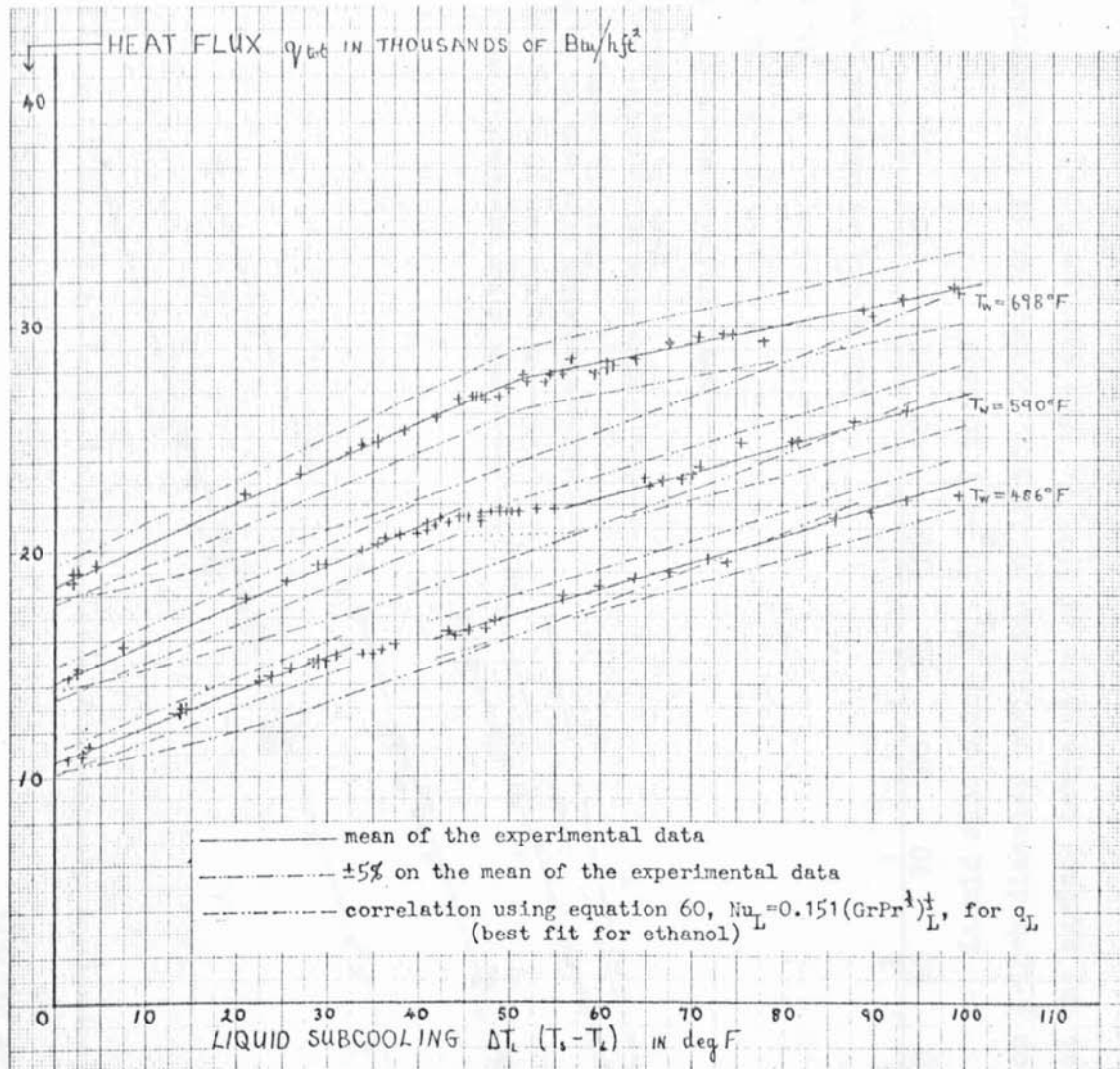


Figure 47. Film boiling of ethanol on $\frac{1}{2}$ -inch diameter horizontal cylinders. Comparison of the experimental data with the proposed correlation of best fit for ethanol (q_L calculated from equation 60). (See section 8.5.)

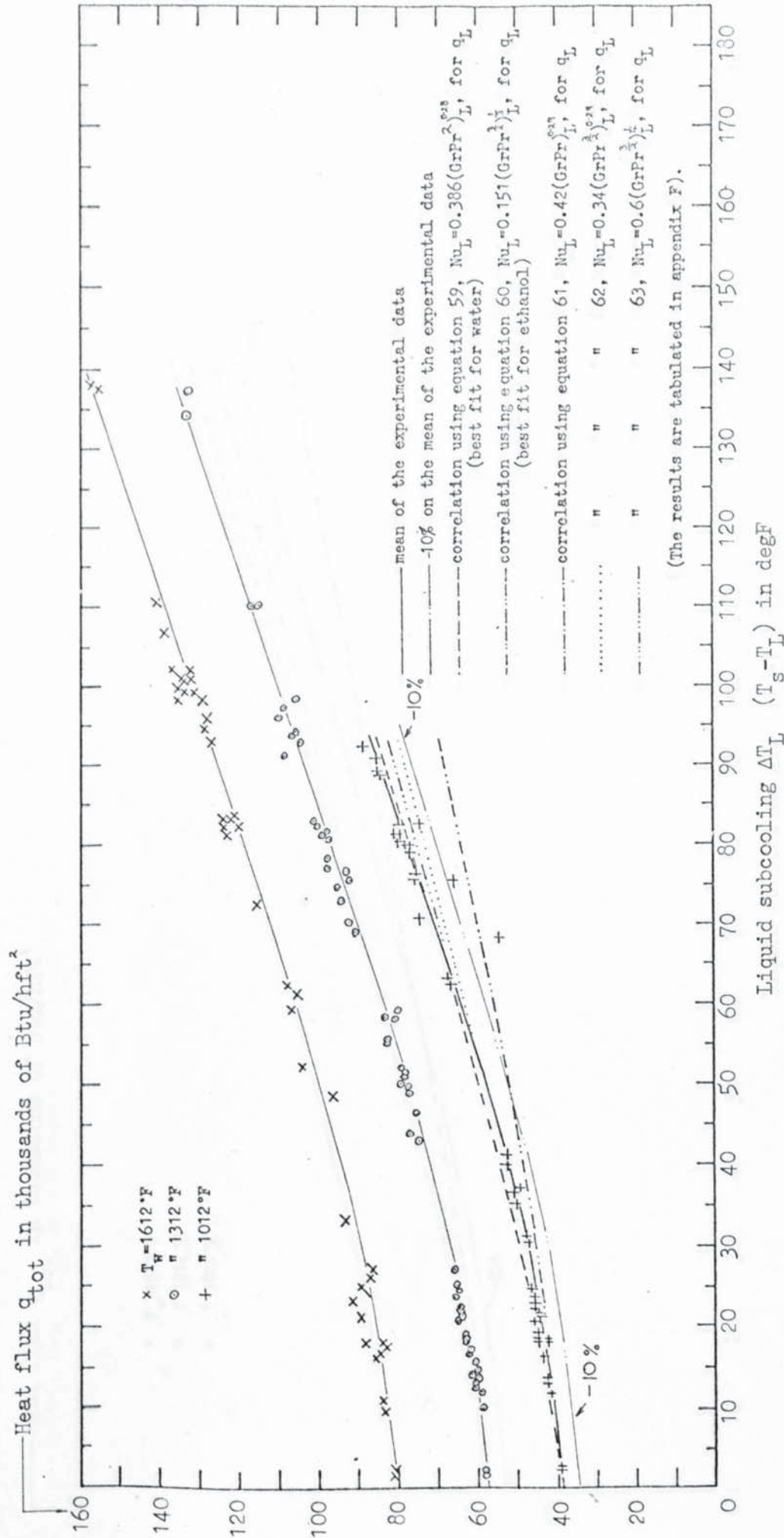


Figure 48. Film boiling of water on $\frac{1}{8}$ -inch diameter horizontal cylinders. Comparison of the experimental data with the proposed correlations at the surface temperature of 1012°F . (See section 8.5.)

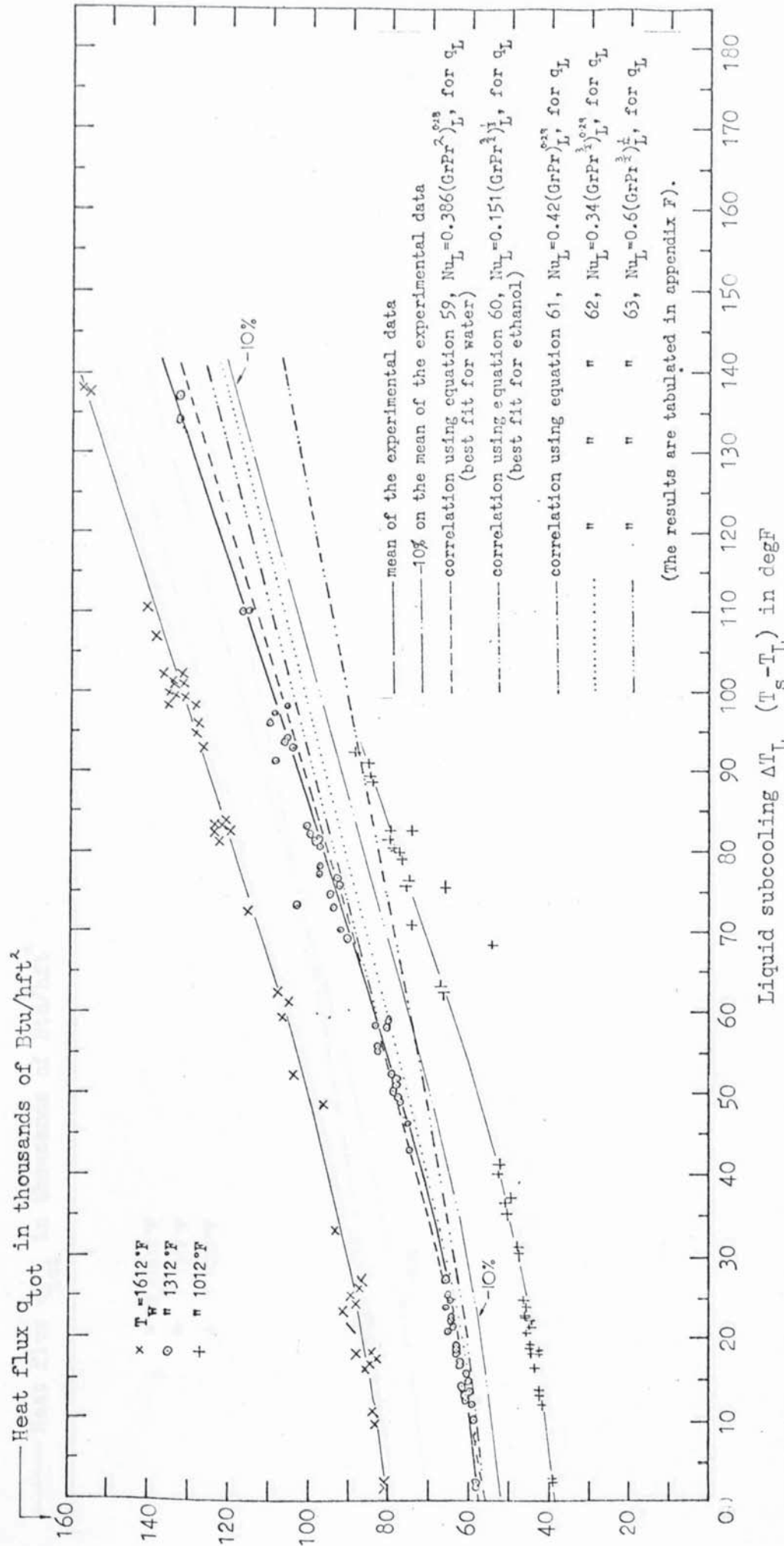


Figure 49. Film boiling of water on $\frac{1}{8}$ -inch diameter horizontal cylinders. Comparison of the experimental data with the proposed correlations at the surface temperature of 1312°F . (See section 8.5.)

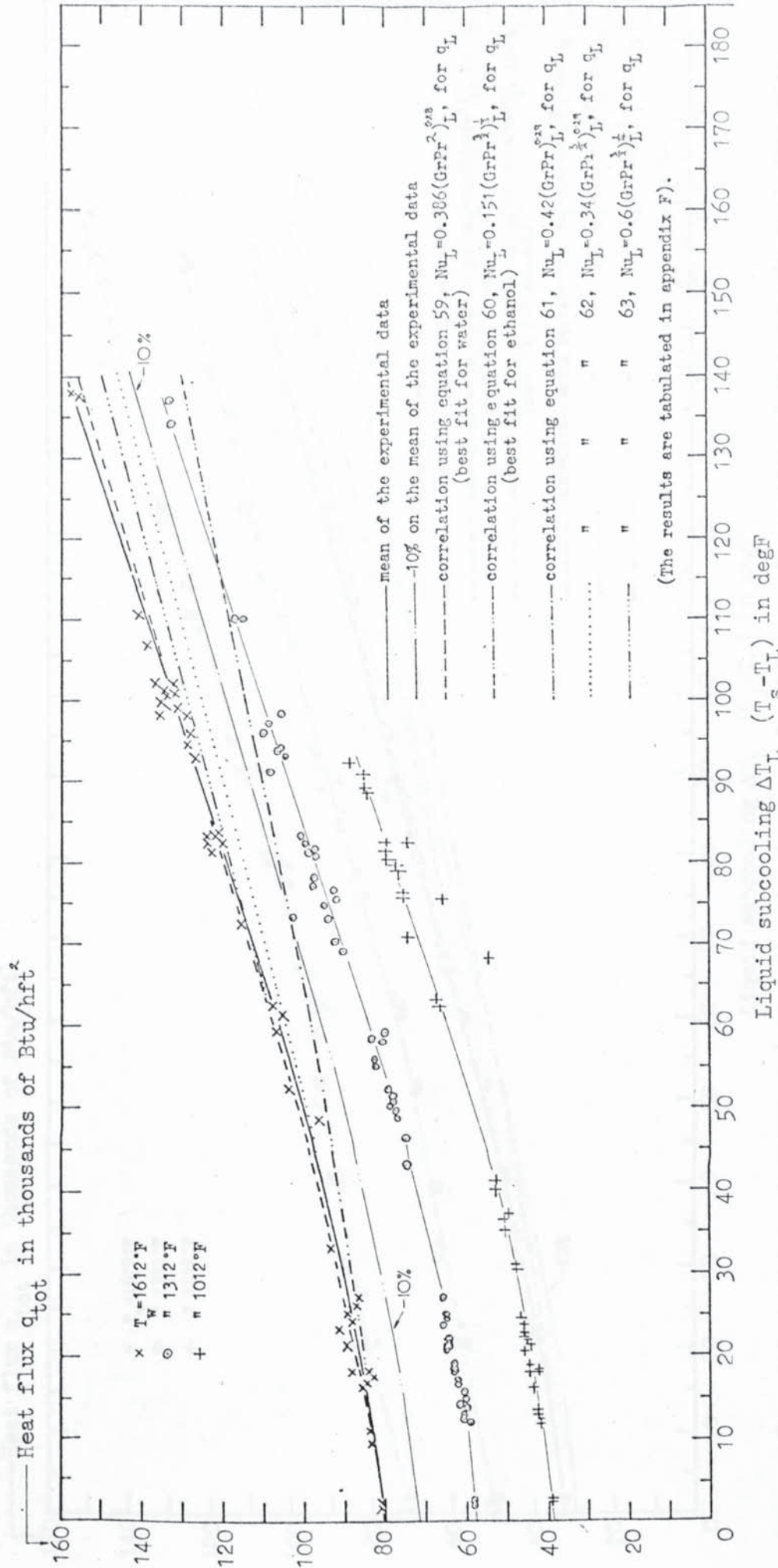
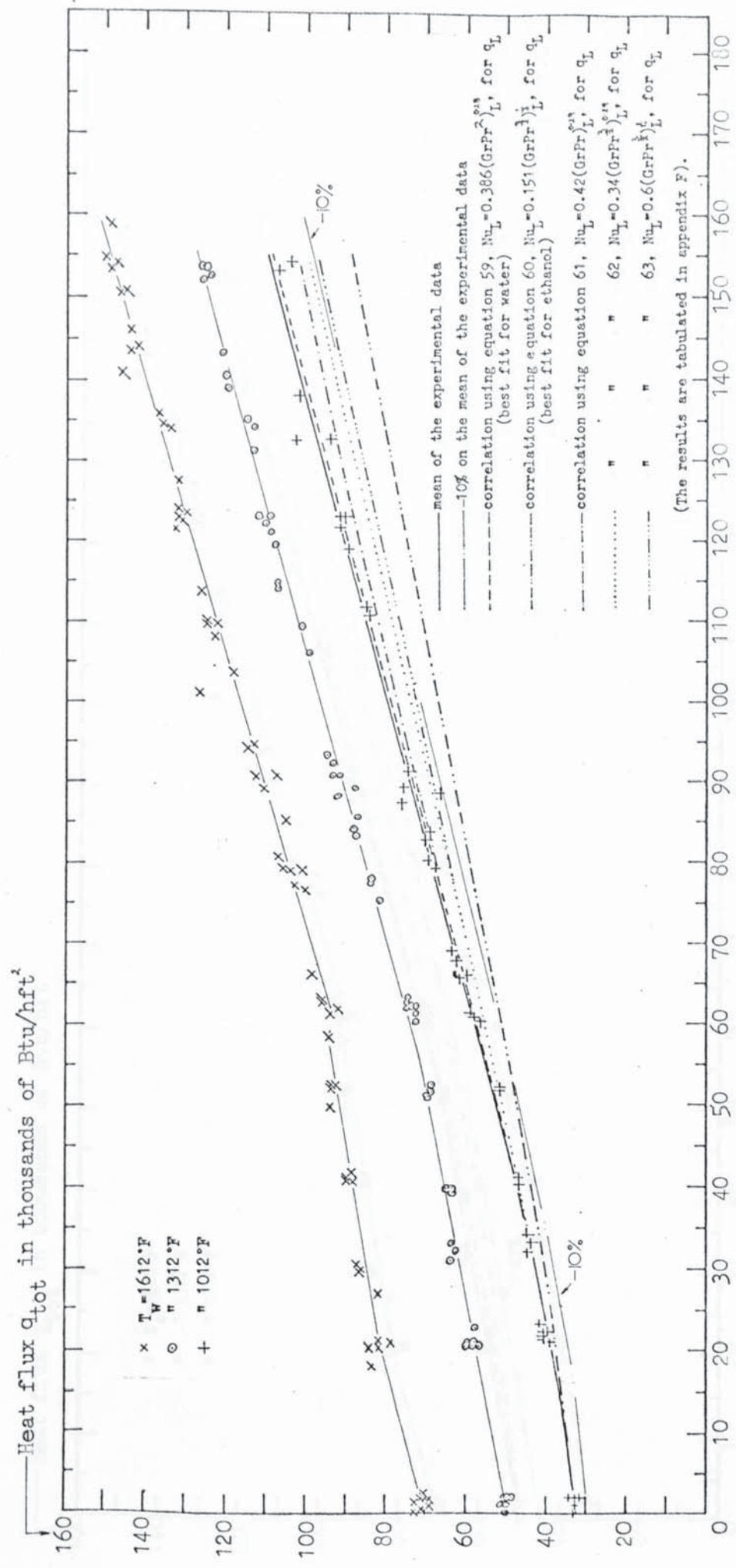


Figure 50. Film boiling of water on $\frac{1}{8}$ -inch diameter horizontal cylinders. Comparison of the experimental data with the proposed correlations at the surface temperature of 1612°F . (See section 8.5.)



Liquid subcooling ΔT_L ($T_s - T_L$) in degF

Figure 51. Film boiling of water on 1/4-inch diameter horizontal cylinders. Comparison of the experimental data with the proposed correlations at the surface temperature of 1012°F. (See section 8.5.)

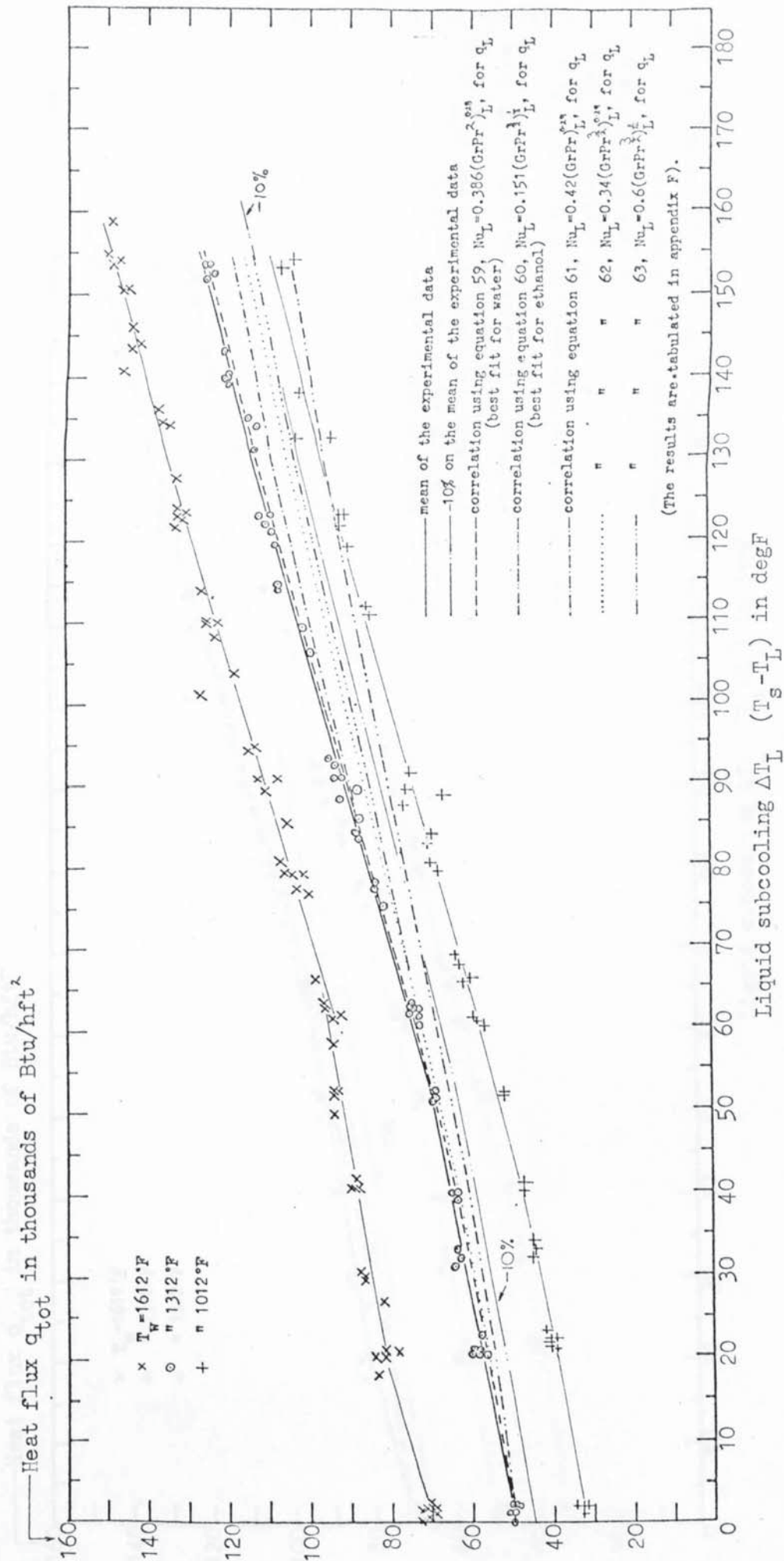


Figure 52. Film boiling of water on $\frac{1}{4}$ -inch diameter horizontal cylinders. Comparison of the experimental data with the proposed correlations at the surface temperature of 1312°F . (See section 8.5.)

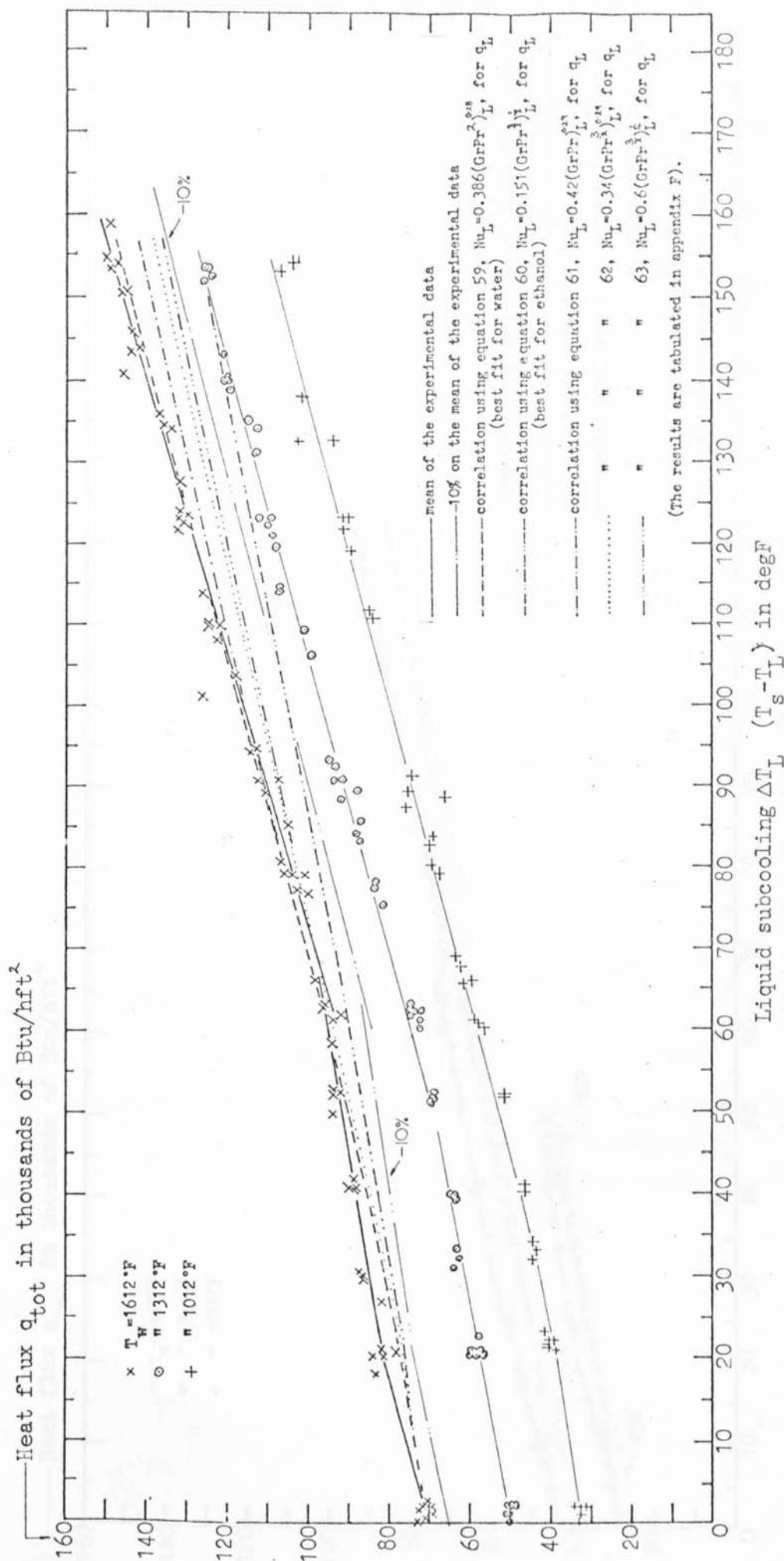


Figure 53. Film boiling of water on $\frac{1}{4}$ -inch diameter horizontal cylinders. Comparison of the experimental data with the proposed correlations at the surface temperature of 1612°F . (See section 8.5.)

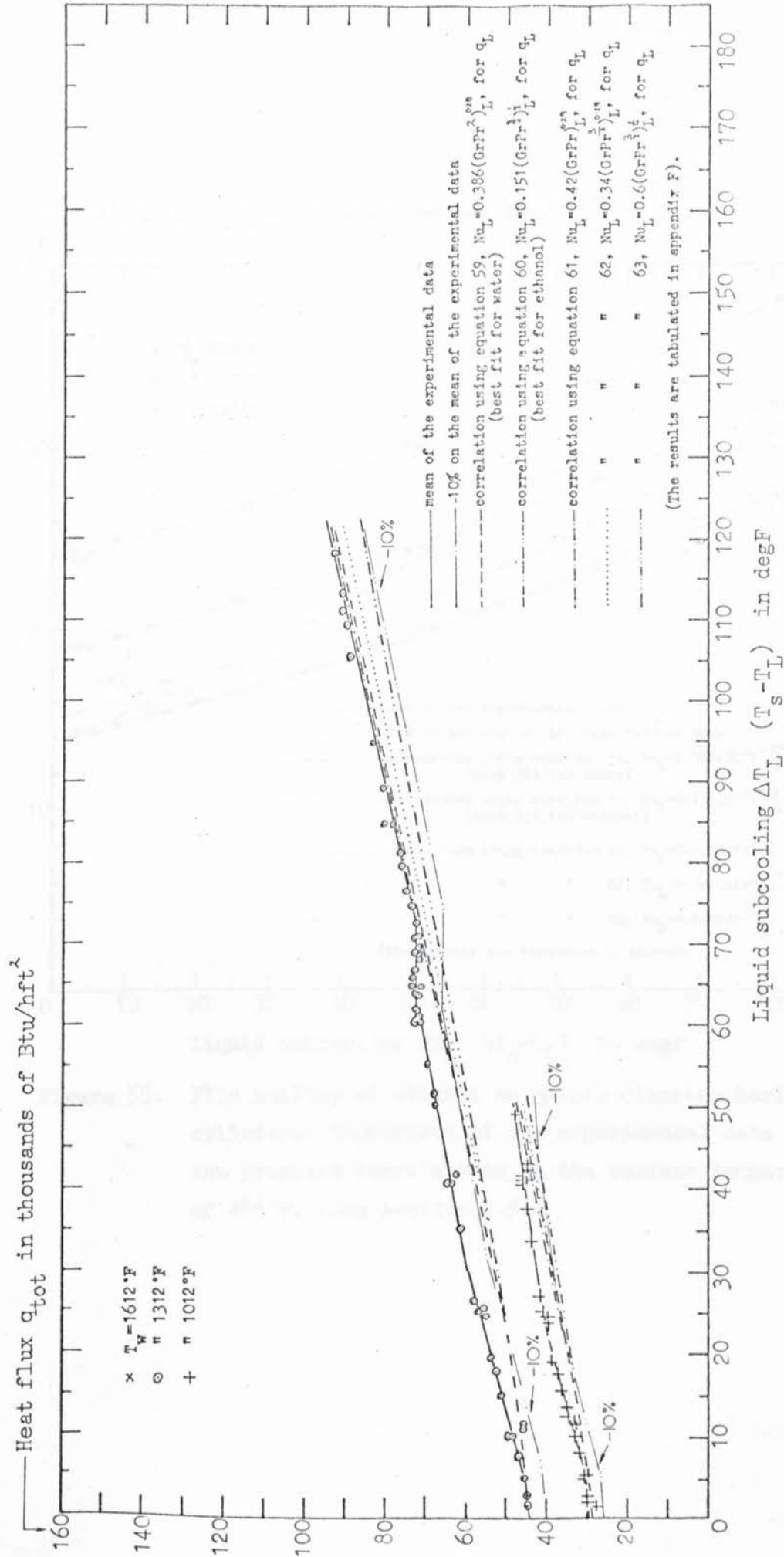


Figure 54. Film boiling of water on $\frac{1}{8}$ -inch diameter horizontal cylinders. Comparison of the experimental data with the proposed correlations at the surface temperatures of 1012°F and 1312°F . (See section 8.5.)

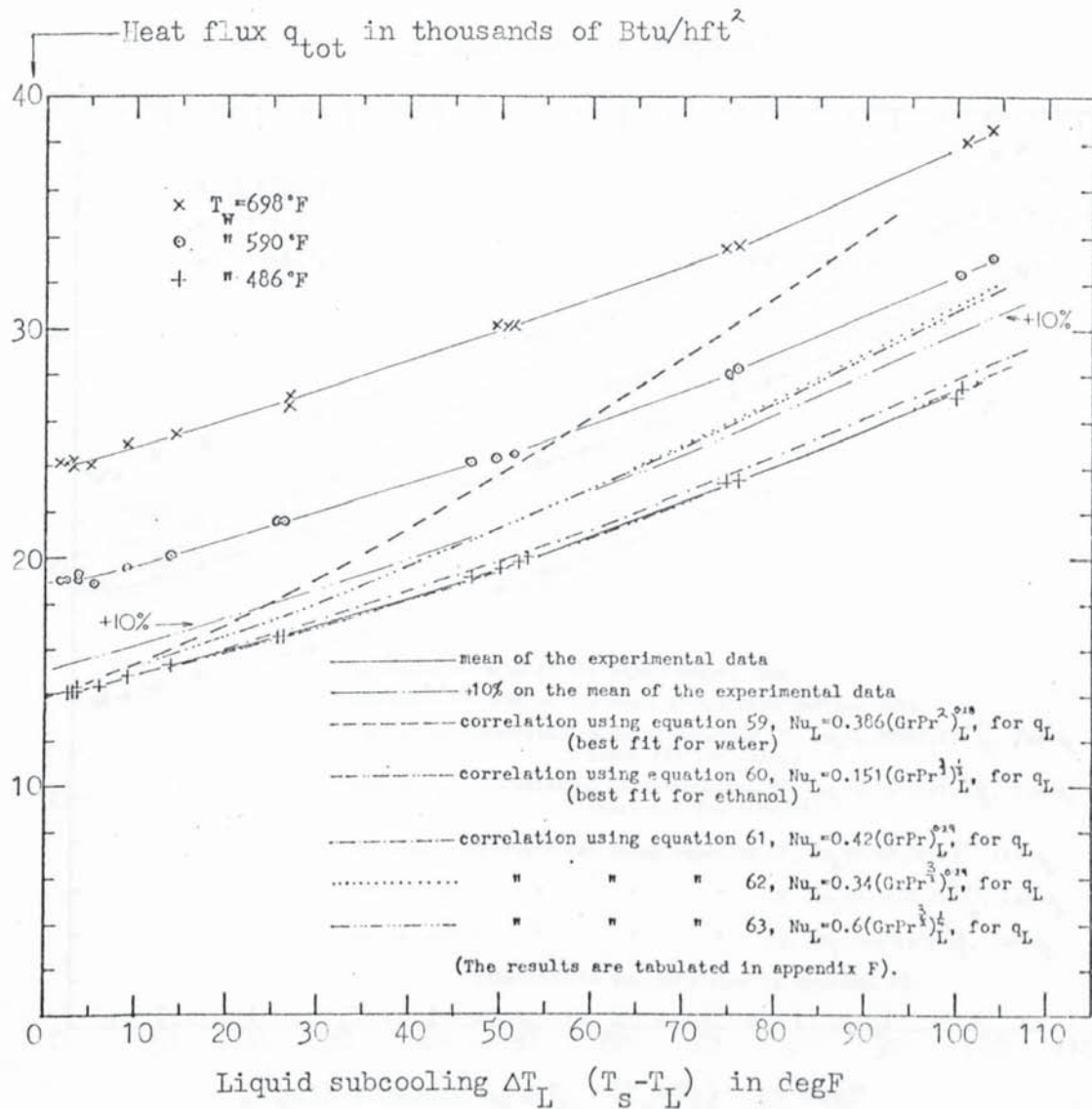


Figure 55. Film boiling of ethanol on $\frac{1}{8}$ -inch diameter horizontal cylinders. Comparison of the experimental data with the proposed correlations at the surface temperature of 486°F . (See section 8.5.)

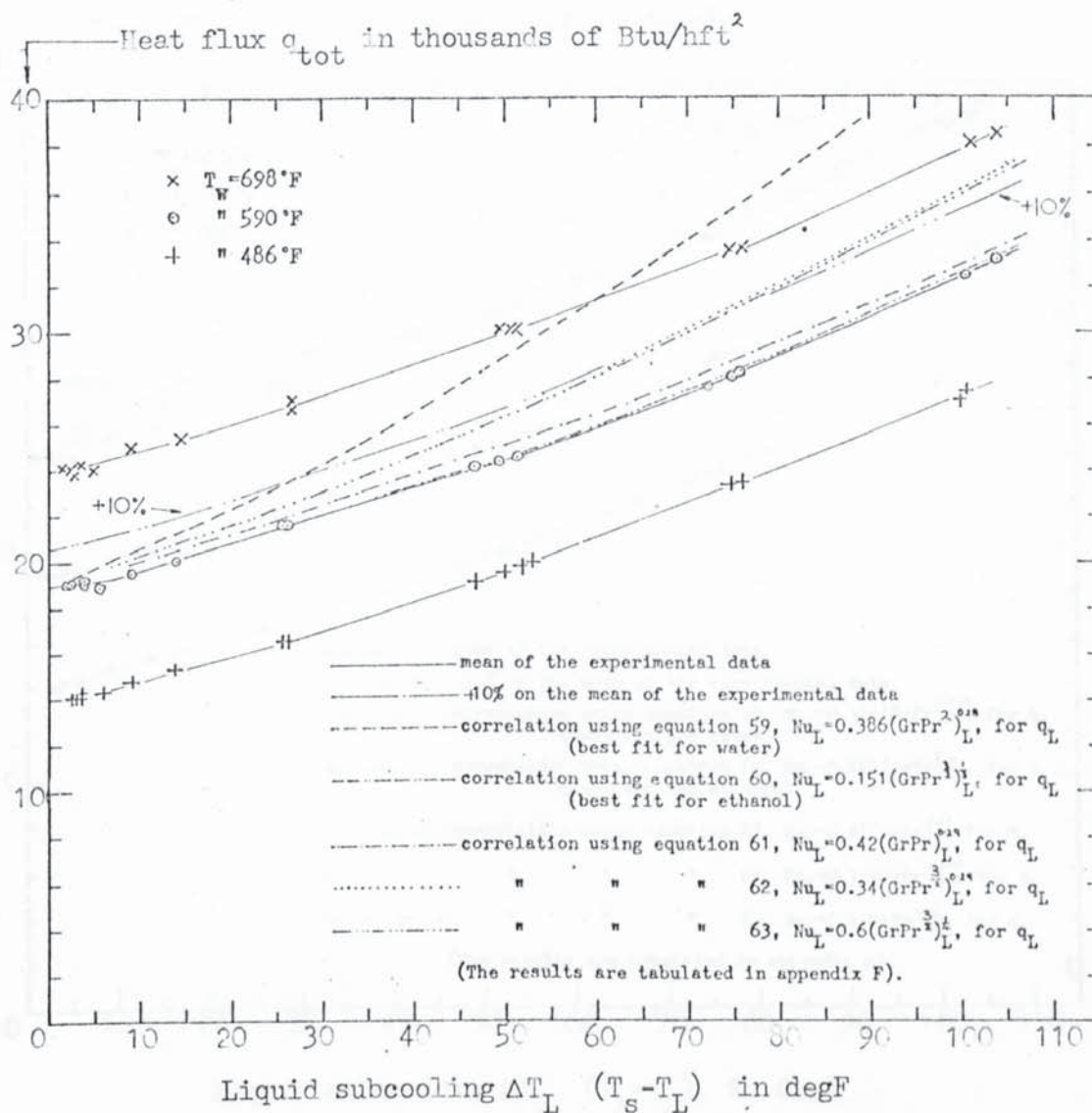


Figure 56. Film boiling of ethanol on $\frac{1}{8}$ -inch diameter horizontal cylinders. Comparison of the experimental data with the proposed correlations at the surface temperature of 590°F . (See section 8.5.)

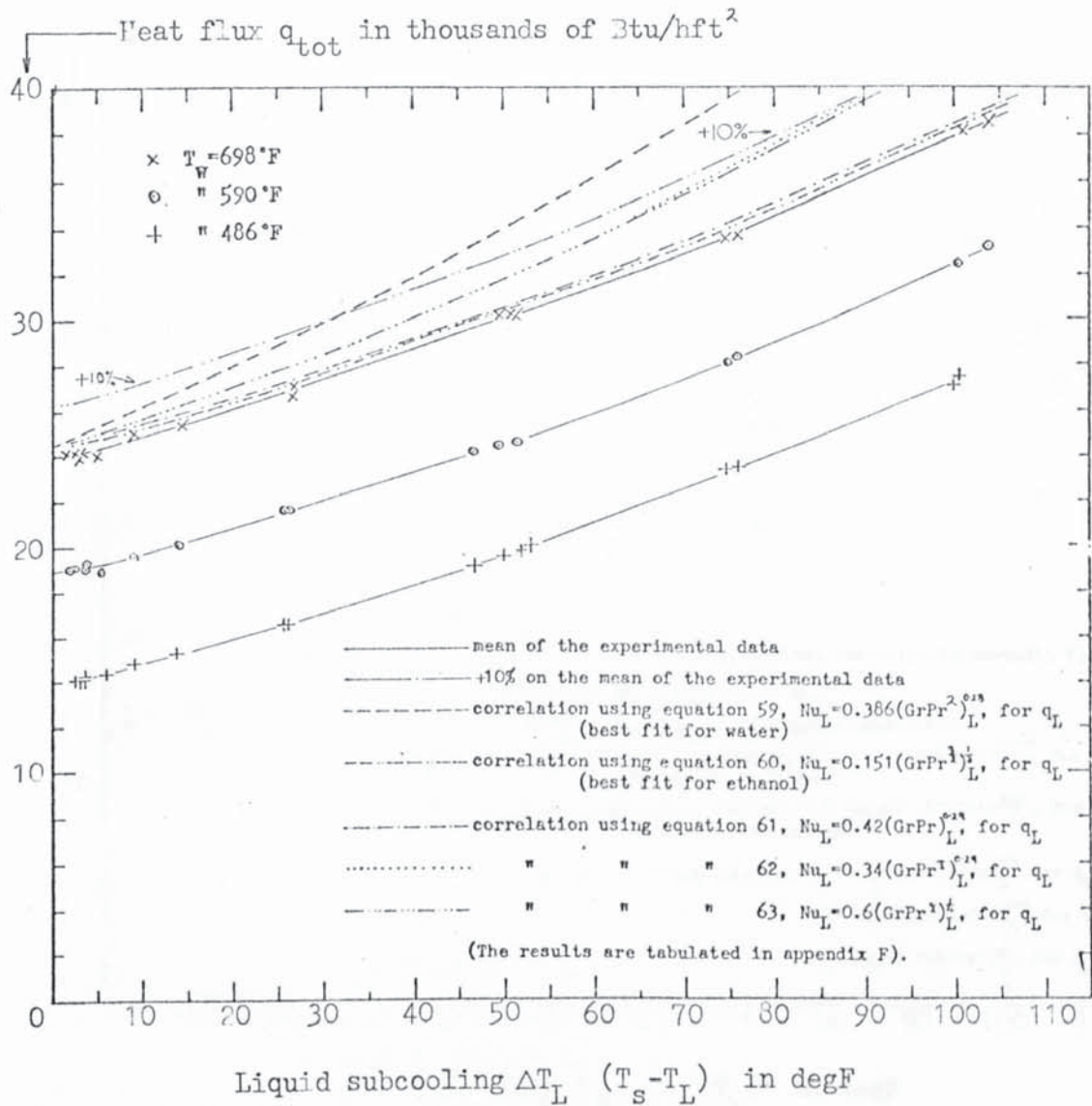


Figure 57. Film boiling of ethanol on $\frac{1}{8}$ -inch diameter horizontal cylinders. Comparison of the experimental data with the proposed correlations at the surface temperature of 698°F . (See section 8.5.)

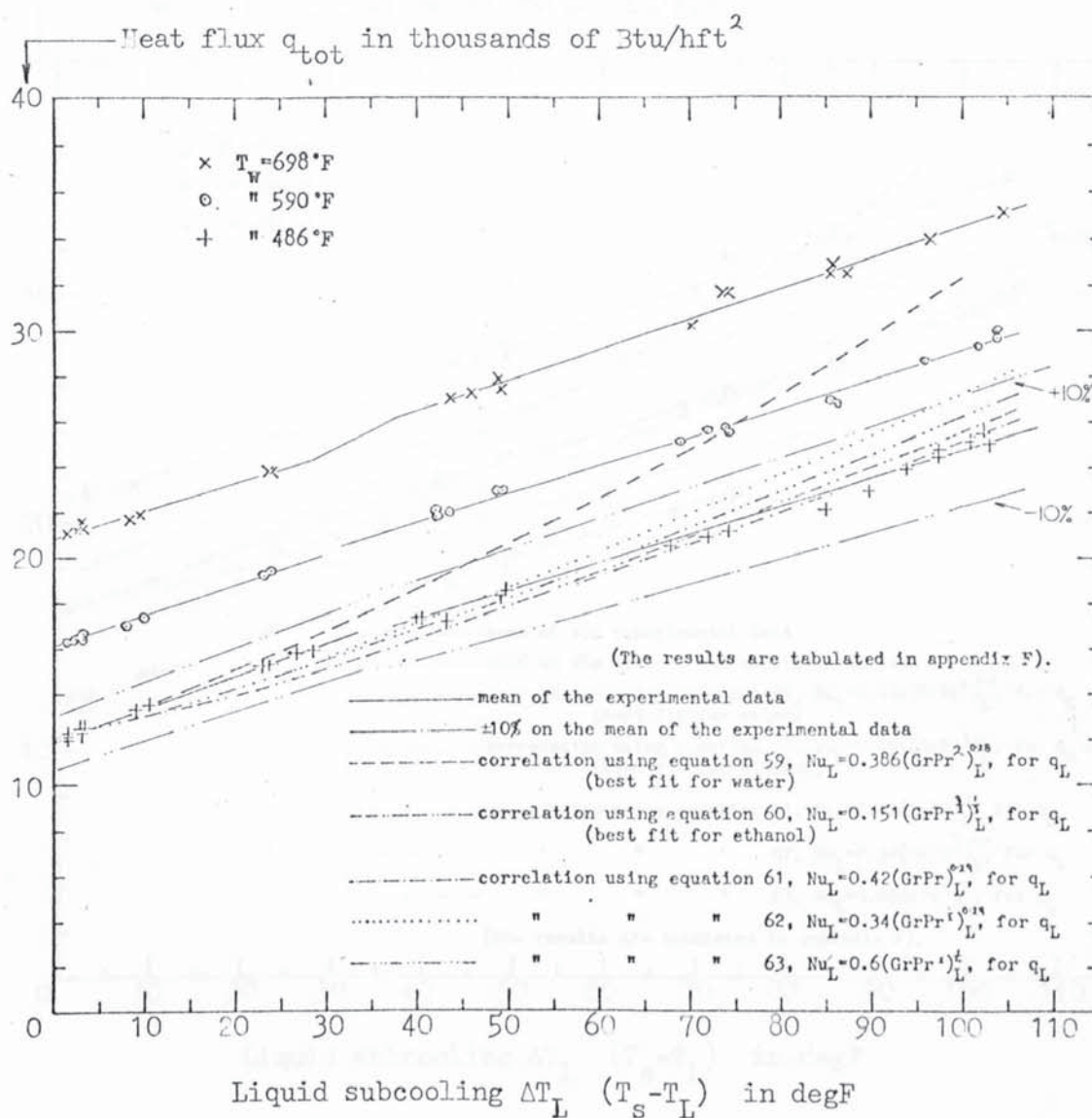


Figure 58. Film boiling of ethanol on $\frac{1}{4}$ -inch diameter horizontal cylinders. Comparison of the experimental data with the proposed correlations at the surface temperature of 486°F . (See section 8.5.)

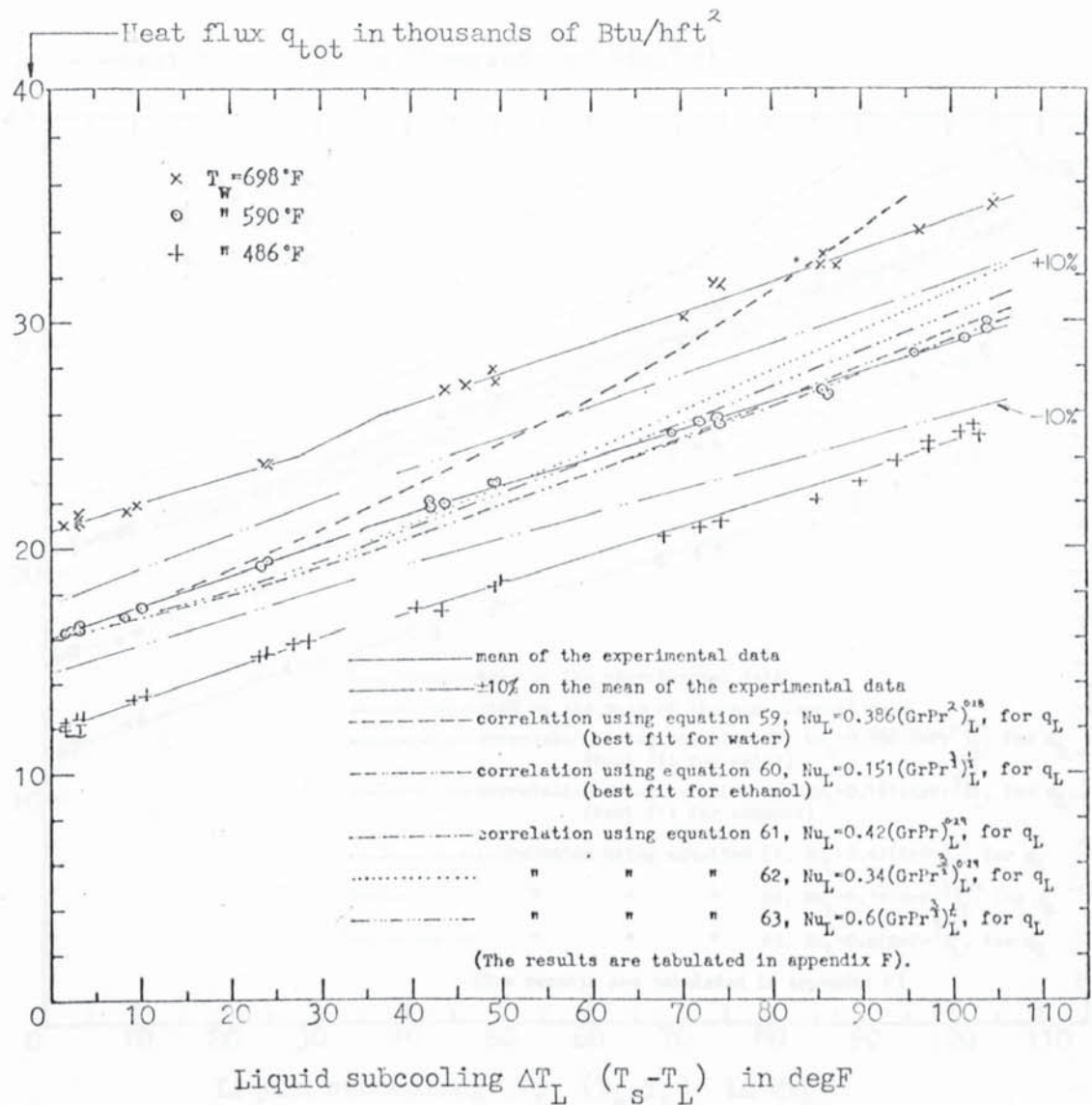


Figure 59. Film boiling of ethanol on $\frac{1}{4}$ -inch diameter horizontal cylinders. Comparison of the experimental data with the proposed correlations at the surface temperature of 590°F . (See section 8.5.)

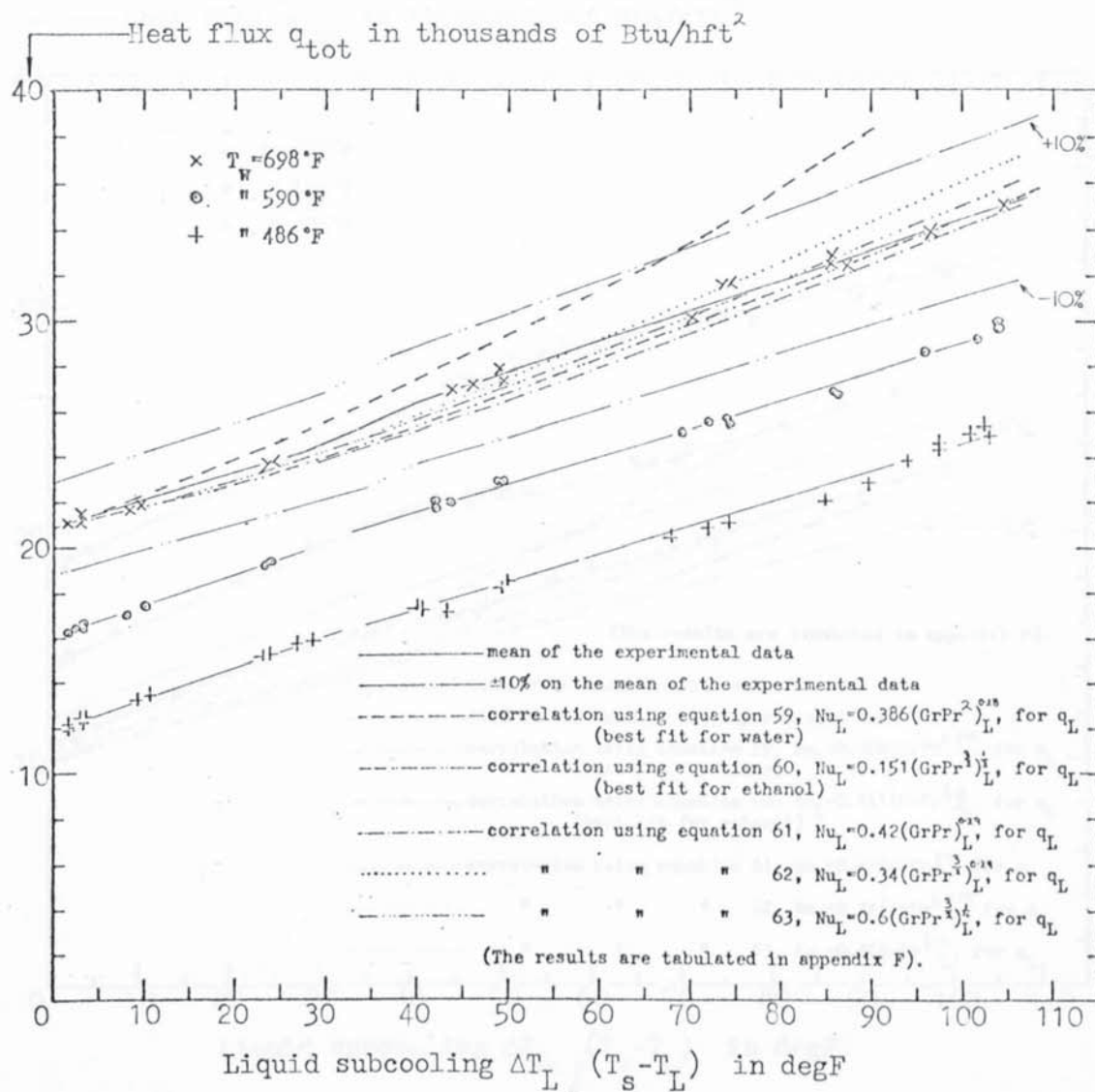


Figure 60. Film boiling of ethanol on $\frac{1}{4}$ -inch diameter horizontal cylinders. Comparison of the experimental data with the proposed correlations at the surface temperature of 698°F . (See section 8.5.)

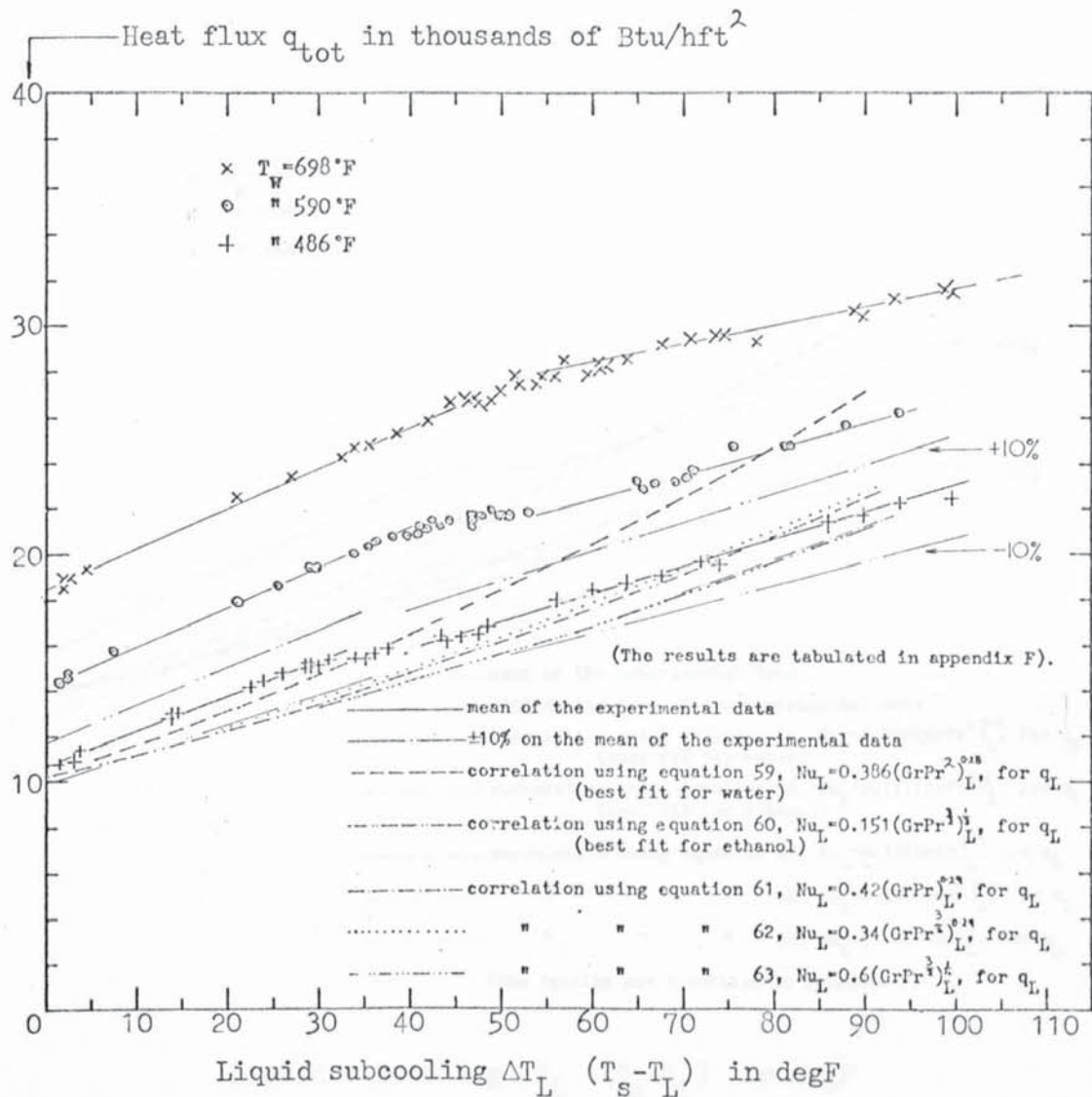


Figure 61. Film boiling of ethanol on $\frac{1}{2}$ -inch diameter horizontal cylinders. Comparison of the experimental data with the proposed correlations at the surface temperature of 486°F . (See section 8.5.)

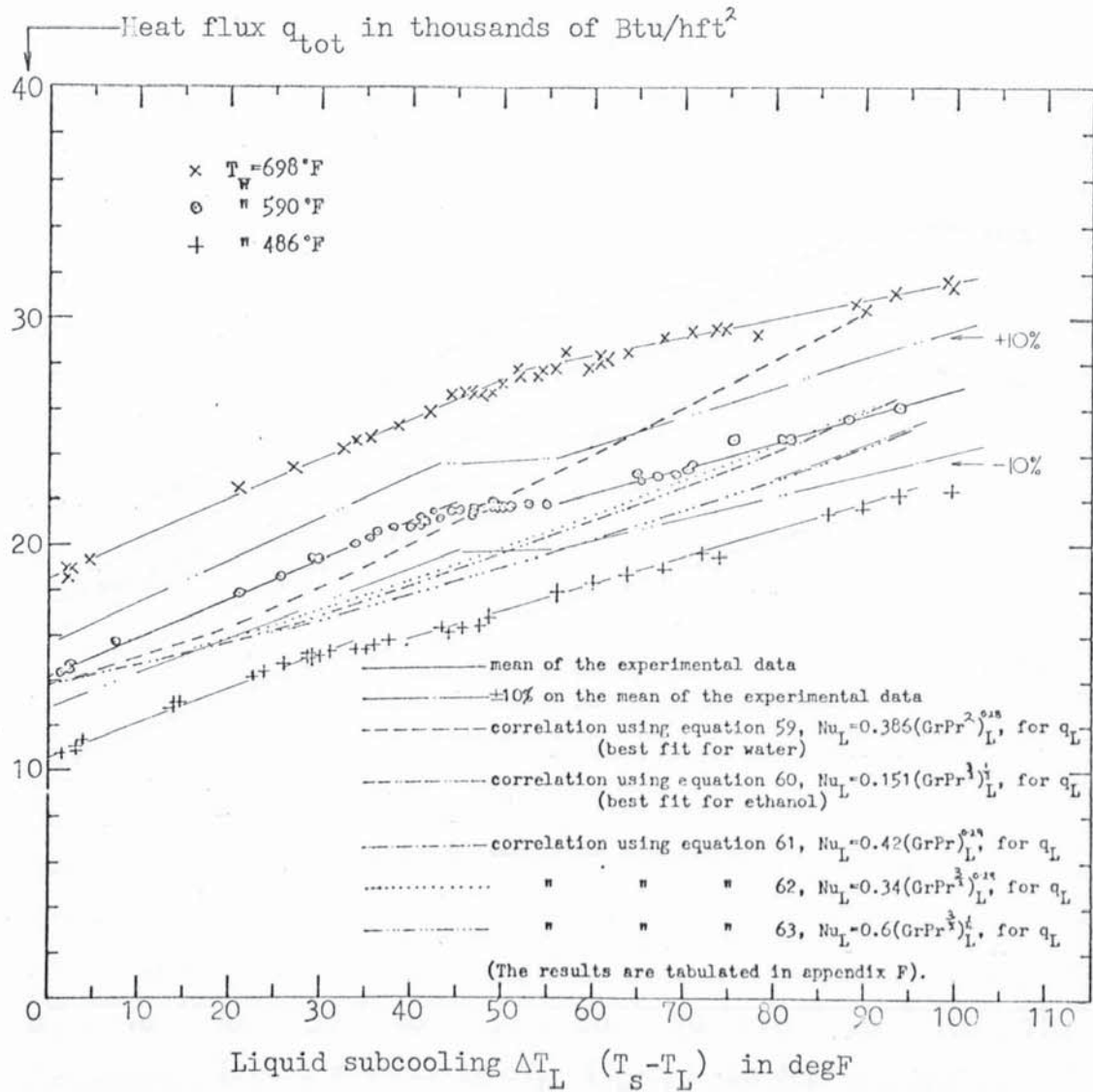


Figure 62. Film boiling of ethanol on $\frac{1}{2}$ -inch diameter horizontal cylinders. Comparison of the experimental data with the proposed correlations at the surface temperature of 590°F . (See section 8.5.)

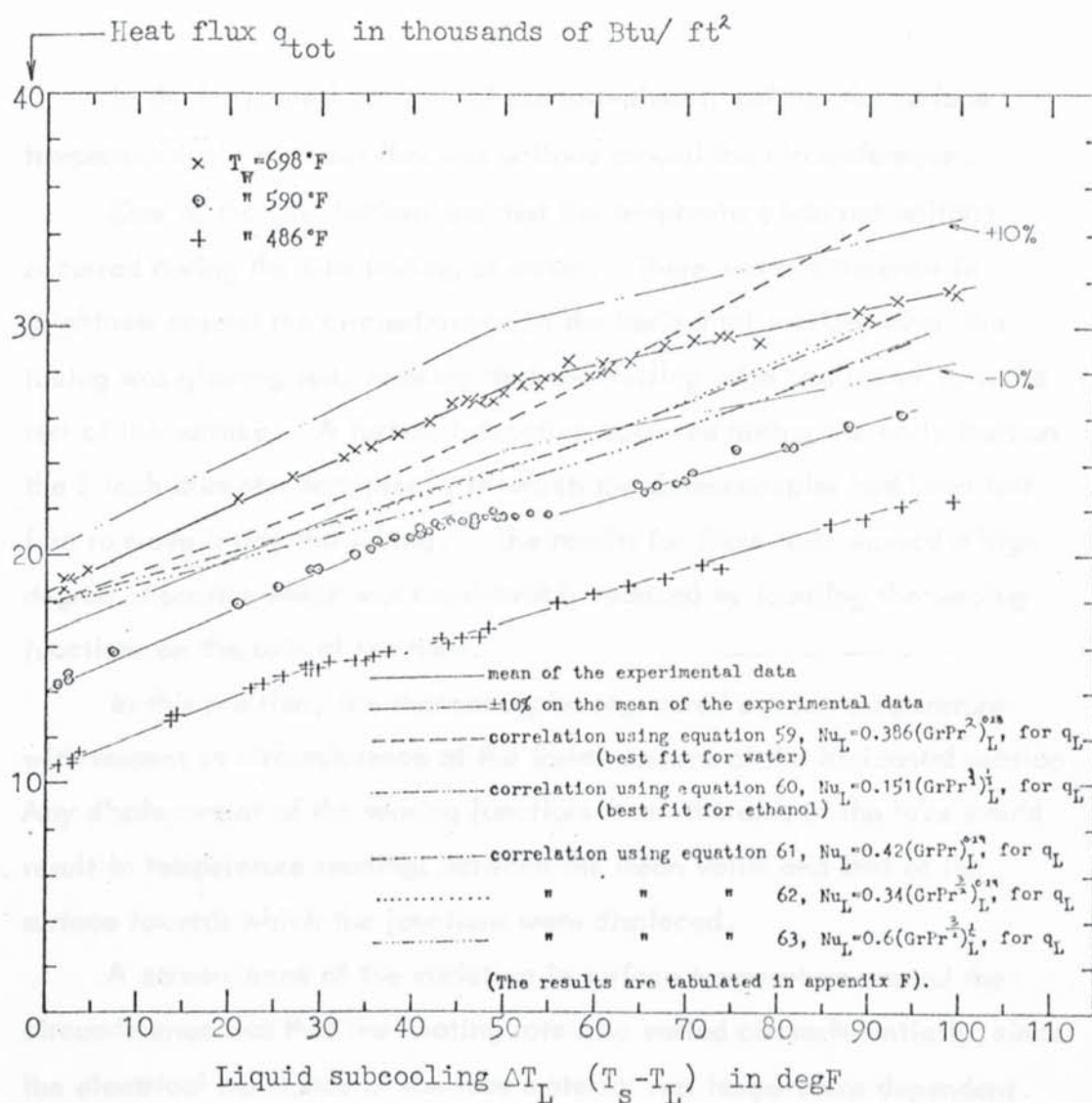


Figure 63. Film boiling of ethanol on $\frac{1}{2}$ -inch diameter horizontal cylinders. Comparison of the experimental data with the proposed correlations at the surface temperature of 698°F . (See section 8.5.)

Appendix A

CIRCUMFERENTIAL VARIATIONS OF SURFACE TEMPERATURE AND HEAT FLUX

In the horizontal sections of the test-pieces, neither the surface temperature nor the heat flux was uniform around the circumference.

One of the first indications that the temperature was not uniform occurred during the film boiling of water. There was a difference in brightness around the circumference in the horizontal sections when the tubing was glowing red, showing that the trailing edge was hotter than the rest of the surface. A further indication occurred during the early tests on the $\frac{1}{4}$ inch diameter test-piece, in which the thermocouples had been left free to move inside the tubing. The results for these tests showed a high degree of scatter which was considerably reduced by locating the sensing junctions on the axis of the tube.

In this position, the thermocouples registered a mean temperature with respect to circumference of the inside surface of the horizontal section. Any displacement of the sensing junctions from the axis of the tube would result in temperature readings between the mean value and that of the surface towards which the junctions were displaced.

A consequence of the variation in surface temperature around the circumference was that the heating rate also varied circumferentially, since the electrical resistance of the tube material was temperature dependent. The hotter, upper parts of the horizontal section were of higher resistance than the colder, lower parts. Since these paths of differing resistance were parallel, then, from the equation $W = E^2/R$ (watts = voltage squared divided by resistance), the heating rate was greater along the bottom of the tube than along the top.

There would of course be a tendency to revert to a condition of uniform surface temperature because heat would be conducted and radiated from the hotter to the colder surfaces.

A qualitative explanation of why the temperature variation occurs depends on the fact that, in laminar convection, heat transfer coefficients are largest at the leading edge and decrease with distance from it. Thus

In the present tests, in which the heating rate is the independent parameter, the surface temperature changed to accommodate the change of heat transfer coefficient.

Appendix B

SOLUTION OF THE INTEGRATED BOUNDARY LAYER EQUATIONS FOR THE LIQUID PHASE

The integrated boundary layer equations for single phase free convection given in reference (52) are :

$$\text{momentum} \quad \frac{d}{dx} \int_0^h u^2 dy = g\beta \int_0^h \Theta dy - \nu \left. \frac{du}{dy} \right|_0 \quad (\text{B1})$$

$$\text{energy} \quad \frac{d}{dx} \int_0^h u \Theta dy = -\alpha \left. \frac{d\Theta}{dy} \right|_0 \quad (\text{B2})$$

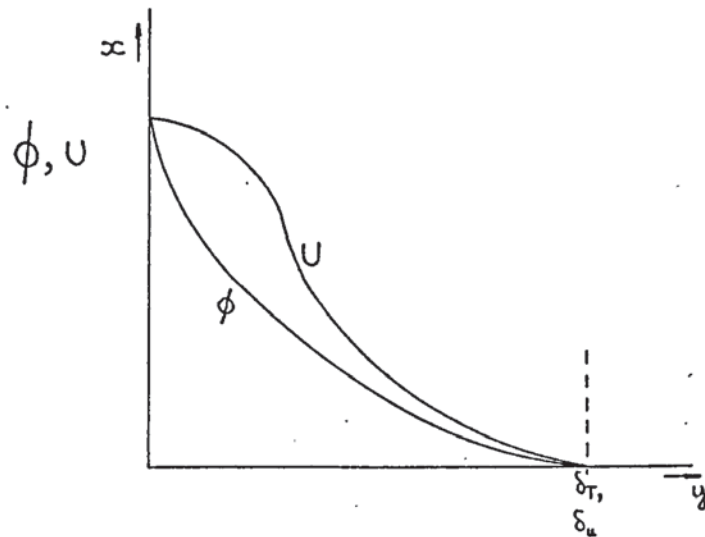
By assuming velocity and temperature profiles an approximate solution of these equations can be achieved from which an approximate equation for heat transfer can be obtained. The value of the numerical coefficient of the heat transfer equation varies slightly according to the profiles assumed, but this is not important because the value of the coefficient is usually selected in the light of experimental data.

The above procedure has been applied to obtain a solution for the liquid heat transfer in subcooled film boiling on a vertical plate. The modification of the coefficient to make the solution apply to the horizontal cylinder as described in section 3.4 was not carried out because of the approximate nature of the solution, but selected from experimental data as mentioned above.

The profiles that were assumed are sketched below and were :

$$\text{temperature} \quad \phi = \frac{\Theta}{\Theta_w} = \frac{T - T_L}{T_s - T_L} = 1 - 2 \left(\frac{y}{\delta_T} \right) + \left(\frac{y}{\delta_T} \right)^2 = \left(1 - \frac{y}{\delta_T} \right)^2 \quad (\text{B3})$$

$$\text{velocity} \quad U = \frac{u}{u_w} = 1 - \frac{3}{2} \left(\frac{y}{\delta_u} \right) + \frac{1}{2} \left(\frac{y}{\delta_u} \right)^3 \quad (\text{B4})$$



The profiles satisfy the following boundary conditions :

temperature	1.	$y = 0$	$\phi = 1$	i.e. $T = T_s$
	2.	$y = \delta_T$	$\phi = 0$	$T = T_L$
	3.	$y = \delta_T$	$\phi' = \frac{d\phi}{dy} = 0$	zero temperature gradient
velocity	4.	$y = 0$	$U = 1$	$u = u_w = u_{\text{maximum}}$
	5.	$y = 0$	$U' = 0$	zero interfacial shear
	6.	$y = \delta_u$	$U = 0$	stationary bulk liquid
	7.	$y = \delta_u$	$U' = 0$	zero velocity gradient

The boundary conditions 4 and 5 arise because it has been assumed that the liquid moves freely, i.e. under its own buoyancy and without any shear at the interface. The theoretical solution by Nishikawa and Ito (53) section 3.7.1 which involved both phases, indicates that for water these boundary conditions are reasonably close approximations at moderate and high subcooling. The fact that velocities in the y - direction are not considered implies that there is no evaporation and condensation.

A relation for the Nusselt number can be obtained from the temperature profile. At any position on the interface the conduction equation gives the local heat flux q_x , as

$$q_x = -k \left. \frac{d\Theta}{dy} \right|_0$$

The local Nusselt number was defined as :

$$Nu_x = \frac{q}{\Theta_w} \cdot \frac{x}{k}$$

Substitution gives

$$Nu_x = - \left. \frac{d\Theta}{dy} \right|_0 \frac{x}{\Theta_w},$$

and from the temperature profile

$$\left. \frac{d\Theta}{dy} \right|_0 = \left. \frac{d\Theta}{dy} \right|_0 \frac{1}{\Theta_w}$$

hence

$$Nu_x = -x \phi = \frac{2x}{\delta_T} \quad (B5)$$

It is often assumed that in free convection the temperature and velocity boundary layers are of equal thickness ($\delta_T = \delta_u$), and the solution was first carried out after making this assumption. The thicknesses are the same, however, only when the value of the Prandtl number is unity. At other values of the Prandtl number the two thicknesses are related by the value of the Prandtl number thus (18) :

$$\delta_u = \delta_T \sqrt{\text{Pr}} \quad (B6)$$

A second solution was therefore carried out using this relationship.

Solution 1 $\delta_u = \delta_T = \delta$

From equations B3 and B4 ,

$$\int_0^h u^2 dy = \int_0^\delta u^2 dy = \frac{13}{35} u_w^2 \delta$$

$$\int_0^h \Theta dy = \int_0^\delta \Theta dy = \frac{1}{3} \Theta_w \delta$$

$$\int_0^h \Theta u \, dy = \int_0^\delta \Theta u \, dy = \frac{4}{15} \Theta_w u_w$$

$$\left. \frac{du}{dy} \right|_0 = 0$$

$$\left. \frac{d\Theta}{dy} \right|_0 = -\frac{2\Theta_w}{\delta}$$

Hence the boundary layer equations B1 and B2 become :

$$\frac{13}{35} \frac{d}{dx} (u_w^2 \delta) = \frac{1}{3} g \beta \Theta_w \delta$$

and

$$\frac{4}{15} \frac{d}{dx} (\Theta_w u_w \delta) = \frac{2}{\delta} \propto \Theta_w$$

By making the substitutions $u_w = Cx^{\frac{1}{2}}$ and $\delta = Kx^{\frac{1}{4}}$ the equations reduce to :

$$C^2 = \frac{28}{39} g \beta \Theta_w$$

and

$$C^2 K^4 = 100 \propto^2$$

$$\text{Hence } \delta = Kx^{\frac{1}{4}} = x^{\frac{1}{4}} \left[\frac{39}{28} \frac{100}{g \beta \Theta_w} \right]^{\frac{1}{4}},$$

$$Nu_x = \frac{2x}{\delta} = 0.583 [Gr_x Pr^2]^{\frac{1}{4}},$$

$$\text{and } Nu = \frac{4}{3} Nu_x = 0.777 [Gr Pr^2]^{\frac{1}{4}}. \quad (B7)$$

A general solution for all similar profiles is therefore :

$$Nu = N [Gr Pr^2]^{\frac{1}{4}}. \quad (B8)$$

Solution 2. $\delta_u = \delta_T \sqrt{\text{Pr}}$

From equations B3 and B4,

$$\int_0^h u^2 dy = \int_0^{\delta_u} u^2 dy = \frac{13}{35} u_w^2 \delta_u ,$$

$$\int_0^h \Theta dy = \int_0^{\delta_T} \Theta dy = \frac{1}{3} \Theta_w \delta_T ,$$

$$\begin{aligned} \int_0^h u \Theta dy &= \int_0^{\delta_T} u \Theta dy = \Theta_w u_w \delta_T \left(\frac{1}{3} - \frac{1}{10\text{Pr}} + \frac{1}{30\text{Pr}\sqrt{\text{Pr}}} \right) \\ &= \Theta_w u_w \delta_T f(\text{Pr}) . \end{aligned}$$

The last integration had to be carried out from 0 to δ_T only because for $y > \delta_T$ the integrand is zero.

Continuing, $\left. \frac{du}{dy} \right|_0 = 0 ,$

and $\left. \frac{d\Theta}{dy} \right|_0 = - \frac{2\Theta_w}{\delta_T}$

By making the substitutions $u_w = Cx^{\frac{1}{2}}$ and $\delta_T = Kx^{\frac{1}{4}}$ the equations reduce to :

$$C^2 = \frac{28}{29} \frac{g\beta\Theta}{\sqrt{\text{Pr}}} ,$$

$$\text{and } C^2 K^4 = \frac{64}{9} \frac{\alpha^2}{(f(\text{Pr}))^2} .$$

$$\text{Hence } \delta_T = Kx^{\frac{1}{4}} = x^{\frac{1}{4}} \left[\frac{64}{9} \frac{39}{28} \frac{\alpha^2}{g\beta\Theta_w} \frac{\sqrt{\text{Pr}}}{(f(\text{Pr}))^2} \right]^{\frac{1}{4}} ,$$

$$\text{Nu}_x = \frac{2x}{\delta} = 1.13 \left[\text{Gr}_x \text{Pr}^{\frac{3}{2}} \right]^{\frac{1}{4}} \left[f(\text{Pr}) \right]^{\frac{1}{2}} ,$$

$$Nu = \frac{4}{3} Nu_x = 1.51 \left[GrPr^{\frac{3}{2}} \right]^{\frac{1}{4}} \left[f(Pr) \right]^{\frac{1}{2}} . \quad (B 9)$$

A general solution for all similar profiles is therefore :

$$Nu = N \left[GrPr^{\frac{3}{2}} \right]^{\frac{1}{4}} \left[\frac{1}{3} - \frac{1}{10Pr} + \frac{1}{30Pr\sqrt{Pr}} \right]^{\frac{1}{2}} . \quad (B 10)$$

Appendix C

EXPERIMENTAL RESULTS

Table C (page 192 to 215)

The experimental results are presented in table C for each of the nominal values of cylinder diameter. The exact values of the diameters are given in appendix E, table E1.

1/8 - inch diameter

Nominal Diameter and Test No.	Test Fluid	Surface Temperature T_w °F	Subcooling ΔT_L degF	Heat Flux q_{tot} Btu/hft ²
1/8 S1.2	Distilled Water	1312	13.5	59 500
3	"	"	15.5	60 300
4	"	"	18	63 200
5	"	"	23.5	65 800
6	"	"	20.5	64 800
7	"	"	19	63 100
8	"	1012	19	44 700
9	"	"	24.5	46 400
10	"	1312	22.5	65 400
11	"	1012	22	45 600
12	"	1312	21	64 100
13	"	1012	21	43 600
1/8 S2.1	De-ionized Water	1312	14	61 500
2	"	1012	16	43 400
3	"	1312	16.5	62 000
4	"	1012	18.5	44 700
5	"	1312	18.5	63 100
6	"	1012	20.3	45 600
9	"	1312	46	75 100
11	"	1612	33	93 500
12	"	1612	25.5	91 500
13	"	"	21	89 600
14	"	"	18	88 200
15	"	"	16.5	84 700
16	"	"	16	85 500
17	"	1312	17	62 300
18	"	1012	18	44 800
22	"	1612	52	104 000
23	"	"	48.3	96 300
28	"	1012	75.3	65 800
29	"	1312	74.5	82 200
30	"	1612	73	103 000
31	"	1312	70.5	74 500
32	"	1012	68	54 500
1/8 S3.1	De-ionized Water	1312	29.5	66 800
2	"	1012	30.3	43 700

Nominal Diameter and Test No.	Test Fluid	Surface Temperature T_w °F	Subcooling ΔT_L degF	Heat Flux q_{tot} Btu/hft ²
1/8 S3.3	De-ionized Water	1312	31	68 200
4	"	1312	41.5	73 600
5	"	"	42.7	75 500
6	"	"	55.3	82 300
7	"	"	55.3	82 300
8	"	"	58	83 200
9	"	"	72.7	94 000
10	"	"	83	101 000
11	"	1012	82.3	79 700
12	"	1312	91	108 500
13	"	"	90.5	104 500
1/8 T1.1	De-ionized Water	1312	74.5	95 000
2	"	"	68.7	90 200
3	"	"	70	92 100
4	"	"	48.7	77 000
5	"	"	49.5	77 500
6	"	"	21.5	64 400
7	"	"	22	65 000
8	"	"	13	60 600
9	"	"	13	60 500
1/8 T2.1	De-ionized Water plus 0.01% teepol	1312	68.7	90 200
2	"	"	68	89 800
3	"	"	84	98 800
4	"	"	83	97 900
5	"	"	92	98 800
6	"	"	94.5	105 500
7	"	1012	93	80 200
9	"	1312	95.7	106 500
10	"	"	45	76 500
11	"	"	46.5	78 800
12	"	"	45.7	77 000
13	"	"	21.5	64 600
14	"	"	21.5	64 600
15	"	"	23.7	65 500
16	"	1612	140	139 000

Nominal Diameter and Test No.	Test Fluid	Surface Temperature T_w °F	Subcooling ΔT_L degF	Heat Flux q_{tot2} Btu/hft ²
1/8T2.18	De-ionized Water plus 0.01% teepol	1612	135.5	143 000
1/8T3.1	De-ionized Water plus 0.01% teepol	1612	103	133 000
2	"	1312	102.3	105 000
3	"	1612	102.3	132 000
4	"	1312	101.5	106 000
5	"	"	82.3	95 500
6	"	1612	82	120 000
7	"	1012	79.5	58 200
8	"	1312	80.5	95 500
9	"	"	77	94 000
10	"	1612	76	118 000
11	"	"	73	116 000
12	"	1012	70	69 000
13	"	1612	73	116 000
14	"	1012	69	68 500
15	"	1612	81.5	120 000
19	"	1012	78	65 000
20	"	"	77	64 000
21	"	"	76	63 500
22	"	"	79.5	74 800
1/8U1.1	De-ionized Water plus 0.01% teepol	1012	70.5	67 600
2	"	1612	69.5	113 000
3	"	"	68	112 000
4	"	1012	65	61 100
5	"	"	65.3	61 100
6	"	1612	41.5	98 000
7	"	1312	41.5	72 200
8	"	1012	41.5	54 400
9	"	1612	41.5	98 500
10	"	1312	41.5	73 200

Nominal Diameter and Test No.	Test Fluid	Surface Temperature T_w °F	Subcooling ΔT_L degF	Heat Flux q_{tot} Btu/hft ²
1/8 U1.11	De-ionized Water plus 0.01% teepol	1012	42.3	54 800
12	"	"	21	44 500
13	"	1612	18.5	86 300
14	"	1012	19.5	43 900
15	"	1612	20	86 800
1/8 V1.1	De-ionized Water plus 0.025% detergent	1612	76.5	114 000
2	"	1312	73.5	89 000
3	"	1612	78.7	116 000
4	"	1312	76	89 500
1/8 V2.1	De-ionized Water	1312	27	65 600
2	"	1612	27	86 500
3	"	1612	26.3	87 100
4	"	1612	17.7	83 000
5	"	1012	18	42 400
6	"	1612	18	84 000
7	"	1012	18	42 800
8	"	1612	61	105 500
9	"	1312	58.3	80 700
10	"	1612	59	105 000
11	"	"	83.5	121 000
12	"	"	82.3	120 000
13	"	"	100.5	134 000
15	"	1312	93.5	106 500
16	"	1612	94.5	129 000
17	"	"	106.7	139 000
18	"	"	99.3	134 000
19	"	1312	95.7	110 000
20	"	1012	92	80 000
21	"	1612	72.3	115 000
22	"	1012	36.3	50 900
23	"	"	35	50 200
24	"	"	22.5	45 300

Nominal Diameter and Test No.	Test Fluid	Surface Temperature T_w °F	Subcooling ΔT_L degF	Heat Flux q_{tot} Btu/hft ²
1/8 V2.25	De-ionized Water	1012	21.5	45 100
26	"	"	11.7	40 900
27	"	"	13	41 500
28	"	"	13	41 500
29	"	1612	11	84 000
30	"	"	9.5	83 500
31	"	1312	10	58 700
32	"	1612	25	89 200
33	"	"	24	88 100
34	"	"	62	108 000
35	"	"	59	107 000
1/8 V3.1	De-ionized Water plus 0.01% detergent	1612	9	83 000
2	"	"	9.5	83 000
3	"	1012	10.5	39 800
4	"	"	12	41 100
5	"	"	26.3	47 500
6	"	"	25	46 600
7	"	"	62.7	66 700
8	"	"	63	66 700
9	"	1612	86	124 000
10	"	"	101.5	137 000
1/8 V4.1	Tapwater	1612	138	157 500
2	"	1312	137	133 000
3	"	"	134	133 000
4	"	1612	137.5	155 500
5	"	1312	77	97 500
6	"	"	78	97 500
7	"	"	50	79 200
8	"	"	52	79 500
9	"	"	14	59 500
10	"	"	12	59 000
11	"	"	24.5	64 800
12	"	"	24.5	64 800
13	"	"	51.5	78 000
14	"	"	51	78 000

Nominal Diameter and Test No.	Test Fluid	Surface Temperature T_w °F	Subcooling ΔT_L degF	Heat Flux q_{tot2} Btu/hft ²
1/8 V4. 15	Tapwater	1312	76.5	92 800
16	"	"	75.3	92 200
17	"	1612	99.7	135 500
18	"	"	98	135 500
1/8 W1. 1	Tapwater	1612	98	129 000
2	"	1312	98	105 500
3	"	1612	99	131 000
4	"	1312	97	108 500
5	"	1612	95.7	128 000
6	"	1312	94	106 000
7	"	1012	90.5	85 500
8	"	"	88.3	84 500
9	"	1612	92.7	127 000
10	"	1312	92.7	104 400
11	"	1012	88.7	84 500
12	"	"	76	75 400
1/8 W2. 1	Tapwater	1012	75.7	76 000
2	"	"	62	66 800
3	"	"	62.7	67 400
4	"	"	41	52 400
5	"	"	39.7	52 400
6	"	"	30.3	47 100
7	"	"	31	47 500
8	"	"	37	49 600
1/8 W3. 1	Tapwater	1612	102	132 500
2	"	"	101	134 500
3	"	"	101	133 500
4	"	"	102	137 000
5	"	1312	110	115 000
1/8 X1. 1	Tapwater	1612	110.5	141 000
2	"	1312	110	117 000
3	Tapwater plus 0.025% teepol	1612	116	142 000
4	"	1312	114.5	84 000
6	"	1612	117.3	144 000
7	"	1312	114.5	84 000
8	"	1612	125.5	147 000

Nominal Diameter and Test No.	Test Fluid	Surface Temperature T_w °F	Subcooling ΔT_L degF	Heat Flux q_{tot} Btu/hft ²
1/8 Y1. 1	Tapwater	1612	2.2	88 000
2	"	1312	2.2	58 000
3	"	1012	2.7	39 000
4	"	1612	2.0	81 000
5	"	1312	2.2	58 000
6	"	1012	2.5	39 000
1/8 Y2. 1	Tapwater (aerated)	1612	83	124 000
2	"	1312	82.7	100 500
3	"	1012	81	79 900
4	"	1612	82	122 000
5	"	1312	81	99 000
6	"	1012	80	79 000
7	"	"	79.5	77 500
8	Tapwater (de-aerated)	1612	82.3	124 000
9	"	1312	81.5	98 100
10	"	1612	81	123 000
11	"	1312	80.5	97 300
12	"	1012	78.7	77 000
13	"	1612	125.5	151 000
14	"	"	124.3	147 000
1/8 ES2.1	Ethanol	698	104	38 600
2	"	590	104	33 200
3	"	698	101	38 200
4	"	590	100.5	32 500
5	"	486	100.5	27 500
6	"	"	100	27 100
7	"	698	74.7	33 600
8	"	590	75	28 100
9	"	"	76	28 400
10	"	486	76	23 500
11	"	698	76	33 700
12	"	486	74.7	23 400
13	"	698	49.7	30 200
14	"	590	49.7	24 400
15	"	486	50	19 600
16	"	698	51	30 200
17	"	590	46.7	24 200

Nominal Diameter and Test No.	Test Fluid	Surface Temperature T_w °F	Subcooling ΔT_L degF	Heat Flux q_{tot2} Btu/hft ²
1/8 ES2.18	Ethanol	486	46.7	19 200
19	"	698	51	30 200
20	"	590	51.5	24 600
21	"	486	52	19 850
22	"	"	53	20 100
23	"	698	26.7	27 100
24	"	590	26.3	21 600
25	"	486	26	16 600
26	"	698	26.7	27 000
27	"	590	26	21 600
28	"	486	26	16 600
29	"	698	14.5	25 400
30	"	590	14	20 050
31	"	486	13.7	15 330
32	"	698	9.3	25 000
33	"	590	9.3	19 530
34	"	486	9.3	15 800
35	"	698	5	24 050
36	"	590	5.5	18 900
37	"	486	6	14 400
38	"	698	3	24 150
39	"	590	3.7	19 100
40	"	486	3.3	14 180
41	"	698	2.5	24 150
42	"	590	2.5	19 100
43	"	486	3	14 180
44	"	698	3	24 150
45	"	590	3.7	19 200
46	"	486	3.3	14 280
47	"	698	1.5	24 150
48	"	590	2	19 000
49	"	486	2.5	14 070

1/4 - inch diameter

Nominal Diameter and Test No.	Test Fluid	Surface Temperature T_w °F	Subcooling ΔT_L degF	Heat Flux q_{tot} Btu/hft ²
1/4 T1. 1	Tapwater	1612	108	123 000
1/4 U1. 1	Tapwater	1612	123.5	130 000
2	"	1312	121.5	109 000
3	"	1612	124	132 000
4	"	"	90.5	112 500
5	"	1312	88	92 000
6	"	1012	87	76 000
7	"	1612	62.3	96 000
8	"	1312	62.3	74 700
9	"	"	61.5	74 700
10	"	1612	21	81 600
11	"	1312	20.7	58 100
12	"	1012	21.5	40 300
13	"	1612	20.3	81 500
14	"	1312	20.3	58 500
15	"	1012	21	40 700
1/4 V1. 1	Tapwater	1612	90.5	107 500
2	"	1312	89	88 000
3	"	1012	88.3	66 200
4	"	1612	85	105 000
5	"	1312	85.3	87 100
6	"	1012	83.5	69 000
7	"	1612	66	94 000
8	"	1312	62	72 500
9	"	1612	61.5	92 000
10	"	1312	60	72 200
11	"	1012	65.7	59 800
12	"	1612	20.7	78 800
13	"	1312	20.3	56 800
14	"	1012	20.7	39 100
15	"	"	22	39 600
16	"	1312	22.5	57 800
17	"	1612	26.7	82 000
18	"	1012	82.3	70 000
19	"	"	68.7	63 500
20	"	"	67.5	62 600
21	"	"	65.3	61 600
1/4 V2. 1	Tapwater	1612	2	70 400

Nominal Diameter and Test No.	Test Fluid	Surface Temperature T_w °F	Subcooling ΔT_L degF	Heat Flux $q_{tot,2}$ Btu/hft ²
1/4 V2.2	Tapwater	1312	2	49 500
3	"	1012	2	32 800
4	"	1312	2	48 800
5	"	1612	1	69 000
6	"	"	2.4	70 400
7	"	1012	2	33 100
8	"	1612	2	70 600
9	"	"	2	70 600
10	"	1312	2	49 900
11	"	1012	2	33 400
1/4 V3.1	Tapwater	1612	40.5	89 000
2	"	1312	39	63 400
3	"	1612	40.5	89 500
4	"	1312	39.7	64 500
5	"	1612	78.7	101 000
6	"	1312	77.5	83 400
7	"	1612	76.5	100 000
8	"	1312	75	81 800
9	"	1012	40	46 700
10	"	"	41	46 700
11	"	"	109.7	122 000
12	"	1312	109.3	101 000
13	"	"	106	99 000
14	"	1612	103.5	118 000
15	"	"	78.7	104 000
16	"	1312	77.5	83 400
17	"	1612	77	103 000
18	"	"	40.5	88 500
19	"	"	41.5	88 500
20	"	1312	39.7	64 100
21	"	1612	146	144 000
22	"	1312	140.3	120 000
23	"	1612	144	142 000
1/4 W1.1	Tapwater	1612	134.5	136 000
2	"	1312	134	113 000
3	"	1612	127.8	132 000
4	"	1312	119.5	108 000
5	"	"	135	115 000
6	"	"	131	113 000

Nominal Diameter and Test No.	Test Fluid	Surface Temperature T_w °F	Subcooling ΔT_L degF	Heat Flux $q_{tot,2}$ Btu/hft ²
1/4 W1. 8	Tapwater	1012	119	89 600
12	"	1612	150.5	146 500
13	"	1312	143	121 000
14	"	1012	138	102 000
15	"	1612	158.7	149 000
16	"	1312	152.5	124 000
17	"	1612	145.7	145 000
18	"	1312	139	119 500
19	"	1012	132.5	94 000
1/4 W2. 1	Tapwater	1012	75.7	76 000
2	"	"	62	66 800
3	"	"	62.7	67 400
4	"	"	41	52 400
5	"	"	39.7	52 400
6	"	"	30.3	47 100
7	"	"	31	47 500
8	"	"	37	49 600
1/4 W3. 1	Tapwater plus 0.025% teepol	1612	134	134 000
2	"	1312	126.5	101 000
3	"	1612	137	136 000
1/4 W4. 1	Tapwater	1312	51	69 600
2	"	1612	49.5	93 700
3	"	"	52	93 700
4	"	"	80.5	107 000
5	"	1312	84	88 000
6	"	"	82.7	87 400
7	"	1612	79	106 000
8	"	1012	80	69 600
9	"	"	79	67 500
10	"	1612	113.7	126 000
11	"	"	109.7	125 000
12	"	"	110	125 000
13	"	1312	114	107 000
14	"	"	114.5	107 000
15	"	1012	111.5	85 000
16	"	"	110.5	84 200

Nominal Diameter and Test No.	Test Fluid	Surface Temperature T_w °F	Subcooling ΔT_L degF	Heat Flux $q_{tot,2}$ Btu/hft ²
1/4 W4.17	Tapwater	1612	143.5	144 000
18	"	"	140.7	146 000
19	"	1312	140.3	120 000
20	"	"	140	121 000
21	"	1012	132.3	103 500
1/4 X1. 1	Tapwater	1612	58	94 000
2	"	"	62.5	96 000
3	"	1312	61	72 700
4	"	"	62.3	73 100
5	"	1012	60	56 600
6	"	"	60.5	57 900
7	"	1612	1.5	72 500
8	"	1312	1.0	50 100
9	"	1012	1.0	32 600
10	"	1612	30	86 600
11	"	1312	32	62 800
12	"	1612	29.5	86 600
13	"	1312	33	63 200
14	"	1012	34	44 200
15	"	"	33	43 600
16	"	1612	94.5	113 000
17	"	"	89	110 500
18	"	1312	90.5	91 500
19	"	"	92	93 100
20	"	1012	91	74 400
21	"	"	90.5	73 500
22	"	1612	123	132 000
23	"	"	122.5	131 000
24	"	1312	122	110 000
25	"	"	123	109 000
26	"	1012	123	91 000
27	"	1012	123	90 500
28	"	1612	154	147 000
29	"	"	153.5	149 000
30	"	1312	153.5	126 000
31	"	"	153.5	125 000
32	"	1012	153	107 000
33	"	1612	65.7	98 500
34	"	1312	62.3	74 400
35	"	1012	61	59 100

Nominal Diameter and Test No.	Test Fluid	Surface Temperature T_w °F	Subcooling ΔT_L degF	Heat Flux q_{tot2} Btu/hft ²
1/4 X1. 36	Tapwater	1612	94	114 500
37	"	1312	93	94 500
38	"	1012	89	75 200
39	"	1612	0	72 800
40	"	1312	0	50 000
41	"	1012	0	
42	"	1612	30.3	87 500
43	"	1312	31	63 600
44	"	1012	32	44 200
45	"	1612	121.5	132 500
46	"	1312	123	112 000
47	"	1012	121.5	91 600
48	"	1312	152	126 000
49	"	1612	154.7	150 000
50	"	1012	154	104 000
51	Tapwater plus 0.025% teepol	1612	154	136 000
52	"	1312	154	111 000
53	"	1612	154	137 000
54	"	1312	154	112 000
55	Tapwater	1612	0.5	70 400
56	"	1312	1.0	51 000
57	"	1012	2.3	34 300
1/4 X2. 1	Tapwater plus 0.025% teepol	1312	77.5	78 600
2	"	1312	77	78 600
3	"	1612	77.5	99 800
4	"	"	77.5	100 100
5	"	1012	77.5	44 400
6	"	"	77.5	44 200
7	"	1312	52	67 300
8	"	"	52.3	67 700
9	"	1612	52.3	88 000
10	"	"	51.5	87 600
11	"	1012	53	51 800

Nominal Diameter and Test No.	Test Fluid	Surface Temperature T_w °F	Subcooling ΔT_L degF	Heat Flux q_{tot} Btu/hft ²
1/4 X2. 12	Tapwater plus 0.025% teepol	1012	51.5	51 400
13	"	1012	77	44 600
14	"	"	52.3	51 400
15	"	"	58.7	54 400
16	"	"	65.3	57 000
17	"	"	71	44 000
18	"	"	74.5	44 000
19	"	"	78	44 400
20	"	"	70	43 600
21	"	"	69	43 400
22	"	"	68	43 400
23	"	"	67	43 200
24	"	"	66	57 300
25	"	"	65	44 000
26	"	"	65	43 000
27	"	"	63	43 100
28	"	"	64	45 900
29	"	"	61	43 400
30	"	"	61	54 900
31	"	"	70	58 400
32	"	"	69	58 400
33	"	1312	70	76 900
35	"	"	102	68 100
36	"	"	102	68 100
37	"	"	102	92 500
38	"	"	102	93 100
39	"	1612	102	117 000
40	"	"	102	117 000
41	"	1312	90	66 500
42	"	"	90	66 900
43	"	"	90	87 900
44	"	"	90	87 500
45	"	"	77	81 500
46	"	"	77	66 500
47	"	1612	125	130 000
48	"	"	123	129 000
49	"	1312	125	71 000
50	"	"	124	71 000
51	"	"	125	101 500

Nominal Diameter and Test No.	Test Fluid	Surface Temperature T_w °F	Subcooling ΔT_L degF	Heat Flux q_{tot}^2 Btu/hft ²
1/4 X2. 52	Tapwater plus 0.025% teepol	1312	124	100 500
53	"	"	122	110 500
1/4 X3. 1	Tapwater plus 0.025% teepol	1012	77.5	60 300
2	"	"	80	60 900
4	"	1312	147	104 000
5	"	"	147	104 000
6	"	"	146.5	72 800
7	"	"	147	106 000
8	"	"	148	75 500
9	"	1612	147	127 800
10	"	"	147.5	128 000
11	"	"	125	127 800
12	"	"	125	127 800
13	"	"	125	118 000
14	"	"	125	106 500
15	"	"	125	118 000
16	"	"	124.7	118 000
17	"	"	124.7	97 000
18	"	"	124.5	97 700
19	"	"	112	118 000
22	"	"	112	117 000
23	"	"	112	116 000
25	"	"	112	115 000
26	"	"	112	117 000
27	"	1012	92.7	67 600
28	"	"	91	66 400
29	"	"	89.5	47 800
30	"	1312	89.5	67 700
31	"	1012	89.5	66 400
24	"	1550	112	115 000
25	"	1590	112	115 000
1/4 ES2. 3	Ethanol	698	87.5	32 500
4	"	590	86	26 800
5	"	486	85	22 100
6	"	698	85.3	32 500

Nominal Diameter and Test No.	Test Fluid	Surface Temperature T_w °F	Subcooling ΔT_L degF	Heat Flux $q_{tot,2}$ Btu/hft ²
1/4 ES3. 1	Ethanol	698	85.7	32 900
2	"	590	85.7	26 900
4	"	698	74	31 700
5	"	"	74	31 700
6	"	590	74	25 700
8	"	"	72	25 600
9	"	486	72	20 900
1/4 ES4. 1	Ethanol	698	49.3	27 400
2	"	590	49.3	22 900
3	"	486	49.7	18 550
4	"	698	49.0	27 900
5	"	590	49	22 900
6	"	486	49.3	18 300
7	"	698	104.5	35 000
8	"	590	104	29 600
9	"	486	102.5	25 400
10	"	698	96.5	33 900
11	"	590	96	28 600
12	"	486	89.7	22 900
13	"	590	90	27 800
14	"	486	103	25 000
15	"	590	101.7	29 200
1/4 ES5. 13	Ethanol	698	3	21 400
14	"	590	3	16 600
15	"	486	3.4	12 400
16	"	590	2.7	16 500
17	"	698	3	21 400
18	"	486	3	12 400
1/4 ES6. 1	Ethanol	698	24	23 800
2	"	590	24	19 400
3	"	486	23.7	15 300
4	"	698	23.7	23 800
5	"	590	23.3	19 200
6	"	486	23	15 200
7	"	698	9.7	21 900
8	"	590	10	17 400
9	"	486	10.5	13 500
10	"	698	8.5	21 700

Nominal Diameter and Test No.	Test Fluid	Surface Temperature T_w °F	Subcooling ΔT_L degF	Heat Flux $q_{tot,2}$ Btu/hft ²
1/4 ES6.11	Ethanol	590	8	17 000
12	"	486	9	13 300
13	"	698	3	21 300
14	"	590	3	16 450
15	"	486	3	12 300
16	"	698	1.5	21 100
17	"	590	1.5	16 200
18	"	486	1.5	12 000
19	"	698	46	27 200
20	"	590	43.7	21 900
21	"	698	43.7	27 000
22	"	590	42	21 900
23	"	486	43.3	17 200
24	"	490	42	21 900
25	"	486	40.5	17 300
26	"	"	40	17 300
27	"	"	26.7	15 800
28	"	"	28.5	15 900
29	"	590	104	29 900
30	"	486	101	25 100
31	"	"	97.6	24 350
32	"	"	97.3	24 700
33	"	"	94	23 800
34	"	"	74.3	21 100
35	"	590	74.3	25 500
36	"	698	70.3	30 250
37	"	590	69	25 100
38	"	486	68	20 450
39	"	"	1.5-2	12 120
40	"	"	1.5	12 120
1/4 ES7. 1	Ethanol	1012	110.3	57 500
2	"	"	107.5	56 600
3	"	"	103.0	56 000
4	"	"	85.0	53 500
5	"	"	79.5	53 200
6	"	"	79.5	53 200
7	"	"	67.7	51 500
8	"	"	64	50 200
9	"	"	63.3	49 800
10	"	"	46	46 400

Nominal Diameter and Test No.	Test Fluid	Surface Temperature T_w °F	Subcooling ΔT_L degF	Heat Flux q_{tot}^2 Btu/hft ²
1/4 ES7.11	Ethanol	1012	46	46 400
12	"	"	46	46 400
13	"	"	26	43 400
14	"	"	26	43 800
15	"	"	10	41 900
16	"	"	10	42 100
17	"	"	2	38 700
18	"	"	2	39 400
19	"	"	106	55 800
20	"	"	102	54 500
21	"	"	97.7	53 000
22	"	"	93	52 800
23	"	"	91	52 800
24	"	"	86.5	53 000
25	"	"	84.5	51 500
26	"	"	79	50 100
27	"	"	76.5	49 700
28	"	"	73	49 400
29	"	"	105	54 700
30	"	"	101.3	52 100
31	"	"	98.5	51 900
32	"	"	94	51 500
33	"	"	86.5	50 000
34	"	"	82.5	49 600
35	"	"	79.5	49 200
39	"	"	90	53 600
40	"	"	85.7	54 200
41	"	"	101.3	54 900
42	"	"	97.3	54 300
43	"	"	91	54 100
44	"	"	86.5	53 200
50	"	"	62.5	51 500
51	"	"	58.5	48 100
52	"	"	57	48 500
1/4 ES8. 1	Ethanol	1012	94	51 100
2	"	"	91.5	50 700
3	"	"	83	49 800
4	"	"	76	49 000
5	"	"	75.5	48 400
6	"	"	73.5	48 100

Nominal Diameter and Test No.	Test Fluid	Surface Temperature T_w °F	Subcooling ΔT_L degF	Heat Flux q_{tot2} Btu/hft ²
1/4 ES8. 9	Ethanol	1012	70.7	47 600
10	"	"	68	47 200
11	"	"	65	47 200
12	"	"	57.5	46 400
13	"	"	53.7	45 500
14	"	"	52.5	45 300

$\frac{1}{2}$ - inch diameter

Nominal Diameter and Test No.	Test Fluid	Surface Temperature T_w °F	Subcooling ΔT_L degF	Heat Flux q_{tot2} Btu/hft ²
$\frac{1}{2}$ Sl. 1	Tapwater	1012	11.7	32 700
2	"	1312	11.3	45 700
3	"	1012	12	33 000
4	"	1312	11	45 500
7	"	1012	1.5	27 250
9	"	"	23.7	39 400
10	"	"	24.5	39 700
11	"	1312	25.5	55 200
12	"	"	24.5	54 900
13	"	1012	43	44 300
14	"	1312	41.5	62 000
15	"	1012	42	44 500
16	"	1612	2	60 800
17	"	1012	41	45 200
18	"	"	41	45 400
21	"	"	5.7	30 400
22	"	"	5.3	29 900
23	"	"	13.5	34 850
24	"	"	33.7	43 400
25	"	"	37.5	44 800
26	"	1312	35	61 100
27	"	1012	41	45 900
28	"	"	40.5	45 900
29	"	1312	40.5	63 900
30	"	"	40.5	63 900
31	"	1012	25	40 900
32	"	1312	25	57 000
33	"	"	26.3	57 700
34	"	1012	19	38 400
35	"	1312	19.5	53 400
36	"	"	17.7	52 100
37	"	1012	17.3	36 800
38	"	"	26.7	41 400
39	"	"	15.5	36 100
40	"	1312	14.7	50 300
41	"	1012	10	32 700
42	"	1312	10	47 900
43	"	1012	12.5	34 600
44	"	1312	12.5	49 100
45	"	1012	8	31 600
46	"	1312	7.5	46 600

Nominal Diameter and Test No.	Test Fluid	Surface Temperature T_w °F	Subcooling ΔT_L degF	Heat Flux q_{tot2} Btu/hft ²
½ SI. 47		1012	5	30 400
48	"	1312	5	45 300
49	"	1012	2.7	29 800
50	"	1312	2.7	44 400
51	"	"	50	67 000
52	"	1012	49	47 400
53	"	1312	51.5	67 300
54	"	"	61.5	72 200
55	"	"	60	71 600
56	"	"	68	71 600
57	"	"	69.5	71 900
58	"	"	61	71 600
59	"	"	68.3	71 600
60	"	"	71	71 600
61	"	"	76.5	74 400
62	"	"	81	76 200
63	"	"	76.5	74 700
64	"	"	74.5	73 500
65	"	"	72.3	72 500
66	"	"	70.5	72 800
67	"	"	68.3	72 100
68	"	"	66.5	72 500
69	"	"	63.5	71 900
70	"	"	64.5	71 900
71	"	"	65.5	73 100
72	"	"	63.5	72 100
73	"	"	60	71 600
74	"	"	55	69 400
75	"	"	64.5	71 900
76	"	"	64.5	73 100
77	"	"	1.5	44 400
78	"	1012	2	29 800
79	"	1312	79.5	75 900
80	"	"	84.5	78 000
81	"	"	89	80 200
82	"	"	94.5	83 000
83	"	"	105.5	88 500
84	"	"	111	90 300
85	"	"	108.5	89 500
86	"	"	118	92 600
87	"	"	113	90 300

Nominal Diameter and Test No.	Test Fluid	Surface Temperature T_w °F	Subcooling ΔT_L degF	Heat Flux $q_{tot,2}$ Btu/hft ²
$\frac{1}{2}$ ES1 . 1	Ethanol	590	7.5	15 750
2	"	698	4.5	19 350
3	"	486	3.7	11 400
4	"	590	72.0	23 700
5	"	486	63.7	18 700
6	"	698	56	27 800
7	"	590	49.6	21 700
8	"	486	43.3	16 400
9	"	698	33.7	24 700
10	"	590	29.0	19 350
11	"	486	26.0	14 800
12	"	698	21.0	22 500
18	"	"	78	29 300
19	"	590	70.3	23 400
20	"	486	67.7	19 000
21	"	590	65.5	22 900
22	"	698	61.5	28 200
23	"	"	60.7	28 100
24	"	486	56.7	17 800
25	"	698	2.5	19 000
26	"	590	2.5	14 650
27	"	486	3.0	11 100
28	"	590	2.5	14 750
29	"	698	2	19 000
30	"	590	3	10 900
31	"	698	93.3	31 200
32	"	"	90	30 400
33	"	590	81	24 800
34	"	486	74	19 500
35	"	590	69	23 200
36	"	698	64	28 500
37	"	"	59.5	27 900
38	"	590	55	21 800
39	"	"	50.5	21 700
40	"	486	47.5	16 500
41	"	"	44	16 200
42	"	698	42	25 900
43	"	590	35.5	20 300
44	"	486	35	15 400
45	"	698	32.5	24 300
46	"	"	27	23 400

Nominal Diameter and Test No.	Test Fluid	Surface Temperature T_w °F	Subcooling ΔT_L degF	Heat Flux q_{tot} Btu/hft ²
$\frac{1}{2}$ ES1.47	Ethanol	590	25.5	18 550
48	"	486	23.7	14 350
49	"	"	22.5	14 200
50	"	590	21.0	17 900
51	"	698	99.5	31 700
52	"	590	93.7	26 200
53	"	486	89.7	21 700
54	"	"	86	21 400
55	"	590	75.5	24 800
56	"	698	74.7	29 600
57	"	"	70.7	29 500
58	"	590	65	23 200
59	"	486	60	18 400
60	"	"	56	17 950
61	"	590	53	21 800
62	"	486	72	19 650
63	"	590	67	23 100
64	"	698	60.7	28 400
65	"	"	54.5	27 800
66	"	590	51	21 700
67	"	486	48.5	16 850
68	"	"	45.5	16 400
69	"	590	42	21 100
70	"	698	38.5	25 300
71	"	"	35.5	24 800
72	"	590	29.7	19 350
73	"	486	29	15 100
74	"	"	99.5	22 400
75	"	"	93.7	22 200
76	"	590	88	25 700
77	"	"	81.7	24 900
78	"	698	73.5	29 600
79	"	"	67.7	29 200
80	"	"	57	28 500
81	"	"	51.5	27 800
82	"	"	44.5	26 700
83	"	590	41	21 200
84	"	"	38	20 700
85	"	486	36	15 600
86	"	"	33.7	15 400
87	"	"	37.5	15 750

Nominal Diameter and Test No.	Test Fluid	Surface Temperature T_w °F	Subcooling ΔT_L degF	Heat Flux q_{tot2} Btu/hft ²
$\frac{1}{2}$ ES1 .88	Ethanol	590	33.7	20 000
89	"	486	31.0	15 300
90	"	698	99	31 700
91	"	"	89	30 700
92	"	590	43.3	21 200
93	"	"	40.5	20 900
94	"	486	29.7	15 100
95	"	"	29	15 050
96	"	"	28.5	15 000
97	"	"	14.5	13 000
98	"	"	14	12 950
99	"	"	13.7	12 800
100	"	590	48	21 700
101	"	"	44.5	21 500
102	"	"	42.5	21 400
103	"	"	40	20 750
104	"	"	36.3	20 600
105	"	"	45.5	21 500
106	"	"	49.0	21 700
107	"	698	49	26 800
108	"	"	47.5	26 700
109	"	590	47	21 600
110	"	"	46.7	26 800
111	"	"	54	27 450
112	"	"	50	27 200
113	"	"	46.7	26 800
114	"	590	49	21 700
115	"	"	46.7	21 400
116	"	"	49	21 800
117	"	"	46.7	21 500
118	"	698	2	18 600
119	"	590	1.5	14 350
120	"	486	1.5	10 750

Appendix D

FLUID PROPERTIES

Table D1 Joint liquid-vapour properties.

Table D2 Properties of the liquids and Gr_L/D^3 .

Table D3 Properties of the vapours and Gr^*/D^3 .

The values of the fluid properties were taken from a number of sources, the reference numbers of which are given in brackets in the tables. The accuracies of the values, where they were given, are quoted below the reference numbers. The properties of the detergent solutions, except for surface tension, have been assumed to be the same as for water.

The modified Grashof number Gr^* , has been defined as follows :

$$Gr^* = \frac{g}{\mu_v^2} \rho_v (\rho_L - \rho_v) D^3$$

The values of the density difference, $(\rho_L - \rho_v)$ were obtained as follows, where the numerical suffices refer to the temperatures at which the densities were evaluated.

For water $\rho_L = \frac{1}{2} (\rho_{212} + \rho_{50}) ,$

and $\rho_v \ll \rho_L$, was neglected.

For ethanol $\rho_L = \frac{1}{2} (\rho_{173} + \rho_{68}) ,$

and $\rho_v = \rho_{380}$

The density of the ethanol vapour was evaluated at 380°F which is the mean temperature of the vapour film for the middle surface temperature of 590°F. The accuracy of the values of Gr^* thus evaluated is discussed in section 6.5. The other properties were evaluated at the mean temperature of $\frac{1}{2} (T_w + T_s)$.

Table D1 Joint liquid-vapour properties

	Water	Detergent solution	Ethanol
Boiling point T_s °F	212	as for water	173 (79)
Surface tension σ at T_s lb _f /ft	4.03×10^{-3} (80)	1.6×10^{-3} (81)	1.2×10^{-3} (82)
Latent heat of vaporization h_{fg} Btu/lb	970.3 (83)	as for water	360 (84)
Critical wavelength λ_c inch $\lambda_c = 2\pi \{g_c \sigma / g (\rho_L - \rho)\}^{\frac{1}{2}}$	0.612	0.384	0.379

TABLE D3. Vapour properties.

Mean Temp. T_m °F	Density ρ_m at T_m lb/ft ³	Viscosity μ at T_m lb/fts	Prandtl No. Pr at T_m	Corresponding surface temp. T_w °F	Gr^* $\frac{D^3}{3}$ /ft ³	Thermal conductivity k at T_m Btu/hftdeg F	Superheat ΔT_v deg F	Specific heat C at T_m Btu/lbdeg F	Non-dim. superheat $Sp = \frac{C \Delta T_v}{h_{fg}}$
WATER	(83)	(83)	(83)			(83)		(83)	
400	0.0288	11.0×10^{-6}	0.97	588	468×10^9	0.0195	376	0.473	0.183
460	0.0269	11.9 "	0.96	708	373 "	0.0213	496		
500	0.0258	12.6 "	0.96	788	319 "	0.0227	576	0.476	0.283
560	0.0242	13.5 "	0.955	908	261 "	0.0247	696		
600	0.0233	14.1 "	0.95	988	230 "	0.0261	776	0.482	0.385
660	0.0221	15.1 "	0.94	1108	191 "	0.0283	896		
700	0.0213	15.7 "	0.94	1188	170 "	0.0298	976	0.490	0.493
760	0.0202	16.7 "	0.93	1308	142.4 "	0.0320	1096	0.494	0.558
800	0.0196	17.3 "	0.92	1388	129 "	0.0336	1176	0.498	0.604
850	0.0188	18.1 "	0.92	1508	112.8 "	0.0356	1296		
900	0.0181	18.9 "	0.92	1588	99.6 "	0.0376	1376	0.507	0.719
950	0.0175	19.6 "		1708	89.5 "	0.0397	1496		
1000	0.0169	20.4 "	0.90	1788	79.8 "	0.0418	1576	0.515	0.836
ETHANOL	(91)	(91)	(91)			(91)		(91)	
212	0.0930	7.25×10^{-6}	0.791	251	2.71×10^{12}	0.0133	78	0.403	0.087
302	0.084	8.27 "	0.79	431	1.85 "	0.0165	258	0.433	0.310
392	0.0737	9.23 "	0.786	611	1.324 "	0.0203	438	0.48	0.584
482	0.0667	10.25 "	0.78	791	0.958 "	0.0243	618	0.517	0.888
572	0.0608	11.2 "	0.773	971	0.742 "	0.0289	798	0.554	1.228
662	0.0558	12.23 "	0.772	1151	0.563 "	0.0334	978	0.589	1.600
752	0.0517	13.25 "	0.771	1331	0.451 "	0.0386	1158	0.624	2.007

Appendix E

REDUCTION OF THE TEST DATA

Table E1	Diameters of the test sections.
Tables E2	Mean values of the experimental results and reduced data for the liquid heat transfer.
E2a	1/8 inch diameter cylinders,
E2b	1/4 inch diameter cylinders,
E2c	1/2 inch diameter cylinders.
Tables E3	Reduced data for saturated film boiling.
E3a	water,
E3b	ethanol.

The test data for water and ethanol have been reduced to dimensionless form by dividing the results into "vapour heat transfer" and "liquid heat transfer", see section 8.3. Average values for the total heat flux q_{tot} , were taken at intervals of subcooling from figures 10 - 12 and 15 - 17. The values of the vapour heat flux q_v , were taken to be the same as the values, q_s , for saturated film boiling. The values of the liquid heat flux q_L , were obtained by subtracting q_s from q_{tot} .

Test sections of the same nominal diameter when cold varied only slightly in actual diameter, by less than 0.001 inch. Therefore, mean values for the diameters were taken and corrected for thermal expansion by adding 0.16% per 100 deg F rise in temperature. In ethanol, the slight differences in diameter at the three surface temperatures were insignificant. In water, the values of the diameters at the intermediate surface temperature were used in the reduction of the data for liquid heat transfer.

The liquid properties were evaluated generally at the mean temperatures, $\frac{1}{2}(T_w + T_s)$ and $\frac{1}{2}(T_L + T_s)$.

Table E1 Diameters of the test sections

Nominal value of diameter (inch)	1/8	1/4	1/2
Average diameter at room temperature (inch)	0.126	0.2515	0.498
Values used in the reduction of the data (inch),			
a) water $T_w = 1012^{\circ}\text{F}$	0.128	0.255	0.505
$T_w = 1312^{\circ}\text{F}$ *	0.1285	0.256	0.507
$T_w = 1612^{\circ}\text{F}$	0.129	0.257	0.510
b) ethanol For all T_w *	0.127	0.254	0.503

* These values of diameter were used in the reduction of the data for liquid heat transfer.

Table E2a. Values of q_{tot} , q_L , Nu_L , Ra_L for $\frac{1}{8}$ -inch dia. cylinders.

ΔT_L degF	q_{tot} Btu/hft ² at T_w (°F) of			$q_L = q_{\text{tot}} - q_s$ Btu/hft ² at T_w (°F) of			Nu_L at T_w (°F) of			Nu_L Mean	$(Gr)_L$	$(GrPr)_L$	$(GrPr^3)_L$	$(GrPr^3)_L$
WATER $\frac{1}{8}$ -inch diameter														
	1012	1312	1612	1012	1312	1612	1012	1312	1612					
152		137 700	159 500		80 200	79 000		16.0	15.82	15.9	62.1×10^3	181×10^3	529×10^3	310×10^3
142		131 100	153 000		73 600	72 500		15.7	15.55	15.6	"	"	"	"
132		124 500	146 500		67 000	66 000		15.42	15.28	15.35	"	"	"	"
122		118 000	140 000		60 500	59 500		15.12	14.95	15.05	"	"	"	"
112		111 400	133 500		53 900	53 000		14.77	14.6	14.68	"	"	"	"
102		104 900	127 100	47 800	47 400	46 600	14.44	14.35	14.2	14.3	"	"	"	"
92	86 300	98 200	120 500	41 000	40 700	40 000	13.82	13.75	13.6	13.72	"	"	"	"
82	79 500	91 900	114 100	34 300	34 400	33 600	13.13	13.21	12.96	13.1	"	"	"	"
72	72 800	85 100	107 700	27 300	27 600	27 200	12.11	12.28	12.16	12.2	"	"	"	"
62	65 800	79 000	101 500	21 000	21 500	21 000	11.07	11.38	11.26	11.2	"	"	"	"
52	59 500	73 000	96 400	14 800	15 500	15 900	9.64	10.12	10.44	10.05	"	"	"	"
42	53 300	67 600	91 600	9 600	10 100	11 100	8.19	8.65	9.54	8.81	"	"	"	"
32	48 100	63 500	87 200	6 000	6 000	6 700	7.42	7.45	8.35	7.7	"	"	"	"
22	44 500	60 500	83 500	2 900	3 000	3 000	6.55	6.8	6.85	6.8	"	"	"	"
12	41 400	57 500	80 500	0	0	0					"	"	"	"
0	38 500										"	"	"	"
ETHANOL $\frac{1}{8}$ -inch diameter														
	486	590	698	486	590	698	486	590	698	Mean				
105	28 100	33 300	38 700	14 100	14 300	14 700	15.3	15.5	16.0	15.6	25.7×10^3	316×10^3	3.90×10^6	1110×10^3
87	25 200	30 100	35 700	11 200	11 100	11 700	14.8	14.7	15.5	15.0	"	"	"	"
69	22 400	27 200	32 700	8 400	8 200	8 700	14.2	13.8	14.7	14.2	"	"	"	"
51	19 700	24 600	30 200	5 700	5 600	6 200	13.1	12.9	14.3	12.2	"	"	"	"
33	17 500	22 300	27 800	3 500	3 300	3 800	12.6	11.9	13.7	11.5	"	"	"	"
15	15 450	20 250	25 500	1 450	1 250	1 500	11.6	10.0	12.0	8.55	"	"	"	"
0	14 000	19 000	24 000	0	0	0					"	"	"	"

Table E2b. Values of q_{tot} , q_L , Nu_L , and Ra_L for $\frac{1}{4}$ -inch dia. cylinders.

ΔT_L degF	q_{tot} Btu/hft ² at T_w (°F) of			$q_L = q_{\text{tot}} - q_s$ at T_w (°F) of			Nu_L at T_w (°F) of			Gr_L	$(GrPr)_L$	$(GrPr^2)_L$	$(GrPr^{\frac{3}{2}})_L$	
WATER $\frac{1}{4}$ -inch diameter														
	1012	1312	1612	1012	1312	1612	1012	1312	1612	Mean				
152	107 800	125 000	147 400	74 800	76 000	77 400	27.8	28.3	28.8	28.3	476 ×10	1.43 ×10	4.37 ×10	2.5 ×10
142	102 400	119 800	141 100	69 400	70 800	71 100	27.6	28.1	28.2	28.0	491 "	1.43 "	4.19 "	2.43 "
132	96 800	114 100	135 500	63 800	65 100	65 500	27.1	27.7	27.9	27.6	512 "	1.43 "	3.99 "	2.39 "
122	91 400	108 600	129 500	58 400	59 600	59 500	26.8	27.4	27.3	27.2	528 "	1.41 "	3.77 "	2.31 "
112	86 000	103 000	123 500	53 000	54 000	53 500	26.4	26.9	26.7	26.7	543 "	1.39 "	3.56 "	2.22 "
102	80 400	97 500	117 500	47 400	48 500	47 500	25.9	26.5	25.9	26.1	557 "	1.37 "	3.37 "	2.15 "
92	75 100	91 900	111 600	42 100	42 900	41 600	25.4	25.9	25.1	25.5	551 "	1.30 "	3.08 "	2.00 "
82	69 800	86 500	105 600	36 800	37 500	35 600	24.8	25.3	24.0	24.7	532 "	1.21 "	2.75 "	1.82 "
72	64 300	81 000	99 700	31 300	32 000	29 700	24.0	24.5	22.8	23.1	518 "	1.13 "	2.46 "	1.67 "
62	59 000	75 000	96 000	26 000	26 000	26 000	23.1	23.1	23.1	23.1	488 "	1.03 "	2.16 "	1.49 "
52	53 600	70 000	92 500	20 600	21 000	22 500	21.7	22.1	23.7	0.91	449 "	0.91 "	1.84 "	1.295 "
42	48 000	66 000	89 200	15 000	17 000	19 200	19.6	22.1	25 0	0.75	382 "	0.75 "	1.47 "	1.05 "
32	43 200	62 000	86 000	10 200	13 000	16 000	17.4	22.2	27.3	0.605	320 "	0.605 "	1.14 "	0.831 "
22	39 500	58 000	82 400	6 500	9 000	12 400	16.1	22.2	30.7	0.436	238 "	0.436 "	0.798 "	0.59 "
12	36 000	54 000	77 000	3 000	5 000	7 000	13.6	22.6	31.6	0.233	131 "	0.233 "	0.415 "	0.311 "
0	33 000	49 000	70 000	0	0	0	0	0	0					
ETHANOL $\frac{1}{4}$ -inch diameter														
	486	590	698	486	590	698	486	590	698	Mean				
105	25 300	29 600	35 100	13 500	13 600	14 200	29.3	29.6	30.9	29.9	206 ×10	2.54 ×10	31.2 ×10	8.81 ×10
87	23 000	27 400	32 600	11 200	11 400	11 700	27.2	27.7	28.4	27.8	206 "	2.39 "	27.8 "	8.14 "
69	20 800	25 100	30 200	9 000	9 100	9 300	30.4	30.7	31.4	30.8	192 "	2.14 "	23.7 "	7.13 "
51	18 600	22 900	27 900	6 800	6 900	7 000	31.3	31.8	32.2		170 "	1.80 "	19.0 "	5.84 "
33	16 600	20 550	25 200	4 800	4 550	4 300	34.6	32.8	31.0		132 "	1.32 "	13.2 "	4.17 "
15	14 000	18 100	22 700	2 200	2 100	1 800	35.2	33.7	28 9		70.1 "	0.690 "	6.61 "	2.14 "
0	11 800	16 000	20 900	0	0	0	0	0	0					

Table E2c. Values of q_{tot} , q_L , Nu_L , Ra_L for $\frac{1}{2}$ -inch dia. cylinders.

ΔT_L degF	q_{tot} Btu/hft ² at T_w (°F) of				$q_L = q_{\text{tot}} - q_s$ at T_w (°F) of				Nu_L at T_w (°F) of			Gr_L	$(GrPr)_L$	$(GrPr^2)_L$	$(GrPr^3)_L$
WATER $\frac{1}{2}$ -inch diameter	1012	1312	1612		1012	1312	1612		1012	1312	1612	Mean			
	94 600	90 200	85 900		50 600	46 200	41 900		46.0	45.6	45.3				
122													10.9 x10	29.3 x10	17.9 x10
112													10.8 "	27.7 "	17.3 "
102													10.7 "	26.2 "	16.8 "
92													10.1 "	23.9 "	15.5 "
82													9.41 "	21.4 "	14.2 "
72													8.77 "	19.1 "	12.95 "
62													7.96 "	16.75 "	11.55 "
52	48 400	67 900			19 400	23 900			40.4	50.0			7.06 "	14.3 "	10.05 "
42	45 400	64 000			16 400	20 000			42.2	51.7			5.82 "	11.4 "	8.55 "
32	42 500	60 000			13 500	16 000			45.6	54.0			4.69 "	8.86 "	6.45 "
22	39 200	54 500			10 200	10 500			49.8	51.4			3.39 "	6.20 "	4.59 "
12	34 000	48 900			5 000	4 900			43.8	44.8			1.81 "	3.22 "	2.42 "
0	29 000	44 000			0	0									
ETHANOL $\frac{1}{2}$ -inch diameter	486	590	698		486	590	698		486	590	698	Mean			
	21 400	25 400	30 600		10 800	11 300	12 100		56.7	59.3	63.5				
87													18.6 x10	216 x10	6.33 x10
69	19 300	23 300	29 100		8 700	9 200	10 600		58.2	61.5	70.1		16.6 "	184 "	5.53 "
51	17 100	21 700	27 600		6 500	7 600	9 100		59.4	69.5	83.1		14.0 "	147 "	4.55 "
33	15 400	19 800	24 200		4 800	5 700	5 700		68.5	81.3	81.3		10.3 "	103 "	3.25 "
15	13 000	16 800	21 200		2 400	2 700	2 700		76.2	85.8	85.8		5.36 "	51.3 "	1.66 "
0	10 600	14 100	18 500		0	0	0								

TABLE E3a

Reduced data for saturated film boiling

	T_w OF	WATER		
		1012	1312	1612
Nominal diameter	Parameter			
1/8 1/4 1/2	q_{tot} Btu/hft ²	38 500 33 000 29 000	57 500 49 000 44 000	80 500 70 000 -
1/8 1/4 1/2	q_{co} Btu/hft ² for $\epsilon_w = 0.75$	34 100 28 600 24 500	47 900 39 400 34 250	62 100 51 400 -
1/8 1/4 1/2	q_{co} Btu/hft ² for $\epsilon_w = 1.0$	32 500 27 000 22 900	44 600 35 800 30 600	55 400 44 600 -
1/8 1/4 1/2	q_{co} Btu/hft ² for $\epsilon_w = 0.9$	33 200 27 600 23 600	45 900 37 400 32 300	58 300 47 800 -
1/8 1/4 1/2	Nu for $\epsilon_w = 0.75$	17.16 28.67 48.63	14.57 23.88 14.11	12.55 20.69 -
1/8 1/4 1/2	Nu for $\epsilon_w = 1.0$	16.36 27.06 45.45	13.57 21.66 36.73	11.19 17.96 -
1/8 1/4 1/2	Nu for $\epsilon_w = 0.9$	16.71 27.67 46.84	13.95 22.63 38.77	11.78 19.24 -
1/8 1/4 1/2	Nu _c for $\epsilon_w = 0.9$	79.9 66.4 56.8	66.5 54.2 46.8	55.9 46.0 -
1/8 1/4 1/2	$Ra_i^* =$ $Gr^* (Pr(\frac{1}{2} + \frac{1}{Sp}))$	0.773×10^6 6.11 " 47.4 "	0.371×10^6 2.94 " 22.8 "	0.207×10^6 1.635 " 12.78 "
1/8 1/4 1/2	$Ra_s^* =$ $Gr^* Pr \frac{1}{Sp}$	0.645×10^6 5.1 " 39.6 "	0.290×10^6 2.29 " 17.8 "	0.151×10^6 1.17 " 9.34 "
1/8 1/4 1/2	$Ra_{\lambda_c}^* =$ $Gr^* Pr \times \frac{1}{Sp} (1 + 0.34 Sp)^2$	0.83×10^6 6.56 " 50.9 "	0.411×10^6 3.25 " 25.2 "	0.236×10^6 1.87 " 14.6 "
1/8 1/4 1/2	$Ra_{\lambda_c}^* =$ $Gr_{\lambda_c}^* Pr (\frac{1}{2} + \frac{1}{Sp})$	359×10^6 207 " 145 "	171×10^6 98.6 " 68.7 "	94.1×10^6 54.3 " 37.9 "
	k Btu/hftdeg F	0.0265	0.032	0.038

TABLE E3b Reduced data for saturated film boiling

		ETHANOL			
		T_w OF	486	590	698
Nominal diameter	Parameter				
1/8 1/4 1/2	q_{tot} Btu/hft ²	14 000 11 800 10 600	19 000 16 000 14 100	24 000 20 900 18 500	
1/8 1/4 1/2	q_{co} Btu/hft ² for $\epsilon_w = 0.75$	13 400 11 200 10 000	18 000 15 000 13 100	22 400 19 300 16 900	
1/8 1/4 1/2	q_{co} Btu/hft ² for $\epsilon_w = 1.0$	13 200 11 000 9 800	17 600 14 600 12 700	21 900 18 800 16 400	
1/8 1/4 1/2	q_{co} Btu/hft ² for $\epsilon_w = 0.9$	13 200 11 000 9 800	17 800 14 800 12 900	22 100 19 000 16 600	
1/8 1/4 1/2	Nu for $\epsilon_w = 0.75$	25.74 43.0 76.1	23.1 38.4 66.5	20.3 35.1 60.8	
1/8 1/4 1/2	Nu for $\epsilon_w = 1.0$	25.3 42.1 74.5	22.5 37.3 64.3	19.9 34.1 59	
1/8 1/4 1/2	Nu for $\epsilon_w = 0.9$	25.4 42.3 74.6	22.8 37.9 65.5	20.1 34.5 59.7	
1/8 1/4 1/2	Nu _c for $\epsilon_w = 0.9$	75.7 63.1 56.2	68.1 56.6 49.4	59.9 34.5 45.0	
1/8 1/4 1/2	$Ra_1^* =$ $Gr^* Pr(\frac{1}{2} + \frac{1}{Sp})$	4.76×10^6 38.1 " 296 "	2.92×10^6 23.4 " 182 "	1.94×10^6 15.5 " 120.4 "	
1/8 1/4 1/2	$Ra_2^* =$ $Gr^* Pr \frac{1}{Sp}$	3.98×10^6 31.9 " 247.4 "	2.29×10^6 18.36 " 142.6 "	1.42×10^6 11.4 " 88.4 "	
1/8 1/4 1/2	$Ra_2^* =$ $Gr^* Pr \times \frac{1}{Sp}(1 + 0.34Sp)^2$	5.11×10^6 40.9 " 318 "	3.23×10^6 25.9 " 201 "	2.21×10^6 17.7 " 137.5 "	
1/8 1/4 1/2	$Ra_{\lambda c}^* =$ $Gr_{\lambda c}^* Pr(\frac{1}{2} + \frac{1}{Sp})$	362×10^6 239 " 182 "	223×10^6 147 " 112.2 "	148×10^6 97.6 " 74.3 "	
	k Btu/hftdeg F	0.0176	0.0198	0.0222	

Appendix FCOMPARISON OF THE CORRELATION FOR HEAT
TRANSFER AND THE EXPERIMENTAL DATA

Table F1	Comparison of data for the 1/8 inch diameter cylinders.
Table F2	Comparison of data for the 1/4 inch diameter cylinders.
Table F3	Comparison of data for the 1/2 inch diameter cylinders.

The values of the total heat flux q_{tot} , have been calculated for water and ethanol at the boiling points (using equation 56), and at intervals of subcooling using all five of the equations for liquid heat transfer (see section 8.5.1). The calculations cover the same ranges of superheat and subcooling as the experimental results. The experimental data have been included in the tables so that numerical comparisons can easily be made.

TABLE F1 Comparison of Data for 1/8 inch diameter cylinder

Equation for Nu_L	T_w °F	q_{tot} Btu/hft ²											
		Water at ΔT_L (deg F) of						Ethanol at ΔT_L (deg F) of					
		0	32	72	112	142	0	33	69	105			
$0.6(GrPr^{\frac{1}{3}})^{\frac{1}{4}}L$	1012/486	37 900	50 500	71 300	93 000		13 900	18 400	24 800	31 800			
	1312/590	56 200	68 800	89 600	111 300	126 800	19 000	23 500	29 900	36 900			
	1612/698	80 300	92 900	113 700	135 400	150 900	24 500	29 000	35 400	42 400			
$0.34(GrPr^{\frac{1}{3}})^{0.29}L$	1012/486	37 900	49 200	68 800	89 400		13 900	18 300	24 900	32 100			
	1312/590	56 200	67 500	87 100	107 700	122 700	19 000	23 400	30 000	37 200			
	1612/698	80 300	91 600	111 200	131 800	146 800	24 500	28 900	35 500	42 700			
$0.151(GrPr^{\frac{1}{3}})^{\frac{1}{3}}L$	1012/486	37 900	46 200	61 000	77 400		13 900	17 300	22 300	28 300			
	1312/590	56 200	64 500	79 300	95 700	107 300	19 000	22 400	27 400	33 400			
	1612/698	80 300	88 600	103 400	119 800	131 400	24 500	27 900	32 900	38 900			
$0.386(GrPr)^{0.28}L$	1012/486	37 900	50 300	72 500	96 900		13 900	19 800	28 700	38 500			
	1312/590	56 200	68 600	90 800	115 200	133 400	19 000	24 900	33 800	43 600			
	1612/698	80 300	92 700	114 900	139 300	157 500	24 500	30 400	39 300	49 100			
$0.42(GrPr)^{0.29}L$	1012/486	37 900	50 600	72 100	93 400		13 900	17 700	22 700	28 700			
	1312/590	56 200	68 900	90 400	111 700	126 400	19 000	22 800	27 800	33 800			
	1612/698	80 300	93 000	114 500	135 800	150 500	24 500	28 300	33 300	39 300			
Experimental data (Table E2a)	1012/486	38 500	48 100	72 800			14 000	17 500	22 400	28 100			
	1312/590	57 500	67 600	91 900	118 000	137 700	19 000	22 300	27 200	33 300			
	1612/698	80 500	91 600	114 100	140 000	159 500	24 000	27 800	32 700	38 700			

TABLE F2 Comparison of data for $\frac{1}{4}$ inch diameter cylinder

Equation for Nu_L	T_w °F	q_{tot} Btu/hft ²									
		Water at ΔT_L (deg F) of					Ethanol at ΔT_L (deg F) of				
		0	32	72	112	152	0	33	69	105	
$0.6(GrPr^{\frac{1}{4}})_L$	1012/486	32 600	43 200	60 700	77 500	96 500	12 000	15 800	21 200	27 000	
	1312/590	49 200	59 800	77 300	94 100	112 900	16 100	19 900	25 300	31 100	
	1612/698	70 900	81 500	99 000	117 200	134 600	20 900	24 700	30 100	35 900	
$0.34(GrPr^{\frac{1}{3}})_L^{0.29}$	1012/486	32 600	43 000	60 900	79 700	98 400	12 000	15 900	21 800	28 100	
	1312/590	49 200	59 600	77 500	96 300	115 000	16 100	20 000	25 900	32 200	
	1612/698	70 900	81 300	99 200	118 000	136 700	20 900	24 800	30 700	37 000	
$0.151(GrPr^{\frac{1}{3}})_L^{\frac{1}{3}}$	1012/486	32 600	41 100	56 000	72 000	87 600	12 000	15 400	20 600	26 300	
	1312/590	49 200	57 700	72 600	88 600	104 200	16 100	19 500	24 700	30 400	
	1612/698	70 900	79 400	94 300	110 300	125 900	20 900	24 300	29 700	35 200	
$0.386(GrPr^{\frac{2}{3}})_L^{0.28}$	1012/486	32 600	43 900	63 600	85 500	107 200	12 000	17 300	24 500	33 700	
	1312/590	49 200	60 500	80 200	102 100	123 800	16 100	21 400	28 600	37 800	
	1612/698	70 900	82 200	101 900	123 800	145 500	20 900	26 200	33 400	42 600	
$0.42(GrPr)_L^{0.29}$	1012/486	32 600	44 300	63 800	83 600	101 600	12 000	15 500	20 500	25 900	
	1312/590	49 200	60 900	80 400	100 200	118 200	16 100	19 600	24 600	30 000	
	1612/698	70 900	82 600	102 100	121 900	139 900	20 900	24 400	29 400	34 800	
Experimental data (Table E2b)	1012/486	33 000	43 200	64 300	86 000	107 800	11 800	16 600	20 800	25 300	
	1312/590	49 000	62 000	81 000	103 000	125 000	16 000	20 550	25 100	29 600	
	1612/698	70 000	86 000	99 700	123 500	147 400	20 900	25 200	30 200	35 100	

TABLE F3

Comparison of data for the $\frac{1}{2}$ inch diameter cylinder

Equation for Nu_L	T_w of	$q_{tot} \text{ Btu/hft}^2$									
		Water at ΔT_L (deg F) of					Ethanol at ΔT_L (deg F) of				
		0	32	72	112	0	33	69	87		
$0.6(GrPr^{\frac{1}{3}})_L$	1012/486	28 400	37 400	52 100	67 600	10 300	13 500	18 000	20 600		
	1312/590	43 400	52 400	67 100	82 600	13 800	17 000	21 500	24 100		
	- /698					17 900	21 100	25 600	28 200		
$0.34(GrPr^{\frac{0.29}{3}})_L$	1012/486	28 400	37 900	54 200	71 700	10 300	13 900	19 200	22 200		
	1312/590	43 400	52 900	69 200	86 700	13 800	17 400	22 700	25 700		
	- /698					17 900	21 500	26 800	29 800		
$0.151(GrPr^{\frac{1}{3}})_L$	1012/486	28 400	36 700	51 800	68 000	10 300	13 700	19 000	21 900		
	1312/590	43 400	51 700	66 800	83 000	13 800	17 200	22 500	25 400		
	- /698					17 900	21 300	26 600	29 500		
$0.386(GrPr^{\frac{0.28}{3}})_L$	1012/486	28 400	38 500	56 100	73 400	10 300	15 100	22 300	26 300		
	1312/590	43 400	53 500	71 100	88 400	13 800	18 600	25 800	29 800		
	- /698					17 900	22 700	29 900	33 900		
$0.42(GrPr^{\frac{0.29}{3}})_L$	1012/486	28 400	39 100	56 900	74 700	10 300	13 500	18 100	20 700		
	1312/590	43 400	54 100	71 900	89 700	13 800	17 000	21 600	24 200		
	- /698					17 900	21 100	25 700	28 300		
Experimental data (Table E2c)	1012/486	29 000	42 500			10 600	15 400	19 300	21 400		
	1312/590	44 000	60 000	72 200	90 200	14 100	19 800	23 300	25 400		
	- /698					18 500	24 200	29 100	30 600		

REFERENCES

- (1) F. KREITH: Principles of Heat Transfer. 2nd ed. International Textbook Co. (1965).
- (2) W.M. ROHSENOW: Heat Transfer with Boiling. Trans. ASHRAE, v72, p7-27, (1966).
- (3) P.J. BERENSON: Experiments on Pool-boiling Heat Transfer. IJHMT v5, p985-99, (1962).
- (4) S.T. HSU: Engineering Heat Transfer. D. Van Nostrand Company, Inc., (1963).
- (5) American Society for Metals: Metals Handbook 8th ed. v2, (1964).
- (6) K. HEINDLHOFER: Quenching: a Mathematical Study of various Hypothesis on Rapid Cooling. The Physical Review vXX, p221-42, (1922).
- (7) M.A. GROSSMAN and E.C. BAIN: Principles of Heat Treatment. American Society for Metals (1964).
- (8) Y. DARDEL: Heat Transfer during Solidification, Heating and Quenching of steel (in French). Editions de la Revue de Métallurgie (1964).
- (9) M. ECONOMOPOULOS and Y. ERNIQUIN: Etude Théorique du Refroidissement d'une Pièce de Forge au cours du Traitement Thermique. CNRM n3, 39-47, (1965).
- (10) V. PASCHKIS and G. STOLZ Jr.: Quenching as a Heat Transfer Problem. J. of metals v8, p1074-5, (1956).
- (11) V. PASCHKIS and G. STOLZ Jr.: How Measurements lead to effective Quenching. The Iron Age p95-97, Nov.22, (1956).
- (12) G. STOLZ Jr., V. PASCHKIS et al: Thermal Considerations in Oil Quenching. JISI v193, p116-123, Oct.(1959).
- (13) V. PASCHKIS: The Coefficient of Heat Transfer during Quenching (in German). Hart Techn Mitt v15, n4, p189-201, (1960). (Translation held by Aston University Library).
- (14) V. PASCHKIS and G. STOLZ Jr.: Research and Development with respect to Heat Transfer in Quenching. Armed Forces Technical Information Agency report no AD 281 854, Arlington 12 Va. U.S.A.
- (15) W. STENZEL and R. SCHULTZE: Evaporative Cooling, Part II:

- Theory of Evaporative Cooling and Measurement of Heat Transfer in Hardening Oils and Salt Solution (in German). *Chemie Ing. Techn.* v30, n11, p720-728, (1958). (Translated by J. SMUTS, London).
- (16) M. TAGAYA and I. TAMURA: Studies on Quenching media (2nd report). The Cooling Ability of various Aqueous Liquids. *Technology Reports of the Osaka University*, v2, n47, (Oct. 1952).
 - (17) F.W. JONES and W.I. PUMPHREY: Some Experiments on Quenching Media. *JISI* v156, p37-54, 524, May (1947).
 - (18) P.E. CARY et al: A new Quenchant for Steel. *Metal Progress* v73, p79-81, March (1958).
 - (19) R.F. HARVEY: Ultrasonic Quenching. *Ultrasonics* v3, p149-151, July-Sept. (1965).
 - (20) R.V. WILLIAMS and B.L. DALTON: The use of an Electric Field to Accelerate Oil Quenching. *BISRA List* 141, June/July (1965).
 - (21) A.D. AKIMENKO: Characteristics of Film Boiling during Surface Water Cooling. *Inzh-fiz. Zhurnal* v7, n6, p32-34 (1964). (Translated by Faraday Translations).
 - (22) N. Yu. TAITIS and A.S. KADINOVA: The Hardening of Tubes by Water Jet. *STAL* in English p525-527, July (1960).
 - (23) D.V. BUDRIN and V.M. KONDRATOV: Quenching in air-water mixtures. *Metal Science and Heat Treatment* p367-370 (1965).
 - (24) L.I. GLADSHTEIN: Use of Sprays for Quenching Low Alloyed Steel. *Metal Science and Heat Treatment* p716-719 (1964).
 - (25) N.A. URUSOVA and I.N. KURILEKH: An Investigation of the Process of Heat Transfer with Nozzle Cooling in the Continuous Casting of Steel. *BISI translation* 5165 (1965).
 - (26) L.L. KARPOV: Quenching in a Stream of Compressed Gases. *Metal Science and Heat Treatment* part 7-8, p581-583 (1966).
 - (27) M.J. SINNOTT and J.C. SHYNE: An Investigation of the Quenching Characteristics of a Salt Bath. *Trans ASM* v44, p758-774 (1952).
 - (28) R. SINCLAIR et al: Assessment of Fluidized Beds for the Heat Treatment of Steel. *JISI* v203, p131-137, Feb. (1965).
 - (29) C.P. BRITTAIN: Traitement Thermique en Bain Fluidisés (in French). *Traitement Thermique* v36, p49-63 (1968).

- (30) L.A. BROMLEY: Heat Transfer in Stable Film Boiling. Chem. Eng. Prog. v46, n5, p221-227 (1950).
- (31) D.P. JORDAN: Film and Transition Boiling. Advances in Heat Transfer v5, edited by T.F. Irvine Jr. and J.P. Hartnett. Academic Press (1968).
- (32) L.A. BROMLEY: Effect of Heat Capacity of Condensate. Ind. Eng. Chem. v44, p2966-9 (1952).
- (33) J.T. BANCHERO et al: Stable Film Boiling of Liquid Oxygen outside single Horizontal Tubes and Wires. Chem. Eng. Prog. Symposium Series v51, part 17, p21-31 (1955).
- (34) B.P. BREEN and J.W. WESTWATER: Effect of Diameter of Horizontal Tubes on Film Boiling Heat Transfer. Chem. Eng. Prog. v58, n7, p67-72 (1962).
- (35) K.J. BAUMEISTER and T.D. HAMILL: Laminar Flow Analysis of Film Boiling from a Horizontal Wire. NASA TN 4035, July (1967).
- (36) P.K. SARMA et al: An Improved Correlation for Film Boiling Heat Transfer on Horizontal Tubes. Can J of Chem.Eng. v46, p398-400 (1968).
- (37) J.A. CLARK: Cryogenic Heat Transfer. Advances in Heat Transfer v5, edited by T.F. Irvine Jr. and J.P. Hartnett. Academic Press (1968).
- (38) Y.Y. HSU and J.W. Westwater: Film Boiling from Vertical Tubes. JAI ChE v4, p58-62 (1958).
- (39) J.C.Y. KOH: Analysis of Film Boiling on Vertical Surfaces. J of HT v84, p55-62 (1962).
- (40) T.H.K. FREDERKING: Laminar Two-Phase Boundary Layers in Natural Convection Film Boiling. ZAMP v14, p207-218 (1963).
- (41) T.H.K. FREDERKING and J. HOPENFIELD: Laminar Two-Phase Boundary Layers in Natural Convection Film Boiling of Subcooled Liquids. ZAMP v15, p388-399 (1964).
- (42) Y.Y. HSU and J.W. WESTWATER: Approximate Theory for Film Boiling from Vertical Surfaces. Chem. Eng. Prog. Symposium Series v56, n30, p15-24 (1960).
- (43) V.M. BORISHANSKII and B.S. FOKIN: Correlation of Heat Transfer Data in Stable Film Boiling on Vertical Surfaces in the Presence of

- Free Liquid Convection in Large Volumes. *Int. Chem. Eng.* v5, n4, p666-668 (1965).
- (44) T.H.K. FREDERKING and J.A. CLARK: Natural Convection Film Boiling on a Sphere. *Adv. in Cryogenic Eng.* v8, p501-506 (1963).
 - (45) T.H.K. FREDERKING et al: Heat Transport and Fluid Motion during Cooldown of Single Bodies to Low Temperatures. *Int. Adv. in Cryogenic Eng.* v10, p353-360 (1965).
 - (46) R.C. HENDRICKS and K.J. BAUMEISTER: Film Boiling from Submerged Spheres. NASA TN D-5124 June (1969).
 - (47) Y.P. CHANG: Wave theory of Heat Transfer in Film Boiling. *J of HT* v81, p1-12, Feb. (1959).
 - (48) P.J. BERENSON: Film-Boiling Heat Transfer from a Horizontal Surface. *J of HT* v83, p351-358, Aug. (1961).
 - (49) E.R. HOSLER and J.W. WESTWATER: Film Boiling on a Horizontal Plate. *ARS Journal* v32, p553-558, April (1962).
 - (50) T.D. HAMILL and K.J. BAUMEISTER: Film Boiling Heat Transfer from a Horizontal Surface as an Optimal Boundary Value Process. 3rd Int. Heat Transfer Conf. Chicago v IV, p59-65 (1966).
 - (51) E.R.G. ECKERT and J.F. GROSS: Heat and Mass Transfer. p191 McGraw-Hill Book Company Inc. (1963).
 - (52) IBID p187.
 - (53) K. NISHIKAWA and T. ITO: Two-Phase Boundary-Layer Treatment of Free-Convection Film Boiling. *IJHMT* v9, p103-115 (1966).
 - (54) W.M. ROHSENOW: Heat Transfer and Temperature Distribution in Laminar Film Condensation. *Trans. ASME* v78, p1645-7 (1956).
 - (55) E.M. SPARROW: The Effect of Radiation on Film-Boiling Heat Transfer. *IJHMT* v7, p229-238 (1964).
 - (56) B.T. LUBIN: Analytical Derivation for Total Heat Transfer Coefficient in Stable Film Boiling from Vertical Plate. *J of HT* v91, p452-453, Aug. (1969).
 - (57) T.D. HAMILL and K.J. BAUMEISTER: Effect of Subcooling and Radiation on Film-Boiling Heat Transfer from a Flat Plate. NASA TN D-3925, Aug. (1967).
 - (58) E.M. SPARROW and R.D. CESS: The Effect of Subcooled Liquid on Laminar Film Boiling *J of HT* v84, p149-156, May (1962).

- (59) M. JAKOB: Heat Transfer v1 p447. John Wiley and Sons, Inc. (1964).
- (60) IBID: p530.
- (61) L.C. BURMEISTER: Effect of Pressure Fluctuations on Laminar Film Boiling. Ph.D. Thesis, Purdue University (1966). (University Microfilms Inc. 66-7394).
- (62) F. TACHIBANA and S. FUKUI: Heat Transfer in Film Boiling to Subcooled Liquids. Int. De in Heat Transfer, ASME, Proc. Int. Heat Transfer Conf. 1961-1962. p219-223.
- (63) W.L. LOSKIEWICZ and S.T. GORCZYCA: The Heat Transfer Coefficient during Cooling in the Hardening Process (in Polish). HUTNIK v23, n7-8, p276-282 (1956).
- (64) K. NISHIKAWA et al: Investigation of Surface Film Boiling under Free Convection (1st Report, An Experiment on Small Wires). Bull JSME v 10, n37, p123-131 (1967).
- (65) W.S. BRADFIELD, R.O. BARKDOL and J.T. BYRNE: Film Boiling on Hydrodynamic Bodies. Convair Scientific Research Note 37, Dec. (1960).
- (66) W.S. BRADFIELD: On the effect of Subcooling on Wall Superheat in Pool Boiling. J of HT v89, p269-270, Aug. (1967).
- (67) T.H.K. FREDERKING et al: Effect of Interfacial Instability on Film Boiling of Saturated Liquid Helium 1 above a Horizontal Surface. AI ChE Journal v12, n2, p238-244 (1966).
- (68) W.S. BRADFIELD: Wave Generation at a Stagnation Point in Stable Film Boiling. Symposium on two-phase flow - Exeter, v2, pA301-A330, June 21-23 (1965).
- (69) J.H. LIENHARD and P.T.Y. WONG: The Dominant Unstable Wavelength and Minimum Heat Flux during Film Boiling on a Horizontal Cylinder. J of HT v86, p220-226, May (1964).
- (70) R. HERMANN: Determination of Heat-Transfer Law for Horizontal Cylinder from Tests with Particular Account taken of the Temperature Characteristic T_e . (VDI Forschungsheft, n379, p1-24; (1936) in German). NACA TM 1366 (1954).
- (71) W.H. McADAMS: Heat Transmission, (3rd Ed). McGraw-Hill Book Co., Inc. Chapter 13.(1954).

- (72) W.H. McADAMS et al: Heat Transfer at High Rates to Water with Surface Boiling. I and EC v41, n9, p1945-53 (1949).
- (73) E.E. O'Brien: On the Flux of Heat through Laminar Wavy Liquid Layers. State Univ. of New York, College of Eng., Stony Brooke. Report n28 (1965) and n28 revised (1966).
- (74) W.S. BRADFIELD: Liquid-Solid Contact in Stable Film Boiling. I and EC Fund. v5, n2, p200-204, May (1966).
- (75) British Standards Institute: B.S. 1042.
- (76) J.B. SIVIOUR and A.J. EDE: Heat Transfer in Subcooled Pool Film Boiling. Fourth Int. Heat Transfer Conf. Paris. paper B.3.12 31st Aug. to 4th Sept. (1970).
- (77) A.E. BERGLES and W.G. THOMPSON Jr: The Relationship of Quench data to Steady-State Pool Boiling Data. IJHMT v13, p55 - 68 (1970).
- (78) S. ROY: (private communication) Dept. of Mech. Eng. University of Aston in Birmingham, Birmingham 4.
- (79) B.P. Chemicals: Bisol Technical Booklet n291, (information on ethanol).
- (80) J.P. HOLMAN: Heat Transfer. 2nd ed. p286. McGraw-Hill Book Company. (1968).
- (81) K. DURHAM (ed): Surface activity and Detergency. Chapter 1. MacMillan and Co. Ltd., (1961).
- (82) International Critical Tables v4, p449. McGraw Hill Book Company (1928).
- (83) E.R.A. Steam Tables. Edward Arnold (Publishers) Ltd. (1967).
- (84) J. TIMMERMANS: Physico-Chemical Constants of Pure Organic Liquids p312 Elsevier Publishing Co. Ltd. (1950).
- (85) International Critical Tables: v3, p27. McGraw-Hill Book Company (1928).
- (86) Handbook of Chemistry and Physics: The Chemical Rubber Co. (1962).
- (87) Engineering Sciences Data Unit (London): Item no. 66024 (1966).
- (88) IBID: Item no. 67030 (1967).
- (89) IBID: Item no. 65009 (1965).
- (90) R.W. GALLANT: Physical Properties of Hydrocarbons Part 8 - Primary Alcohols. Hydrocarbon Processing, v45, n10, Oct. (1966).

- (91) S.S. KUTATE LADZE and V.M. BORISHANSKII: A Concise Encyclopedia of Heat Transfer. Pergamon Press (1966).
- (92) E.G. BRENTARI and R.V. SMITH: Nucleate and Film Pool Boiling Design Correlations for O_2 , N_2 , H_2 and He. Int. Adv. In Cryogenic Eng. v10, p325-341 (1965).
- (93) C.T. SCIANCE et al: Film Boiling Measurements and Correlation for Liquefied Hydrocarbon Gases. Chem. Eng. Prog. Symposium Series v63, n77, p115-119 (1967).